



UNIVERSIDADE ESTADUAL PAULISTA  
"JÚLIO DE MESQUITA FILHO"  
Campus de São José do Rio Preto

Programa de Pós-Graduação em Genética

---

**MATEUS RODRIGUES BEGUELINI**

**ANÁLISE ULTRAESTRUTURAL E IMUNOCITOQUÍMICA DA  
ESPERMATOGÊNESE E NUCLEOLOGÊNESE DE MORCEGOS**

São José do Rio Preto  
2012

**MATEUS RODRIGUES BEGUELINI**

**ANÁLISE ULTRAESTRUTURAL E IMUNOCITOQUÍMICA DA  
ESPERMATOGÊNESE E NUCLEOLOGÊNESE DE MORCEGOS**

Tese apresentada como parte dos requisitos para obtenção do título de **Doutor em Genética**, junto ao Programa de Pós-Graduação em Genética, do Instituto de Biociências, Letras e Ciências Exatas da Universidade Estadual Paulista "Júlio de Mesquita Filho", Campus de São José do Rio Preto.

Orientadora: Prof<sup>ª</sup> Dr<sup>ª</sup>. Eliana Morielle Versute

Co-orientador: Prof. Dr. Sebastião Roberto Taboga

Beguelini, Mateus Rodrigues.

Análise ultraestrutural e imunocitoquímica da espermatogênese e nucleologênese de morcegos / Mateus Rodrigues Beguelini. - São José do Rio Preto : [s.n.], 2012.

222 f. : il. ; 30 cm.

Orientador: Eliana Morielle-Versute

Tese (doutorado) - Universidade Estadual Paulista, Instituto de Biociências, Letras e Ciências Exatas

1. Morcego - Reprodução. 2. Espermatogênese. 3. Nucleologênese. 4. Chiroptera. I. Morielle-Versute, Eliana. II. Universidade Estadual Paulista, Instituto de Biociências, Letras e Ciências Exatas. III. Título.

CDU - 599.4

Ficha catalográfica elaborada pela Biblioteca do IBILCE  
Campus de São José do Rio Preto – UNESP

**MATEUS RODRIGUES BEGUELINI**

**ANÁLISE ULTRAESTRUTURAL E IMUNOCITOQUÍMICA DA  
ESPERMATOGÊNESE E NUCLEOLOGÊNESE DE MORCEGOS**

Tese apresentada como parte dos requisitos para obtenção do título de **Doutor em Genética**, junto ao Programa de Pós-Graduação em Genética, do Instituto de Biociências, Letras e Ciências Exatas da Universidade Estadual Paulista "Júlio de Mesquita Filho", Campus de São José do Rio Preto.

Banca Examinadora

Prof<sup>ª</sup>. Dr<sup>ª</sup>. Eliana Morielle Versute – UNESP – São José do Rio Preto  
(Orientadora)

Prof<sup>ª</sup>. Dr<sup>ª</sup>. Shirlei Maria Recco-Pimentel – UNICAMP – Campinas

Prof<sup>ª</sup>. Dr<sup>ª</sup>. Cleida Aparecida de Oliveira – UFMG – Belo Horizonte

Prof. Dr. Carlos Alberto Vicentini – UNESP – Bauru

Prof<sup>ª</sup>. Dr<sup>ª</sup>. Isabel Cristina Cherici Camargo – UNESP – Assis



Dedico esse trabalho

Aos meus pais, Augusto Beguelini e Ercília Rodrigues Beguelini, por todo o sacrifício, renúncia, amor e compreensão que me dispuseram ao longo dessa longa jornada.

Meu caráter e tudo que conquistei, devo a vocês!  
Essa conquista não é só minha, mas de vocês também.

# Agradecimento Especial

À Professora Doutora Eliana Morielle Versute pela paciência, compreensão e confiança em mim depositada, além de todo o conhecimento a mim transmitido e, acima de tudo, pelo convívio e amizade.

**Sincera Gratidão, Admiração e Respeito!**

Ao Professor Doutor Sebastião Roberto Taboga por confiar na minha capacidade tanto em pesquisa quanto em orientação, além do convívio, amizade e respeito a mim dedicado durante todos esses anos.

Ao técnico Luiz Roberto Falleiros Junior por todo o auxílio durante esses quatro anos de pesquisa, pelas muitas risadas e pelo bom convívio.

"Na vida ,nem sempre encontramos o caminho certo, no entanto, sempre existem pessoas iluminadas que nos auxiliam a trilha-los da melhor forma possível"

# Agradecimentos

Agradeço a todas as pessoas que me auxiliaram, direta ou indiretamente, na realização deste trabalho, em especial:

A todos os meus familiares pela força e incentivo que sempre me deram, em especial meus tios **Mário** e **Joana**, meu primo **Caíque**, meu afilhado **Gabriel**, minha querida prima **Lucinéia** e meus sobrinhos **Vitória** e **Mikael**;

Aos meus velhos amigos e companheiros que tanto me auxiliaram nessa jornada: **Alessandro**, **Henrique**, **Gilberto**, **Wecksley** e **Kauan**.

Aos novos amigos que me acolheram nessa etapa final: **Roberto**, **Paulo**, **Daniel**, **Gilson**, **Diego**, **Alexandre** e **Zé**;

As minhas lindas amigas, que moram no meu coração: **Tatiane**, **Sabrina**, **Silze**, **Gisele** e **Mayara**;

A **Rose Cervates** e **Wellington Zanucoli** por toda atenção, carinho, força e suporte que me proporcionaram. Espero contar com vocês por toda a vida;

A meus companheiros do laboratório de Chiroptera: **Bruno** e **Larissa**;

A meus amigos do laboratório de Microscopia e Microanálise: **Ana Paula**, **Bianca**, **Bruno**, **Camila**, **Carol Fradsen**, **Diego**, **Egon**, **Eloísa**, **Filipe**, **Maê**, **Manoel**, **Mariana Marcielo**, **Mariana Zanateli**, **Marina**, **Ricardo**, **Samantha**, **Simone** e **Vanessa**;

A "minhas pupilas": **Ana Carolina**, **Caroline**, **Fabiane** e **Larissa**; e ao **André**;

Ao meu "braço direito" nessa caminhada, **Cíntia**, por toda a sua doação, dedicação e afinho. Sincera Amizade, Companheirismo e Respeito!

As Professoras Doutoras **Karina de Cassia Faria**, **Fernanda Cristina Alcântara dos Santos** e **Rejane Maira Góes** pelo auxílio na pesquisa;

Aos funcionários dos Departamentos de Biologia e Zoologia e Botânica, em especial aos técnicos **Jorge** e **Rosana**;

Aos funcionários da Seção de Pós-graduação, em especial a **Rosemar**;

A CAPES pela bolsa de estudos concedida; e a FAPESP pelo auxílio financeiro;

**A todos, Muito obrigado!**

"Posso ter defeitos, viver ansioso e ficar irritado algumas vezes, mas não esqueço de que minha vida é a maior empresa do mundo. E que posso evitar que ela vá à falência.

Ser feliz é reconhecer que vale a pena viver, apesar de todos os desafios.

Ser feliz é deixar de ser vítima dos problemas e se tornar um autor da própria história.

**PEDRAS NO CAMINHO? GUARDO TODAS, UM DIA VOU CONSTRUIR UM CASTELO..."**

(Fernando Pessoa)

## RESUMO

Embora o processo de reprodução tenha sido objeto de estudo em muitos mamíferos, relativamente pouca atenção tem sido dada a esse estudo em morcegos, apesar dessa ser uma grande e diversa classe de organismos, que apresenta diferentes estratégias reprodutivas para ajustar esses animais às várias condições ecológicas e comportamentais as quais estão submetidos. Da mesma forma, em geral todas as observações sobre o ciclo nucleolar foram feitas a partir da análise de células mitóticas. Assim, o intuito do presente estudo foi analisar características reprodutivas e do ciclo nucleolar meiótico de espécies de morcegos Neotropicais. No epitélio seminífero, três tipos de espermatogônias foram reconhecidos: A<sub>d</sub>, A<sub>p</sub> e B. Essas após entrarem em meiose, passam por duas divisões celulares e formam espermatídes haplóides, que sofrem diferenciação, compactando seu DNA, alongando seu núcleo e formando o flagelo e acrossomo, num processo que, em microscopia eletrônica de transmissão, pode ser dividido em doze fases. Observamos que o processo de espermiogênese ocorre de forma semelhante em *Platyrrhinus lineatus*, *Molossus molossus* e *Myotis nigricans* e que os espermatozóides de *P. lineatus* e *M. molossus* apresentam semelhanças, como o formato mais alongado da cabeça, a presença do perforatorium e espessamentos nas fibras densas externas 1, 5 e 6. Por outro lado, *M. nigricans* apresenta a ausência de perforatorium e espessamentos nas fibras axilares 1, 5, 6 e 9. Comparando os padrões reprodutivos de *Artibeus planirostris* e *M. nigricans*, observamos que, apesar de ambos serem espécies Neotropicais, eles diferem acentuadamente em sua reprodução. *Artibeus planirostris* apresenta um perfil de espermatogênese ativo durante todo o ano, possivelmente apresentando um padrão poliéstrico bimodal, com dois picos de acentuada produção espermatogênica, um em setembro e outro em fevereiro. Por outro lado, *M. nigricans* apresenta um ciclo reprodutivo anual caracterizado por apresentar dois períodos de regressão testicular, perfil

ainda não observado em nenhum outro morcego ou mamífero. A nucleologênese nas diferentes espécies analisadas ocorre de maneira semelhante ao observado na divisão mitótica de muitos mamíferos, onde os componentes nucleolares podem se comportar de até quatro formas durante a divisão meiótica, dissolver-se no nucleoplasma, deslocar-se para o citoplasma, associar-se às regiões pericromossomais ou ficar ligado às RONS durante toda a divisão; com a variação no posicionamento cromossômico não influenciando significativamente na nucleologênese meiótica. Por outro lado, percebemos que o número de RONS exerce alguma influência na nucleologênese onde, espécies que possuem maior número de RONS, apresentam maior número de nucléolos por célula interfásica, maior número de sítios de desorganização e uma maior quantidade de material nucleolar e expressão de nucleolina nas células em divisão. Com esses resultados inéditos esclarecemos alguns aspectos da espermatogênese e da nucleologênese de morcegos, assim como levantamos dados que podem ser utilizados em análises filogenéticas multifatoriais, para uma melhor elucidação das relações filogenéticas entre as espécies de morcegos.

**PALAVRAS-CHAVE:** Espermatogênese, Espermiogênese, Chiroptera, Nucleologênese, Sazonalidade.

**ABSTRACT**

*Although the process of reproduction has been studied in many mammals, relatively little attention has been given to this study in bats, this large and diverse order of organisms, which presents different reproductive strategies to adjust the animals to various environmental conditions and behaviors that they are inserted. Likewise, in general all studies on the nucleolar cycle were made based on the analysis of mitotic cells. Thus, the purpose of this study was to analyze the reproductive characteristics and the nucleolar meiotic cycle of Neotropical bat species. In the seminiferous epithelium, three types of spermatogonia were recognized:  $A_b$ ,  $A_p$  and B. These, after enter in meiosis, undergo two cell divisions to form haploid spermatids, which undergo differentiation, compressing their DNA, stretching its nucleus and forming the acrosome and flagellum, a process that, in transmission electron microscopy, can be divided into twelve stages. We note that the process of spermiogenesis occurred similarly in *Platyrrhinus lineatus*, *Molossus molossus* and *Myotis nigricans* and that the spermatozoon of *P. lineatus* and *M. molossus* have similarities, as the more elongated shape of the head, the presence of perforatorium and thickening in the outer dense fibers 1, 5 and 6. On the other hand, *M. nigricans* did not present the perforatorium and the thickening was presented in the fibers 1, 5, 6 and 9. Comparing the reproductive patterns of *Artibeus planirostris* and *M. nigricans*, we observed that, although both are Neotropical species, they differ markedly in their reproduction. *Artibeus planirostris* presents an active pattern of spermatogenesis throughout the year, possibly exhibiting a polyestral bimodal pattern, with two pronounced peaks of spermatogenic production, one in September and another in February. On the other hand, *M. nigricans* has an annual reproductive cycle endowed with two periods of testicular regression, a profile never before observed in any bat or other*

*mammal. The process of nucleologenesis in the different species analyzed occurs in a manner similar to that observed in mitotic division of many mammals, where the nucleolar components can behave as four forms during meiotic division: dissolved in the nucleoplasm; move to the cytoplasm; associate to perichromosomal regions; or linked to NORs throughout the division; with the variation in chromosome positioning does not significantly affecting the meiotic nucleologenesis. On the other hand, we noticed that the number of NORs exerts some influence on nucleologenesis, where species that have a higher number of NORs, present a higher number of nucleoli in interphase cells, most sites of disruption, a greater amount of nucleolar material and expression of nucleolina in dividing cells. With these new results we clarify some aspects of spermatogenesis and nucleologenesis of bats, as well as gather data that can be used in phylogenetic analysis, to better elucidate the phylogenetic relationships among species of bats.*

**KEYWORDS:** Spermatogenesis, Spermiogenesis, Chiroptera, Nucleologenesis, Seasonality.



## SUMÁRIO

<b>I.</b>	<b>INTRODUÇÃO</b> .....	13
	1. Morcegos: aspectos gerais .....	13
	2. A Ordem Chiroptera.....	16
	2.1. Família Phyllostomidae .....	20
	2.2. Família Molossidae .....	21
	2.1. Família Vespertilionidae .....	22
	3. Reprodução .....	24
	3.1. Espermatogênese .....	26
	3.2. Controle Hormonal da Espermatogênese – Função das Células Acessórias.....	29
	4. Nucleologênese.....	31
<b>II.</b>	<b>OBJETIVOS</b> .....	37
<b>III.</b>	<b>CAPÍTULO 1: Ultrastructure of spermatogenesis in the white-lined broad-nosed bat, <i>Platyrrhinus lineatus</i> (Chiroptera: Phyllostomidae) .....</b>	38
<b>IV.</b>	<b>CAPÍTULO 2: Ultrastructural characteristics of spermatogenesis in Pallas's Mastiff bat, <i>Molossus molossus</i> (Chiroptera: Molossidae) .....</b>	53
<b>V.</b>	<b>CAPÍTULO 3: Ultrastructural characteristics of the spermatogenesis in Black Myotis Bat, <i>Myotis nigricans</i> (Chiroptera: Vespertilionidae), during the four phases of its annual reproductive cycle .....</b>	67

<b>VI. CAPÍTULO 4: Análise comparativa da ultraestrutura das células espermatogênicas e do espermatozóide de morcegos .....</b>	<b>110</b>
<b>VII. CAPÍTULO 5: Annual Reproductive Cycle of Males of the Flat-faced Fruit-eating Bat, <i>Artibeus planirostris</i> (Chiroptera: Phyllostomidae) .....</b>	<b>115</b>
<b>VIII. CAPÍTULO 6: Two Process of Testicular Regression, not Directly Linked to Apoptosis, Are Peculiar Events of the Annual Reproductive Cycle of the Black Myotis Bat, <i>Myotis nigricans</i> (Chiroptera: Vespertilionidae) .....</b>	<b>142</b>
<b>IX. CAPÍTULO 7: Análise da nucleogênese em morcegos .....</b>	<b>176</b>
<b>X. DISCUSSÃO GERAL E CONCLUSÕES.....</b>	<b>203</b>
<b>XI. REFERÊNCIAS BIBLIOGRÁFICAS.....</b>	<b>211</b>

# I. INTRODUÇÃO

## 1. Morcegos: aspectos gerais

Os morcegos pertencem a uma das ordens mais diversa e distinta de Mammalia, a ordem Chiroptera (*chiro* = mão, *ptera* = asa); sendo os únicos mamíferos que apresentam a habilidade de vôo ativo. Essa capacidade é compartilhada unicamente com as aves e répteis pterossauros extintos, sendo possível, devido à transformação de seus membros superiores em asas. No entanto, diferente da regressão de ossos observada em aves (três dígitos) e nos pterossauros (quatro dígitos), suas asas são únicas, apresentando um grande desenvolvimento dos cinco dígitos, que atualmente tem tido seu desenvolvimento, ontogenia e evolução extensivamente estudadas (SEARS et al., 2006; WETHERBEE et al., 2006; SEARS, 2008; HOCKMAN et al., 2009; NOLTE et al., 2009; SHEN et al., 2010).

A capacidade de voar permitiu aos morcegos explorar o meio aéreo, onde o número de predadores e competidores é relativamente menor, o que lhes possibilitou uma ampla distribuição e dispersão, assim como proporcionou a possibilidade de utilizar diferentes tipos de abrigos e alimentos (MARCHESIN e MORIELLE-VERSUTE, 2002).

Os morcegos ocorrem em quase todo o planeta, só não sendo encontrados em locais muito frios, como nos pólos, locais muito quentes e em algumas ilhas oceânicas isoladas (Fig. 1). Eles estão presentes em uma ampla variedade de *habitats*, desde florestas e matas conservadas, a áreas degradadas e ambientes altamente antropomórficos, como nossas cidades (SIMMONS, 2005). No ambiente natural, estão freqüentemente associados a *habitats* aquáticos (rios, córregos, lagos e canais), onde são favorecidos pela facilidade de alimentação, pois muitas vezes esses locais atraem um grande número de insetos, que são a principal fonte de alimento para muitas espécies. Algumas espécies se adaptaram bem ao ambiente urbano, podendo ser encontradas se alimentando em nossos parques, praças e principais vias de acesso, bem como habitando em forros, dosséis, frestas, etc. de nossas residências.

A rica diversidade de fontes de alimento, propiciada pelo meio aéreo, proporcionou aos morcegos a capacidade de desenvolverem a mais diversa variedade de hábitos alimentares dentre todos os mamíferos, onde observamos desde espécies carnívoras, insetívoras, frugívoras, nectarívoras, a espécies hematófagas. A ampla variedade de alimentos utilizados varia de frutos, néctar, pólen, partes florais, folhas, insetos, outros artrópodos, pequenos peixes, anfíbios, lagartos, aves, pequenos mamíferos até o sangue (FENTON, 1992).

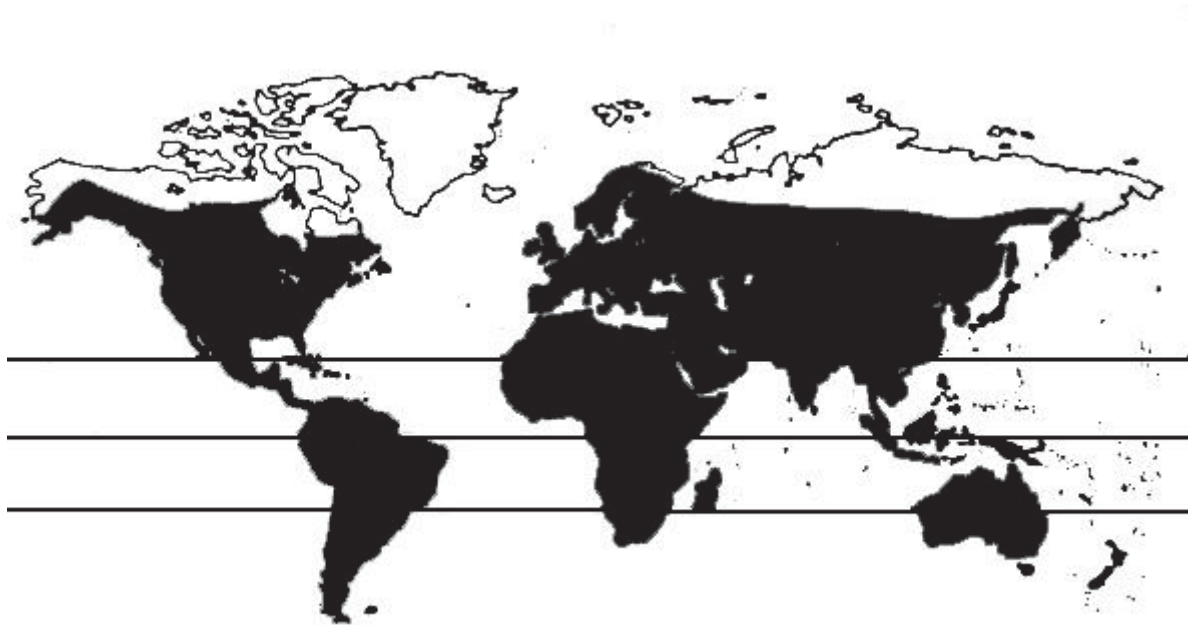


**Figura 1.** Mapa mostrando a distribuição da ordem Chiroptera no mundo. Áreas em negro demonstram a presença de morcegos. (Fonte: <http://www.saudeanimal.com.br/distr.htm>).

Outra importante característica que possibilitou a ocupação do meio aéreo noturno e também a diversificação de hábitos alimentares foi à capacidade de ecolocalização; que é o fenômeno onde a laringe é capaz de produzir sons de frequências complexas que são moduladas pelas cavidades bucal e nasal, em algumas espécies amplificadas por apêndices nasais, e discernidas por uma rica inervação ligada ou ao trago, anti-trago ou diretamente ao tímpano (SPEAKMAN, 2001). Esse “sexto sentido” está presente na maioria dos morcegos

(exceto os megaquirópteros) e funciona como um radar, onde o animal é capaz de localizar os diferentes obstáculos, assim como suas presas e, dessa forma, se orientar.

Em decorrência dessa ampla capacidade de locomoção e da grande variedade de hábitos alimentares, os morcegos desempenham diversas funções ecológicas, sendo importantes no controle populacional de insetos; na polinização e dispersão de sementes, sendo um dos principais agentes na regeneração de “habitats” fragmentados; assim como contribuindo para o controle de populações de pequenos vertebrados em áreas naturais, pela predação direta (carnívoros) ou por ação indireta, via doenças (hematófagos: *Desmodus rotundus*, *Diaemus youngi* e *Diphylla eucadata*) (BOYLES et al., 2011).

Embora sejam animais de grande importância ecológica, os morcegos são também reservatórios naturais de agentes infecciosos, e potenciais transmissores de graves doenças, como a raiva, histoplasmosse, entre outras (ROSA et al., 2006).

A importância desses animais, dos pontos de vista ecológico, econômico e médico-sanitário, aliada ao conjunto de características peculiares a esse grupo, tornaram os morcegos alvos de intensos estudos sob diversos enfoques. No entanto ainda encontramos diversas incongruências sistemáticas, taxonômicas e evolutivas; assim como falta de conhecimentos acerca de aspectos ecológicos, fisiológicos e reprodutivos; mostrando que a ordem necessita de outros estudos que complementem esses resultados e dêem condições para uma melhor resolução dessas incongruências.

## 2. A Ordem Chiroptera

A ordem Chiroptera constitui a segunda maior ordem de mamíferos, apresentando cerca de 200 gêneros e 1100 espécies amplamente distribuídas (REIS et al., 2007). Está classicamente dividida em duas subordens: Megachiroptera e Microchiroptera. A primeira é encontrada exclusivamente no Velho Mundo e compreende uma única família (Pteropodidae) com 42 gêneros e 186 espécies, enquanto que a segunda está amplamente distribuída por todo o globo, envolvendo 17 famílias e 930 espécies (SIMMONS, 2005).

A subordem Megachiroptera apresenta as maiores formas de morcegos, conhecidas como “raposas voadoras”, com algumas espécies dos gêneros *Pteropus* e *Acerodon* apresentando envergadura de 1,7 metros. De forma geral, apresentam o segundo dedo provido de unha, olhos grandes e bem desenvolvidos, não possuem sistema de ecolocalização e são, na sua grande maioria, frugívoros (NOWAK, 1999).

Os morcegos da subordem Microchiroptera são cosmopolitas, apresentam a extraordinária capacidade de ecolocalização, ampla variação de hábitos alimentares, e possuem o segundo dedo desprovido de unha (REIS et al., 2006).

No Brasil são encontrados 64 gêneros e 165 espécies de Microchiroptera, pertencentes a nove famílias: Phyllostomidae (40 gêneros e 92 espécies), Molossidae (7 gêneros e 24 espécies), Vespertilionidae (5 gêneros e 22 espécies), Emballonuridae (7 gêneros e 15 espécies), Mormoopidae (1 gênero e 4 espécies), Noctilionidae (1 gênero e 2 espécies), Thyropteridae (1 gênero e 4 espécies), Furipteridae (1 gênero e 1 espécie) e Natalidae (1 gênero e 1 espécie). Dessas, Phyllostomidae, Moormopidae, Noctilionidae, Thyropteridae, Furipteridae e Natalidae são encontradas exclusivamente nas Américas, enquanto que Molossidae, Vespertilionidae e Emballonuridae também ocorrem no velho mundo (REIS et al., 2006).

Embora os morcegos sejam extraordinariamente bem sucedidos, eles permanecem como um dos grupos menos conhecidos em relação a muitos aspectos, como os evolutivos e reprodutivos.

A origem e as relações evolutivas da ordem ainda são muito controversas. Classicamente Chiroptera é considerado um grupo monofilético alocado na superordem Archonta, juntamente com Primates, Dermoptera e Scandentia. Isso pressupõe que Megachiroptera e Microchiroptera são subordens proximamente relacionadas (isto é, formam um clado), e que suas características compartilhadas, incluindo a habilidade de voar, estariam presentes em seu ancestral comum mais recente (SIMMONS, 1994; 1995). Dessa forma, haveria somente uma origem do vôo ativo em mamíferos; contudo, outros pesquisadores (SMITH e MADKOUR, 1980; PETTIGREW, 1986; PETTIGREW e JAMIESON, 1987; PETTIGREW et al., 1989; PETTIGREW, 1995) desafiaram esta visão tradicional propondo que os megaquirópteros são mais relacionados à Dermoptera e aos primatas do que aos microquirópteros, sugerindo que o grupo é na verdade difilético. Nikaido e colaboradores (2000), baseado em dados moleculares, sugeriram que Chiroptera é mais relacionado com Fereuungulata (Carnívora + Perissodactyla + Certatiodactyla) do que com Archonta e Van den Bussche e Hofer (2004) encontraram indícios que reforçam esta hipótese.

Dentro de Chiroptera, a monofilia de Microchiroptera e as relações entre suas diferentes famílias são também motivos de muito debate. Estudos filogenéticos clássicos propuseram quatro grupos monofiléticos para a subordem (SMITH, 1976): Emballonuroidea (Emballonuridae + Rhinopomatidae + Craseonycteridae), Rhinolophoidea (Nycteridae + Megadermatidae + Rhinolophidae + Hipposideridae), Noctilionoidea (Noctilionidae + Mormoopidae + Phyllostomidae) e Vespertilionoidea (Mystacinidae + Molossidae + Myzopodidae + Thyropteridae + Furipteridae + Natalidae + Vespertilionidae). Esta hipótese foi questionada por vários trabalhos subsequentes (VAN VALEN, 1979; PIERSON, 1986;

NOVACEK, 1991; SIMMONS, 1998) e atualmente observamos que a morfologia suporta a monofilia de microquirópteros vivos, no entanto, estudos de DNA não concordam com a morfologia e sugerem que os microquirópteros são parafiléticos, com Megadermatidae (*Macroderma*, *Megaderma*) e Rhinolophidae (*Rhinolophus*, *Hipposideros*), representantes da superfamília Rhinolophoidea, formando um clado com megaquirópteros (Yinpterochiroptera) em vez de com outros microquirópteros (Yangochiroptera) (TEELING et al., 2005).

Dentro das principais famílias dois níveis de questões têm sido extensivamente abordados: o primeiro refere-se à posição da família dentro de Microchiroptera, sua relação com outras famílias e aos agrupamentos supragenéricos e, o outro, aponta para os conflitos entre as relações filogenéticas dentro da família, que culminaram no reconhecimento e definição dos gêneros. Um exemplo disso são os relacionamentos não muito bem estabelecidos que aparecem em várias famílias e gêneros, entre os quais podemos citar: as dúvidas no posicionamento das subfamílias Tomopeatinae (Molossidae ou Vespertilionidae) e Desmodontinae (agora considerado grupo irmão dos demais filostomídeos); dúvidas no número de subfamílias de Phyllostomidae e Vespertilionidae e mesmo no inter-relacionamento entre elas, assim como no posicionamento e relação de seus gêneros; e a problemática nos relacionamentos inter e intragenéricos em *Myotis*, *Eptesicus* e *Pipistrellus* da família Vespertilionidae; *Artibeus* e *Sturnira* da família Phyllostomidae; *Eumops* e *Molossus* da família Molossidae, entre outros (KOOPMAN, 1984, 1993, 1994; SIMMONS e GEISLER, 1998; JONES et al., 2002; BAKER et al., 2003; MARCHESIN e MORIELLE-VERSUTE, 2006).

Controvérsias também são observadas quanto à origem, evolução e irradiação adaptativa da ordem. Dentro de Microchiroptera encontramos um consenso na hipótese de que a maioria deles tenham se originado no Velho Mundo, a partir de onde se radiaram adaptativamente para outras regiões do mundo, inclusive a América. Esta hipótese é suportada



pela presença de representantes das famílias Emballonuridae, Rhinolophidae, Megadermatidae, Vespertilionidae e Molossidae em sítios arqueológicos da Europa datados do Terciário Médio (SMITH, 1976).

Smith (1976) sugere que a maioria das famílias de Microchiroptera originou-se, aparentemente, da radiação adaptativa dos embalonurídeos, rinolofídeos e vespertilionídeos. Com base no grau de especialização morfológica, sugere-se que os embalonurídeos teriam chegado primeiro aos trópicos do Novo Mundo (SIMMONS e GEISLER, 1998), sendo um possível ancestral dos noctilionídeos, mormoopídeos e filostomídeos, sendo seguidos pelos vespertilionídeos, que seriam, aparentemente, o estoque de onde derivaram as famílias Natalidae, Thyropteridae e Furipteridae (SMITH, 1976).

No entanto, Hood e Baker (1986) não detectaram homologias cromossômicas quando compararam os cromossomos de espécies de Phyllostomidae e Emballonuridae e estudos recentes, com base na distribuição das espécies, em dados fósseis e em filogenias com seqüências de DNA mitocondrial e nuclear sugerem que Noctilionoidea (Noctilionoidea: Furipteridae, Moormopidae, Noctilionidae, Phyllostomidae e Thyropteridae + Natalidae) forma um clado monofilético, que tem sua origem no hemisfério sul, com o mais recente ancestral comum sendo compartilhado com a família Mystacinidae durante o eoceno médio na África (VAN DEN BUSSCHE e HOOFER, 2004, TEELING et al., 2005, LIM, 2009), e não com Emballonuridae.

Similarmente, estudos do nosso laboratório mostram uma extensa homologia cromossômica partilhada entre espécies de Phyllostomidae e Molossidae (FARIA e MORIELLE-VERSUTE, 2006), assim como grande semelhança entre a ultraestrutura de seus espermatozóides (BEGUELINI et al., 2011a; BEGUELINI et al., 2012), mostrando que a hipótese de que Phyllostomidae esteja mais proximamente relacionado à Molossidae e não à Emballonuridae não pode ser descartada.

Toda essa complexidade faz de Chiroptera um grupo alvo de muitas especulações. Os relacionamentos evolutivos de muitos táxons ainda não foram investigados em detalhe e com alta representatividade, assim como inúmeras incongruências são observadas entre os estudos já feitos. Tudo isso demonstra que a ordem Chiroptera necessita de maiores estudos, que angariem caracteres morfológicos, genéticos, citogenéticos, bioquímicos, moleculares, etc., que quando avaliados conjunta e comparativamente possam fornecer subsídios para melhores interpretações de suas relações evolutivas, taxonômicas e filogenéticas.

### **2.1. Família Phyllostomidae**

A família Phyllostomidae é a mais diversificada da região neotropical, contando atualmente com cerca de 160 espécies divididas em 57 gêneros. Trata-se de um clado endêmico do Novo Mundo, com registros que se estendem do sudoeste dos Estados Unidos da América até o norte da Argentina (REIS et al., 2006). É, dentre todas as famílias de mamíferos, a mais diversificada em termos de estratégias alimentares (insetívoros, onívoros, frugívoros, carnívoros, nectarívoros e hematófagos). A principal característica morfológica do grupo é o apêndice nasal em forma de folha, presente na maioria das espécies, mas modificado em forma de ferradura nas espécies hematófagas.

A origem monofilética dessa família é suportada pela congruência de dados morfológicos, citogenéticos, bioquímicos e moleculares (BAKER et al., 1989; SIMMONS e GEISLER, 1998; JONES et al., 2002). No entanto, as relações filogenéticas dentro do grupo têm sido alvo de intenso debate, principalmente em relação ao reconhecimento de subfamílias e tribos. Jones e Carter (1976) reconheceram seis subfamílias: Desmodontinae, Phyllostominae, Glossophaginae, Carrollinae, Stenodermatinae e Phyllonycterinae. Já Wetterer e colaboradores (2000), analisando tanto dados morfológicos quanto sítios de restrição e cromossomos sexuais, reconheceram mais uma subfamília, a Brachyphyllinae. Cabe destacar

ainda que Baker e colaboradores (2003), com base em dados moleculares propuseram uma nova classificação com 11 subfamílias reconhecidas (Macrotinae, Micronycterinae, Desmodontinae, Lonchorhininae, Phyllostominae, Glossophaginae, Lonchophyllinae, Carollinae, Glyphonycterinae, Rhinophyllinae e Stenodermatinae).

Aparentemente, a grande irradiação adaptativa dos filostomídeos foi uma resposta a exploração de diferentes tipos de alimentos e habitats presentes no Novo Mundo (SMITH, 1976); no entanto, apesar dos vários estudos, pouco ainda se sabe sobre alguns aspectos de sua biologia, como os fisiológicos e reprodutivos; além de suas incongruências em sistemática e evolução.

## **2.2. Família Molossidae**

Molossidae é uma família cosmopolita composta por 16 gêneros e 86 espécies de morcegos insetívoros, amplamente distribuídos em regiões tropicais e temperadas de todo o mundo (SIMMONS, 2005). Caracterizam-se por apresentar a “cauda livre”, isto é, a cauda não fica inteiramente contida no uropatágio; e asas longas e estreitas, que demonstram uma adaptação ao voo rápido e manobrável, necessário à caça de insetos (REIS et al., 2007).

Sua sistemática e evolução são ainda bastante incertas, gerando muitas questões relativas à posição da família dentro de Microchiroptera e aos agrupamentos supragenéricos, assim como conflitos entre as várias proposições de relações filogenéticas dentro da família, que culminariam no reconhecimento e definição de seus gêneros (MARCHESIN e MORIELLE-VERSUTE, 2006).

Classicamente a família Molossidae era composta por uma única família, Molossinae, a qual incluía todos os molossídeos; no entanto, baseados em seqüências de DNA (SUDMAN, 1994) e em análises filogenéticas a partir de diferentes conjuntos de dados (SIMMONS, 1998), vários autores propuseram a inclusão da subfamília Tomopeatinae, antes

considerada uma subfamília de Vespertilionidae, em Molossidae. Esses autores demonstraram que *Tomopeas* estava mais relacionado aos molossídeos que aos vespertilionídeos e a inclusão deste em Molossidae não alterou o monofiletismo da família (SIMMONS e GEISLER, 1998; MARCHESIN e MORIELLE-VERSUTE, 2006).

Similarmente, os relacionamentos filogenéticos entre os gêneros e espécies de Molossidae são bastante controversos. O grande número de espécies aliado a sobreposição de caracteres de alguns gêneros, como *Eumops* e *Molossus*, fazem com que o reconhecimento e diferenciação de suas espécies sejam difíceis (GREGORIN e TADDEI, 2002). Todas essas incongruências são possivelmente devidas à escassez de estudos representativos dos táxons, uma vez que se trata de espécies difíceis de coletar, devido às suas características de comportamento e hábito.

### 2.3. Família Vespertilionidae

Vespertilionidae é a maior e mais diversificada família de Chiroptera, apresentando 48 gêneros e 407 espécies (SIMMONS, 2005; REIS et al., 2007), o que corresponde a aproximadamente um terço de todas as espécies de morcegos viventes; é verdadeiramente cosmopolita, ocorrendo em todos os continentes, com algumas espécies atingindo regiões temperadas frias e ilhas oceânicas, tais como Bermudas, Galápagos e Havaí (KOOPMAN, 1970).

Os vespertilionídeos possuem olhos pequenos, nenhum apêndice nasal (rudimentar em *Nyctophilus* e em *Pharotis*), suas caudas são relativamente longas e estão contidas em toda a extensão da membrana interfemural, formando um “V” bem definido. Esta grande família inclui uma larga escala de tamanhos. Alguns morcegos pesam somente quatro gramas, visto que outros pesam até 50 gramas (REIS et al., 2007).

Cinco subfamílias eram geralmente propostas para Vespertilionidae: Vespertilioninae, Myotinae, Miniopterinae, Murinae e Kerivoulinae (SIMMONS, 1998; SIMMONS e GEISLER, 1998). No entanto, Simmons (2005) reconheceu a existência de mais uma subfamília (Antrozoinae), aumentando o número para seis. Dessas, as três últimas são claramente monofiléticas (SIMMONS, 1998).

Apenas Vespertilioninae e Myotinae ocorrem no Brasil, com aproximadamente 24 espécies pertencentes a cinco gêneros (*Eptesicus*, *Histiotus*, *Lasiurus*, *Myotis* e *Rhogeessa*), todas elas se alimentando de insetos (BARCLAY e BRIGHAM, 1991; REIS et al., 2007).

No Hemisfério Norte, muitas de suas espécies realizam movimentos migratórios ou hibernam (CRICHTON e KRUTZSCH, 2000), comportamentos que, embora não comprovados, são sugeridos para representantes da América do Sul (REIS et al., 2007).

A sistemática, ao nível familiar; o reconhecimento dos gêneros e espécies e a filogenia de Vespertilionidae são altamente controversos, em decorrência do grande número de espécies alocados em poucos gêneros, como *Myotis* que apresenta mais de 100 espécies; dos poucos estudos constantes na literatura; da dificuldade na coleta desses animais; e do pequeno número de caracteres morfológicos adequados para sua classificação taxonômica (MARCHESIN e MORIELLE-VERSUTE, 2006).

### 3. Reprodução

A ordem Chiroptera apresenta algumas características reprodutivas singulares dentre todos os mamíferos, como o fato de algumas espécies entrarem em hibernação e apresentarem nesse período um processo de regressão dos túbulos seminíferos, onde apenas espermatogônias e células de Sertoli podem ser observadas (RACEY, 1974; KUROHMARU et al., 2002; LEE, 2003; LEE e MORI, 2004). Possivelmente, de forma a adaptar-se a esse período de hibernação; muitas espécies desenvolveram características únicas como: um prolongado armazenamento de espermatozóides na cauda do epidídimo nos machos e/ou no corno uterino nas fêmeas; assincronia entre os períodos de espermatogênese e o de cópula, assim como um retardo na ovulação, fertilização e/ou implantação do embrião no trato reprodutor feminino (ANAND-KUMAR, 1965; RACEY, 1979; RASWEILER, 1993; CRICHTON e KRUTZSCH, 2000; ENCARNAÇÃO et al., 2004; SHARIFI et al., 2004, BEGUELINI et al., 2009; 2011a).

Aliado a isso, a maioria das espécies de morcegos já estudadas apresenta aparentemente um sistema de cópula poligínico, no qual um macho copula com várias fêmeas (sistema de haréns); e/ou poliândrico, onde a fêmea copula em seqüência com vários machos, com a paternidade aparentemente fora do harém; enquanto que uma minoria aparenta possuir um sistema monogâmico. A maioria das relações de morcegos é promíscua, com os indivíduos que copularam não mantendo nenhuma relação nem antes nem depois da cópula. Assim, seu sistema de cópula pode variar desde a formação de grupos de um macho para múltiplas fêmeas; múltiplos machos para múltiplas fêmeas; até um único macho para uma única fêmea; com essa composição podendo variar no número de integrantes e podendo estar organizada durante todo o ano ou apenas por um período (sazonal) (CRICHTON e KRUTZSCH, 2000).

Caracteristicamente, morcegos gestam um único concepto em cada gestação, a exceção de alguns membros de Vespertilionidae, como *Lasiurus borealis*, que podem gestar até quatro. O período de gestação varia amplamente entre as espécies e, em alguns casos, pode variar dentro da mesma espécie devido a retardos no desenvolvimento (GOPALAKRISHNA e BADWAIK, 1993; HAYSEN et al., 1993).

Comparados a outros mamíferos, morcegos geralmente têm um grande porte ao nascimento, apresentando uma massa corporal que representa aproximadamente 20-30% do peso materno, mas que pode chegar a até 43%, dependendo da espécie (KURTA e KUNZ, 1987); e também uma grande longevidade, possivelmente devida à reduzida taxa de mortalidade que o ambiente aéreo noturno lhe propiciou e ao grande tamanho que sua prole apresenta no período de independência (BARCLAY, 1995).

Por sua ampla distribuição geográfica, os morcegos sofrem considerável influência dos fatores abióticos sobre suas estratégias reprodutivas. Espécies que ocorrem em altas latitudes tendem a possuir um padrão monoéstrico de reprodução intimamente associado com a hibernação e diretamente influenciado pela temperatura (CRICHTON e KRUTZSCH, 2000). Entretanto, em espécies tropicais, os ciclos reprodutivos estão fortemente associados com a estação chuvosa. Estes fatores climáticos (temperatura e pluviosidade) combinados com a viabilidade do suplemento alimentar influenciam diretamente nos ciclos reprodutivos dos quirópteros tropicais, proporcionando diferentes possibilidades de ciclos reprodutivos, desde padrões monoéstricos e poliéstricos bimodais, até espécies que se reproduzem ao longo de todo o ano (FLEMING et al., 1972; TADDEI, 1976).

Isso demonstra que a morfologia, fisiologia e as estratégias reprodutivas, em Chiroptera, são amplamente complexas e diversas, variando dependendo da latitude e do hábitat que os morcegos habitam, variando dentro da mesma família, gênero ou mesmo dentro de uma mesma espécie (BRADBURY e VEHRENCAMP, 1977; TADDEI, 1980).

### 3.1. Espermatogênese

A espermatogênese é um processo ordenado e complexo de divisão celular e diferenciação pelo qual células-tronco se transformam em espermatozóides. Ocorre nos túbulos seminíferos dos testículos (Fig. 2) que em humanos produzem aproximadamente 120 milhões de espermatozóides diariamente. A manutenção dessa impressionante produção diária requer uma coordenação das divisões celulares mitóticas das espermatogônias, para repor as reservas de células-tronco e para sofrerem a diferenciação em espermatócitos, divisões meióticas dos espermatócitos para produzir espermátides, que contém um número haplóide de cromossomos, e diferenciação das espermátides em espermatozóides maduros (MATSUMOTO, 1996).

A regularidade do processo espermatogênico está ligada aos processos genéticos, transcricionais, traducionais e reguladores, onde o ciclo é mantido por uma grande rede de reações que vai desde a ativação e desativação gênica, até a produção de proteínas que coordenam as divisões celulares. Toda essa cascata de reações e diferenciação tem atraído muitos estudos, devido a esse processo envolver muitas mudanças radicais tanto na forma como na fisiologia e bioquímica das células.

Nos adultos esse processo contínuo pode ser dividido em três fases distintas: a mitótica, a meiótica e a espermiogênese; cada uma sendo caracterizada por mudanças morfológicas e bioquímicas do citoplasma e núcleo celular.

A fase mitótica, também chamada de proliferativa ou espermatogonial, é caracterizada pelas divisões mitóticas das células-tronco (espermatogônias), que vão originar novas células, parte da qual irá servir para a renovação da população de células-tronco e outras que entrarão no processo de divisão e diferenciação. As espermatogônias predestinadas a entrarem em meiose ainda sofrerão algumas divisões mitóticas formando outros tipos de espermatogônias que, ao final das mitoses, serão deslocadas para o compartimento adluminal



e entrarão em uma prolongada fase de meiose, como espermatócitos. Todos os tipos celulares subsequentes ficarão no compartimento adluminal, passando entre junções celulares de células de Sertoli adjacentes e serão dependentes dessas células para terem acesso a nutrientes e hormônios necessários a sua diferenciação (COSTA e PAULA, 2003).

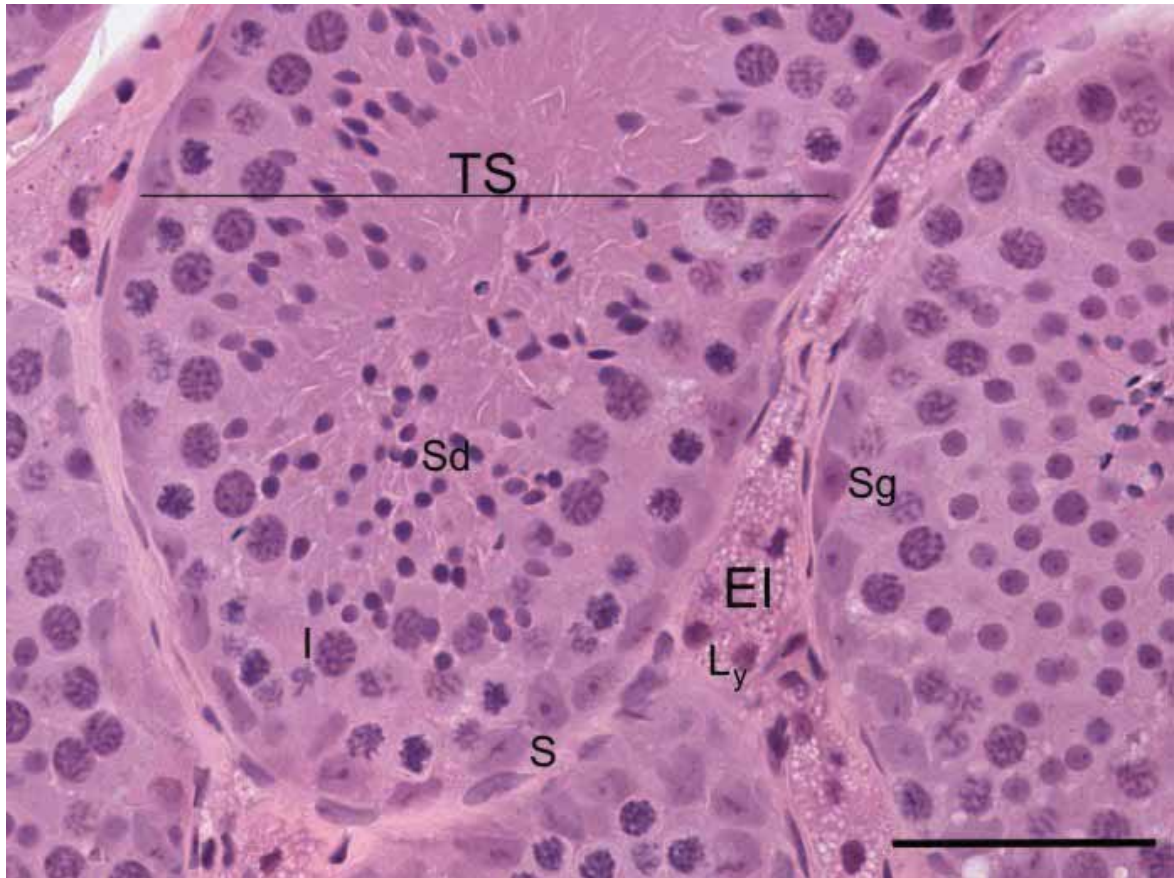


**Figura 2.** Arranjo geral do epitélio testicular de morcegos (*Platyrrhinus lineatus*), coloração por Hematoxilina-Eosina. Túbulo seminífero (TS), espaço intersticial (EI), célula de Sertoli (S), espermatogônia (Sg), espermatócito primário (I), espermatídeos (Sd) e células de Leydig ( $L_y$ ). Barra = 50  $\mu$ m.

O próximo passo da espermatogênese corresponde à fase meiótica, processo no qual os espermatócitos passam pelas duas divisões meióticas originando espermatídeos haplóides (RUSSELL et al., 1990). Nesse período são observadas todas as reações preparatórias para a divisão celular, como a inibição da transcrição, a duplicação do DNA e a formação dos complexos sinaptonêmicos, com a gradual condensação da cromatina ao seu

redor; assim como a ocorrência da desorganização e reorganização nucleolar e das duas divisões meióticas para a formação das espermatídes haplóides (PARVINEN et al., 1991; LODISH et al., 2005).

A última e mais longa fase da espermatogênese corresponde a espermiogênese, processo que, através de mudanças morfológicas progressivas, faz com que espermatídes arredondadas se diferenciem em espermatozóides alongados que se tornam aptos a locomoção e fertilização (CLERMONT, 1972). Estas modificações incluem: o desenvolvimento do acrossomo que, apesar de possuir características semelhantes entre os mamíferos, uma espécie difere das outras nos detalhes de sua formação e na sua forma final na região anterior do espermatozóide; a condensação e o alongamento do núcleo, onde as histonas associadas à cromatina nuclear são substituídas por protaminas, assim há uma remodelagem das fibras de cromatina que passam a ser mais compactas; e quase ao mesmo tempo, a formação do flagelo e acúmulo de mitocôndrias. Associado a esses eventos, ocorre uma redução progressiva do volume citoplasmático pela liberação de corpos residuais (WARD e COFFEY, 1991; COSTA e PAULA, 2003). Após esses processos as espermatídes são liberadas para o lúmen do túbulo seminífero, passando a serem chamadas de espermatozóides, fechando o ciclo da espermatogênese.

Embora o processo de espermatogênese tenha sido objeto de estudo em muitos mamíferos, pouca atenção tem sido dada a esse estudo em morcegos, apesar dessa ser uma grande e diversa classe de organismos, que apresentam diferentes estratégias reprodutivas para ajustar esses animais às várias condições ecológicas e comportamentais as quais estão submetidos.

### 3.2. Controle Hormonal da Espermatogênese – Função das Células Acessórias

A espermatogênese em mamíferos requer a ação de um complexo conjunto de peptídeos e hormônios esteróides que, através de uma grande rede de interações e cascatas de reações, regulam o funcionamento do epitélio seminífero. Esses mensageiros hormonais são críticos, não somente por regularem o desenvolvimento das células germinativas, mas também por regularem a proliferação e o funcionamento dos diferentes tipos de células somáticas testiculares, que são requeridas para o funcionamento normal dos testículos (McLACHLAN et al., 2002).

Dentre essas temos as células de Leydig, que são células intersticiais cuja função principal parece ser a produção de testosterona (MENDIS-HANDAGAMA, 1997); as células mióides que circundam os túbulos seminíferos e fornecem suporte físico e movimento contrátil a estas estruturas (MAEKAWA et al., 1996); e as células de Sertoli, que estão localizadas junto à lâmina basal dos túbulos seminíferos, com seu citoplasma envolvendo as células germinativas e estendendo-se até o lúmen tubular. Dentre as funções que desempenha, podem-se destacar: formação da barreira hematotesticular; suporte estrutural e nutricional das células germinativas; responsabilidade pela progressão das células germinativas, em diferenciação, em direção ao lúmen; liberação dos espermatozóides para o lúmen tubular, processo conhecido como espermição; fagocitose de células germinativas degeneradas e corpos residuais; secreção de fluidos e proteínas para banhar as células germinativas em desenvolvimento e conduzir os espermatozóides através dos túbulos em direção à *rete testis* (RUSSELL e GRISWOLD, 1993).

Cada um destes tipos celulares é alvo direto de um ou mais hormônios, cujas ações são essenciais para manter a fertilidade masculina. Essa regulação parece ser feita principalmente pelos hormônios folículo estimulante (FSH) e luteinizante (LH), que são

hormônios glicoproteicos secretados pela glândula pituitária; e pela testosterona (HOLDCRAFT e BRAUN, 2004a).

A expressão de receptores de FSH apenas nas células de Sertoli (RANNIKKI et al., 1995) e de LH, primariamente, apenas nas células de Leydig (LEI et al., 2001), pressupõe diferentes funções para esses hormônios. O papel principal do FSH na espermatogênese parece estar ligado à estimulação da proliferação das células de Sertoli (HECKERT e GRISWOLD, 2002), lembrando que o número dessas células determina diretamente o número de células germinativas do epitélio (SHARPE, 1994). Já o do LH estaria ligado à regulação da síntese de testosterona pelas células de Leydig (HOLDCRAFT e BRAUN, 2004a).

A testosterona (T) e seus metabólitos, diidrotestosterona (DHT) e estradiol (E2), são hormônios primordiais na regulação do desenvolvimento e da diferenciação das células germinativas, bem como da diferenciação sexual. Nos machos, a T assume o papel principal, tanto no desenvolvimento morfológico como na função reprodutiva, embora o E e seus receptores (ER), principalmente o  $\alpha$  (ER $\alpha$ ), claramente desempenhem algum papel na manutenção da fertilidade masculina. No entanto, esses efeitos parecem ser indiretos e secundários (LEE et al., 2000).

Em contraste com o papel dos estrógenos, os andrógenos e a função de seu receptor (AR) são essenciais para a adequada diferenciação sexual e para a manutenção da espermatogênese. A atividade do AR é regulada pela T e DHT, cuja ligação desencadeia sua translocação nuclear e ativa sua função reguladora transcricional (LINDZEY et al., 1994). No testículo, o AR é expresso nas células de Leydig, mióides, e de Sertoli (ZHOU et al., 2002). A expressão nas células de Leydig e mióides é contínua, com o próprio AR desempenhando um importante papel na regulação dos níveis de T, através de um feedback autócrino sobre as células de Leydig, com a inibição da síntese e secreção de LH pela hipófise (AMORY e BREMNER, 2001). Já a expressão nas células de Sertoli parece ocorrer de forma estágio-

dependente, além de ser um requisito essencial a normal ocorrência da espermatogênese. Pelo menos três etapas da espermatogênese parecem apresentar dependência à expressão de AR: a progressão através da meiose I; as etapas do alongamento das espermátides; e a fase final da espermiogênese (HOLDCRAFT e BRAUN, 2004a, 2004b; WANG et al., 2009).

Assim, a célula de Sertoli apresenta um papel crucial no desenvolvimento das células germinativas e na regulação da espermatogênese, recebendo sinais endócrinos circulantes e fatores parácrinos das células de Leydig, peritubular e células germinativas, integrando esses sinais, e secretando produtos que controlam o desenvolvimento das células germinativas e modulam a função de outras células testiculares, incluindo sua própria função (MATSUMOTO, 1996).

#### **4. Nucleologênese**

O nucléolo é a estrutura celular mais facilmente visível, mesmo sem coloração e *in vivo*, em microscopia de luz, o que é possível graças ao seu índice de refração mais elevado do que o dos outros elementos do núcleo e do citoplasma. Seu tamanho e forma dependem do estado funcional celular, variando conforme a espécie e, dentro de uma espécie, de tecido para tecido e mesmo de célula para célula. Quanto mais forte a sobrecarga funcional celular, maior será o nucléolo (MELLO, 2001). Ele é um grande domínio nuclear reunido em torno dos genes ribossomais (DNAr); quando em eucariotos superiores, o RNA ribossomal (RNAr) 47S é transcrito, transformado em 18S, 5,8S e 28S RNAr, e montado com o 5S RNAr e proteínas necessárias para produção das pequenas (18S RNAr) e das grandes (5,8S, 28S e 5S RNAr) subunidades do ribossomo (HERNANDEZ-VERDUN, 2011).

A função principal do nucléolo é a biogênese dos ribossomos, fenômeno que envolve uma série de eventos como a transcrição do DNAr, o processamento dos pré-RNAr e a reunião de partículas pré-ribossomais (SCHEER e HOCK, 1999). No entanto ele é um

domínio plurifuncional envolvido na resposta ao stress; na biogênese de partículas de ribonucleoproteínas independentes das subunidades do ribossomo; além de estar ligado a cadeia de propagação de várias doenças, como o câncer e infecções virais, entre outras ações (BOISVERT et al., 2007; HISCOX, 2007).

Presentemente o nucléolo é um dos mais surpreendentes e bem estudados sub-compartimento do núcleo. Quando observado em microscopia eletrônica, o nucléolo de eucariotos superiores contém três componentes principais: o centro fibrilar (CF), o componente fibrilar denso (CFD) e o componente granular (CG); com esta estruturação refletindo a compartimentalização dos mecanismos relacionados à produção dos ribossomos. O CF contém centenas de cópias de genes DNAr arranjados em tandem, em vários locos cromossômicos denominados regiões organizadoras nucleolares (RONs). Apesar dos vários genes, somente um subconjunto deles está normalmente ativo e este parece ter uma localização mais periférica, estendendo-se para o CFD, onde são observados os RNAr recém transcritos. No CG, o mais periférico, vão ocorrer os eventos finais do processamento dos transcritos de RNAr, com a formação das partículas pré-ribossomais que serão translocadas para o citoplasma através dos poros nucleares (CARMO-FONSECA et al., 2000, HERNANDEZ-VERDUN, 2011).

Durante o ciclo celular, alterações na forma e tamanho dos nucléolos podem ocorrer, em consequência do papel funcional dos vários domínios nucleolares, que se desorganizam e reorganizam durante o ciclo. A grande produção de ribossomos em interfase mantém a compartimentalização nucleolar, no entanto quando a célula entra em divisão, essa produção para, desencadeando a desorganização nucleolar (SIRRI et al., 2000). Essa desorganização é um processo sequencial, que começa no início da divisão com a desagregação ordenada dos complexos de processamento do CG e depois do CFD, seguida pela repressão da transcrição da RNA polimerase I (pol I). Estima-se que essa transcrição

diminua em cerca de 30% durante o início da prófase e para ao seu fim (GÉBRANE-YOUNÈS et al., 1997).

As várias classes de compartimentos nucleolares distribuem-se então para diferentes regiões da célula, no entanto, o aparelho ou maquinário transcricional, pol I e seus fatores de transcrição, permanecem associados às RONS durante toda a divisão (SAVINO et al., 2001). Contrariamente a esse, os componentes do processamento dos pré-RNAs são encontrados, no mínimo, em dois diferentes sítios: na região pericromossomal e no citoplasma. Eles se dispõem em volta dos cromossomos no início da prometáfase e permanecem até o início da telófase (DUNDR et al., 1997) e, no citoplasma, aparecem constituindo numerosas partículas esféricas relativamente grandes. Elas aparecem na anáfase, diminuem em número na telófase e eventualmente desaparecem na fase G1 (DUNDR et al., 1997; DUNDR e OLSON, 1998).

No início e durante a mitose, vários fatores de transcrição específicos da pol I são fosforilados pela Cdk1 ciclina quinase B; com essas fosforilações sendo necessárias para se estabelecer e manter a supressão da transcrição do DNAr. Da mesma forma, a fosforilação das proteínas do processamento nucleolar é modificada durante a mitose. A proteína NPM/B23, uma ribonucleoproteína específica do componente granular, é um dos alvos da Cdk1 ciclina quinase B durante a mitose. A fosforilação da NPM/B23 começa na prófase inicial e é revertida pela PP1 fosfatase apenas na anáfase. Esta fosforilação diminui a afinidade de ligação do RNA-NPM/B23, ocasionando a liberação desta proteína do nucléolo durante a prófase e desencadeando a desorganização nucleolar. Assim percebemos que tanto a desorganização do nucléolo quanto a inativação da transcrição do DNAr parecem ocorrer pela mesma via, mas com a desagregação dos complexos de processamento nucleolar precedendo a inativação da transcrição (HEIX et al., 1998; SIRRI et al., 1999; NEGI e OLSON, 2006).



Os diferentes trabalhos voltados ao estudo da nucleologênese têm mostrado que a reorganização nucleolar inicia-se no final da anáfase ou início da telófase (SCHEER et al., 1993; FOMPROIX et al., 1998); e depende da coordenação entre a reativação da transcrição do DNAr e o recrutamento e ativação dos complexos de processamento de RNAr. Esses complexos estão presentes na célula por serem estocados, durante a mitose, em locais denominados de corpúsculos pré-nucleolares (PNBs). Assim, a reestruturação do novo nucléolo no início da intérfase envolve a ativação da maquinaria de transcrição, já em associação com os genes de DNAr; a formação de corpos nucleolares transitórios, os PNBs; e da translocação dos complexos de ribonucleoproteínas dos PNBs aos locais de transcrição (HERNANDEZ-VERDUN et al., 2002).

Como durante a mitose, a transcrição da pol I é reprimida pela atividade da Cdk1 ciclina quinase B, no final da mitose a reativação de sua transcrição depende da inibição dessa atividade. Essa inibição parece ser controlada pela ação das fosfatases PP1 e PP2A. Assim observamos que a inibição/ativação da transcrição do DNAr é resultado do equilíbrio entre fosforilação/desfosforilação de seus sítios e da distribuição local e atividade dessas enzimas (HERNANDEZ-VERDUN, 2011).

O principal sinal para a reorganização nucleolar é a reativação da transcrição do DNAr, no entanto, foi demonstrado que somente a reativação não possui a capacidade de organizar completamente um nucléolo, com essa montagem sendo também depende das proteínas e dos complexos de processamento presentes no compartimento pericromossômico e nos PNBs (DOUSSET et al., 2000; SIRRI et al., 2002). Assim, a completa reorganização depende do recrutamento dos complexos de processamento dos PNBs para os nucléolos em formação, em primeiro lugar para reorganizar o CFD (fibrilarina) e depois o CG (Nop52) (MURO et al., 2010).



Interessante notar que, em algumas células que contêm uma grande abundância de complexos nucleolares, ocorre a formação de aglomerados denominados “nucleolus derived foci” (NDFs), os quais tendem a deslocar-se para o citoplasma durante a divisão. A utilização também desse material na reconstrução do nucléolo das células filhas é ainda intensamente discutida (DUNDR et al., 1997; DUNDR et al., 2000).

Apesar das diferentes abordagens sobre a nucleologênese, há ainda muito a ser entendido, uma vez que, apesar do fenômeno ser comum a todas as células eucariotas, alguns aspectos devem ser particulares a cada organismo ou espécie. Além disso, a maioria dos estudos foi realizado em cima do processo mitótico, com pouco ou nenhum estudo do processo meiótico. Deve ser considerado aqui, que nas células somáticas a transcrição é suspensa no início do ciclo de condensação cromossômica, mas nas células gaméticas os genes ribossomais são ativos durante a prófase I - leptóteno, zigóteno e início do paquíteno, nos espermátocitos, e até o diplóteno, nos oócitos (WACHTLER e STHAL, 1993).

Como citado anteriormente, as RONS fazem parte do centro fibrilar, e, portanto, são indispensáveis à formação do nucléolo. Não só em mamíferos, mas em vários outros grupos de organismos, o número e a posição das RONS variam amplamente entre as espécies. Na maioria dos mamíferos as RONS são encontradas nos autossomos, mas em algumas espécies, elas ocorrem também nos cromossomos sexuais.

O número de RONS ativas corresponde ao número máximo de nucléolos que podem ser encontrados em células interfásicas, todavia, o número de RONS que são ativas em cada célula pode variar. A ativação diferencial de RONS conduz a uma variação no número e tamanho dos nucléolos, porém não é a única responsável, uma vez que existem modificações cíclicas na morfologia dos nucléolos durante o ciclo celular, assim como fusão nucleolar, resultante de movimento, crescimento e aproximação dos nucléolos.

O número de RONS em espécies de morcegos é variável, assim como é variável o número de RONS ativas e de nucléolos. Também é característico uma taxa elevada de fusão nucleolar (VOLLETH, 1987; MORIELLE e VARELLA-GARCIA, 1988).

A variação no número de RONS é grande, podendo ser destacado a presença de um par em espécies de diferentes famílias como *Platyrrhinus lineatus*, *Molossus rufus* e *Lasiurus ega*, até 3 e 5 pares nas espécies *Artibeus lituratus* e *Myotis nigricans* (MORIELLE-VERSUTE et al., 1996; MARCHESIN e MORIELLE-VERSUTE, 2002). No entanto, essa variação não ocorre somente no número, mas também em seu posicionamento onde, devido a rearranjos, elas podem estar localizadas em diferentes lócus cromossômicos, com o extremo de *Carollia perspicillata*, que apresenta as RONS no cromossomo X.

Em geral todas as observações sobre RONS e nucléolos em morcegos foram feitas a partir da análise de células somáticas. Em decorrência da escassez de informações e do interessante aspecto envolvendo a nucleologênese, uma análise de células meióticas, envolvendo a caracterização das RONS e nucléolos, é interessante.

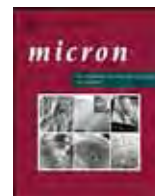
## II. OBJETIVOS

Com base no exposto, a presente tese teve como objetivos principais:

1. Analisar sob o enfoque de ultraestrutura as células espermatogênicas de *P. lineatus* (Phyllostomidae), *M. molossus* (Molossidae) e *M. nigricans* (Vespertilionidae), com ênfase a ultraestrutura dos espermatozoides; caracterizando-os, a fim de verificar se há variação interespecífica.
2. Avaliar o efeito da sazonalidade na morfologia testicular dos morcegos das espécies *A. planirostris* e *M. nigricans*, por meio da análise de material obtido em coletas seriadas e consecutivas (mês a mês).
3. Analisar o comportamento dos subcompartimentos nucleolares durante a divisão meiótica, investigando se a variação no número e posicionamento cromossômico das RONS influencia na nucleogênese.
4. Reunir informações morfológicas que quando avaliadas conjuntamente e comparativamente possam fornecer subsídios para interpretações de relações evolutivas e taxonômicas para o grupo Chiroptera.

### III. CAPÍTULO 1

## **Ultrastructure of spermatogenesis in the white-lined broad-nosed bat, *Platyrrhinus lineatus* (Chiroptera: Phyllostomidae)**



## Ultrastructure of spermatogenesis in the white-lined broad-nosed bat, *Platyrrhinus lineatus* (Chiroptera: Phyllostomidae)

Mateus R. Beguelini<sup>a</sup>, Cintia C.I. Puga<sup>b</sup>, Sebastião R. Taboga<sup>a,\*</sup>, Eliana Morielle-Versute<sup>b</sup>

<sup>a</sup> Department of Biology, São Paulo State University – UNESP/IBILCE, 15054-000 São José do Rio Preto, São Paulo, Brazil

<sup>b</sup> Department of Zoology and Botany, São Paulo State University – UNESP/IBILCE, 15054-000 São José do Rio Preto, São Paulo, Brazil

### ARTICLE INFO

#### Article history:

Received 18 August 2010

Received in revised form 11 February 2011

Accepted 13 February 2011

#### Keywords:

Chiroptera

Spermatogenesis

Spermiogenesis

Synaptonemal complex

Ultrastructure

### ABSTRACT

Spermatogenesis, the remarkable process of morphological and biochemical transformation and cell division of diploid stem cells into haploid elongated spermatozoa, is one of the most complex cell differentiations found in animals. This differentiation process has attracted extensive studies, not only because the process involves many radical changes in the cell shape and biochemistry, but also because the phases and steps of differentiation have provided a better basis for analyzing the seminiferous epithelium cycle. Thus, this study aimed to characterize ultrastructurally the spermatogenesis process in the bat *Platyrrhinus lineatus* in order to provide a basis for determining the stages of spermatogenesis and to facilitate comparisons of the process between bat species and other vertebrates. Based on ultrastructural characteristics three main types of spermatogonia could be accurately identified: A<sub>d</sub>, A<sub>p</sub> and B; the differentiation of spermatids was clearly divided into 12 steps (steps 1–3: Golgi phase, steps 4–5: cap phase, steps 6–9: acrosomal phase and steps 10–12: maturation phase). The ultrastructure of spermatozoa, Leydig cells and Sertoli cells was characterized; and some processes including nucleolar disorganization and the formation of synaptonemal complexes, acrosome and chromatoid body were discussed. Based on our results we may conclude that the spermatogenic process of *P. lineatus* follows the pattern of mammals with some specificity, as the process of formation of the acrosome and the presence of the perforatorium. By other side, the simpler ultrastructure of its spermatozoon shows a pattern more closely related to the sperm cells of humans and other primates.

© 2011 Elsevier Ltd. All rights reserved.

### 1. Introduction

Spermatogenesis, the remarkable process of morphological and biochemical transformation and cell division of a diploid stem cell into a haploid elongated spermatozoon, is one of the most complex cell differentiations found in animals. During this process, the stem cell spermatogonias proliferate and differentiate, duplicate their DNA and proceed through meiosis, forming haploid spermatids. The spermatid reduces its cell volume more than a hundred times, radically changes its shape and produces a number of morphologically elaborate organelles including the acrosome, the midpiece and the flagellum (Lin et al., 1997). This differentiation process has attracted extensive studies, not only because the process involves many radical changes in the cell shape and biochemistry, but also because the phases and steps of differentiation have provided a better basis for analyzing the seminiferous epithelium cycle.

\* Corresponding author at: Rua Cristóvão Colombo n° 2265, Jardim Nazareth, 15054-000 São José do Rio Preto, São Paulo, Brazil. Tel.: +55 17 32212386; fax: +55 17 32212374.

E-mail address: [taboga@ibilce.unesp.br](mailto:taboga@ibilce.unesp.br) (S.R. Taboga).

Furthermore, the ultrastructure of the spermatozoon has been the subject of considerable investigation in several animal groups over the past 30 years and is an important indicator of phylogenetic relationships (Rouse and Robson, 1986; Jamieson, 1987, 1995; Jamieson et al., 1993; Mori, 1994; Phillips et al., 1997; Teixeira et al., 1999b; Korn et al., 2000; Fernandes et al., 2001; Garda et al., 2002; Costa et al., 2004; Gwo et al., 2004; Vieira et al., 2005; Soon-Jeong et al., 2006).

Although the main morphological events of spermatogenesis are generally similar in the majority of eutherian mammals, some taxa show many unique characteristics. In spite of the scarcity of published information on the process of spermatogenesis in Chiroptera, bats show some exclusive reproductive characteristics. Some species enter into hibernation and present testicular regression when only spermatogonia and Sertoli cells can be observed in the seminiferous tubules (Racey, 1974; Kurohmaru et al., 2002; Lee, 2003; Lee and Mori, 2004). Possibly in order to adapt to the hibernation period, many species have developed mechanisms such as prolongation of sperm storage in the cauda epididymis in males and in the uterine cornua in females; asynchrony between the spermatogenesis and the period of mating; delayed ovulation, fertilization and implantation in the female reproductive tract; and

exceptional ultrastructural morphology of the spermatozoa, as observed in *Noctilio leporinus* (Anand-Kumar, 1965; Racey, 1979; Rasweiler, 1993; Phillips et al., 1997; Crichton and Krutzsch, 2000; Encarnaç o et al., 2004; Sharifi et al., 2004).

Thus, this study aimed to characterize the process of bat spermatogenesis ultrastructurally in order to provide a basis for determining the stages of spermatogenesis and to facilitate comparisons of the process between species of bats and those of other vertebrates.

The species examined herein is *Platyrrhinus lineatus*, a relatively small phyllostomid bat (mean adult weight: 20 g) that is found from subtropical South America to southern Mexico, presents four broad white stripes on the head and possesses a distinct white stripe that extends along the dorsum from the occipital to the base of the interfemoral membrane. It is a frugivorous species that inhabits large forests and also small forest fragments (urban or rural) and forms small harems of 7–15 females per male (Willig and Hollander, 1987). According to Costa et al. (2007), it is a polyestric species that present a great breeding season (average of 10.6 months), with females showing a peak in pregnancies in August–October and another in January–February and absence of pregnancy only in April–July, by other side, scrotal males were observed throughout the year.

## 2. Materials and methods

### 2.1. Animals, tissue collection and processing

Five sexually mature specimens of *P. lineatus* (E. Geoffroy, 1810) were analyzed. The animals were collected in northwest S o Paulo State, Brazil (49W22'45" 20S49'11") between June 2008 and May 2009, and were deposited in the Chiroptera collection at the S o Paulo State University (UNESP-IBILCE).

The ethics committee at S o Paulo State University (UNESP) authorized all experimental procedures (Process: 013/09–CEEA) whereas the capture and captivity of bats were authorized by the Brazilian institution responsible for wild animal care (Instituto Brasileiro do Meio Ambiente, IBAMA–Process: 02027.001957/2006-02).

After the sacrifice of animals, the testes and epididymis were removed, perforated and fixed by immersion in a solution of 3% glutaraldehyde plus 0.25% tannic acid in Millonig buffer (pH 7.3) containing 0.54% glucose for 24 h (Cotta-Pereira et al., 1976). After washing with the same buffer, the samples were post-fixed with 1% osmium tetroxide for 2 h, dehydrated in graded series of acetone, and included in Araldite 502 Resin (Electron Microscopy Sciences, Hatfield, PA, USA). Ultrathin sections (50 nm) were made using diamond knives, stained with 2% uranyl acetate for 30 min (Watson, 1958), followed by 2% lead citrate in sodium hydroxide for 10 min (Venable and Coggeshall, 1965) and analyzed in a Leo-Zeiss 906 Transmission Electron Microscope (Cambridge, United Kingdom) at the “Prof. Dr. Celso Abbade Mour o” Center for Microscopy (IBILCE-UNESP).

## 3. Results

### 3.1. Spermatogonias

Based on ultrastructural features only three main types of spermatogonias could be accurately identified for the bat species *P. lineatus*: the dark type A – A<sub>d</sub>, the pale type A – A<sub>p</sub> and type B.

#### 3.1.1. Type A<sub>d</sub> spermatogonia

The type A<sub>d</sub> usually presents an elliptical shape, adheres firmly to the basal lamina, with which it forms projections and depres-

sions, and is surrounded by Sertoli cells in the basal compartment of the germinal epithelium (Fig. 1A). It has an oval nucleus containing a finely granular and highly electron-dense chromatin (with clusters of condensed chromatin); a single, large, granular and irregularly shaped nucleolus, usually centrally located. It presents a small cytoplasm, also intensely stained, with few organelles, where some mitochondria, few extensions of endoplasmic reticulum (smooth and rough) and fine cytoplasmic granulations (ribosomes and/or glycogen) can be observed.

#### 3.1.2. Type A<sub>p</sub> spermatogonia

The type A<sub>p</sub> presents a more elongated shape, its adhesion to the basal lamina is less pronounced, showing projections and depressions lower than type A<sub>d</sub>, and it is also surrounded by Sertoli cells in the basal compartment of the germinal epithelium (Fig. 1B). It has an oval nucleus, containing a finely granular homogeneous chromatin but this nucleus stains very lightly compared to A<sub>d</sub> ones; it has a large granular nucleolus that is most often singular and rarely double (Fig. 1C). This type has larger cytoplasm, also intensely stained, with mitochondria, a few extensions of endoplasmic reticulum (smooth and rough), Golgi complex, centrioles and fine cytoplasmic granulations (ribosomes and/or glycogen). It is interesting to observe the presence of large chromatoid body in this spermatogonia type (Fig. 1D).

#### 3.1.3. Type B spermatogonia

The adhesion of Type B cells to the basal lamina is the smallest among all spermatogonias, both in the contact area and the degree of adhesion, where their connection to it is almost flat, with small projections and depressions (Fig. 1E). It is laterally surrounded by Sertoli cells and in the top is in contact with cells of the adluminal compartment (spermatocytes). It has a round nucleus containing homogeneous chromatin but with clumps of condensed chromatin mainly associated with the nuclear envelope (Fig. 1F). It presents a single large granular nucleolus, more compact and centrally located and less frequently two nucleoli. The cytoplasmic organelles observed are similar to those of type A<sub>p</sub>. It was observed the presence of a chromatoid body also in this spermatogonia type (not documented).

### 3.2. Pre-leptotene spermatocytes

During this phase the cell begins to lose contact with the basal lamina because the cytoplasmic processes of Sertoli cells are interposed between the cell and the basal lamina (Fig. 1G). Thus, the cell starts its ascent toward the tubule lumen through the adluminal compartment. Many of them are completely detached from the basal lamina. The cell presents a circular shape, with a circular nucleus containing homogeneous chromatin but with discrete clumps of condensed chromatin mainly associated with the nuclear envelope. The cytoplasm is small, with few organelles.

### 3.3. Meiotic phases: the spermatocytes

With the progression of the cells to meiotic division, the most evident changes are chromatin condensation, the formation of synaptonemal complexes and the nucleolar disruption.

The process of chromatin condensation begins early in leptotene spermatocytes. In the transition from pre-leptotene to leptotene spermatocytes, the cells move away from the basal lamina to the adluminal compartment, the nucleus increases in size and the chromatin begins to condense, forming small clumps of condensed chromatin that associate on the periphery of a new nuclear component, the synaptonemal complex. Despite the beginning of the nuclear condensation, the nucleus of leptotene spermatocytes still presents an uncondensed appearance, and



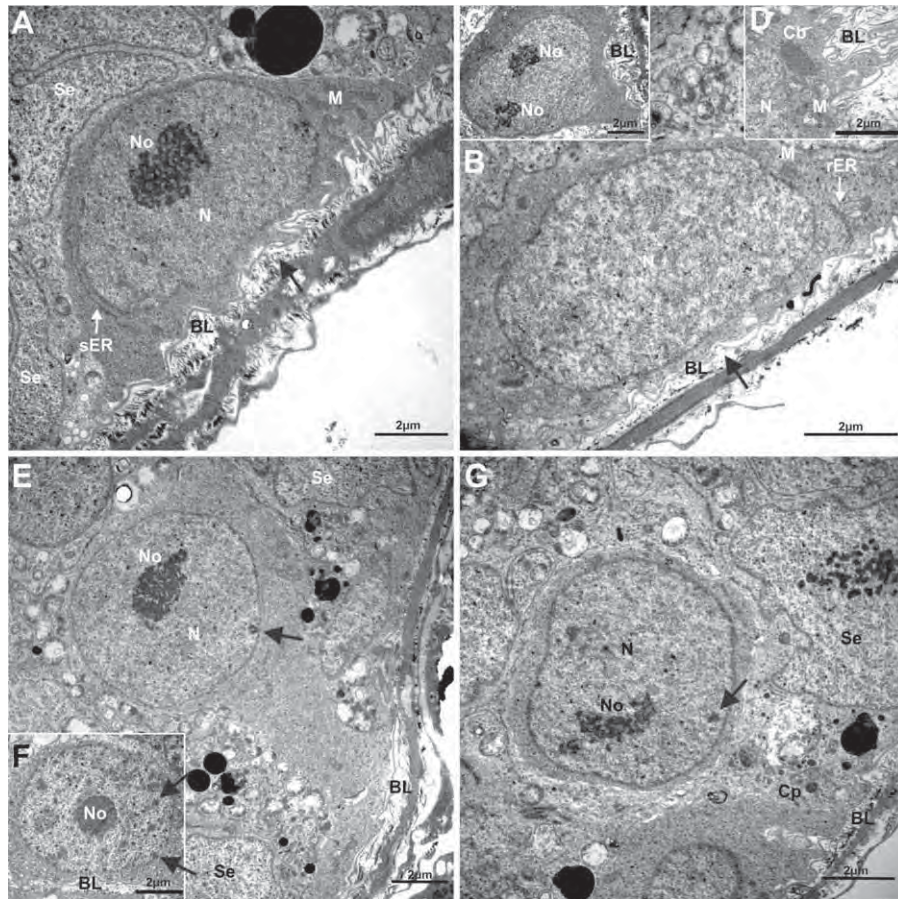


**Fig. 1.** Electron micrographs of the pre-meiotic cells of *Platyrhynchus lineatus*. (A) Type A<sub>4</sub> spermatogonia. Note the high degree of adhesion to the basal lamina (arrow). (B–D) Type A<sub>6</sub> spermatogonia. Note an intermediate degree of adhesion to the basal lamina (B, arrow), the presence, in rare cases, of two nucleoli (C) and the chromatoid body (D). (E and F) Type B spermatogonia. Note the smallest degree of adhesion to the basal lamina (E) and the presence of clusters of condensed chromatin in the nucleus (F, arrow). (G) Pre-leptotene spermatocytes. Note the loss of the contact with the basal lamina, the formation of points of condensed chromatin (arrow) in the nucleus and the cytoplasmic projections of Sertoli cells. (BL, basal lamina; Cb, chromatoid body; Cp, cytoplasmic projection of Sertoli cell; M, mitochondria; N, nucleus; No, nucleolus; rER, rough endoplasmic reticulum; Se, Sertoli cell; sER, smooth endoplasmic reticulum).

the cytoplasm shows few organelles (Fig. 2A). From zygotene to diakinesis spermatocytes the condensation of chromatin occurs gradually, mainly on the periphery of the synaptonemal complexes, forming distinctive blocks, the homologous chromosomes (Fig. 2B–F).

The structure of synaptonemal complexes resembles a ribbon that presents three laterally juxtaposed portions: two external portions of high electron density and a central thin line of intermediate electron density (Fig. 2D), while small oblique zipper-like filaments transverse this structure, both ends of which are attached to the nuclear envelope in single ends (Fig. 2A and B, arrow-heads). At these attachment sites the double membrane of the nucleus presents a high electron density (Fig. 2D, asterisk), while the intermediate part extends out in a loop to the central portions of the nucleus (Fig. 2C, arrow-head). They were first observed in leptotene spermatocytes and tended to disappear in final diplotene (Fig. 2B–E).

The nucleolus seems still to be morphologically organized in leptotene and early zygotene spermatocytes (Fig. 2A and B), presenting a compact electron-dense form, generally centrally located. These characteristics indicate that the morphological disorganization begins later. In late zygotene and/or early pachytene the nucleolus loses its morphology, beginning its disruption (Fig. 2C), and presents a fragmented shape, while small electron-dense fragments, possibly nucleolar fragments, can be seen near the nucleolus

(Fig. 2C, arrows). In diplotene the nucleolar fragments can be observed associated with certain chromosomal regions (Fig. 2E, arrow) and the nucleolar fragments are more conspicuous. In diakinesis the number of nucleolar fragments decreases greatly, but certain parts can still be observed to be associated with a single chromosomal region (Fig. 2F, arrow). In addition, during the diakinesis we observed a structural framework between the paired chromosomes (Fig. 2F).

In metaphase, the chromatin condensation peaks while the synaptonemal complexes are unobservable, the nuclear envelope is broken, the centrioles are already positioned on opposite poles and the microtubules are linked to chromosomes that align in the equatorial region of the cell (Fig. 2G).

After alignment, the spindle fibers are shortened during anaphase and the nuclear envelope is restored (telophase) giving rise to two secondary spermatocytes. These come in rapid cell division, producing four haploid spermatids, which will undergo cellular differentiation, transforming them into spermatozoa. The limited time in which these events occur hampers the observation of these phases by electron microscopy.

#### 3.4. Spermiogenesis

The differentiation of spermatids can be clearly divided into 12 steps according to the morphological changes that occur during the



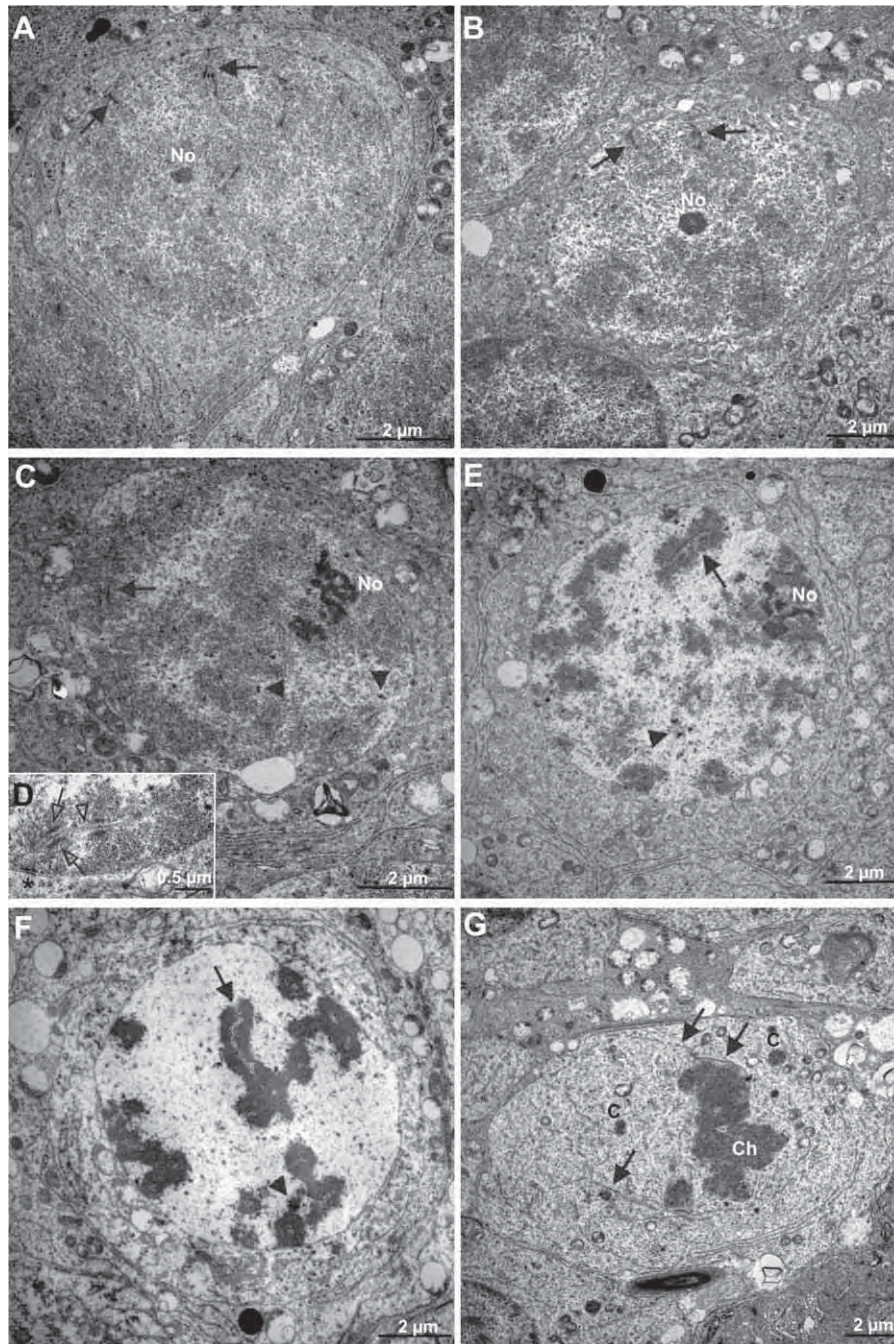


**Fig. 2.** Electron micrographs of the meiotic cells (meiosis I) of *Platyrhynchus lineatus*. (A) Leptotene, (B) Zygotene, (C and D) Pachytene, (E) Diplotene, (F) Diakinesis, and (G) Metaphases. Note the increase in the degree of chromatin condensation around the synaptonemal complexes (A–F, arrows); the structure of the synaptonemal complexes formed by three laterally juxtaposed portions: two highly electron-dense external portions (D, hollow arrows) and a central thin median electron-dense line (D, hollow arrow-head); the disorganization of the nucleolus (arrow-heads, nucleolar materials dispersed) from leptotene (A) to diplotene (E) with certain parts associated with a single chromosomal region in diakinesis (F, arrow); the structural framework in the middle of the chromosomes in diakinesis (F, arrow-head); the break of the nuclear envelope in the metaphases (G, arrows) and that the centrioles are already positioned on opposite poles of the cell (C, centrioles; Ch, chromosomes; No, nucleolus).

formation of the acrosome and the flagellum as well as the elongation and condensation of the nucleus. Steps 1–3 corresponded to the Golgi phase of spermatid development, steps 4–5 to the cap phase, steps 6–9 to the acrosomal phase and steps 10–12 to the maturation phase.

#### 3.4.1. Step 1 spermatids

The Step 1 spermatids correspond to the cells newly formed from the second meiotic division and present little differentiation (Fig. 3A). They are characterized by a spherical nucleus containing

condensed chromatin points and a concentrated mass of chromatin attached to the nuclear envelope, with a single large nucleolus (Fig. 3B). Rough endoplasmic reticulum and mitochondria can be found throughout the cytoplasm. Centrioles can be seen near the plasma membrane. The Golgi complex is poorly developed and is associated with small vesicles, which are the precursors of the proacrosomal vacuole, and is also often near or associated with the chromatoid body. It is interesting to note the intercellular bridges that connect adjacent spermatids, forming something that resembles a syncytium.



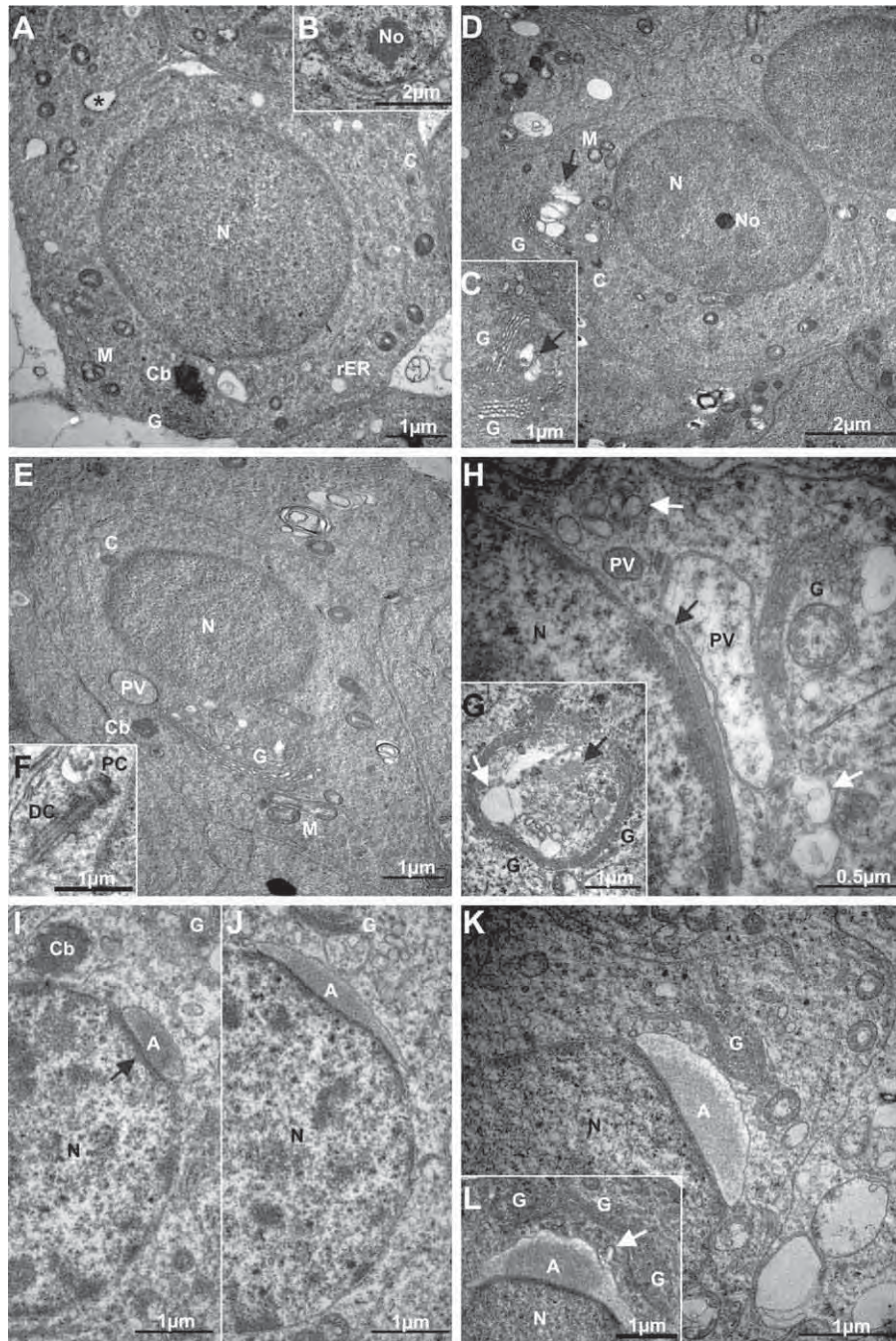


**Fig. 3.** Electron micrographs of the spermatids showing the spermiogenesis process in *Platyrhynchus lineatus*. (A and B) Step 1 spermatids. Note the little differentiation of this type of spermatid, the nuclei are spherical and present a single and large nucleolus (B). The chromatoid body and the Golgi complex are closely related. The centrioles are seen in the proximity of the plasma membrane and mitochondria are scattered throughout the cytoplasm. (C and D) Step 2 spermatids. Note the great development of the Golgi complex and the formation of proacrosomal vesicles (C, arrow), which tend to increase in number starting to fuse with each other to form large proacrosomal vacuoles (D, arrow). Clusters of mitochondria are associated with this complex. The dislocation of centrioles to the vicinity of the Golgi complex was also observed. (E and F) Step 3 spermatids. Note the fusion of the proacrosomal vesicles that forms a large proacrosomal vacuole (E). The Golgi complex, chromatoid body and clusters of mitochondria were intimately associated. The dislocation of centrioles to the pole opposite the acrosome formation is also observed and the distal centriole is starting its development to form the axoneme (F). (G–I) Step 4 spermatids. Note the formation of two types of proacrosomal vacuoles (G–H): the electron-dense type is less numerous, forms smaller proacrosomal vacuoles with round and compact shape, and was the first to join the nuclear envelope (black arrows); the electron-lucid type is produced in greater number and forms large and irregular proacrosomal vacuoles, which join latter to the nuclear envelope (white arrows). The proacrosomal vacuoles greatly increase during this step and attach to the nuclear envelope to form a concavity in the nucleus, with the contact of the both membranes presenting a more electron-dense appearance (I, arrow). Note the proximity of the chromatoid body to the region of the acrosome formation (I). (J–L) Step 5 spermatids. Note the intimately association of the acrosome with the nuclear envelope (J) and, inside it the presence of two types of components, a more electron-dense type, which occupies the central region in contact with the nuclear envelope and a translucent component that surrounds the electron-dense component and stays in contact with the outer membrane (K and L). The production and subsequent fusion of proacrosomal vesicles to the acrosome by the Golgi complex continues in this step (L, arrow) (A, acrosome; C, centrioles; Cb, chromatoid body; DC, distal centriole; G, Golgi complex; M, mitochondria; N, nucleus; No, nucleolus; PC, proximal centriole; PV, proacrosomal vacuole; rER, rough endoplasmic reticulum; \*, intercellular bridge).

#### 3.4.2. Step 2 spermatids

The nucleus remains spherical, with points of condensed chromatin and a concentrated mass of chromatin attached to nuclear envelope, with a single large nucleolus. In this step the Golgi complex presents a high level of development, greatly increasing in size and number of cisterns, whose vesicles start to fuse with each other to form large proacrosomal vesicles (Fig. 3C), which tend to increase in number (Fig. 3D). Chromatoid body and clusters of mitochondria are associated with this complex. The dislocation of centriole to the vicinity of the Golgi complex was also observed. Other cellular organelles are similar to those observed in Step 1 spermatids.

#### 3.4.3. Step 3 spermatids

The nuclear morphology is very similar to that observed in Step 2 spermatids, in which the numerous proacrosomal vesicles observed are now fused to form a large proacrosomal vacuole adjacent to the nucleus (Fig. 3E). The dislocation of centrioles to the pole opposite to the acrosome formation is also observed; these centrioles position themselves right next to the nucleus whose concavity accommodates the proximal centriole. Meanwhile, the distal centriole starts its development to form the axoneme (Fig. 3F), which had already reached the external side of the cell. The Golgi complex, chromatoid body and mitochondrial clusters were intimately associated. Other cellular organelles are similar to those observed in Step 2 spermatids.

#### 3.4.4. Step 4 spermatids

In this step we observed that the Golgi complexes in *P. lineatus* produce two types of proacrosomal vesicles: one electron-dense and the other electron-lucid (Fig. 3G). The electron-dense vesicles, produced in smaller numbers, form smaller proacrosomal vacuoles with a round compact shape, and were the first to adhere to the nuclear envelope (Fig. 3H, black arrow). The electron-lucid vacuoles are produced in greater number, and form large and irregular proacrosomal vacuoles, which adhere latter to the nuclear envelope (Fig. 3H, white arrow). The proacrosomal vacuoles greatly increase during this step and attach to the nuclear envelope to form a concavity in the nucleus (Fig. 3I). The membranes both of the proacrosomal vacuole and of the nucleus are thinner and their contact has a more electron-dense appearance (Fig. 3I, arrow).

The nuclear shape remains spherical, although inside the nucleus the chromatin condensation starts forming large blocks throughout the nucleus and increasing the amount of chromatin associated with the nuclear envelope. Other cellular organelles are similar to those observed in Step 3 spermatids. It is interesting to note the proximity of the chromatoid body to the region of the acrosome formation (Fig. 3I).

#### 3.4.5. Step 5 spermatids

During this step the acrosome associates more intimately with the nuclear envelope and begins to cover the nucleus (Fig. 3J), occupying nearly a quarter of its entire surface (Fig. 3K and L). Inside the acrosome two types of components were observed, a more electron-dense and fibrous component, which occupies the central region in contact with the nuclear envelope and an amorphous translucent component that surrounds the electron-dense component and stays in contact with the outer membrane of the acrosome (Fig. 3K and L). The production and subsequent fusion of proacrosomal vesicles to the acrosome by the Golgi complex continue in this step (Fig. 3L, arrow).

#### 3.4.6. Step 6 spermatids

During this phase the acrosome begins to condense, presenting a strong electron-dense granular matrix, it compacts and expands, forming a cap that covers a large surface of the nucleus (Fig. 4A). The Golgi complex, now poorly developed, begins to regress while

the axoneme extends greatly. Associated with the developing flagellum, connected to the annulus, was observed the presence of a granular electron-dense mass, probably the chromatoid body (Fig. 4B).

#### 3.4.7. Step 7 spermatids (Fig. 4C)

During this step the nucleus migrates toward the plasma membrane, the cytoplasm starts to migrate to the caudal region of the cell and the acrosomes cover a great portion of the nuclear surface. In the distal region of the acrosome occurs the development of an elevation associated with microtubules (arrow). It is interesting to note the beginning of the nucleolar disorganization.

#### 3.4.8. Step 8 spermatids

During this step, the cytoplasm dislocates to the posterior pole of the cell and the nucleus attaches to the plasma membrane (Fig. 4D). The acrosomes present a small compact format, which involves the entire anterior region of the nucleus. In this phase we observed the formation of the manchette, which attaches to the elevation of the acrosome, produced in the anterior step, and will subsequently assist in nuclear elongation (Fig. 4D, arrow). The large allocation of microtubules to form the manchette is easily observed (Fig. 4E).

#### 3.4.9. Step 9 spermatids

During this step the nuclear elongation evolves (Fig. 4F–I), where the longitudinal manchette, connected to the nuclear ring (Fig. 4H), has its fibers gradually shortened, pulling the acrosomes and making it cover the entire rostral end of the nucleus, which now assumes an arrow-shape (Fig. 4I). The major changes in the nucleolar fragmentation occur during this step (Fig. 4G), and at the end of this phase, the nucleolus could not be observed.

#### 3.4.10. Step 10 spermatids

At this step the nuclear ring completes its dislocation to the posterior region of the nucleus, the annulus starts its caudal migration and the organization of the midpiece begins, with the mitochondrial clusters associating with the axial filament (Fig. 5A). The formation of the perforatorium in the rostral region of the nucleus was also observed (Fig. 5B).

#### 3.4.11. Step 11 spermatids

The spermatid heads in Step 11 become long and compact and begin to present a prominent perforatorium (Fig. 5C–E). The tail presents large allocation and alignment of mitochondrial clusters to the midpiece (Fig. 5C).

#### 3.4.12. Step 12 spermatids

In this step the spermatids have achieved the basic format of the spermatozoon, with the mitochondrial sheath, from the midpiece, and the fibrous sheath, from the principal piece, already organized (Fig. 5F). The cytoplasm moved almost completely out of the spermatids. This is the last stage before the process of spermiation: released of the spermatozoa in the tubular lumen and formation of the residual bodies, which contains many organelles not included in the spermatozoa, as Golgi complex, mitochondria and chromatoid bodies (Fig. 5G).

### 3.5. Ultrastructure of the spermatozoon (Fig. 6)

#### 3.5.1. Spermatozoon head

The spermatozoon had a dorso-ventrally flattened, arrow-like head. Externally it is covered by a plasma membrane, which is free at the top of the nucleus, with a space separating it from the outer acrosomal membrane, and attached to its final portion, in the terminal region of the acrosome, the equatorial segment. Below it is the acrosome, which extends up to one third of its extension from



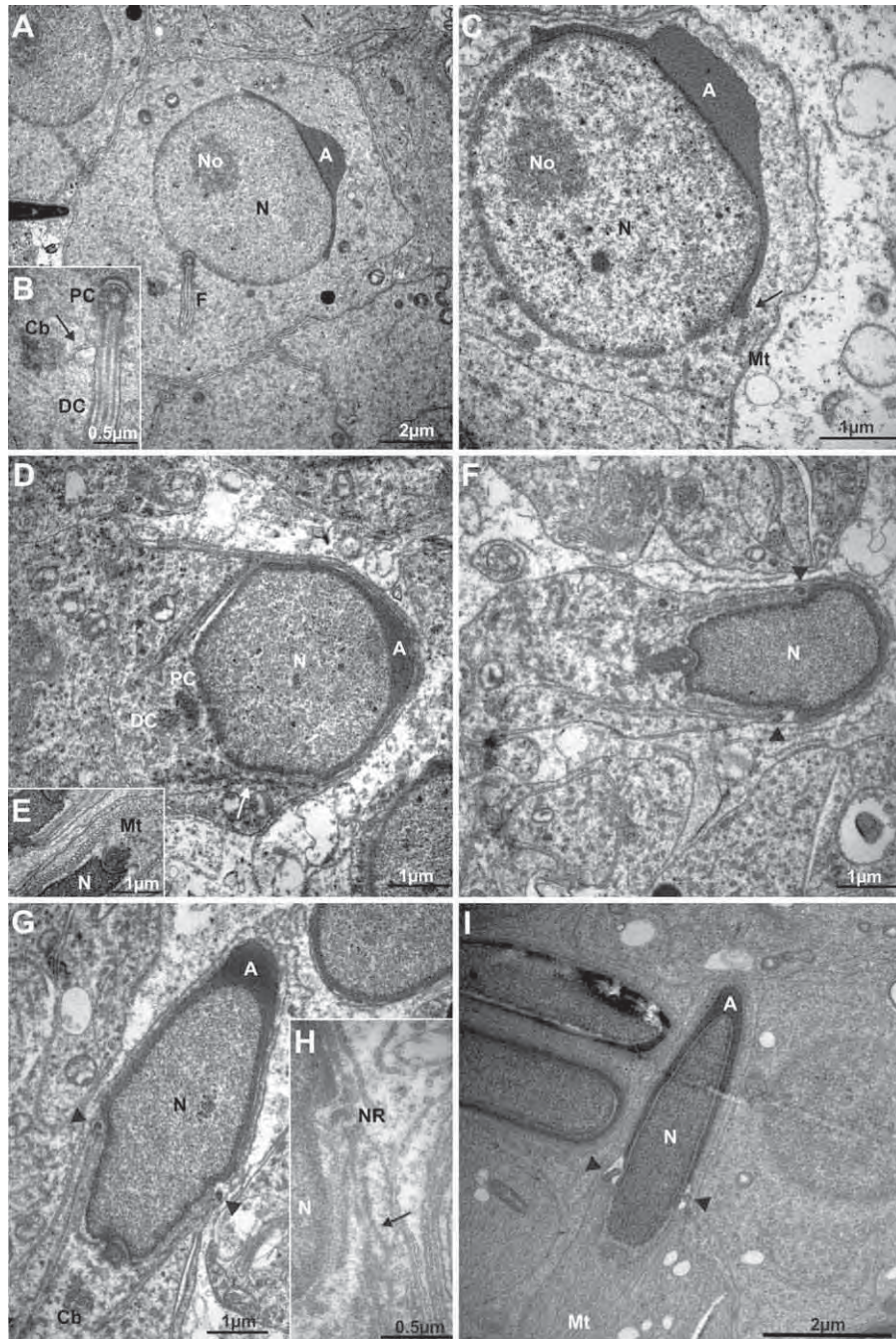


**Fig. 4.** Electron micrographs of the spermatids showing the spermiogenesis process in *Platyrrhinus lineatus*. (A and B) Step 6 spermatids. Note that the acrosome condenses, compacts and expands forming a cap of strong electron-dense granular matrix, that covers a large surface of the nucleus (A) and the association of the chromatoid body to the developing flagellum, connected to the annulus (arrow) (B). (C) Step 7 spermatid. Note the migration of the nucleus toward the plasma membrane; the beginning of the nucleolar disorganization; and the development of an elevation in the distal region of the acrosome that associates with microtubules. (D and E) Step 8 spermatids. Note the attachment of the nucleus to the plasma membrane and the formation of the microtubular manchette (E), which attaches to the elevation of the acrosome (D, arrow). (F–I) Early (F), middle (G and H) and late (I) Step 9 spermatids. Note that the nuclear elongation occurs in this step, when the longitudinal manchette (H, arrow), connected to the nuclear ring (arrow-heads) has its fibers gradually shortened, pulling the acrosomes and making it cover the entire rostral end of the nucleus, which now assumes an arrow-shape (I) (A, acrosome; Cb, chromatoid body; DC, distal centriole; F, flagellum; Mt, microtubules; N, nucleus; No, nucleolus; NR, nuclear ring; PC, proximal centriole).

the rostral region of the nucleus and covers approximately three fourths of its length; it is surrounded by the outer acrosomal membrane, which externally associates at some points with the plasma membrane, and internally by the inner acrosome membrane, which is in contact with a reduced subacrosomal space. Extending from the inner acrosomal membrane to the middle of the acrosome is the perforatorium, which has a spear-like or trident form. The acrosome has a granular matrix less electron-dense than the nucleus. Below it, between it and the nucleus, is a small pale space, the

subacrosomal space, which covers the rostral end of the nucleus, until the equatorial segment. The arrow-shaped nucleus contains homogenous, electron-dense chromatin.

### 3.5.2. Neck

The base of the nucleus has a concavity where the implantation fossa is formed. The basal plate attaches to the nucleus and fills the implantation fossa, but extends only to the vicinity of the redundant nuclear membrane. The proximal centriole is directly



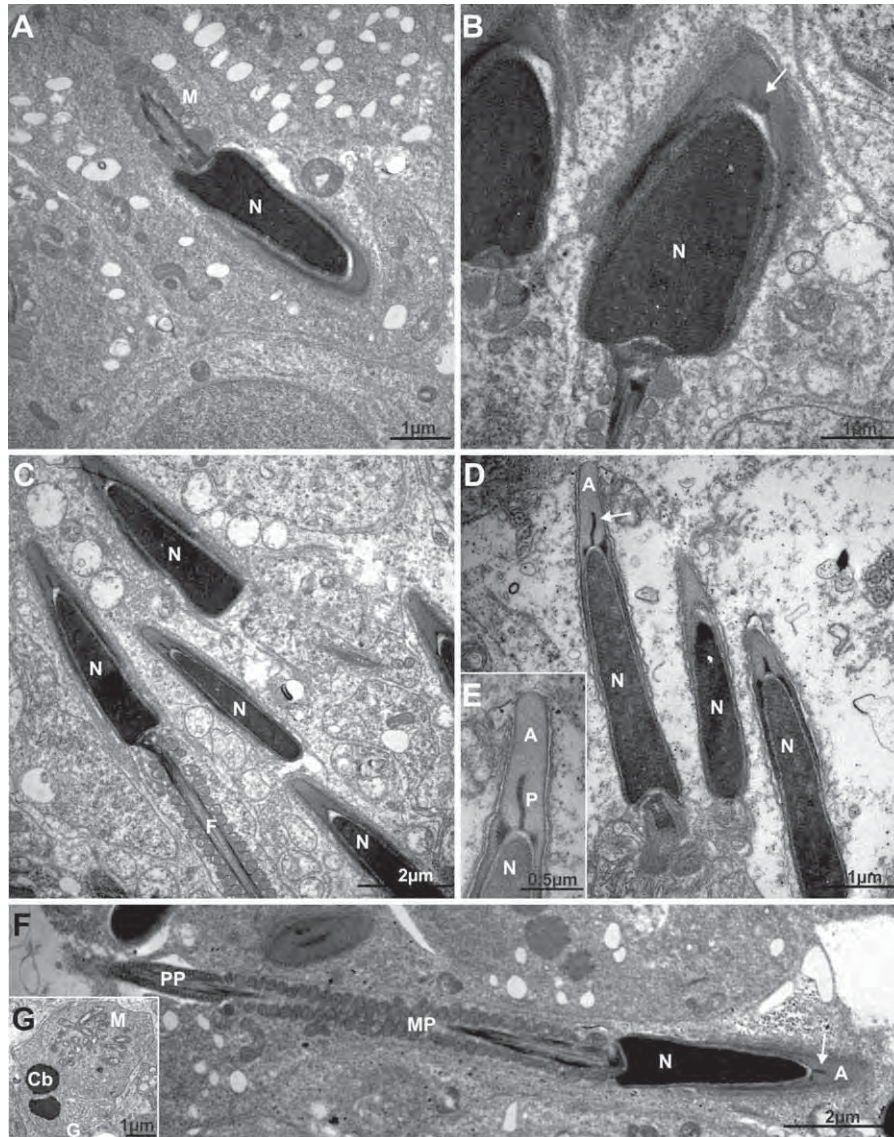


**Fig. 5.** Electron micrographs of the spermatids showing the spermiogenesis process in *Platyrrhinus lineatus*. (A and B) Step 10 spermatids. Note that at this step the nuclear ring completes its dislocation to the posterior region of the nucleus, the annulus commences its caudal migration and the organization of the midpiece begins, with the clusters of mitochondria associating with the axial filament (A), and the formation of the perforatorium in the rostral region of the nucleus (B, arrow). (C–E) Step 11 spermatids. Note that the head of the spermatids have become long, compact and possess a prominent perforatorium (C–E). In the tail a large allocation and alignment of mitochondrial clusters to the midpiece are observed (C). (F) Step 12 spermatid. Note that at this step the spermatids have achieved the basic format of the spermatozoon, with the mitochondrial sheath from the midpiece and the fibrous sheath from the principal piece already organized. (G) Residual bodies. Note that it contains many organelles not included in the spermatozoa, as Golgi complex, mitochondria and chromatoid bodies (A, acrosome; Arrows, perforatorium; Cb, chromatoid body; F, flagellum; G, Golgi complex; M, mitochondria; MP, midpiece; N, nucleus; P, perforatorium; PP, principal piece).

attached to the basal plate and the redundant nuclear membrane is extensive.

### 3.5.3. Midpiece

The midpieces are slightly shorter and contain approximately 30 mitochondrial gyres. The arrangement of the mitochondria is similar to those described in other mammalian spermatozoa, where one pair of mitochondria comprises a gyre.

In a cross-section of the midpiece, the outer dense fibers are arranged in a horseshoe fashion and show bilateral symmetry: Fiber 1 is the largest and presents a bilobular shape while fibers 3 and 8 remain aligned with the central fibrils of the axial filament complex, forming the dorsoventral axis (X–Y) that asymmetrically separates the complex, with a major compartment containing four dense fibers (4, 5, 6 and 7) and a minor compartment including three (1, 2 and 9); and the fibers 5 and 6 are larger than the others.

In the uppermost level of the midpiece lie satellite fibers in close proximity to all outer dense fibers, but in greater quantity in fibers 1, 5 and 6, while throughout most of the midpiece, they are found only in association with the inner aspect of fibers 5 and 6.

The position of the cytoplasmic droplet is variable, and it can be observed as high as the neck or as low as the midpiece terminus vicinity. Droplets always contain an abundance of membranes.

An annulus is found caudal to the last mitochondrial gyre. Immediately caudal to the annulus the tail diameter lessens abruptly and gives rise to the principal piece.

### 3.5.4. Principal piece

The principal piece is longer than the middle piece. In the upper region of the principal piece the outer dense fibers 3 and 8 terminate and projections from the fibrous sheath extend into the position those fibers had occupied. The remaining outer dense fibers tend

to diminish in diameter as they become more posterior and disappear in the end portion of the principal piece. In the same manner, the fibrous sheath projections tend to diminish throughout the principal piece.

### 3.5.5. End piece

The transition from principal piece to end piece was not easily observed, but cross-sections of end pieces were frequently noted. The uppermost level of the end piece presents only the axial filament enclosed by the plasma membrane, while throughout its length the organization of the axial filament is lost and in the terminus of the end piece only 11 microtubules, without a distinct form, were observed.

## 3.6. Auxiliary cells

### 3.6.1. Sertoli cell (Fig. 7A and B)

The parenchyma of the seminiferous tubules of the bat testis are mainly composed of cytoplasm of the Sertoli cells, which are associated with the basal lamina and exhibit extensive cytoplasmic processes that enveloped all the associated germ cells and proceed into the lumen.

The cell presents two different regions: basal and apical. In the basal region is localized the nucleus, which is large and irregularly shaped, displaying large infoldings. It presents a highly euchromatic and homogeneous nucleoplasm with a fine fibrillo-granular texture, scarce points of heterochromatin, and a prominent nucleolus. The nucleolus appears dispersed, occupying a great nuclear area. The perinuclear cytoplasm was occupied by many multivesicular bodies and a few electron-dense bodies. The rest of the basal cytoplasm exhibited a high concentration of subcellular structures including the endoplasmic reticulum, Golgi complex, mitochondria and ribosomes. The smooth endoplasmic reticulum predominates over rough endoplasmic reticulum. Some cytoplasmic regions present single but conspicuous *lamellae anellata* derived from the nuclear envelope.

Few lipid droplets were observed in the basal region whereas the apical region presented large compacted masses of smooth endoplasmic reticulum, and together with mitochondria, surrounded the differentiating spermatids (not documented).

### 3.6.2. Leydig cell (Fig. 7C–E)

The seminiferous tubules of the *P. lineatus* testis are surrounded by an interstitial tissue, composed of a great amount of extracellular matrix, nerve bundles, blood and lymphatic vessels, immune cells and Leydig interstitial cells.

The most typical Leydig cell morphology is irregular polygonal cells, found singly or in clusters within the interstitial tissue. These cells are separated from each other by thin extracellular spaces. The nuclei are generally large, undefined (circular to oval), and possess a greater portion of granular euchromatin and clusters of heterochromatin localized at some points throughout the nucleus, associated with the nuclear envelope and with a single large nucleolus. In favorable sections the peripheral nucleoli appear dark, with a lighter central amorphous component. This nucleolar configuration is considered indicative of a synthetically active cell.

The Leydig cell cytoplasm is vast and presents a highly secretory aspect, with a great portion of such cytoplasm occupied by the endoplasmic reticulum (Fig. 7D) and vesicles (Fig. 7E). The endoplasmic reticulum is found predominantly in the smooth form. This reticulum was organized as a compact network of anastomosing cisterns that surrounds the nucleus and other organelles. When the cisterns surround lipid droplets, they usually form concentric layers. Cisterns of rough endoplasmic reticulum are only occasionally seen near the plasma membrane and nucleus, and are continuous with the smooth. Three spherical bodies are observed:

the lipid droplets, the electron-dense bodies and the multivesicular bodies. The lipid droplets are relatively large with round vesicles that are distributed irregularly or in groups. They present a pale and homogeneous component and are not surrounded by membrane. The electron-dense bodies resemble endosomal-lysosomal bodies that are frequently seen near the cell surface and near the lipid droplets. The association of the electron-dense bodies with lipid droplets is frequently observed. The multivesicular bodies are irregular, membrane-bound vesicles, located in the Golgi region as well as more peripherally in the cytoplasm.

## 4. Discussion

Spermatogenesis is a complex, highly ordered process of cell division and differentiation by which spermatogonial stem cells give rise to mature spermatozoa. It is a process that may be divided into three functionally distinct phases: the proliferation phase, the meiotic phase and spermiogenesis (Clermont, 1972; Matsumoto, 1996).

The proliferation phase is related to the process of stem cell renewal, where some spermatogonia divide to replenish the stem cell pool and others undergo mitotic divisions, become committed to further differentiation, and produce spermatocytes (Russell et al., 1990). Spermatogonias are present in the basal compartment of the seminiferous tubule and are separated from other developing germ cells by Sertoli cell tight junctions.

The recognition and classification of spermatogonia were proposed by several authors. However, these classifications are based mainly on two groups of spermatogonial features: (1) the association between the cells and their topographical arrangement in relation to the basal lamina, in which the most complex classification recognizes a series of nine spermatogonia in rodent species –  $A_s$ ,  $A_{pr}$ ,  $A_{al}$ ,  $A_1$ ,  $A_2$ ,  $A_3$ ,  $A_4$ , In and B (de Rooij, 2001; Chiarini-Garcia and Russell, 2002); and (2) the nuclear morphology, chromatin condensation and position within the seminiferous epithelium, where the number of spermatogonia are variable, but three main types are observed in all studies –  $A_d$ ,  $A_p$  and B (Smithwick et al., 1996; Ehmcke et al., 2005; Bakst et al., 2007; Beguelini et al., 2009).

In the present study, only three spermatogonia types could be accurately identified and characterized ( $A_d$ ,  $A_p$  and B). These data corroborate the previous work of Beguelini et al. (2009), which employed several light microscopy stains, observing the same three types of spermatogonia in *P. lineatus* and five other bat species. However, the careful observation of the spermatogonial self-renewal and differentiation demonstrates that this is a continuous process, where the delimitation of a higher number of phases could render the classification arbitrary.

Based on this consideration, on different classifications adopted and in results obtained we propose that the spermatogonial differentiation process in bats begins with the true spermatogonial stem cell, denominated  $A_d$ . These cells are probably quiescent and under paracrine factors of Sertoli and/or Leydig cells (Tähhä, 1986; Petersen and Söder, 2006) can be stimulated to divide, thus replenishing the stem cell pool and forming cells committed to further differentiation. At the end of mitotic divisions is produced a different cell type, the type B spermatogonia which represent the cell destined to differentiate in spermatocytes and enter into meiotic division.

Among the scarce studies published on spermatogonial differentiation in bats, we found that in all cases the three main spermatogonia types are present (Singwi and Lall, 1983; McGuckin and Blackshaw, 1987; Saidapur and Patil, 1992; Lee, 2003; Beguelini et al., 2009), showing that this process may be similar in all these species, with only a few species-specific peculiarities. For example, the ultrastructure of the three spermatogonia types in *P. lineatus*



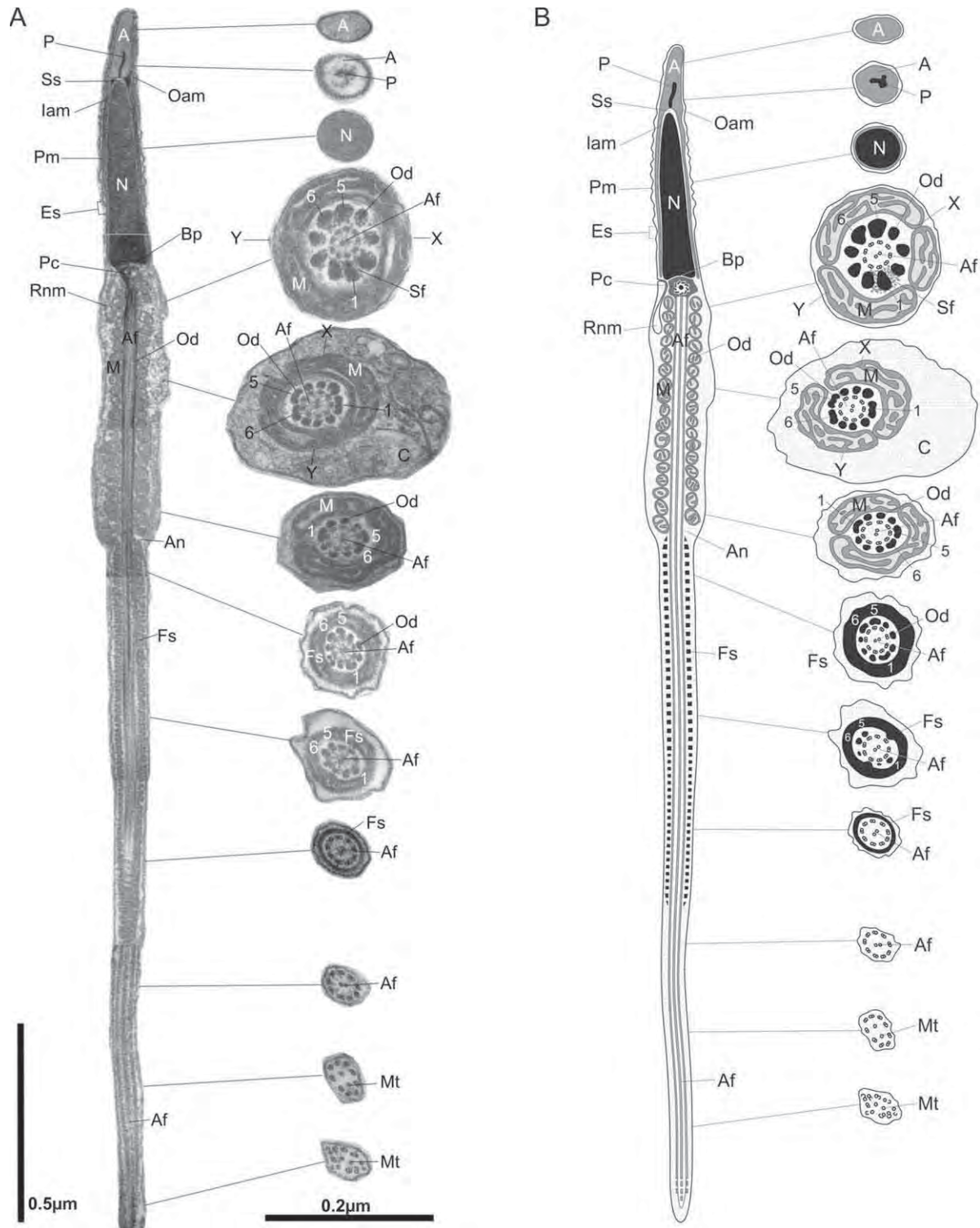


**Fig. 6.** Schematic figure of the ultrastructure of the spermatozoon of the *Platyrrhinus lineatus*. (A) Ultrastructure of the spermatozoon in longitudinal and corresponding transverse sections. Drawn from several TEM micrographs. (B) Correspondent diagram of spermatozoon of *Platyrrhinus lineatus* in longitudinal and corresponding transverse sections (A, acrosome; Af, axial filament; An, annulus; Bp, basal plate; C, cytoplasmic droplet; Es, equatorial segment; Fs, fibrous sheat; lam, inner acrosomal membrane; M, mitochondria; Mt, microtubules; N, nucleus; Oam, outer acrosomal membrane; Od, outer dense fibers; P, perforatorium; Pc, proximal centriole; Pm, plasma membrane; Rnm, redundant nuclear membrane; Sf, satellite fibers; Ss, subacrosomal space; X–Y, axis X–Y).

characterized herein were very similar to those observed by Lee (2003) in *Myotis macrodactylus*, despite the fact that the two species are geographically and phylogenetically distant (Wetterer et al., 2000; Teeling et al., 2005).

The next step of spermatogenesis corresponds to the meiotic phase, the process in which spermatocytes undergo meiotic divi-

sions that give rise to haploid spermatids (Russell et al., 1990). The meiotic process begins with a single round of DNA replication (Lodish et al., 2005) in pre-leptotene spermatocytes, which increases their nuclear size, transforming them into leptotene spermatocytes and beginning the cycle of cell division. Leptotene spermatocytes present the commencement of the formation of

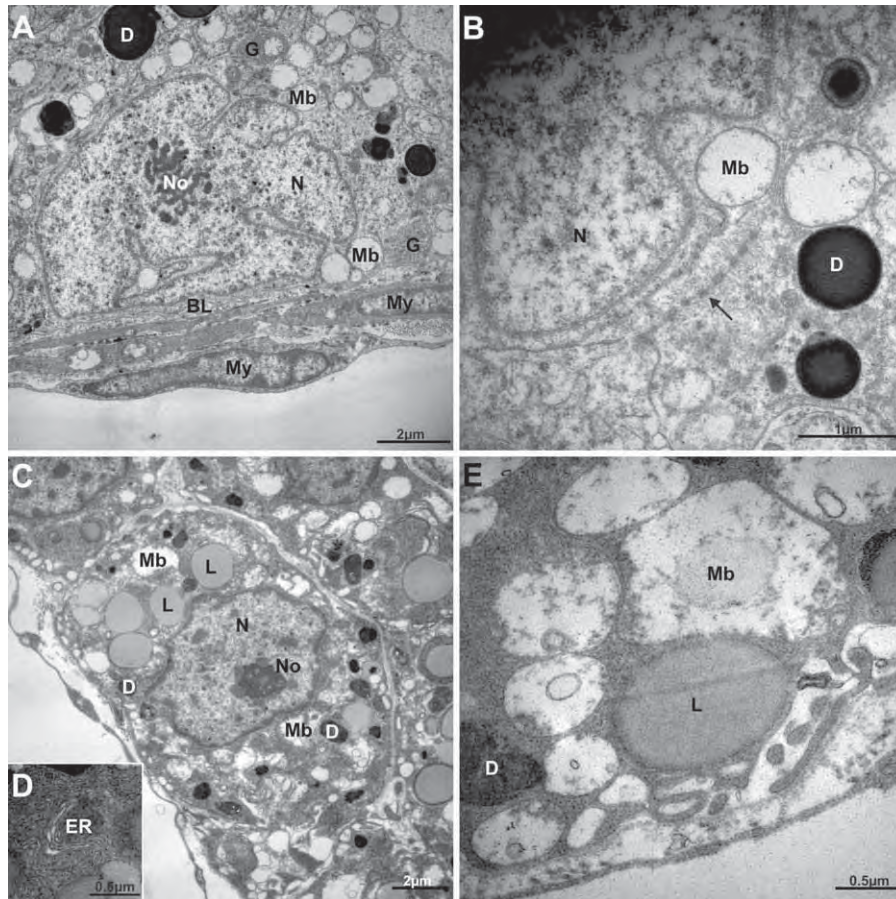


**Fig. 7.** Electron micrographs of the auxiliary cells of the bat *Platyrrhinus lineatus*. (A) The basal region of a Sertoli cell. Note the large and irregularly shaped nucleus presenting great infoldings and a dispersed nucleolus. The perinuclear cytoplasm was occupied by many multivesicular bodies and a few electron-dense bodies. Observe the presence of myoid cells below the basal lamina. (B) Cytoplasmic region presenting single but conspicuous *lamellae anellata* derived from the nuclear envelope (arrow). (C–E) Leydig cells. Note the large and undefined nucleus with a single and large nucleolus and the vast and highly secretory cytoplasm with great portion of them occupied by the endoplasmic reticulum (D) and vesicles (E) (BL, basal lamina; D, electron-dense bodies; ER, endoplasmic reticulum; G, Golgi complex; L, lipid droplets; Mb, multivesicular bodies; My, Myoid cell; N, nucleus; No, nucleolus).

synaptonemal complexes and, consequently, the beginning of the nuclear condensation.

We observed that the synaptonemal complex is composed of two longitudinal lateral elements (LE) and an enclosed central region, the latter of which contains a longitudinal central element (CE) that is joined to the LEs by thin protein transverse filaments. Its structure is very similar to observe in many other species (Schleirmacher and Schmidt, 1973; Solari and Moses, 1973; Gillies, 1975; Zickler and Kleckner, 1999; Hunter, 2003; Page and Hawley, 2004) showing that it is a prominent and evolutionarily well-conserved structure. Its initial formation in leptotene spermatocytes and the disappearance in diplotene were also observed by other researchers (Schleirmacher and Schmidt, 1973; Page and Hawley, 2004), however, the observation of vestiges of the synaptonemal complexes during diakinesis, in our study, indicates the possibility that the CE protein elements are maintained between the homologues chromosomes.

Another interesting process that occurs during meiosis and has already been studied in many species is the nucleolar cycle. It is reported that during the cell divisions the nucleolus disrupts and the behavior of its subcomponents can vary interspecifically (Dundr et al., 1997; Leung et al., 2004; Chen et al., 2005; Hernandez-Verdun, 2006). The most common type of behavior is that in which the nucleolus is disrupted during prophase and reappears during telophase; however, other patterns have been observed, as the nucleolar semi-persistence and persistence

already observed in different families of bugs (Garcia-Tavares and Vilela de Azeredo-Oliveira, 1997; Cattani and Papeschi, 2004), plants (Frew and Bowen, 1929; Ramanujam, 1938; Gori, 1956) and mammals (Heneen and Nichols, 1966).

The present study corroborates the previous work of Beguelini et al. (in press) which analyzes the nucleolar behavior in five species of Brazilian bats, including *P. lineatus*, using different cytogenetic approaches (Ag-NOR, acridine orange and fluorescent *in situ* hybridization). It is observed that the morphological nucleolar disruption begins in zygotene whereas with the progression of chromatin condensation the nucleolus disrupts and its components can be viewed as irregular markings on nucleoplasm, points associated with perichromosomal regions or great portions associated with a single chromosomal portion, the nucleolus organizer region (NOR).

The last and longest phase of spermatogenesis corresponds to spermiogenesis, the process in which a round spermatid differentiates into a mature spermatozoon that is capable of motility and fertilization (Clermont, 1972). The number of steps in the differentiation of spermatids into spermatozoa varies in different species and several studies have described between 6 and 16 steps (Gunawardana, 1977; Singwi and Lall, 1983; Lin and Jones, 1993; Góes and Dolder, 2002; Segatelli et al., 2002; Nakai et al., 2004). This accentuated difference in the number of steps is mainly linked to two particularities: the final morphology of the spermatozoon head (the more elaborate the structure, the greater the number



of steps) and the methods used by each author to analyze the process.

In the present study the spermiogenesis of *P. lineatus* was subdivided into 12 steps, a greater number relative to the seven steps observed by Beguelini et al. (2009) in the same species. This difference is related to the methods used in each study, where the ultrastructural analysis is more distinctive than the light microscopy staining. This number is also greater than that observed by Lee (2003) in *Myotis macrodactylus*, despite the fact that both studies used ultrastructural analysis. Nevertheless, this number was not higher than observed by Morigaki et al. (2001) in *Pteropus vampyrus* and *Rhinolophus cornutus*, by Saidapur and Patil (1992) in *Rousettus leschenaulti* and by Singwi and Lall (1983) in *Rhinopoma kinneari*, which on the basis of acrosome formation system, identified 13, 14 and 16 steps, respectively.

During spermiogenesis some unique events occur including the condensation of the nuclear chromatin, formation of the acrosome, elimination of the residual cytoplasm, and development of the flagellum (Suphamungmee et al., 2008). Although this process is similar in the majority of animals (Gunawardana and Scott, 1977; Lalli and Clermont, 1981; Chatchavalvanich et al., 2005; Zhang et al., 2007; Suphamungmee et al., 2008) some species-specific variations have been observed.

In the majority of mammals an electron-dense acrosomal granule is found inside the acrosome during its formation (Kurohmaru et al., 1994; Segatelli et al., 2000; Suphamungmee et al., 2008). In the present study, we also observed an electron-dense material inside the acrosome of *P. lineatus*; however, differently from the above mentioned authors, it is not the granular form but rather a fibrous mass that is associated with the nuclear envelope. Segatelli et al. (2000) and Suphamungmee et al. (2008) observed that the acrosome of the Mongolian gerbil (*Meriones unguiculatus*) and *Tupaia glis*, respectively, was formed by small vesicles that already contain these granules inside them, whereas in *P. lineatus*, we observed that their Golgi complexes produce two different types of proacrosomal vesicles, one electron-dense, that attaches first to the nucleus, and other electron-lucid that attaches later, a pattern not observed in other species.

The chromatoid body that was first described by Benda (1891) in spermatocytes of the rat, mouse, guinea pig and several other mammals, was rarely observed in the spermatocytes of *P. lineatus*. Moreover, it was present in types A<sub>p</sub> and B spermatogonia and in spermatids, indicating that this organelle is not unique to spermatocytes, and is indeed present in most spermatogenic cells, as proposed by Peruquetti et al. (2008).

The origin of this structure remains unclear and its real function is widely discussed (Fawcett et al., 1970; Söderström and Parvinen, 1976; Peruquetti et al., 2008). Despite not knowing the origin of this structure, our observations indicate that the chromatoid body is formed at the beginning of spermatid differentiation; plays an important role in the acrosome formation, during the first steps; assists in the tail formation; and is eliminated at the end of the process within the residual bodies; as observed by other researchers (Fawcett et al., 1970; Söderström and Parvinen, 1976; Tang et al., 1982; Soley, 1994; Peruquetti et al., 2008).

As a highly specialized cell, it is expected that the morphology of the spermatozoon is specific to each species, or at least is similar between closely related species, so that structural differences may possibly indicate taxonomic differences. Thus, currently the observation and analysis of the ultrastructure of the spermatozoon have been used as an important tool in the identification and classification of taxa of several groups of organisms, ranging from amphibians (Garda et al., 2002, 2004; Costa et al., 2004) and reptiles (Teixeira et al., 1999a,b,c, 2002; Giugliano et al., 2002; Vieira et al., 2005) to some groups of mammals (Mori, 1994; Soon-Jeong et al., 2006).

Within the Chiroptera order, the studies related to the spermatozoon ultrastructure are still scarce, with only some studies related to megachiropteran species (Rouse and Robson, 1986) and another showing the unconventional morphology of the greater bulldog bat, *Noctilio leporinus* (Phillips et al., 1997).

The ultrastructure of the spermatozoon of the small Neotropical phyllostomid bat, *P. lineatus*, shows that it presents a small compact arrow-like head, very similar to that observed in the Korean vespertilionid bat, *M. macrodactylus* (Lee, 2003). However, it is endowed with a perforatorium, which has a spear-like or trident form, not observed in *M. macrodactylus*.

If the typical mammalian sperm model usually consists of a dorsoventrally flattened, ovate, ensiform or falciform head (Fawcett, 1970), the spermatozoon of the *P. lineatus* deviates widely from this pattern. However, its morphology differs from other mammals such as marsupials (Lin et al., 1997; Lin and Rodger, 1999; Lin and Jones, 2000; Johnston et al., 2004; Lloyd et al., 2008), the chinchilla, ground squirrel, Guinea pig, Mongolian gerbil, mouse and Russian hamster (Fawcett, 1970; Tanii et al., 1999; Segatelli et al., 2000) on account of a simpler spermatozoon head morphology. Similarly, several rodents show a relatively enlarged acrosome (Fawcett and Phillips, 1970) not observed in the bats analyzed.

Thus, our data demonstrate that the spermatogenic process of *P. lineatus* follows the pattern of mammals with some specificity, as the process of formation of the acrosome and the presence of the perforatorium. By other side, the simpler ultrastructure of its spermatozoon shows a pattern more closely related to the sperm cells of humans and other primates (Fawcett, 1970; Hoffer et al., 1981; Holt and Moore, 1984).

## Acknowledgements

Technical help from Luiz Roberto Falleiros Junior and Rosana Silistino de Souza Santos is highly appreciated. The authors acknowledge for Raduan Alexandre Soleman by the design of the spermatozoa diagram. The scholarship awarded to Mateus Rodrigues Beguelini by the Brazilian Research Foundation (CAPES) is also gratefully acknowledged. Financial support from the São Paulo State Research Foundation (FAPESP) and the Brazilian Research Foundation (CAPES) is gratefully acknowledged.

## References

- Anand-Kumar, T.C., 1965. Reproduction in the rat-tailed bat *Rhinopoma kinneari*. *J. Zool.* 147, 147–155.
- Bakst, M.R., Akuffo, V., Trefil, P., Brillard, J.P., 2007. Morphological and histochemical characterization of the seminiferous epithelial and Leydig cells of the turkey. *Anim. Reprod. Sci.* 97, 303–313.
- Beguelini, M.R., Moreira, P.R.L., Faria, K.C., Marchesin, S.R.C., Morielle-Versute, E., 2009. Morphological characterization of the testicular cells and seminiferous epithelium cycle in six species of Neotropical bats. *J. Morphol.* 270, 943–953.
- Beguelini, M.R., Marchesin, S.R.C., Azeredo-Oliveira, M.T.V., Morielle-Versute, E. Nucleolar behavior during meiosis in males of phyllostomid bats (Chiroptera, Mammalia). *Genet. Mol. Res.*, in press.
- Benda, C., 1891. Neue Mitteilungen über die Entwicklung der Genitaldrüsen und die Metamorphose der Samenzellen (Histogenese der Spermatozoen). *Verhandlungen der Berliner Physiologischen Gesellschaft. Arch. Anat. Physiol.* 1891, 549–552.
- Cattani, M.V., Papeschi, A.G., 2004. Nucleolus organizing regions and semi-persistent nucleolus during meiosis in *Spartocera fusca* (Thunberg) (Coreidae, Heteroptera). *Hereditas* 140, 105–111.
- Chatchavalvanich, K., Thongpan, A., Nakai, M., 2005. Ultrastructure of spermiogenesis in a freshwater stingray, *Himantura signifier*. *Ichthyol. Res.* 52, 379–385.
- Chen, D., Dunder, M., Wang, C., Leung, A., Lamond, A., Misteli, T., Huang, S., 2005. Condensed mitotic chromatin is accessible to transcription factors and chromatin structural proteins. *J. Cell. Biol.* 168, 41–54.
- Chiarini-Garcia, H., Russell, L.D., 2002. Characterization of mouse spermatogonia by transmission electron microscopy. *Reproduction* 123, 567–577.
- Clermont, Y., 1972. Kinetics of spermatogenesis in Mammals: seminiferous epithelium cycle and spermatogonial renewal. *Physiol. Rev.* 52, 198–236.
- Costa, G.C., Vieira, G.H.C., Teixeira, R.D., Garda, A.A., Colli, G.R., Bão, S.N., 2004. An ultrastructural comparative study of the sperm of *Hyla pseudopseudis*, *Scinax*



- rostratus, and *S. squalirostris* (Amphibia: Anura: Hylidae). *Zoomorphology* 123, 191–197.
- Costa, L.M., Almeida, J.C., Esbérard, C.E.L., 2007. Dados de reprodução de *Platyrrhinus lineatus* em estudo de longo prazo no Estado do Rio de Janeiro (Mammalia, Chiroptera, Phyllostomidae). *Iheringia Série Zoológica, Porto Alegre* 97 (2), 152–156.
- Cotta-Pereira, G., Rodrigo, F.G., David-Ferreira, J.F., 1976. The use of tannic acid–glutaraldehyde in the study of elastic related fibers. *Stain Technol.* 51, 7–11.
- Crichton, E.G., Krutzsch, P.H., 2000. *Reproductive Biology of Bats*. Academic Press, London, UK, p. 528.
- de Rooij, D.G., 2001. Proliferation and differentiation of spermatogonial stem cells. *Reproduction* 121, 347–354.
- Dundr, M., Meier, U.T., Lewis, N., Rekosh, D., Hammarskjöld, M.-L., Olson, M.O.J., 1997. A class of nonribosomal nucleolar components is located in chromosome periphery and in nucleolus-derived foci during anaphase and telophase. *Chromosoma* 105, 407–417.
- Ehmcke, J., Luetjens, C.M., Schlatt, S., 2005. Clonal organization of proliferating spermatogonial stem cells in adult males of two species of non-human Primates, *Macaca mulatta* and *Callithrix jacchus*. *Biol. Reprod.* 72, 293–300.
- Encarnação, J.A., Dietz, M., Kierdorf, U., 2004. Reproductive condition and activity pattern of male Daubenton's bats (*Myotis daubentonii*) in the summer habitat. *Mamm. Biol.* 69, 163–172.
- Fawcett, D.W., 1970. A comparative view of sperm ultrastructure. *Biol. Reprod. Suppl.* 2, 90–127.
- Fawcett, D.W., Phillips, D.M., 1970. Recent observations on the ultrastructure and development of the mammalian spermatozoon. In: *Comparative Spermatology*, Publication of Accademia de Lincei, Rome Italy. Academic Press, New York.
- Fawcett, D.W., Eddy, E.M., Phillips, D.M., 1970. Observations on the fine structure and relationships of the chromatoid body in Mammalian spermatogenesis. *Biol. Reprod.* 2, 129–153.
- Fernandes, A.P., Curi, G., França, F.G.R., Bão, S.N., 2001. Nuclear changes and acrosome formation during spermiogenesis in *Euchistus heros* (Hemiptera: Pentatomidae). *Tissue Cell* 33 (3), 286–293.
- Frew, P.E., Bowen, R.H., 1929. Nucleolar behaviour in the mitosis of plant cells. *Quart. J. Microsc. Sci.* 2 (73), 197–212.
- Garcia-Tavares, M., Vilela de Azeredo-Oliveira, M.T., 1997. Pattern of nucleolar activity during spermiogenesis in triatomines (Heteroptera Reduviidae) as analysed by silver staining. *Cytobios* 89, 93–103.
- Garda, A.A., Colli, G.R., Aguiar-Júnior, O., Recco-Pimentel, S.M., Bão, S.N., 2002. The ultrastructure of the spermatozoa of *Epipedobates flavopictus* (Amphibia, Anura Dendrobatidae), with comments on its evolutionary significance. *Tissue Cell* 34 (5), 356–364.
- Garda, A.A., Costa, G.C., Colli, G.R., Bão, S.N., 2004. Spermatozoa of Pseudinae (Amphibia, Anura Hylidae), with a test of the hypothesis that sperm ultrastructure correlates with reproductive modes in Anurans. *J. Morph.* 261, 196–205.
- Gillies, C.B., 1975. Synaptonemal complex and chromosome structure. *Annu. Rev. Genet.* 9, 91–109.
- Giugliano, L.G., Teixeira, R.D., Colli, G.R., Bão, S.N., 2002. Ultrastructure of spermatozoa of the lizard *Ameiva ameiva*, with considerations on polymorphism within the family Teiidae (Squamata). *J. Morph.* 253, 264–271.
- Góes, R.M., Dolder, H., 2002. Cytological steps during spermiogenesis in the house sparrow (*Passer domesticus* Linnaeus). *Tissue Cell* 34, 273–282.
- Gori, C., 1956. Persistenza nucleolare durante la mitosi nel genere *Reseda*. *Caryologia* 9, 45–55.
- Gunawardana, V.K., 1977. Stages of spermatids in the domestic fowl: a light microscope study using Araldite sections. *J. Anat.* 123, 351–360.
- Gunawardana, V.K., Scott, M.G.A.D., 1977. Ultrastructural studies on the differentiation of spermatids in the domestic fowl. *J. Anat.* 124 (3), 741–755.
- Gwo, J.C., Yang, W.T., Kuo, M.C., Takemura, A., Cheng, H.Y., 2004. Spermatozoal ultrastructures of two marine perciform teleost fishes, the *Paraupeneus spilurus* (Mullidae) and the rabbitfish, *Siganus fuscus* (Siganidae) from Taiwan. *Tissue Cell* 36, 63–69.
- Heneen, W.K., Nichols, W.W., 1966. Persistence of nucleoli in short term and long term cell cultures and in direct bone marrow preparations in mammalian materials. *J. Cell Biol.* 31, 543–561.
- Hernandez-Verdun, D., 2006. Nucleolus: from structure to dynamics. *Histochem. Cell Biol.* 123, 127–137.
- Hoffer, A.P., Shalev, M., Frisch, D.H., 1981. Ultrastructure and maturational changes in spermatozoa in the epididymis of the pigtailed monkey, *Macaca nemestrina*. *J. Androl.* 3, 140–146.
- Holt, W.V., Moore, H.D.M., 1984. Ultrastructural aspects of spermatogenesis in the common marmoset (*Callithrix jacchus*). *J. Anat.* 138, 175–188.
- Hunter, N., 2003. Synaptonemal complexities and commonalities. *Mol. Cell.* 12, 533–535.
- Jamieson, B.G.M., 1987. *The Ultrastructure and Phylogeny of Insect Spermatozoa*. Cambridge University Press, Cambridge, pp. 1–309.
- Jamieson, B.G.M., 1995. Evolution of tetrapod spermatozoa with particular reference to amniotes. In: Jamieson, B.G.M., Ausio, J., Justine, J.L. (Eds.), *Advances in Spermatozoal Phylogeny and Taxonomy*, 166. *Mém Mus Nat d'Hist Nat, Paris*, pp. 343–358.
- Jamieson, B.G.M., Lee, M.S.Y., Long, K., 1993. Ultrastructure of the spermatozoon of the internally fertilizing frog *Ascaphus truei* (Ascaphidae: Anura: Amphibia) with phylogenetic considerations. *Herpetologica* 49, 52–65.
- Johnston, S.D., Daddow, L., Carrick, F.N., Jamieson, B., 2004. Observations of spermiogenesis and epididymal sperm maturation in the rufous hare wallaby, *Lagorchestes hirsutus* (Metatheria, Mammalia). *Acta Zool. (Stockholm)* 85, 53–58.
- Korn, N., Thurston, R.J., Pooser, B.P., Scott, T.R., 2000. Ultrastructure of spermatozoa from Japanese quail. *Poultry Sci.* 79, 407–414.
- Kurohmaru, M., Kobayashi, H., Hattori, S., Nishida, T., Hayashi, Y., 1994. Spermatogenesis and ultrastructure of a peculiar acrosomal formation in the musk shrew, *Suncus murinus*. *J. Anat.* 185, 503–509.
- Kurohmaru, M., Saruwatari, T., Kimura, J., Mukohyama, M., Watanabe, G., Taya, K., Hayashi, Y., 2002. Seasonal changes in spermatogenesis of Japanese Lesser Horseshoe bat, *Rhinolophus cornutus* from a morphological viewpoint. *Okajimas Folia Anat. Jpn.* 79 (4), 93–100.
- Lalli, M., Clermont, Y., 1981. Structural changes of the head components on the rat spermatid during late spermiogenesis. *Am. J. Anat.* 160, 419–434.
- Lee, J.H., 2003. Cell differentiation and ultrastructure of the seminiferous epithelium in *Myotis macrodactylus*. *Korean J. Electron Microsc.* 33 (1), 25–39.
- Lee, J.H., Mori, T., 2004. Annual cycle of the seminiferous epithelium of *Myotis macrodactylus*. *J. Fac. Agric. Kyushu Univ.* 49 (2), 355–365.
- Leung, A.K.L., Gerlich, D., Miller, G., Lyon, C., Lam, Y.W., Lleres, D., Daigle, N., Zomerdijs, J., Ellenberg, J., Lamond, A.L., 2004. Quantitative kinetic analysis of nucleolar breakdown and reassembly during mitosis in live human cells. *J. Cell Biol.* 166, 787–800.
- Lin, M., Jones, R.C., 1993. Spermiogenesis and spermiation in the Japanese quail (*Coturnix coturnix japonica*). *J. Anat.* 183, 525–535.
- Lin, M., Jones, R.C., 2000. Spermiogenesis and spermiation in a monotreme mammal, the platypus, *Ornithorhynchus anatinus*. *J. Anat.* 196, 217–232.
- Lin, M., Rodger, J.C., 1999. Acrosome formation during sperm transit through the epididymis in two marsupials, the tammar wallaby (*Macropus eugenii*) and the brushtail possum (*Trichosurus vulpecula*). *J. Anat.* 194, 223–232.
- Lin, M., Harman, A., Rodger, J.C., 1997. Spermiogenesis and spermiation in a marsupial, the tammar wallaby (*Macropus eugenii*). *J. Anat.* 190, 377–395.
- Lloyd, S., Carrick, F., Hall, L., 2008. Unique features of spermiogenesis in the Musky Rat-kangaroo: reflection of a basal lineage or a distinct fertilization process? *J. Anat.* 212, 257–274.
- Lodish, H., Berk, A., Matsudaira, P., et al., 2005. *Molecular Cell Biology*, 5th ed. WH Freeman & Co, Nova Iorque.
- Matsumoto, A.M., 1996. Spermatogenesis. In: Adashi, E.Y., Rock, J.A., Rosenwaks, Z. (Eds.), *Reproductive Endocrinology, Surgery and Technology*. Lippincott-Raven Publishers, Philadelphia, pp. 360–384.
- McGuckin, M.A., Blackshaw, A.W., 1987. Cycle of the seminiferous epithelium in the grey-headed fruit bat, *Pteropus poliocephalus*. *Aust. J. Biol. Sci.* 40, 203–210.
- Mori, T., 1994. Phylogenetic implications of sperm ultrastructure in Japanese Insectivores. *Sci. Mamm. Jpn.* 34, 51–57.
- Morigaki, T., Kurohmaru, M., Kanai, Y., Mukohyama, M., Hondo, E., Yamada, J., Agung-priyono, S., Hayashi, Y., 2001. Cycle of the seminiferous epithelium in the Java fruit bat (*Pteropus vampyrus*) and the Japanese Lesser Horseshoe bat (*Rhinolophus cornutus*). *J. Vet. Med. Sci.* 63, 773–779.
- Nakai, M., Van Cleeff, J.K., Bahr, J.M., 2004. Stages and duration of spermatogenesis in the domestic ferret (*Mustela putorius furo*). *Tissue Cell* 36, 439–446.
- Page, S.L., Hawley, R.S., 2004. The genetics and molecular biology of the synaptonemal complex. *Annu. Rev. Cell Dev. Biol.* 20, 525–558.
- Peruquetti, R.L., Assis, I.M., Taboga, S.R., Azeredo-Oliveira, M.T.V., 2008. Meiotic nucleolar cycle and chromatoid body formation during the rat (*Rattus norvegicus*) and mouse *Mus musculus* spermiogenesis. *Micron* 39, 419–425.
- Petersen, C., Söder, O., 2006. The Sertoli cell – a hormonal target and “Super” nurse for germ cells that determines testicular size. *Hormone Res.* 66, 153–161.
- Phillips, D.M., Rasweiler, J.J., Murwali, F., 1997. Giant, accorioned sperm acrosomes of the greater bulldog bat, *Noctilio leporinus*. *Mol. Reprod. Dev.* 48, 90–94.
- Racey, P.A., 1974. The reproductive cycle in male noctule bats, *Nyctalus noctula*. *J. Reprod. Fertil.* 41, 169–182.
- Racey, P.A., 1979. The prolonged storage and survival of spermatozoa in Chiroptera. *J. Reprod. Fertil.* 56, 391–402.
- Ramanujam, S., 1938. Cytogenetical studies in the Oryzaeae: I. Chromosome studies in the Oryzaeae. *Ann. Bot. (Lond.)* 2, 107–125.
- Rasweiler, J.J., 1993. Pregnancy in Chiroptera. *J. Exp. Zool.* 266, 495–513.
- Rouse, G.W., Robson, S.K., 1986. An ultrastructural study of megachiropteran (Mammalia: Chiroptera) spermatozoa: implications for chiropteran phylogeny. *J. Submicrosc. Cytol.* 18, 137–152.
- Russell, L.D., Ettlin, R.A., Sinha-Hikin, A.P., Clegg, E.D., 1990. Mammalian spermatogenesis. In: Russell, L.D., Ettlin, R.A., Sinha-Hikin, A.P. (Eds.), *Clegg Histological and Histopathological Evaluation of the Testis*. Cache River Press, Clearwater, pp. 1–40.
- Saidapur, S.K., Patil, S.B., 1992. Kinetics of spermatogenesis in megachiropteran bat, *Rousettus leschenaulti* (Desmarest): seminiferous epithelial cycle, frequency of stages, spermatogonial renewal and germ cell degeneration. *Indian J. Exp. Biol.* 30, 1037–1044.
- Schleirmacher, E., Schmidt, W., 1973. Changes of the synaptonemal complex at the end of pachytene. *Humangenetik* 19, 235–245.
- Segatelli, T.M., Almeida, C.C.D., Pinheiro, P.F.F., Martinez, M., Padovani, C.R., Martinez, F.E., 2000. Ultrastructural study of acrosome formation in Mongolian gerbil (*Meriones unguiculatus*). *Tissue Cell* 32 (6), 508–517.
- Segatelli, T.M., Almeida, C.C.D., Pinheiro, P.F.F., Martinez, M., Padovani, C.R., Martinez, F.E., 2002. Kinetics of spermatogenesis in the Mongolian gerbil (*Meriones unguiculatus*). *Tissue Cell* 34 (1), 7–13.
- Sharifi, M., Ghorbani, R., Akmal, V., 2004. Reproductive cycle in *Pipistrellus kuhlii* (Chiroptera, Vespertilionidae) in western Iran. *Mammalia* 68 (4), 323–327.
- Singwi, M.S., Lall, S.B., 1983. Spermatogenesis in the non-scrotal bat – *Rhinopoma kinneari* Wroughton (Microchiroptera: Mammalia). *Acta Anat.* 116, 136–145.

- Smithwick, E.B., Young, L.G., Gould, K.G., 1996. Duration of spermatogenesis and relative frequency of each stage in the seminiferous epithelial cycle of the chimpanzee. *Tissue Cell* 28, 357–366.
- Söderström, K., Parvinen, M., 1976. Transport of material between the nucleus, the chromatoid body and the Golgi complex in the early spermatids of the rat. *Cell Tissue Res.* 168, 335–342.
- Solari, A.J., Moses, M.J., 1973. The structure of the central region in the synaptonemal complexes hamster and cricket spermatocytes. *J. Cell Biol.* 56, 145–152.
- Soley, J.T., 1994. Centriole development and formation of the flagellum during spermiogenesis in the ostrich (*Struthio camelus*). *J. Anat.* 185, 301–313.
- Soon-Jeong, J., Joo-Cheol, P., Heung-Joong, K., Chun, S.B., Myung-Hee, Y., Do-Seon, L., Moon-Jin, J., 2006. Comparative fine structure of the epididymal spermatozoa from three Korean shrews with considerations on their phylogenetic relationships. *Biocell* 30 (2), 279–286.
- Suphamungmee, W., Wanichanon, C., Vanichviriyakit, R., Sobhon, P., 2008. Spermiogenesis and chromatin condensation in the common tree shrew, *Tupaia glis*. *Cell Tissue Res.* 331, 687–699.
- Tähkä, K.M., 1986. Current aspects of Leydig cell function and its regulation. *J. Reprod. Fertil.* 78, 367–380.
- Tang, X.M., Lalli, M.F., Clermont, Y., 1982. A cytochemical study of the Golgi apparatus of the spermatid during spermiogenesis in the rat. *Am. J. Anat.* 163, 283–294.
- Tanii, I., Yoshinaga, K., Toshimori, K., 1999. Morphogenesis of the acrosome during the final steps of rat spermiogenesis with special reference to tubulobulbar complexes. *Anat. Rec.* 256, 195–201.
- Teeling, E.M., Springer, M.S., Madsen, O., Bates, P., O'Brien, S.J., Murphy, W.J., 2005. A molecular phylogeny of bats illuminates biogeography and the fossil record. *Science* 307, 580–584.
- Teixeira, R.D., Colli, G.R., Bão, S.N., 1999a. The ultrastructure of the spermatozoa of the worm lizard *Amphisbaena alba* (Squamata, Amphisbaenidae) and the phylogenetic of amphisbaenians. *Can. J. Zool.* 77, 1254–1264.
- Teixeira, R.D., Colli, G.R., Bão, S.N., 1999b. The ultrastructure of the spermatozoa of the lizard *Micrablepharus maximiliani* (Squamata, Gymnophthalmidae), with considerations on the use of sperm ultrastructure characters in phylogenetic reconstruction. *Acta Zool. (Stockholm)* 80, 47–59.
- Teixeira, R.D., Vieira, G.H.C., Colli, G.R., Bão, S.N., 1999c. Ultrastructural study of spermatozoa of the neotropical lizards, *Tropidurus semitaeniatus* and *Tropidurus torquatus* (Squamata, Tropiduridae). *Tissue Cell* 31 (3), 308–317.
- Teixeira, R.D., Scheltinga, D.M., Trauth, S.E., Colli, G.R., Bão, S.N., 2002. A comparative ultrastructural study of spermatozoa of the teiid lizards *Cnemidophorus gularis gularis*, *Cnemidophorus ocellifer*, and *Kentropyx altamazonica* (Reptilia, Squamata, Teiidae). *Tissue Cell* 34 (3), 135–142.
- Venable, J.H., Coggeshall, R.A., 1965. A simplified lead citrate stain for use in electron microscopy. *J. Cell Biol.* 25, 407–408.
- Vieira, G.H.C., Colli, G.R., Bão, S.N., 2005. Phylogenetic relationships of corytophanid lizards (Iguania, Squamata, Reptilia) based on partitioned and total evidence analyses of sperm morphology, gross morphology, and DNA data. *Zool. Scripta* 34 (6), 605–625.
- Watson, M.L., 1958. Staining tissue section of electron microscopy with heavy metals. *J. Biophys. Biochem. Cytol.* 4, 475–478.
- Wetterer, A.L., Rockman, M.V., Simmons, N.B., 2000. Phylogeny of phyllostomid bats (Mammalian: Chiroptera): data from diverse morphological systems, sex chromosomes, and restriction sites. *Bull. Am. Mus. Nat. Hist.* 248, 200.
- Willig, M.R., Hollander, R.R., 1987. *Vampyrops lineatus*. In: *Mammalian Species*, vol. 275. The American Society of Mammalogists, pp. 1–4.
- Zhang, L., Han, X.K., Li, M.Y., Bao, H.J., Chen, Q.S., 2007. Spermiogenesis in soft-shelled turtle, *Pelodiscus sinensis*. *Anat. Rec.* 209, 1213–1222.
- Zickler, D., Kleckner, N., 1999. Meiotic chromosomes: integrating structure and function. *Annu. Rev. Genet.* 33, 603–754.

## IV. CAPÍTULO 2

### **Ultrastructural characteristics of spermatogenesis in Pallas's Mastiff bat, *Molossus molossus* (Chiroptera: Molossidae)**

Artigo aceito à publicação na revista “Microscopy Research and Technique”, 2012.

# Ultrastructural Characteristics of Spermatogenesis in Pallas's Mastiff Bat, *Molossus molossus* (Chiroptera: Molossidae)

MATEUS R. BEGUELINI,<sup>1</sup> SEBASTIÃO R. TABOGA,<sup>1</sup> AND ELIANA MORIELLE-VERSUTE<sup>2\*</sup>

<sup>1</sup>Department of Biology, UNESP—Univ Estadual Paulista, São José do Rio Preto, São Paulo 15054-000, Brazil

<sup>2</sup>Department of Zoology and Botany, UNESP—Univ Estadual Paulista, São José do Rio Preto, São Paulo 15054-000, Brazil

**KEY WORDS** Chiroptera; *Molossus molossus*; spermatogenesis; spermiogenesis

**ABSTRACT** Despite the large number of species, their wide distribution, and unique reproductive characteristics, Neotropical bats have been poorly studied, and important aspects of the reproduction of these animals have not been elucidated. We made an ultrastructural analysis of spermatogenesis in *Molossus molossus* (Molossidae). The process of spermatogonial differentiation is similar to that found in other bats and is also relatively similar to that of Primates, with three main spermatogonia types: A<sub>d</sub>, A<sub>p</sub>, and B. Meiotic divisions proceed similarly to those of most mammals, and spermiogenesis is clearly divided into 12 steps, in the middle of the range known for bats (9–16 steps). Formation of the acrosome is similar to that known from other mammals; however, the ultrastructure of spermatozoa was found to have unique characteristics, including many wavy acrosomal projections on its surface, which seems to be specific for the family Molossidae. Comparing the ultrastructure of the spermatozoon of *M. molossus* with other bats already study, we observed that three characters vary: morphology of the outer dense fibers, of the perforatorium, and of the spermatozoon head. The great similarity of morphological characters between *M. molossus* and *Platyrrhinus lineatus* suggests that *M. molossus* is more closely related to the Phyllostomidae than to the Rhinolophidae and the Vespertilionidae. *Microsc. Res. Tech.* 00:000–000, 2012. © 2012 Wiley Periodicals, Inc.

## INTRODUCTION

The bats belong to the second largest order of mammals, the Chiroptera, with ~200 genera and 1,100 species widely distributed among tropical and temperate regions (Reis et al., 2007; Simmons, 2005). They inhabit a wide variety of habitats, colonizing from natural to urban environments, and thus are submitted to a large variety of abiotic factors, including latitude, temperature, rainfall, and photoperiod (Fleming et al., 1972).

In response to all these factors, the bats have evolved some unique adaptations, including testicular regression during hibernation, prolongation of sperm storage in the cauda epididymis in males and in the uterine cornua in females, asynchrony between spermatogenesis and the mating period, delayed ovulation, fertilization and implantation (Beguelini et al., 2009, 2011a), and great differences in the ultrastructural morphology of the spermatozoa (Breed and Leigh, 1985; Fawcett and Ito, 1965; Phillips et al., 1997; Sang-Sick et al., 1999). All these differences probably evolved as adaptations to the habitat of each species; the morphology of the cells and physiology of the processes apparently adapt in response to abiotic stimuli. As each species colonizes different places and has different behaviors and requirements, it is expected that each bat species will have unique reproductive characteristics.

The reproductive characteristics of the bats of the temperate and tropical regions of the Old World have been extensively studied (Crichton and Krutzsch, 2000; Encarnação et al., 2004; Racey and Tam, 1974; Sharifi et al., 2004), mainly from an ecological-behavioral perspective; however, the Neotropical bats have been poorly evaluated, and almost no studies have addressed spermatogenesis.

Spermatogenesis is a highly regulated and synchronized process of cellular differentiation, whereby stem cells proliferate, divide meiotically, and gradually differentiate into highly specialized haploid cells, spermatozoa (Costa and Paula, 2003; Matsumoto, 1996). The main events of this process are generally similar in most mammals (Adachi et al., 1992; Foote et al., 1972; Kurohmaru et al., 2002; Osman and Ploen, 1986; Oud and de Rooij, 1977; Painter, 1923; Swierstra and Foote, 1963; Wodsedalek, 1914); however, variations in the process among and within orders, families, and taxa are frequently observed (Lin and Jones, 2000; Lin et al., 1997; Phillips et al., 1997), being mainly determined by variations in the final structure of the spermatozoon (Beguelini et al., 2011a; Jamieson, 1995).

This differentiation process has attracted extensive studies of a wide variety of species, not only because the process involves numerous radical changes in cell shape, biochemistry, and gene regulation, but also because variations in the ultrastructure of the spermatozoon have been used as an important tool in the identification of species (Lin and Jones, 2000; Lin et al., 1997; Phillips et al., 1997).

This differentiation process has attracted extensive studies of a wide variety of species, not only because the process involves numerous radical changes in cell shape, biochemistry, and gene regulation, but also because variations in the ultrastructure of the spermatozoon have been used as an important tool in the identification of species (Lin and Jones, 2000; Lin et al., 1997; Phillips et al., 1997).

\*Correspondence to: Eliana Morielle-Versute, Department of Zoology and Botany, UNESP—Univ. Estadual Paulista—Rua Cristóvão Colombo no. 2265, Jardim Nazareth, São José do Rio Preto, São Paulo 15054-000, Brazil. E-mail: morielle@ibilce.unesp.br

Received 14 October 2011; accepted in revised form 1 December 2011

DOI 10.1002/jemt.22005

Published online in Wiley Online Library (wileyonlinelibrary.com).



tification and classification of taxa of various groups of organisms (Costa et al., 2004; Garda et al., 2004; Giugliano et al., 2002; Soon-Jeong et al., 2006; Vieira et al., 2005).

The large number of species, their wide distribution and the lack of studies, have hindered the elucidation of the taxonomic, phylogenetic and evolutionary patterns of bats; therefore, further studies that provide distinctive taxonomic characters are necessary.

*Molossus molossus* is a small member of the family Molossidae, insectivorous bats that are an important component of Brazilian fauna (Eger, 2007). It occurs in the Netherlands Antilles and Trinidad and Tobago, and across northern South America, south throughout the greater Amazon basin into Ecuador, Peru, Bolivia, Paraguay, Uruguay, and northern Argentina (Eger, 2007; Reis et al., 2007; Simmons, 2005). *M. molossus* is a species that is well adapted to urban areas, often using human constructions as roosts (Eger, 2007; Reis et al., 2007), a behavior that has ecological, social, economic, and medical health implications. It is the most common bat in the urban areas in Brazil. Although it is known to be polyestric with two annual reproductive breeding seasons in Brazil, one in March–April and another in November, and sexually active males are found almost year round (Beguelini et al., 2010; Fabián and Marques, 1989); information about the reproductive process in males is scarce. Thus, we made an ultrastructural analysis of spermatogenesis in *M. molossus*.

## MATERIALS AND METHODS

### Animals, Collection, and Licenses

Five sexually mature males of *M. molossus* (Pallas, 1766) were analyzed. The bats were classified as adults based on the body weight, complete ossification of the metacarpal epiphyses, wear of the teeth (De Knecht et al., 2005), positioning of the testes, and the presence of sperm inside the cauda epididymis.

The animals were collected in northwest São Paulo State, Brazil (49W22'45" 20S49'11") between August and November 2008 and were deposited in the Chiroptera collection at São Paulo State University (UNESP-IBILCE).

The ethics committee of the São Paulo State University (UNESP) authorized all experimental procedures (Process: 013/09—CEEA); the capture and captivity of the bats were authorized by the Brazilian institution responsible for wild animal care (Instituto Brasileiro do Meio Ambiente, IBAMA—Process: 02027.001957/2006-02).

### Transmission Electron Microscopy

After the sacrifice of the animals, the testes and cauda epididymis were removed, perforated, and fixed by immersion in a solution of 3% glutaraldehyde plus 0.25% tannic acid in Millonig buffer (pH 7.3), containing 0.54% glucose, for 24 h. After washing with the same buffer, the samples were postfixated with 1% osmium tetroxide for 2 h, dehydrated in graded series of acetone, and included in Araldite 502 Resin (Electron Microscopy Sciences, Hatfield, PA). Ultrathin sections (50 nm) were made using diamond knives, stained with 2% uranyl acetate for 30 min (Watson, 1958), followed by 2% lead citrate in sodium hydroxide for 10 min (Venable and Coggeshall, 1965); they were analyzed in a

Leo-Zeiss 906 Transmission Electron Microscope (Cambridge, UK) at the “Prof. Dr. Celso Abbade Mourão” Center for Microscopy (IBILCE-UNESP).

## RESULTS

### Spermatogonia

Three main types of spermatogonia were identified in *M. molossus*, based on ultrastructural features: the dark type A – A<sub>d</sub>, the pale type A – A<sub>p</sub>, and type B.

Type A<sub>d</sub> spermatogonia (Fig. 1A) are usually isolated cells located in the basal compartment of the germinal epithelium; they are surrounded by Sertoli cells and are adhered to the basal lamina. It is the smallest type of spermatogonium and has an elliptical shape. The nucleus is oval, occupies most of the cell, and contains finely granular chromatin, with clusters of condensed chromatin and a single, large, granular, and irregularly shaped nucleolus, usually centrally located. The cell has little cytoplasm, with few mitochondria, some endoplasmic reticulum (smooth and rough), and fine cytoplasmic granulations (ribosomes and/or glycogen).

Type A<sub>p</sub> spermatogonia (Fig. 1B) are also present in the basal compartment; however, adhesion to the basal lamina is less pronounced. They have a more elongated shape, with relatively more cytoplasm, containing mitochondria, some endoplasmic reticulum (smooth and rough), Golgi complex, centrioles, and fine cytoplasmic granulations (ribosomes and/or glycogen). They have an oval nucleus, containing finely granular chromatin and a large granular nucleolus; rarely, there are two nucleoli.

The first difference observed between spermatogonia types A<sub>p</sub> and B is loss of adhesion to the basal lamina. Type B spermatogonia start the process of ascension into the adluminal compartment, gradually dislocating the cytoplasm to the upstream regions of the basal compartment (Fig. 1C), consequently losing contact with the basal lamina (Fig. 1D). The nuclei are round and contain large clumps of condensed chromatin, mainly associated with the nuclear envelope, and a single large and granular nucleolus, compact, and centrally located; less frequently, there are two nucleoli. The cytoplasm is almost circular, with clusters of mitochondria, a few endoplasmic reticulum extensions (smooth and rough), a Golgi complex, and fine cytoplasmic granulations (ribosomes and/or glycogen).

Groups of up to eight type-B spermatogonia were observed to remain connected by intercellular bridges (Figs. 1E and 1F).

### Meiotic Phase: The Spermatocytes

During the meiotic phase, groups of type B spermatogonia move away from the basal lamina to the adluminal compartment, the nucleus increases in size, and the chromatin begins to condense. During this process, formation of the synaptonemal complexes begins, and, consequently, there is a gradual process of chromatin condensation and nucleolar disruption.

The ribbon shape of the synaptonemal complexes (two external portions of high electron density and a central thin line of intermediate electron density, which are transversed by small oblique zipper-like filaments) was first observed in leptotene spermatocytes (Fig. 2A) and tended to disappear in final diplotene-dia-



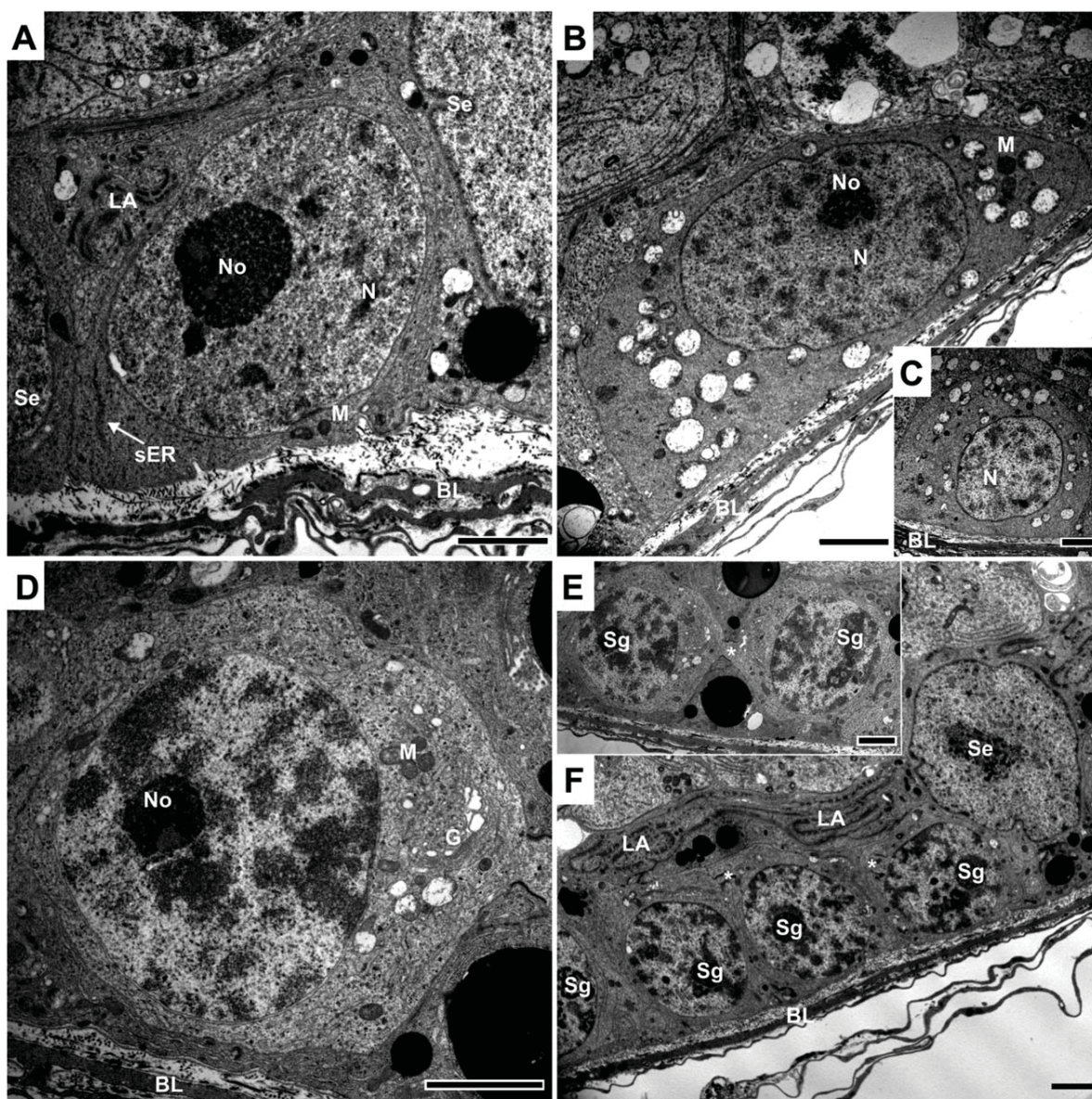


Fig. 1. Electron micrographs of the spermatogonial types of *Molossus molossus*. **A:** Type  $A_4$  spermatogonia. Note the small size of this cell type; the nucleus occupies most of its cytoplasm, and there are lamellae anellata (LA), derived from the nuclear envelope, in the cytoplasm of the Sertoli cells. **B:** Type  $A_1$  spermatogonia. Note the more elongated shape of this cell type, with a relatively greater proportion of cytoplasm. **C–F:** Type B spermatogonia. Note that this cell type starts the process of ascension into the adluminal compartment,

migrating the cytoplasm to the upstream regions of the basal compartment (C), losing contact with the basal lamina (D). This cell type forms groups of two (E) to eight cells that remain connected to each other by intercellular bridges (F). (BL, basal lamina; G, Golgi complex; M, mitochondria; N, nucleus; No, nucleolus; Se, Sertoli cell; sER, smooth endoplasmic reticulum; Sg, spermatogonia; \*intercellular bridge. Scale bars = 2  $\mu$ m.

kinesis (Figs. 2D and 2E). Both ends were individually attached to the nuclear envelope, with the nuclear envelope presenting a high-electron density at these attachment sites (Fig. 2B). On the other hand, the intermediate part extended out in a loop to the central portions of the nucleus (Figs. 2B and 2C).

Along with the formation of the synaptonemal complexes, we observed onset of chromatin condensation. The chromatin associates at the edge of the synaptonemal complexes and begins to condense, forming clumps

of condensed chromatin. These clumps were small in leptotene spermatocytes (Fig. 2A); the nucleus still had an uncondensed appearance; however, from zygotene to diakinesis, the condensation of chromatin occurred gradually, forming distinctive blocks at the edges of the synaptonemal complexes (Figs. 2B–2E).

The nucleolus still seems to be morphologically organized in leptotene and zygotene spermatocytes (Figs. 2A and 2B), presenting a compact electron-dense form. However, in early pachytene, the nucleolus loses



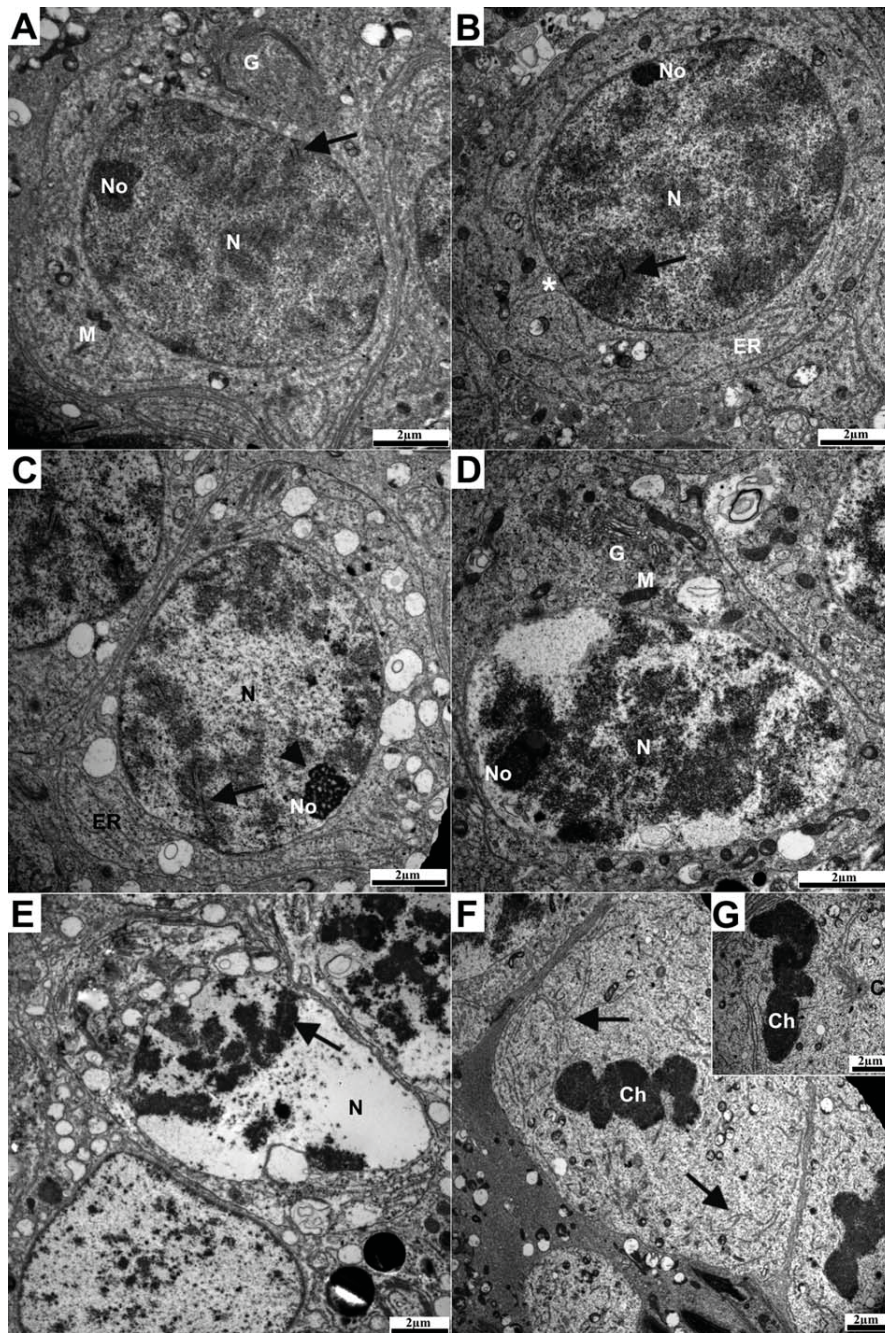


Fig. 2. Electron micrographs of the meiotic cells (meiosis I) of *Molossus molossus*. **A:** Leptotene. **B:** Zygotene. **C:** Pachytene. **D:** Diplotene. **E:** Diakinesis. **F, G:** Metaphases. Note the increase in the degree of chromatin condensation around the synaptonemal complexes (A–C, arrows); the disorganization of the nucleolus from leptotene (A) to diplotene (D), with a great nucleolar fragmentation in pachytene (arrow-head); the structural framework in the middle of

its morphological integrity, beginning disruption, appearing fragmented (Fig. 2C). In diakinesis, the nucleolus is no longer observed, and the number of nucleolar fragments decreases considerably (Fig. 2E).

The spermatocytes presented few organelles; however, Golgi complexes, clusters of mitochondria, and

the chromosomes in diakinesis (E, arrow); the breakdown of the nuclear envelope during metaphase (F, arrows); the centrioles are already positioned on opposite poles of the cell, with the microtubules linked to chromosomes (G). (C, centrioles; Ch, chromosomes; ER, endoplasmic reticulum; G, Golgi complex; M, mitochondria; N, nucleus; No, nucleolus).

extensions of endoplasmic reticulum (smooth and rough) were easily observed (Figs. 2A–2E).

Chromatin condensation peaked in metaphase, the nucleolus and the synaptonemal complexes disappeared, the nuclear envelope broke apart (Fig. 2F, arrows), the centrioles became positioned at opposite

poles, and the microtubules became linked to the chromosomes, which aligned in the equatorial region of the cell (Fig. 2G).

After the alignment, the spindle fibers became shortened during anaphase, and the nuclear envelope was restored (telophase), giving rise to two secondary spermatocytes. These began rapid cell division, producing four haploid spermatids, which underwent cellular differentiation, transforming into spermatozoa. The limited time during which these events occur hampers observation of these phases by electron microscopy.

### Spermiogenesis

During spermiogenesis, morphological changes that occurred during differentiation of spermatids into spermatozoa were clearly divided into four phases with 12 steps: the Golgi phase, steps 1–4; the cap phase, steps 5–8; the acrosomal phase, steps 9–10; and the maturation phase, steps 11–12.

**Golgi Phase.** This phase is characterized by initiation of the differentiation process, in which cells newly formed from the second meiotic division enter into spermiogenesis process. The main changes during this phase are the development of the Golgi complex, formation of proacrosomal vesicles and the proacrosomal vacuole, and initial formation of the acrosome and flagellum, which can be divided into four steps (1–4).

Step 1 spermatids correspond to the haploid cells derived from the second meiotic division and present little differentiation (Fig. 3A). They have a large and spherical nucleus, with scattered clusters of condensed chromatin and a single nucleolus (Fig. 3B); there are few extensions of endoplasmic reticulum and mitochondria, dispersed throughout the cytoplasm, and a Golgi complex associated with small vesicles that are the precursors of the proacrosomal vacuole (Fig. 3C). The chromatoid body is often near or associated with the Golgi complex (Fig. 3C).

In step 2 spermatids, the nucleus remains spherical and has little chromatin condensation (Fig. 3D). On the other hand, the Golgi complex develops considerably, increasing in size, producing more cisterns and vesicles, which start to fuse with each other to form large proacrosomal vesicles (Fig. 3E). Electron-dense granules form within the larger proacrosomal vesicles (Figs. 3D and 3E, arrows), and the chromatoid body becomes associated with this complex (Fig. 3D); intercellular bridges connect adjacent spermatids, forming something that resembles a syncytium (Fig. 3D, asterisk); there is initial development of the centrioles to form the axoneme (Fig. 3F). Other cellular organelles were similar to those observed in step 1 spermatids.

In step 3 spermatids, the numerous proacrosomal vesicles fused to form a large proacrosomal vacuole adjacent to the nucleus (Fig. 3G). The positioning of this vacuole caused the formation of a concavity in the nucleus; however, there were few changes in the nuclear morphology, with the formation of some scattered clusters of condensed chromatin. Dislocation of centrioles and chromatoid bodies to the pole opposite to that of acrosome formation and intercellular bridges were also observed. Other cellular organelles were similar to those observed in step 2 spermatids.

In step 4 spermatids, the proacrosomal vacuole firmly attaches to the nuclear envelope, forming a con-

cavity in the nucleus (Fig. 3H). The contact of the membranes of the proacrosomal vacuole and of the nucleus was more electron-dense (Fig. 3H, arrow). The nuclear shape remained spherical; although inside the nucleus, the chromatin condensation started forming large blocks of condensed chromatin throughout (Fig. 3H, arrowhead). Other cellular organelles were similar to those observed in Step 3 spermatids.

**Cap Phase.** During this phase, the proacrosomal vacuole flattened against the nucleus and began to extend laterally, forming the acrosomal cap and defining the cranial pole of the spermatid. Similarly, the centrioles migrated to the opposite pole, forming the flagellum and defining the caudal pole of the spermatid. This phase can be divided into four steps (5–8).

During step 5, the proacrosomal vacuole associated more intimately with the nuclear envelope, beginning to cover the nucleus (Figs. 3I and 3K), forming the acrosomal cap. Two types of components were observed inside this vacuole, a more electron-dense component that occupied the central region in contact with the nuclear envelope and a translucent component that surrounded the electron-dense component (Figs. 3I and 3K). The production of additional acrosomal vesicles by the Golgi complex and their subsequent fusion to the acrosomal cap continued in this step. There were also intercellular bridges in this step (Fig. 3J).

In step 6, the spermatids already lined up in the cranio-caudal plane, with the acrosome being formed in the cranial region and the axoneme implanted in the caudal region of the nucleus (Fig. 4A). The acrosomal cap began to condense, presenting a stronger electron-dense matrix, and expanded, covering a large proportion of the surface of the nucleus.

The acrosomal cap of the step 7 spermatids already covered half of the nuclear surface; distally, they developed an elevation (Fig. 4B) that will be associated with microtubules.

In step 8 spermatids, the nucleus approached to the plasma membrane (Fig. 4C) and the cytoplasm dislocated to the posterior pole of the cell. The acrosomal cap presented a more compact format, which filled the entire anterior region of the nucleus; attachment of large and translucent proacrosomal vesicles to the cap was also common in this step (Figs. 4C and 4D). Numerous microtubules formed the manchette, which later attached to the elevation of the acrosomal cap, produced in the anterior step, subsequently contributing to nuclear elongation (Figs. 4C and 4D).

**Acrosome Phase.** Nuclear elongation and condensation occur in this phase, which can be divided into two steps (9–10).

During step 9, there is nuclear elongation (Figs. 4E–4I); the fibers of the longitudinal manchette (Fig. 4F), connected to the nuclear ring (Figs. 4H and 4I), are gradually shortened, pulling the acrosomes, so that it covers the entire rostral end of the nucleus, which now assumes an arrow-shape (Fig. 4I). Nuclear condensation occurs gradually along the nuclear elongation (Figs. 4E–4I), causing major nucleolar fragmentation (Fig. 4E); at the end of this phase, the nucleolus was no longer observed. The flagellum in formation develops considerably during this phase, with formation of the nuclear fossa, positioning of the centriolar adjunct, and elongation of the axonema (Fig. 4E).



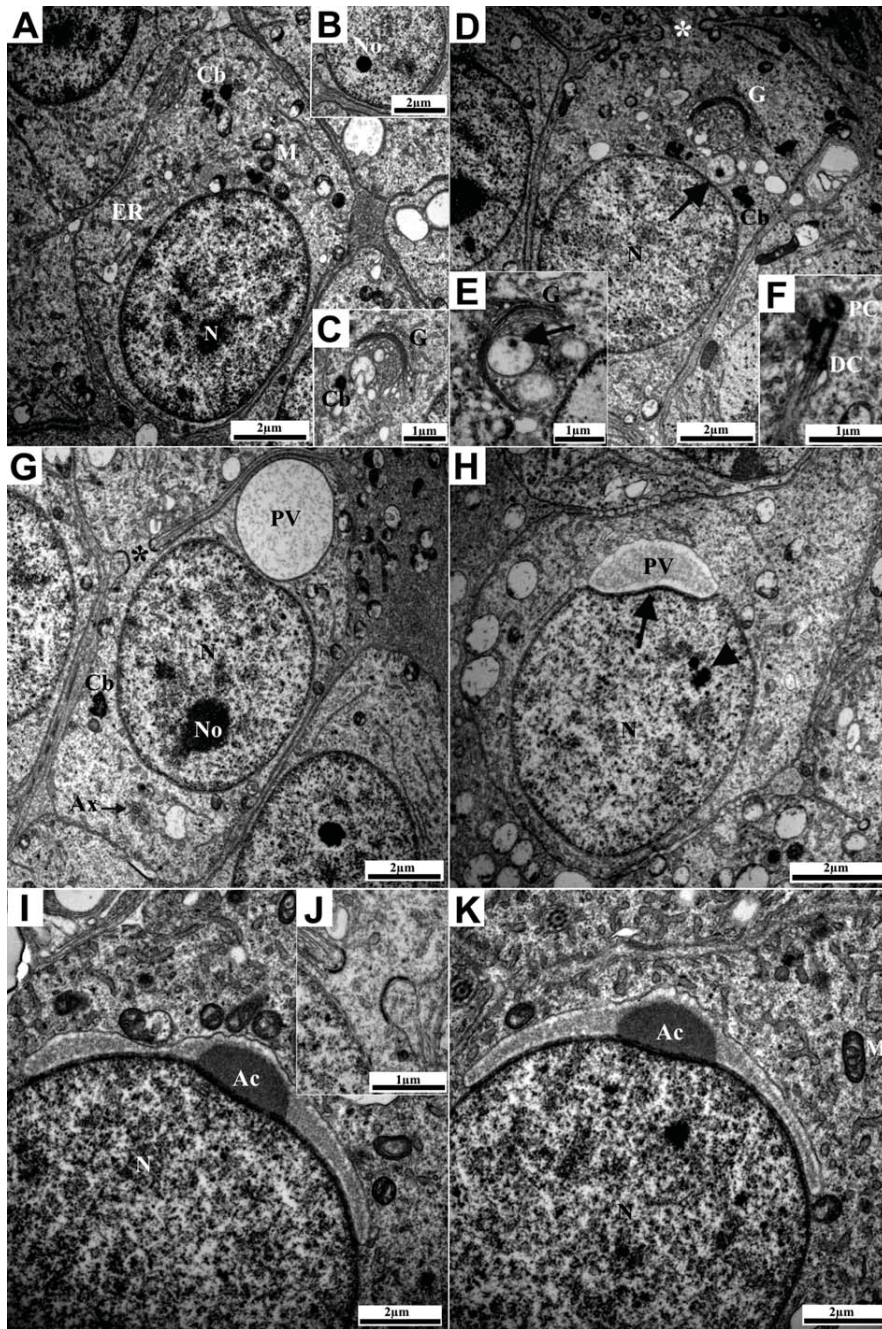


Fig. 3. Electron micrographs of the spermatids of *Molossus molossus*. **A–C:** Step 1 spermatids. Note that there is little differentiation in this type of spermatid. The nuclei are spherical, with a single nucleolus (B); the Golgi complex presents few proacrosomal vesicles (C); and the chromatoid body is closely associated with them (C). **D–F:** Step 2 spermatids. Note the considerable development of the Golgi complex and the formation of large proacrosomal vesicles that present electron-dense granules (D, E, arrows) along with intercellular bridges (D, \*) and initial development of the axoneme (F). **G:** Step 3 spermatid. Note the large proacrosomal vacuole adjacent to the nucleus, dislocation of centrioles, and chromatoid bodies to the pole opposite the acrosome formation and the intercellular bridges (\*). **H:** Step 4 sper-

matid. Note the attachment of the proacrosomal vacuole to the nuclear envelope, forming a concavity in the nucleus, with the contact of the two membranes presenting a more electron-dense appearance (arrow) and the beginning of chromatin condensation (arrow-head). **I–K:** Step 5 spermatids. Note the intimate association of the acrosomal cap with the nuclear envelope and two types of components inside it, a more electron-dense type and another translucent type (I and K), and intercellular bridges (J). (Ac, acrosomal cap; Ax, axonema; Cb, chromatoid body; DC, distal centriole; ER, endoplasmic reticulum; G, Golgi complex; M, mitochondria; N, nucleus; No, nucleolus; PC, proximal centriole; PV, proacrosomal vacuole; \*intercellular bridge).



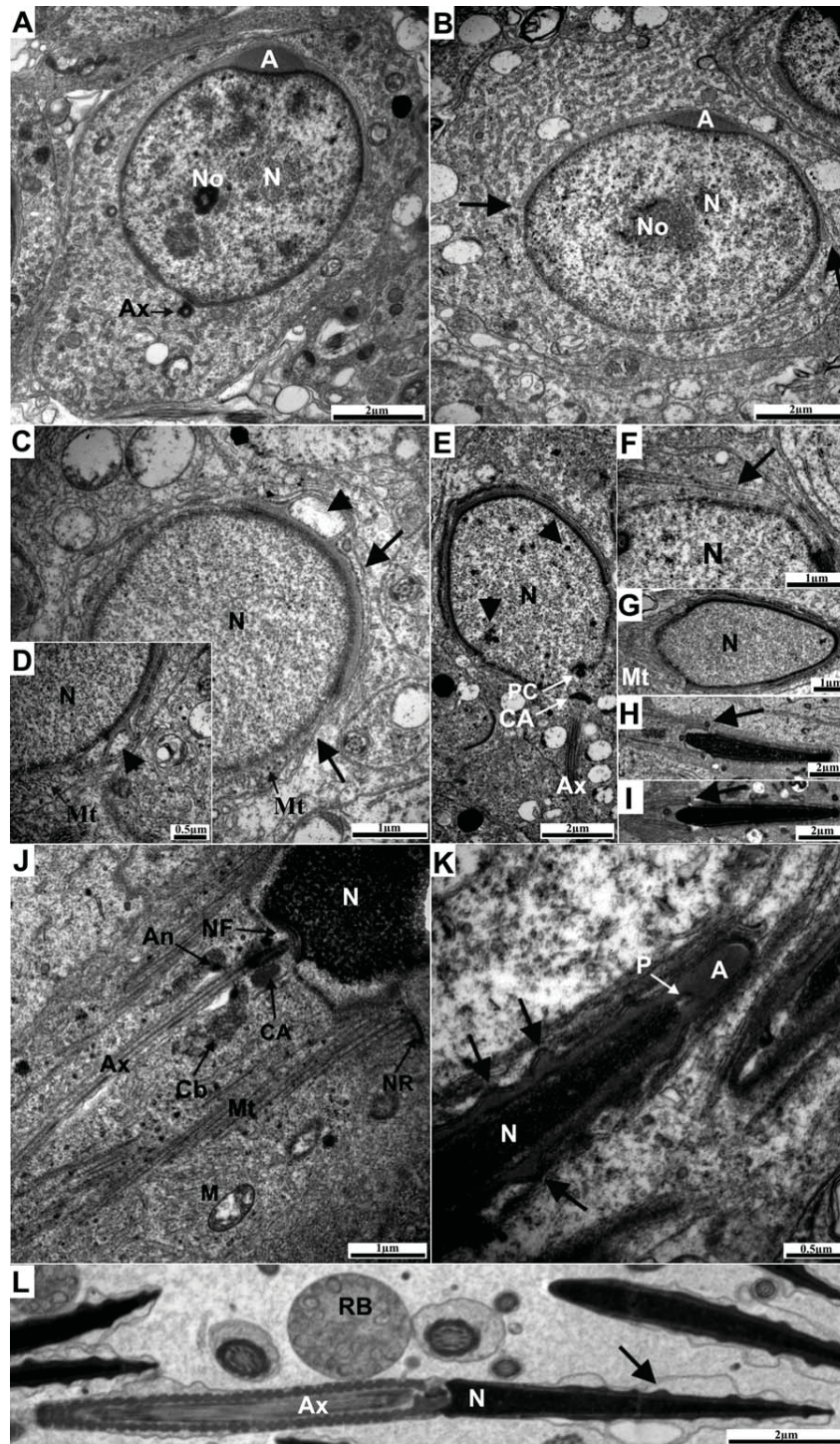


Fig. 4. Electron micrographs of the spermatids of *Molossus molossus*. **A:** Step 6 spermatid. Note the expansion of the acrosomal cap, which covers most of the nuclear surface and contains a strong electron-dense matrix. **B:** Step 7 spermatid. Note the development of an elevation in the distal region of the acrosome (arrows). **C, D:** Step 8 spermatids. Note the approach of the nucleus to the plasma membrane (arrows), the attachment of large and translucent proacrosomal vesicles to the acrosome (arrow-heads); and the allocation of microtubules to the microtubular manchette in formation (Mt). **E-I:** Early (E-G), middle (H), and late (I) step 9 spermatids. Note that major changes in nucleolar fragmentation (E, arrow-heads), nuclear elongation, and condensation gradually occur in this step, when the longitudinal manchette (F, arrow), connected to the nuclear ring (H, I, arrows) has its fibers gradually shortened, pulling the acrosomes, making it cover the entire rostral end of the nucleus, which now

assumes an arrow shape (I). **J:** Step 10 spermatid. Note that at this step, the nuclear ring completes its dislocation to the posterior region of the nucleus, the annulus commences its caudal migration, and the organization of the midpiece begins. **K:** Step 11 spermatid. Note the beginning of the formation of the perforatorium in the rostral region of the nucleus and the acrosomal projections, forming lateral blisters on the spermatozoon surface (arrows). **L:** Step 12 spermatid/spermatozoa observed in the caput epididymis. Note that at this step, the spermatids have achieved the basic format of the spermatozoa, with a pleated head (arrow), and the residual bodies contain many organelles not included in the spermatozoa. (A, acrosome; An, annulus; Ax, axonema; CA, centriolar adjunct; Cb, chromatoid body; M, mitochondria; Mt, microtubules; N, nucleus; NF, nuclear fossa; No, nucleolus; NR, nuclear ring; P, perforatorium; PC, proximal centriole; RB, residual body).

At step 10, the nuclear ring completes its dislocation to the posterior region of the nucleus, the nucleus reaches its highest level of chromatin condensation, the nuclear fossa is almost completed, and the annulus is intimately associated with the chromatoid body and starts its caudal migration; and recruitment of the mitochondrial clusters for the organization of the mid-piece begins (Fig. 4J).

**Maturation Phase.** The differentiation process for the formation of spermatozoa is completed during this phase. The acrosome and nucleus complete their elongation and condensation, and the spermatozoon head assumes its final form. Similarly, the mid, principal, and end pieces are organized, forming the functional flagellum. Residual spermatid cytoplasm becomes retained at the luminal edge of the Sertoli cells after release of the spermatozoa into the seminiferous lumen (spermiation process). All these final processes can be divided into two steps (11–12).

In step 11, the spermatid heads become long and compact. At this step, formation of the perforatorium begins in the rostral region of the nucleus (Fig. 4K), and local accumulations of acrosomal materials give rise to lateral blisters on the spermatozoon surface, the acrosomal projections (Fig. 4K). The tail has a large allocation of mitochondria, which are aligned to the midpiece; organization of the principal and end pieces begins.

In step 12, the spermatids complete their differentiation, attaining the basic format of the spermatozoon, with acrosomal projections in the spermatozoon head; the mid, principal, and end pieces in the tail are already organized. After final organization of the spermatozoon, it is released into the tubular lumen (spermiation process). Along with it, a large amount of cytoplasm (residual bodies), which contains many organelles not included in the spermatozoa, were also released (Figs. 4L and 5F); these seem to be degraded only in the epididymis.

### Ultrastructure of the Spermatozoon

**Spermatozoon Head.** The spermatozoon has a dorso-ventrally flattened, spatulate-like head (Fig. 5F) that, when cut sagittally, appears to be arrow-shaped (Figs. 5A and 5B). The arrow-shaped nucleus occupies almost the entire head, presenting an extremely dense and homogeneous matrix (Figs. 5C and 5D). The inner acrosomal membrane is close related to the nuclear membrane, forming a pale and small, but continuous, subacrosomal space between the two membranes, which covers the rostral end of the nucleus, up to the equatorial segment (Fig. 5A). However, at the apical edge, the inner acrosomal membrane extends to the anterior region, to the middle of the acrosome, forming the perforatorium, which has a spear-like form (Fig. 5C). The acrosome covers approximately four-fifths of the nuclear length, has a highly homogeneous electron-dense matrix, presents many wavy acrosomal projections (Fig. 5C), and is surrounded by the outer acrosomal membrane. Externally, the spermatozoon head is covered by a large amount of plasma membrane, which is free along most of its length, forming a space that separates it from the outer acrosomal membrane; however, in the terminal region of the acrosome, it is

attached to the nuclear envelope, in the region of the equatorial segment (Figs. 5A and 5B).

**Neck (Fig. 5D).** The neck, or connecting piece, corresponds to the place where the proximal and distal centrioles attach/associate with the nucleus, connecting the tail to the sperm head. At the base of the nucleus, the proximal centriole develops a concavity where the implantation fossa is formed. Within this complex, we found, just beneath the nuclear envelope, the basal plate and, below it, the capitulum. The central portion of the capitulum directly associates with the axial filament (distal centriole), and its marginal portions associate with the anterior part of the nine outer dense fibers, forming the segmented columns. Lateral to this complex, we observed a small amount of redundant nuclear membrane and below, the beginning of the midpiece.

**Midpiece.** The midpiece is composed of the axial filament, which is surrounded by the nine outer dense fibers; these are surrounded by the mitochondrial sheath. This sheath is slightly shorter and contains ~35 mitochondrial gyres, which are helically organized around the longitudinal outer dense fibers; one pair of mitochondria comprises a gyre. The mitochondrial end-to-end junctions are randomly distributed along the course of the helix (Figs. 5A and 5B).

In cross-section, we observed that the outer dense fibers are arranged in a horseshoe fashion and show bilateral symmetry: fiber 1 is the largest and presents a bilobular shape; fibers 3 and 8 remain aligned with the central fibrils of the axial filament complex, forming the dorsoventral axis ( $X$ - $Y$ ), which asymmetrically separates the complex; fibers 5 and 6 are larger than the others. In the anterior portion of the midpiece, the outer dense fibers are surrounded, on their concave surface, by satellite fibers, with fibers 1, 5, and 6 being most numerous. However, the satellite fibers are not present throughout most of the midpiece (Figs. 5A and 5B).

The cytoplasmic droplet was only rarely observed, with the plasma membrane frequently closely applied to the mitochondrial sheath; however, when present, its position was variable; it was observed as high as the neck and as low as the midpiece terminus vicinity. It always contained an abundance of membranes.

We found the circular structure of the annulus in the terminal region of the midpiece. It was closely associated with the plasma membrane; in the anterior portion, it was also associated with last mitochondrial gyre, and in the posterior portion, with the fibrous sheath (Fig. 5E).

**Principal Piece.** The main difference between the midpiece and the principal piece was the mitochondrial sheath in the former and the fibrous sheath in the latter (Fig. 5E). The principal piece is longer than the midpiece.

In the anterior portion of the principal piece, projections from the fibrous sheath extended into the position of the outer dense fibers 3 and 8, forming the longitudinal column that supports the helical fibers of the fibrous sheath (Figs. 5A and 5B). Similarly, the remaining outer dense fibers tended to diminish in diameter from the anterior to posterior, disappearing in the middle portion of the principal piece; the fibrous sheath projections tended to diminish throughout the principal piece.



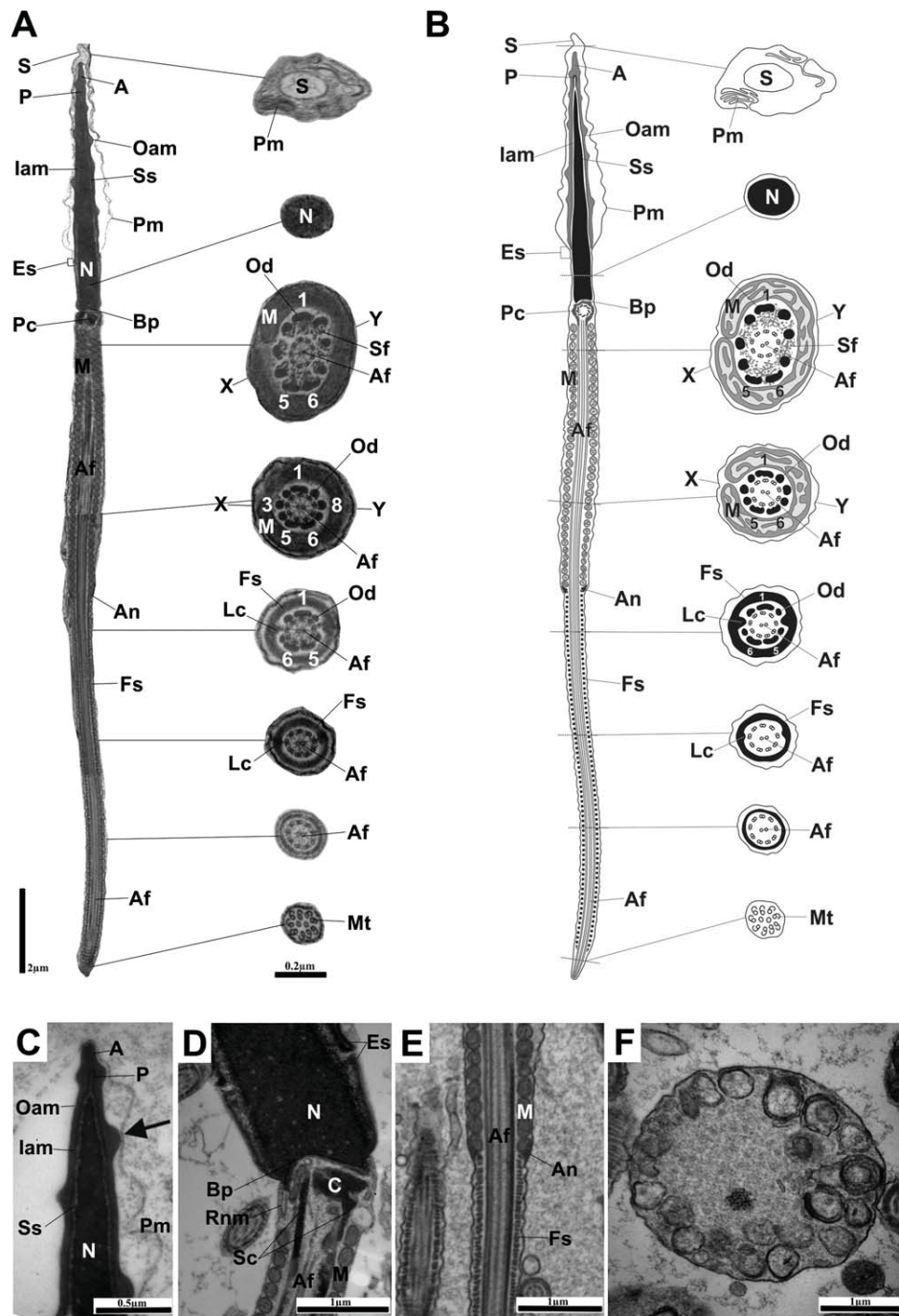


Fig. 5. Schematic figure of the ultrastructure of the spermatozoon of *Molossus molossus* in transmission (TEM). **A:** Ultrastructure of the spermatozoon in longitudinal and corresponding transverse sections. Drawn from several TEM micrographs. **B:** Corresponding diagram of a *M. molossus* spermatozoon in longitudinal and corresponding transverse sections. **C:** TEM micrograph of the head region. Note the presence of the perforatorium and acrosomal projections (arrow). **D:** TEM micrograph of the neck region. **E:** TEM micrograph of the transitional region from the midpiece to the principal piece. Note the change of the mitochondrial sheath for the fibrous sheath and the presence of

the annulus. **F:** TEM micrograph of the residual body. (A, acrosome; Af, axial filament; An, annulus; Bp, basal plate; C, capitulum; Es, equatorial segment; Fs, fibrous sheath; Iam, inner acrosomal membrane; Lc, longitudinal column; M, mitochondria; Mt, microtubules; N, nucleus; Oam, outer acrosomal membrane; Od, outer dense fibers; P, perforatorium; Pc, proximal centriole; Pm, plasma membrane; Rnm, redundant nuclear membrane; S, space between the plasma membrane and the outer dense membrane; Sc, segmented column; Sf, satellite fibers; Ss, subacrosomal space; X-Y, Axis X-Y).

**End Piece (Figs. 5A and 5B).** The transition from principal piece to end piece was not easily observed, but cross-sections of end pieces were frequently noted. The uppermost level of the end piece had only the axial filament enclosed by the plasma membrane; throughout its length, the organization of the axial filament was lost; at the terminus of the end piece, there were only 11 microtubules, without a distinct form.

#### Auxiliary Cells

**Sertoli Cell.** As in other mammals, the Sertoli cells of *M. molossus* are irregular cells that extend from the basal lamina to the lumen of the seminiferous tubules and envelope all the associated germ cells. They present two different regions: basal and apical.

The basal region corresponds to the lowest part of the epithelium, which is closely associated with the basal lamina. It usually contains the nucleus, which is large and irregularly shaped, displaying large infoldings; there is a highly euchromatic and homogeneous nucleoplasm, very little heterochromatin, and a prominent nucleolus (Figs. 6A and 6B). The nucleus may be more closely associated with the basal lamina, showing a more horizontally elongated shape (Fig. 6A) or be farther away, showing a vertically elongated shape (Fig. 6B), depending on the stage of the seminiferous epithelium cycle.

The basal cytoplasm was occupied by many mitochondria (Fig. 6A), electron-dense bodies (Fig. 6B), few extensions of *lamellae anellata* (Fig. 6B), the endoplasmic reticulum, and the Golgi complex.

The apical region had a high concentration of subcellular structures, including Golgi complexes and mitochondria (Fig. 6C), a large amount of endoplasmic reticulum (Fig. 6D), ribosomes, and a large amount of *lamellae anellata* (Figs. 6E–6G), surrounding the differentiating spermatids (Fig. 6C). This region also had a large number of intercellular junctions (Fig. 6H).

**Leydig Cell.** The Leydig cells make up the largest portion of the interstitial tissue of *M. molossus*. They are irregular cells, which may be found singly or in clusters. Their nuclei are generally large, undefined (ranging from circular to oval), with a greater portion of granular euchromatin and clusters of heterochromatin located in some regions throughout the nucleus and associated with the nuclear envelope; they have a single and large nucleolus (Fig. 6I).

The cytoplasm is extensive, with a large portion occupied by the endoplasmic reticulum (Figs. 6I–6K), predominantly in the smooth form, along with mitochondria (Figs. 6I–6K) and spherical bodies (Figs. 6I–6K). The reticulum is organized as a compact network of anastomosing cisterns that surround the nucleus and other organelles. The mitochondria present a wide variety of formats, from elongated with transverse cristae (Fig. 6J), to circular with waveform cristae (Fig. 6K).

Two spherical bodies were observed: lipid droplets and electron-dense bodies. The lipid droplets were relatively large, round-shaped, with a pale and homogeneous component, and they were not surrounded by membranes (Figs. 6I–6K). The electron-dense bodies resembled endosomal-lysosomal bodies; they were frequently seen near the cell surface and near the lipid droplets (Fig. 6I).

#### DISCUSSION

The process of spermatogonial differentiation in *M. molossus* appears to be similar to that of other bats (Beguelini et al., 2009, 2011a; Lee, 2003; McGuckin and Blackshaw, 1987; Saidapur and Patil, 1992; Singwi and Lall, 1983) and to be closely related to that known for Primates (Cavicchia and Dym, 1978; Ehmcke et al., 2005, 2006), with three main spermatogonia types: A<sub>d</sub>, A<sub>p</sub>, and B. As we found in a previous study (Beguelini et al., 2011a), the A<sub>d</sub> spermatogonia is the “true” spermatogonial stem cell, which divides mitotically, re-establishing the number of stem cells and forming type A<sub>p</sub>; this latter type is more active and divides mitotically, producing type B, which is the cell destined to differentiate and enter into meiotic division. This process is similar in most species of bats.

The meiotic divisions proceed in a manner similar to those of most mammals, with the formation of the synaptonemal complexes, gradual nuclear condensation around them, and consequent nucleolar disruption. The observation of nucleolar fragmentation and the scattering of nucleolar fragments throughout the nucleus in pachytene spermatocytes is similar to what was observed in our previous studies (Beguelini et al., 2011a,b); similarly, the observation of nucleolar components in the cytoplasm during meiotic division demonstrated that dislocation of nucleolar components from the nucleus to the cytoplasm occurs frequently.

The spermiogenesis process tends to be species-specific, presenting different characteristics in each species. The number of steps in spermatid differentiation in bats varies widely, from 9 in *Myotis macrodactylus* (Lee, 2003), 10 in *Rhinolophus ferrumequinum korai* (Lee et al., 1992), 13 in *Pteropus vampyrus* and *Rhinolophus cornutus* (Morigaki et al., 2001), 14 in *Rousettus leschenaulti* (Saidapur and Patil, 1992), to 16 steps in *Rhinopoma kinneari* (Singwi and Lall, 1983). Although *M. molossus* belongs to a different family than *Platyrrhinus lineatus*, another Neotropical species (Beguelini et al., 2011a), it also had 12 steps in the spermiogenesis process.

The process of acrosome formation in *M. molossus* is similar to that found in other mammals; the acrosome is formed by proacrosomal vesicles that already contain an electron-dense granule (Kurohmaru et al., 1994; Segatelli et al., 2000; Suphamungmee et al., 2008); however, it differs from that found in *P. lineatus*, which produces two different types of proacrosomal vesicles (Beguelini et al., 2011a). On the other hand, the many wavy acrosomal projections on the acrosomal surface that we found in *M. molossus* seems to be rare. Berrios et al. (1978) observed similar projections in a South American rodent, *Octodon degus*, and Nicander and Bane (1966), in lagomorphs; however, the quantity, positioning, and shape were different from the *M. molossus*. Breed and Leigh (1985) also observed these projections in three genera of Australian molossid bats (*Chaerophon*, *Mormopterus*, and *Tadarida*); consequently, this characteristic appears to be common in the Molossidae.

Comparing the ultrastructure of the spermatozoon of *M. molossus* with other bats already studied, we observed that three characters vary: morphology of the outer dense fibers, presence and morphology of the perforatorium/apical body, and spermatozoon head morphology.



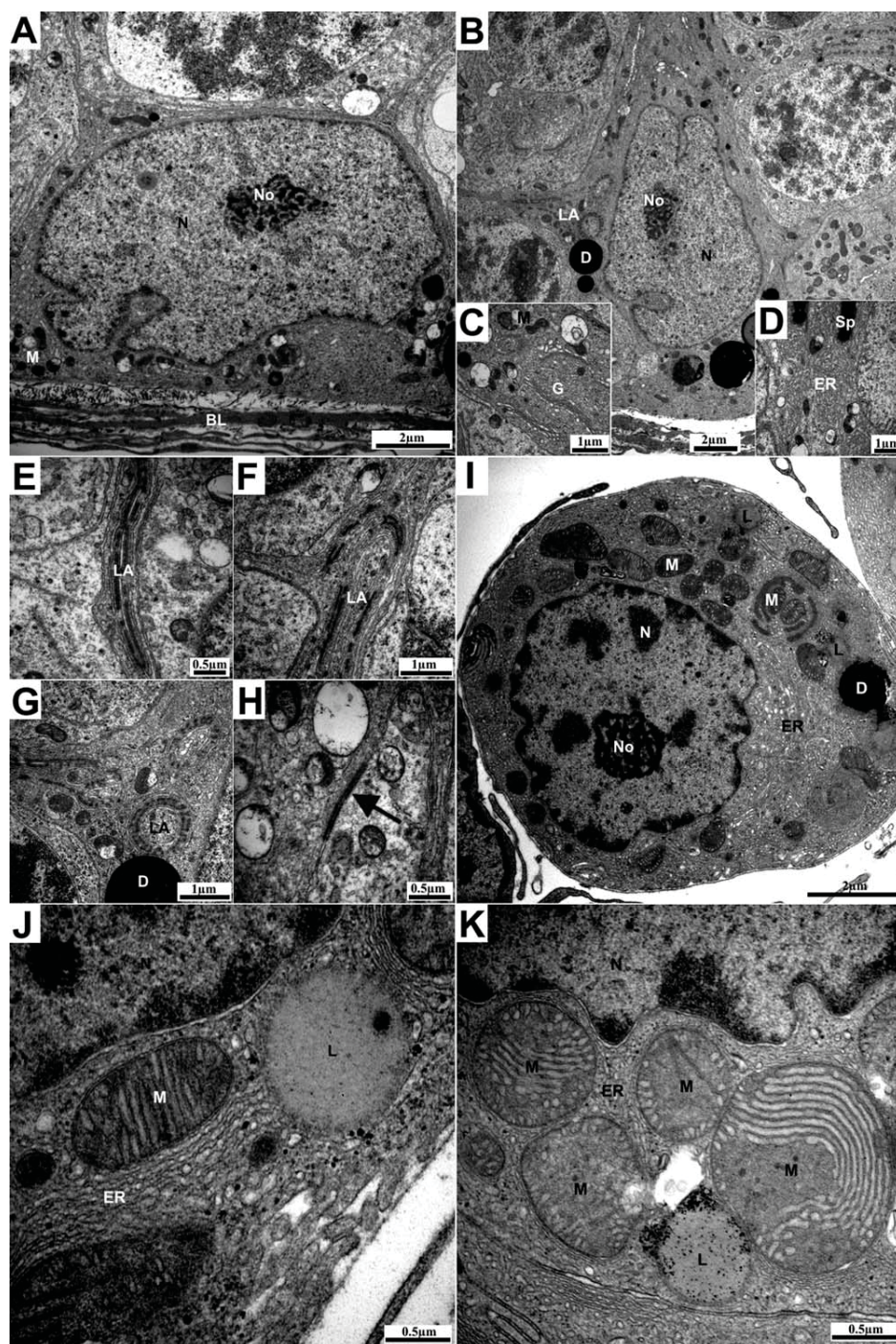


Fig. 6. Electron micrographs of the auxiliary cells of the bat *Molossus molossus*. A-H: Sertoli cells. I-K: Leydig cells. A, B: The basal region of a Sertoli cell. Note the large, irregularly and horizontally elongated shaped nucleus with large infoldings and a prominent nucleolus, and the perinuclear cytoplasm, which contains many mitochondrial clusters (A). Depending on the stage of the seminiferous epithelium cycle in that the epithelium is found, the nucleus may have a vertically elongated shape (B). C-H: Apical region. Note the high concentration of subcellular structures, including the Golgi complexes and mitochondria (C) and the endoplasmic reticulum (D), the large amount of lamellae anellata (E-G), and the presence of intercellular

junctions (H, arrow). I: Note the large and undefined nuclei of the Leydig cell, with a greater portion of granular euchromatin and clusters of heterochromatin localized at some regions throughout the nucleus and associated with the nuclear envelope, the single and large nucleolus and the large amount of endoplasmic reticulum, mitochondria and spherical bodies. J, K: Cytoplasm of Leydig cells. Note that the mitochondria present a wide variety of formats, from elongated with transverse cristae (J) to circular with waveforms cristae (K). (BL, basal lamina; D, electron-dense bodies; ER, endoplasmic reticulum; G, Golgi complex; L, lipid droplets; LA, lamellae anellata; M, mitochondria; N, nucleus; No, nucleolus; Sp, spermatid).



The morphology of the outer dense fibers presented two different patterns: one with the outer dense fibers 1, 5, 6, and 9 larger than the others and the other with only 1, 5, and 6 being larger. The first pattern includes the Rhinolophidae (Lee et al., 1992; Oh et al., 1985; Sang-Sick et al., 1999), Miniopteridae (Sang-Sick et al., 1999), and Vespertilionidae (Fawcett and Ito, 1965; Lee, 2003; Son et al., 1997) species, and the second includes the Neotropical species *M. molossus*—Molossidae (present study) and *P. lineatus*—Phyllostomidae (Beguelini et al., 2011a).

The perforatorium is absent or poorly developed in the Vespertilionidae (Fawcett and Ito, 1965) and Noctilionidae (Phillips et al., 1997), little developed in the Rhinolophidae (Lee et al., 1992; Oh et al., 1985), and well developed in the Molossidae (Breed and Leigh, 1985, present study) and *P. lineatus*—Phyllostomidae (Beguelini et al., 2011a).

Unusual characters in the spermatozoon head are also typical in some families, such as the extraordinarily large, flat, and eccentrically inserted head with accordion-like folds of the Noctilionidae (Phillips et al., 1997) and the many wavy acrosomal projections of the Molossidae (Breed and Leigh, 1985, present study).

The great similarity of morphological characters between *M. molossus* and *P. lineatus* suggests that *M. molossus* is more closely related to the Phyllostomidae (Beguelini et al., 2011a) than to Rhinolophidae and Vespertilionidae.

#### ACKNOWLEDGMENTS

The authors thank Luiz Roberto Falleiros Junior and Rosana Silistino de Souza Santos for their technical help and Raduan Alexandre Soleman for preparing the spermatozoa diagram. A scholarship awarded to Mateus Rodrigues Beguelini by the Brazilian Research Foundation (CAPES) and the financial support by Fundação de Amparo à Pesquisa do Estado de São Paulo Grant n° 2009/16181-9 are also gratefully acknowledged.

#### REFERENCES

- Adachi Y, Kurohmaru M, Hattori S, Hayashi Y. 1992. Spermatogenesis in the Watase's shrew, *Crocidura watasei*. A light and electron microscopic study. *Exp Anim* 41:295–303.
- Beguelini MR, Moreira PRL, Faria KC, Marchesin SRC, Morielle-Versute E. 2009. Morphological characterization of the testicular cells and seminiferous epithelium cycle in six species of Neotropical bats. *J Morphol* 270:943–953.
- Beguelini MR, Sergio BFS, Leme FLJ, Taboga SR, Morielle-Versute E. 2010. Morphological and morphometric characteristics of the epididymis in the Neotropical bats *Eumops glaucinus* and *Molossus molossus* (Chiroptera: Molossidae). *Chiropt Neotrop* 16:769–779.
- Beguelini MR, Puga CCI, Taboga SR, Morielle-Versute E. 2011a. Ultrastructure of spermatogenesis in the white-lined broad-nosed bat, *Platyrrhinus lineatus* (Chiroptera: Phyllostomidae). *Micron* 42:586–599.
- Beguelini MR, Marchesin SRC, Azeredo-Oliveira MTV, Morielle-Versute E. 2011b. Nucleolar behavior during meiosis in four species of phyllostomid bats (Chiroptera, Mammalia). *Genet Mol Res* 10:552–565.
- Berrios M, Fléchon JE, Barros C. 1978. Ultrastructure of *Ocotodon degus* spermatozoa with special reference to the acrosome. *Am J Anat* 151:39–54.
- Breed WG, Leigh C. 1985. Sperm head morphology of Australian molossid bats with special reference to the acrosomal structure. *Mammalia* 49:403–406.
- Cavicchia JC, Dym M. 1978. Ultrastructural characteristics of monkey spermatogonia and preleptotene spermatocytes. *Biol Reprod* 18:219–228.
- Costa DS, Paula TAR. 2003. Espermatogênese em mamíferos. *Scientia* 4:53–72.
- Costa GC, Vieira GHC, Teixeira RD, Garda AA, Colli GR, Bão SN. 2004. An ultrastructural comparative study of the sperm of *Hyla pseudopseudis*, *Scinax rostratus*, and *S. squalirostris* (Amphibia: Anura: Hylidae). *Zoomorphology* 123:191–197.
- Crichton EG, Krutzsch PH. 2000. Reproductive biology of bats. London: Academic Press, UK.
- De Knecht LV, Silva JA, Moreira EC, Sales GL. 2005. Morcegos capturados no município de Belo Horizonte, 1999–2003. *Arq Bras Med Vet Zootec* 57:576–583.
- Eger JL. 2007. Family Molossidae. In: *Mammals of South America: Marsupials, Xenarthrans, Shrews and Bats*. Gardner AL, editor. Chicago: University Chicago Press. pp. 399–439.
- Ehmcke J, Luetjens CM, Schlatt S. 2005. Clonal organization of proliferating spermatogonial stem cells in adult males of two species of non-human Primates, *Macaca mulatta* and *Callithrix jacchus*. *Biol Reprod* 72:293–300.
- Ehmcke J, Wistuba J, Schlatt S. 2006. Spermatogonial stem cells: Question, models and perspectives. *Hum Reprod Upd* 12:275–282.
- Encarnação JA, Dietz M, Kierdorf U. 2004. Reproductive condition and activity pattern of male Daubenton's bats (*Myotis daubentonii*) in the summer habitat. *Mammal Biol* 69:163–172.
- Fabián ME, Marques RV. 1989. Contribuição ao conhecimento da biologia reprodutiva de *Molossus molossus* Pallas, 1766 (Chiroptera, Molossidae). *Ver Bras Zool* 6:603–610.
- Fawcett DW, Ito S. 1965. The fine structure of bat spermatozoa. *Am J Anat* 116:567–610.
- Fleming TH, Hooper ET, Wilson DE. 1972. Three Central American bat communities: Structure, reproductive cycles and movement patterns. *Ecology* 53:555–569.
- Footo RH, Swierstra EE, Hunt WL. 1972. Spermatogenesis in the dog. *Anat Rec* 173:341–352.
- Garda AA, Costa GC, Colli GR, Bão SN. 2004. Spermatozoa of Pseudinae (Amphibia, Anura, Hylidae), with a test of the hypothesis that sperm ultrastructure correlates with reproductive modes in Anurans. *J Morphol* 261:196–205.
- Giughiano LG, Teixeira RD, Colli GR, Bão SN. 2002. Ultrastructure of spermatozoa of the lizard *Ameiva ameiva*, with considerations on polymorphism within the family Teiidae (Squamata). *J Morphol* 253:264–271.
- Jamieson BGM. 1995. Evolution of tetrapod spermatozoa with particular reference to amniotes. In: Jamieson BGM, Ausio J, Justine JL, editors. *Advances in spermatozoal phylogeny and taxonomy*. Paris: Mémoires du Muséum National d'Histoire Naturelle. pp. 343–358.
- Kurohmaru M, Kobayashi H, Hattori S, Nishida T, Hayashi Y. 1994. Spermatogenesis and ultrastructure of a peculiar acrosomal formation in the musk shrew, *Suncus murinus*. *J Anat* 185:503–509.
- Kurohmaru M, Saruwatari T, Kimura J, Mukohyama M, Watanabe G, Taya K, Hayashi Y. 2002. Seasonal changes in spermatogenesis of Japanese Lesser Horseshoe bat, *Rhinolophus cornutus* from a morphological viewpoint. *Okajimas Folia Anat Japan* 79:93–100.
- Lee JH. 2003. Cell differentiation and ultrastructure of the seminiferous epithelium in *Myotis macrodactylus*. *Kor J Electron Microsc* 33:25–39.
- Lee JH, Choi BJ, Son SW. 1992. Spermiogenesis in the Korean Greater Horseshoe Bat, *Rhinolophus ferrumequinum korai*. *Kor J Electron Microsc* 22:97–117.
- Lin M, Jones RC. 2000. Spermiogenesis and spermiation in a monotreme mammal, the platypus, *Ornithorhynchus anatinus*. *J Anat* 196:217–232.
- Lin M, Harman A, Rodger JC. 1997. Spermiogenesis and spermiation in a marsupial, the tammar wallaby (*Macropus eugenii*). *J Anat* 190:377–395.
- Matsumoto AM. 1996. Spermatogenesis. In: Adashi EY, Rock JA, Rosenwaks Z, editors. *Reproductive Endocrinology, Surgery and Technology*. Philadelphia: Lippincott-Raven. pp. 360–384.
- McGuckin MA, Blackshaw AW. 1987. Cycle of the seminiferous epithelium in the grey-headed fruit bat, *Pteropus poliocephalus*. *Aust J Biol Sci* 40:203–210.
- Morigaki T, Kurohmaru M, Kanai Y, Mukohyama M, Hondo E, Yamada J, Agungpriyono S, Hayashi Y. 2001. Cycle of the seminiferous epithelium in the Java fruit bat (*Pteropus vampyrus*) and the Japanese Lesser Horseshoe bat (*Rhinolophus cornutus*). *J Vet Med Sci* 63:773–779.
- Nicanter L, Bane A. 1966. Fine structure of the sperm head in some mammals with particular reference to the acrosome and subacrosomal substance. *Zeitschrift Zellforschung Mikrosk Anatom* 72:496–514.
- Oh YK, Mori T, Uchida TA. 1985. Spermiogenesis in the Japanese Greater Horseshoe Bat, *Rhinolophus ferrumequinum Nippon*. *J Fac Agric Kyushu Uni* 29:203–209.

- Osman DI, Ploen L. 1986. Spermatogenesis in the camel (*Camelus dromedarius*). *Anim Reprod Sci* 10:23–26.
- Oud JL, de Rooij DG. 1977. Spermatogenesis in the Chinese hamster. *Anat Rec* 187:113–124.
- Painter TS. 1923. Studies in mammalian spermatogenesis. II. The spermatogenesis of man. *J Exper Zool* 37:291–336.
- Phillips DM, Rasweiler JJ, Murwali F. 1997. Giant, accordioned sperm acrosomes of the greater bulldog bat, *Noctilio leporinus*. *Mol Reprod Dev* 48:90–94.
- Racey PA, Tam WH. 1974. Reproduction in male *Pipistrellus pipistrellus* (Mammalia: Chiroptera). *J Zool* 172:101–122.
- Reis NR, Peracchi AL, Pedro WA, Lima IP. 2007. Morcegos do Brasil. Londrina: Universidade Estadual de Londrina.
- Saidapur SK, Patil SB. 1992. Kinetics of spermatogenesis in megachiropteran bat, *Rousettus leschenaulti* (Desmarest): Seminiferous epithelial cycle, frequency of stages, spermatogonial renewal and germ cell degeneration. *Ind J Exp Biol* 30:1037–1044.
- Sang-Sick K, Jung-Hun L, Sung-Won S, Byung-Jin C. 1999. Morphological comparison of spermatozoa in the Korean greater horseshoe bat (*Rhinolophus ferrumequinum korai*) and long-fingered bat (*Miniopterus schreibersi fuliginosus*). *Kor J Electron Microsc* 29:1–10.
- Segatelli TM, Almeida CCD, Pinheiro PFF, Martinez M, Padovani CR, Martinez FE. 2000. Ultrastructural study of acrosome formation in Mongolian gerbil (*Meriones unguiculatus*). *Tissue Cell* 32:508–517.
- Sharifi M, Ghorbani R, Akmal V. 2004. Reproductive cycle in *Pipistrellus kuhlii* (Chiroptera, Vespertilionidae) in western Iran. *Mammalia* 68:323–327.
- Simmons NB. 2005. Order Chiroptera. In: Wilson DE, Reeder DM, editors. *Mammal species of the world: A taxonomic and geographic reference*. Baltimore: Johns Hopkins University Press. pp. 312–529.
- Singwi MS, Lall SB. 1983. Spermatogenesis in the non-scrotal bat—*Rhinopoma kinneari* Wroughton (Microchiroptera: Mammalia). *Acta Anatom* 116:136–145.
- Son SW, Lee JH, Cheon HM. 1997. Spermiogenesis in the Korean Daubenton's Bat (*Myotis daubentonii ussuriensis*). *Dev Reprod* 1:9–24.
- Soon-Jeong J, Joo-Cheol P, Heung-Joong K, Chun SB, Myung-Hee Y, Do-Seon L, Moon-Jin J. 2006. Comparative fine structure of the epididymal spermatozoa from three Korean shrews with considerations on their phylogenetic relationships. *Biocell* 30:279–286.
- Suphamungmee W, Wanichanon C, Vanichviriyakit R, Sobhon P. 2008. Spermiogenesis and chromatin condensation in the common tree shrew, *Tupaia glis*. *Cell Tissue Res* 331:687–699.
- Swierstra EE, Foote RH. 1963. Cytology and kinetics of spermatogenesis in the rabbit. *J Reprod Fertil* 5:309–322.
- Venable JH, Coggeshall RA. 1965. A simplified lead citrate stain for use in electron microscopy. *J Cell Biol* 25:407–408.
- Vieira GHC, Colli GR, Bao SN. 2005. Phylogenetic relationships of corytophanid lizards (Iguania, Squamata, Reptilia) based on partitioned and total evidence analyses of sperm morphology, gross morphology, and DNA data. *Zool Scripta* 34:605–625.
- Wodsdalek JE. 1914. Spermatogenesis of the horse with special reference to the accessory chromosome and chromatoid body. *Biol Bull* 27:295–326.
- Watson ML. 1958. Staining tissue section of electron microscopy with heavy metals. *J Biophys Biochem Cytol* 4:475–478.



## V. CAPÍTULO 3

**Ultrastructural characteristics of the spermatogenesis in Black  
Myotis Bat, *Myotis nigricans* (Chiroptera: Vespertilionidae),  
during the four phases of its annual reproductive cycle**

Artigo a ser submetido à publicação na revista “Reproduction, Fertility and Development”.

**Ultrastructural characteristics of the spermatogenesis in Black Myotis Bat, *Myotis nigricans* (Chiroptera: Vespertilionidae), during the four phases of its annual reproductive cycle**

Mateus R. Beguelini<sup>A</sup>, Sebastião R. Taboga<sup>A</sup>, Eliana Morielle-Versute<sup>B\*</sup>

<sup>A</sup>*Department of Biology, UNESP – Univ Estadual Paulista, São José do Rio Preto, São Paulo, Brazil, 15054-000;*

<sup>B</sup>*Department of Zoology and Botany, UNESP – Univ Estadual Paulista, São José do Rio Preto, São Paulo, Brazil, 15054-000*

**Running head:** Active and inactive testes of *Myotis nigricans*.

\*Corresponding author: Eliana Morielle-Versute – Rua Cristóvão Colombo n° 2265, Jardim Nazareth, 15054-000, São José do Rio Preto, São Paulo, Brazil. Tel.: +55 17 32212369. FAX: + 55 17 32212374. E-mail address: morielle@ibilce.unesp.br

**ABSTRACT**

*Myotis nigricans* is an endemic species of vespertilionid bat, from the Neotropical region, that resembles temperate zone bats in their reproductive cycle; presenting an annual reproductive cycle dotted of two process of testicular regression. Thus, this study aimed to ultrastructurally evaluates the process of spermatogenesis and the morphological changes of spermatogenic cells during the four phases of its annual reproductive cycle. Its annual reproductive cycle could be divided into four phases: active; deactivating; regressed and reactivating periods; with all presenting distinct characteristics. The active period was similar to other bats, presenting the complete occurrence of the spermatogenesis, with three main types of spermatogonia: A<sub>d</sub>, A<sub>p</sub> and B; and 12 steps in spermatid differentiation; however, it differed having the outer dense fibers 1, 5, 6 and 9 larger than the others. These three types of spermatogonia suffer considerably morphologic changes from deactivating to the regressed period, and in the reactivating, they return to the basic morphology, reactivating the spermatogenesis. In conclusion, our study described the process of spermatogenesis, the ultrastructure of the spermatozoa and the distinct morphologic variations in the ultrastructure of the spermatogenic cells of *M. nigricans* during the four different periods of its annual reproductive cycle.

**Keywords:** Spermogenesis, Testicular regression.

## INTRODUCTION

*Myotis nigricans* is an endemic species of vespertilionid bat, from the Neotropical region, which present unique characteristics regarding its reproductive pattern. Wilson and Findley (1971) and Krutzsch (1979) proposed that its reproductive cycle is geographically variable, with animals from Paraguay presenting an active pattern trough the year; from Panama presenting an active pattern during most of the year, but becomes reproductively quiescent for approximately three months; and animals from Mexico more closely resembling temperate zone bats in their reproductive condition at certain times of the year.

Similarly, Beguelini *et al* (2012a) demonstrated that animals from São Paulo State - Brazil, resembles temperate zone bats in their reproductive cycle, however, their annual reproductive cycle present not one but two process of testicular regression, a pattern never observed in any other species. The authors also observed that the two period of regression were not linked to apoptotic process and that this pattern seems to be not directly linked to any seasonal abiotic variation.

Recently, the process of spermatogenesis in bats has been object of a number of studies (Morigaki *et al.* 2001; Kurohmaru *et al.*, 2002; Lee 2003; Lee and Mori 2004; Sharifi *et al.* 2004; Beguelini *et al.* 2009; Beguelini *et al.* 2011a; Beguelini *et al.* 2012b). Despite, the main events are similar in most species, variations in the process among and within families and taxa are frequently observed (Fawcett and Ito 1965; Singwi and Lall 1983; Breed and Leigh 1985; Oh *et al.* 1985; Lee *et al.* 1992; Saidapur and Patil 1992; Son *et al.* 1997; Phillips *et al.* 1997; Sang-Sick *et al.* 1999; Beguelini *et al.* 2011a; Beguelini *et al.* 2011b). However, studies related to the ultrastructural investigation of the process of testicular regression and activation are scarce or nonexistent.

Due to all these interesting characteristics and the lack of information about the reproduction of this species in South America, the aim of this study was to ultrastructurally

characterize its spermatogenesis and to evaluate the differences between the phases of their reproductive cycle (active, deactivating, regressed and reactivating periods).

## **MATERIALS AND METHODS**

### ***Study Area, Capture and Licenses***

The animals were collected in the city of São José do Rio Preto, in northwest of São Paulo State, Brazil, (49W22'45" 20S49'11"). The capture was performed between September 2008 and February 2009 at night, using five mist-nets (3 m x 6 m) set to intercept bats flying 1–3 m above the ground. The nets were precisely set on possible flight paths or exit shelters.

The capture and captivity of bats were authorized by the Brazilian institution responsible for wild animal care (Instituto Brasileiro do Meio Ambiente, IBAMA – Processes: 02027.001957/2006-02 and 21707-1) whereas the ethics committee at São Paulo State University (UNESP) authorized all experimental procedures (Process: 013/09 – CEEA). The animals were treated according to the recommendations of the Committee on Care and Use of Laboratory Animals from the Institute of Laboratory Animal Resources, National Research Council, “Guide for the Care and Use of Laboratory Animals” (Committee on Care and Use of Laboratory Animals, 1980).

### ***Species, Aging and Experiment***

The species analyzed was the exclusively Neotropical Vespertilionidae bat, *Myotis nigricans*. It is not listed as endangered in the International Union for Conservation of Nature (IUCN) Red List of Threatened Species, however, it is a scarce and difficult to collect species, thus we took care to not disturb the females and only few adult males were used in this study.

The bats were aged as adult based on the body weight, complete ossification of the metacarpal-phalangeal epiphyses, wear of the teeth (De Knecht *et al.* 2005), positioning of the testes and the presence of sperm inside the testes and/or cauda epididymis.

Twenty sexually male mature specimens were used in this study, with five animals collected in each period of the testicular cycle (four sample groups): 1. active (September); 2. deactivating (October); 3. regressed (November); 4. reactivating (January-February). These periods of collection were determined based on the reproductive cycle of the species, described by Beguelini *et al.* (2012a).

### ***Processing of Animals***

After the sacrifice of animals by cervical dislocation, the testes and epididymis were removed, perforated and fixed by immersion in a solution of 3% glutaraldehyde plus 0.25% tannic acid in Millonig buffer (pH 7.3) containing 0.54% glucose for 24 h. After washing with the same buffer, the samples were post-fixed with 1% osmium tetroxide for 2 hours, dehydrated in graded series of acetone, and included in Araldite 502 Resin (Electron Microscopy Sciences, Hatfield, PA, USA). Ultrathin sections (50 nm) were made using diamond knives, stained with 2% uranyl acetate for 30 minutes, followed by 2% lead citrate in sodium hydroxide for 10 minutes and analyzed in a Leo-Zeiss 906 Transmission Electron Microscope (Cambridge, United Kingdom) at the "Prof. Dr. Celso Abbade Mourão" Center for Microscopy (IBILCE-UNESP).

All the specimens are housed in the Chiroptera collection at the São Paulo State University (DZSJRP- UNESP).

## RESULTS

### *Active Period: Spermatogenesis*

During the active period, the process of spermatogenesis occurred completely and naturally: the mitotic divisions of the spermatogonia generated the spermatocytes, which by meiotic divisions produced the spermatids that passed by spermiogenesis, transforming them into spermatozoa. Despite the regular function of the epithelium, the well-defined fixed cell associations of the seminiferous epithelium cycle were not observed even in this period; where different types of associations were presented: two spermatocytes generations associated with two or three types of spermatids to stages with only pre-leptotene spermatocytes and two types of spermatids.

Despite the asynchrony in the seminiferous epithelium cycle, *M. nigricans* also presented three main types of spermatogonia, during the active period: the dark type A - A<sub>d</sub>, the pale type A - A<sub>p</sub> and type B.

### *Spermatogonia*

The type A<sub>d</sub> spermatogonia was always enclosed in the basal compartment of the germinal epithelium, surrounded by Sertoli cells and adhered to the basal lamina, forming projections and depressions with it. It was in contact, in the upper regions, with spermatocytes or directly with spermatids. Its nucleus contained a finely granular and highly electron-dense chromatin (with clusters of condensed chromatin) and from one to three large, granular/fragmented and irregularly shaped nucleoli (**Fig. 1A-B**). It presented a cytoplasm also intensely stained, doted of some mitochondria, few extensions of endoplasmic reticulum (smooth and rough), Golgi complex and fine cytoplasmatic granulations, ribosomes and/or glycogen (**Figs. 1A**).

The type  $A_p$  presented a less pronounced adhesion to the basal lamina, showing projections and depressions lower than type  $A_d$ , and it was also surrounded by Sertoli cells in the basal compartment (**Fig. 1C**). It had an oval nucleus, containing a finely granular homogeneous chromatin and a larger cytoplasm, with mitochondria, a few extensions of endoplasmic reticulum (**Fig. 1E**), Golgi complex and fine cytoplasmic granulations (ribosomes and/or glycogen). It is interesting to observe the presence of large chromatoid bodies in this type of spermatogonia (**Fig. 1D**).

The Type B spermatogonia started the process of ascension into the adluminal compartment, gradually dislocating the cytoplasm to the upstream regions of the basal compartment (**Fig. 1F**), consequently losing contact with the basal lamina (**Fig. 1G**). It had a round nucleus containing homogeneous chromatin but with clumps of condensed chromatin mainly associated with the nuclear envelope (**Fig. 1F**), and presented from one (**Fig. 1F**) to three (**Fig. 1G**) large nucleoli. The organelles presented in their cytoplasm were similar to those of type  $A_p$ , and the chromatoid body was also observed (**Fig. 1G**).

#### *Meiotic Phases: The Spermatocytes*

During this phase, groups of type B spermatogonia moved away from the basal lamina to the adluminal compartment, transforming them in spermatocytes and entering in meiotic division. During the divisions, the most evident changes corresponded to the chromatin condensation, the formation of synaptonemal complexes and the nucleolar disruption.

The process of chromatin condensation began early in leptotene spermatocytes (**Fig. 2A**) and proceeded gradually, mainly on the periphery of the synaptonemal complexes (**Figs. 2A-D**), forming distinctive blocks (the homologues chromosomes) that achieved their higher condensation in metaphases (**Fig. 2F**).



The structure of the synaptonemal complexes, which resembles a ribbon that presents three laterally juxtaposed portions, were first observed in leptotene spermatocytes and tended to disappear in final diplotene diakinesis (**Figs. 2A-D**).

Along with the formation of the synaptonemal complexes and the gradual onset of chromatin condensation, the nucleolar disruption occurred. Despite the nucleoli of *M. nigricans* already presented a fragmented shape since spermatogonia, during the meiotic phase, these nucleoli suffered a more accentuated process of fragmentation, which began early in leptotene spermatocytes (**Fig. 2A**), gradually extended (**Fig. 2B-D**) still the diakinesis and seemed to end in metaphases, where the nucleolar fragments are no longer found (**Fig. 2F**). It is interesting to note the presence of a great amount of *lamellae anellata* during the meiotic phase (**Fig. 2E**).

In metaphases, the chromatin condensation peaked, while the synaptonemal complexes and the nucleolar fragments were unobservable (**Fig. 2F**). After the alignment of the chromosomes, the spindle fibers were gradually shortened during anaphase and the nuclear envelope was restored (telophase) giving rise to two secondary spermatocytes (**Fig. 2G**). These came in rapid cell division (meiosis II), producing four haploid spermatids, which underwent cellular differentiation (spermiogenesis), transforming them into spermatozoa. The limited time during which these events occur hampers observation of these phases (meiosis II) by electron microscopy.

### *Spermiogenesis*

Based on ultrastructural characteristics, the differentiation of spermatids could be clearly divided into 12 steps: steps 1-4 corresponded to the Golgi phase of spermatid development, steps 5-8 to the cap phase, steps 9-10 to the acrosomal phase and steps 11-12 to the maturation phase.

*Step 1 spermatids*

The step 1 spermatids corresponded to the cells newly formed from the second meiotic division, presented little differentiation and were the cells destined to enter into process of spermiogenesis. They had a spherical nucleus containing a finely granular homogeneous chromatin, with most often a single and compact nucleolus (**Fig. 3A**). Few extensions of endoplasmic reticulum and mitochondria were dispersed throughout their cytoplasm, and a Golgi complex associated with small vesicles, which are the precursors of the proacrosomal vacuole, was also observed (**Fig. 3B**). It is interesting to note the intercellular bridges that connect adjacent spermatids, forming something that resembles a syncitium (**Fig. 3A**).

*Step 2 spermatids*

In this step the Golgi complex underwent a process of development, increasing in size and number of cisterns, and also increasing the production of proacrosomal vesicles, which started to fuse with each other to form large proacrosomal vesicles (**Fig. 3C**). It is interesting to note the proximity of the chromatoid body to this complex. Other cellular organelles were similar to those observed in Step 1 spermatids.

*Step 3 spermatids*

The morphology of this step was very similar to that observed in Step 2 spermatids; however, now the numerous proacrosomal vesicles fused, forming a large proacrosomal vacuole that stayed adjacent to the nucleus (**Fig. 3D-E**). The dislocation of centrioles to the opposite pole to the acrosome formation was also observed. Other cellular organelles were similar to those observed in Step 2 spermatids.

*Step 4 spermatids*

The proacrosomal vacuole greatly increased during this step and attached to the nuclear envelope, forming a concavity in the nucleus (**Fig. 3F** and **H**). The Golgi complex remained associated with/in proximity of the proacrosomal vacuole (**Fig. 3H**), continuously secreting proacrosomal vesicles. By other side, at the opposite pole, the centrioles underwent a considerable process of development, with the formation of the flagellum. Associated with the developing flagellum, connected to the annulus, was observed the presence of a granular electron-dense mass, probably the chromatoid body (**Fig. 3G**).

*Step 5 spermatids*

During this step the acrosome associated more intimately with the nuclear envelope and began to cover the nucleus (**Fig. 3I**). The production and subsequent fusion of proacrosomal vesicles to the acrosome by the Golgi complex continued in this step (**Fig. 3J**).

*Step 6 spermatids*

The acrosome began to condense during this step, presenting a more electron-dense matrix; it compacted and expanded, forming a cap that covers a large surface of the nucleus (**Fig. 3K**). The Golgi complex began to regress while the axoneme extends greatly.

*Step 7 spermatids (Fig. 4A-B)*

During this step the nucleus migrated toward the plasma membrane, the cytoplasm started to migrate to the caudal region of the cell and the acrosomes covered a great portion of the nuclear surface. The fusion of large proacrosomal vesicles to the acrosome was easily observed in this step (**A**, arrows). In the distal region of the acrosome occurred the development of an elevation that is associated with microtubules (**B**, arrows).

*Step 8 spermatids*

In this step we observed the formation of the microtubular manchette, which attached to the elevation of the acrosome, produced in the anterior step, and subsequently assisted in nuclear elongation (**Fig. 4C**); and the dislocation of the cytoplasm to the posterior pole of the cell.

*Step 9 spermatids*

During this step the nuclear elongation evolved (**Figs. 4D-H**), where the longitudinal manchette, connected to the nuclear ring (**Fig. 4D**), had its fibers gradually shortened, pulling the acrosomes and making it cover the entire rostral end of the nucleus, which assumed an arrow-shape (**Fig. 4H**).

*Step 10 spermatids*

At this step the nuclear ring completed its dislocation to the posterior region of the nucleus (**Fig. 4I**) and the annulus started its caudal migration (**Fig. 4J**). The nucleus completed their chromatin condensation and the presence of a perforatorium was not observed (**Fig. 4K**). The organization of the midpiece began, with the great allocation and association of clusters of mitochondria to the axial filament (**Fig. 4L**).

*Step 11 spermatids*

In this step the mitochondrial sheath, from the midpiece, was almost completely organized (**Fig. 4M**) and the organization of the fibrous sheath, from the principal piece, took place (**Fig. 4N**).

*Step 12 spermatids (not documented)*

In this step the spermatids had achieved the basic format of the spermatozoon, with the cytoplasm moved almost completely out of the spermatids. This was the last stage before the process of spermiation: released of the spermatozoa in the tubular lumen and formation of the residual bodies, which contained many organelles not included in the spermatozoa, as Golgi complex, mitochondria and chromatoid bodies.

*Ultrastructure of the Spermatozoon**Spermatozoon Head*

The spermatozoon had an arrow-like head that were occupied almost completely by the nucleus, which presented an extremely dense and homogeneous matrix (**Fig. 5A**). Externally it was covered by a plasma membrane, which was free at the top of the nucleus, with a space separating it from the outer acrosomal membrane. Below it was the acrosome that presented a small size, covering only one third of the nuclear length and presenting also an extremely dense and homogeneous matrix (**Fig. 5B**). The presence of the subacrosomal space between the nuclear and inner acrosomal membranes was always noted; however, the perforatorium was absent (**Fig. 5B**).

*Neck (Fig. 5C)*

The base of the nucleus had a concavity where the basal plate attached to the nucleus, connecting the tail to the sperm head. At the base of the nucleus, the proximal centriole developed a concavity where the implantation fossa was formed. Within this complex we found, just beneath the nuclear envelope, the basal plate and, below it, the capitulum. The central portion of the capitulum directly associated with the axial filament (distal centriole), and its marginal portions associated with the anterior part of the nine outer dense fibers,

forming the segmented columns. Lateral to this complex, we observed a small amount of redundant nuclear membrane and below, the beginning of the midpiece.

#### *Midpiece*

The midpiece was composed by the axial filament, which is surrounded by the nine outer dense fibers; and these were surrounded by the mitochondrial sheath. In transversal cross-sections, we observed that the outer dense fibers were arranged in a horseshoe fashion and showed bilateral symmetry: Fibers 1, 5, 6 and 9 were larger than the others and presented a bilobular shape, while fibers 3 and 8 remained aligned with the central fibrils of the axial filament complex, forming the dorso-ventral axis (X-Y), which asymmetrically separated the complex (**Fig. 5D**).

An annulus was found caudal to the last mitochondrial pair. Immediately caudal to the annulus the tail diameter lessens abruptly and gave rise to the principal piece (**Fig. 5E**).

The position of the cytoplasmic droplet was variable, and it could be observed as high as the neck or as low as the midpiece terminus vicinity. Droplets always contained an abundance of membranes (**Fig. 5I**).

#### *Principal Piece*

In the upper region of the principal piece the outer dense fibers terminated (**Fig. 5F**) and projections from the fibrous sheath extended into the position those fibers had occupied. The fibers 3 and 8 disappeared, giving rise to the longitudinal columns that supported the helical fibers of the fibrous sheath (**Fig. 5G**). In the same manner, the fibrous sheath projections tended to diminish throughout the principal piece.



### *End Piece*

The transition from principal piece to end piece was not easily observed, but cross-sections of end pieces were frequently noted. The uppermost level of the end piece presented only the axial filament enclosed by the plasma membrane (**Fig. 5H**), while throughout its length, the organization of the axial filament was lost and in the terminus of the end piece only 11 microtubules, without a distinct form, were observed.

### *Deactivating Period*

During the deactivating period, all the cells that entered in differentiation seemed to proceed still the end, with no accentuated differences in the process of spermatogenesis and without processes of cell degeneration; however, the formation of new cells to enter in differentiation seemed sharply decreases or did not occur.

We noted that the basal compartment tended to present a more firmly cell association and a higher electron-density than the adluminal compartment; the Sertoli cells tended to be in the basal compartment, with the nucleus closed related to the basal lamina, and in association with the spermatogonia. By other side, the adluminal compartment seemed to present a relaxation in the cellular connections, presenting several intra and intercellular vacuoles (**Fig. 6A**), and a more detached association in the proximity of the lumen (**Fig. 6B**). Despite these differences, the ultrastructure of the related cell types seemed to be similar to that of the active period, and few sporadic apoptotic cells was observed.

The process of deactivation extended until the total regression of the epithelium, where only spermatogonia and Sertoli cells can be observed; thus beginning the regressed period.

### ***Regressed Period***

The regressed period corresponded to the period in which the spermatogenesis ceased, thus, its epithelium was composed only by spermatogonia and Sertoli cells (**Fig. 6C**).

Three main types of spermatogonia were also observed in the regressed testes, types A<sub>d</sub>, 1 e 2; however, not all they seemed to present the same characteristics of the three types discerned in the anterior periods.

The type A<sub>d</sub> spermatogonia seemed to be similar to that observed in anterior periods, being isolated cells adhered to the basal lamina and presenting a compacted shape. It was the rarest type observed, being rarely met in the epithelium (**Fig. 6C**, arrow).

The type 1 spermatogonia were great cells that presented oval shape; they could be adhered or released from the basal lamina and were completely surrounded by Sertoli cells (**Fig. 6C-D**). Their nucleus were round-to-oval, presented a finely granular and highly electron-dense chromatin (with clusters of condensed chromatin) and from one to three nucleoli (**Fig. 6D** and **F**). Their cytoplasm were large and less electron-dense, presenting some mitochondria, few extensions of endoplasmic reticulum (smooth and rough), Golgi complex and fine cytoplasmatic granulations, ribosomes and/or glycogen. It is interesting to observe the presence of large lipid droplets inside this spermatogonia type (**Fig. 6F**).

The type 2 spermatogonia were the cells that are above the line formed by the nuclei of Sertoli cells (**Fig. 6C**). These cells seemed to present a smaller size than the type 1, presenting a smaller cytoplasm almost entirely occupied by their large nucleus (**Fig. 6G**). The few organelles observed were similar to type 1; however, the presence of lipid droplets was not detected.

The presence of few sporadic apoptotic cells was also observed (**Fig. 6E**).

### ***Reactivating Period***

The reactivating period corresponded to the period in which the spermatogenesis restarted; thus, the epithelium began to develop, producing new cells that enter in meiotic division and differentiation (**Fig. 7A**).

The spermatogonia were reactivated and the three main types can be seen again: types A<sub>d</sub>, A<sub>p</sub> (**Fig. 7A-B**) and B (**Fig. 7A and C**); presenting similar characteristics to the active period.

We could observe, in most seminiferous tubules, the presence of a great amount of apoptotic cells (**Fig. 7D**). They were observed in both compartments (basal and adluminal), presenting a large compact concentration of cellular components in the cytoplasm (**Fig. 7E**) and an anomalous chromatin attached to the nuclear envelope (**Fig. 7F**). The detachment of part of the cytoplasm, forming apoptotic bodies was also observed (**Fig. 7E**).

This reactivation was slow, thus most of seminiferous tubules cross-sections was occupied basic by Sertoli cells, spermatogonia and primary spermatocytes (**Fig. 7A**). However, over time, the spermatocytes completed the meiotic division and became spermatids that initiated the process of differentiation into spermatozoa, thus completing the spermatogenesis and entering in the testicular active period.

### ***Changes in the morphology of the Auxiliary Cells during the periods***

#### ***Sertoli Cell***

In the active period, the Sertoli cells presented the basic mammalian morphology, presenting two different regions: basal and apical. In the basal region was localized the nucleus, which was large and irregularly shaped, displaying large infoldings. It presented a highly euchromatic and homogeneous nucleoplasm with scarce points of heterochromatin, and a prominent nucleolus. The nucleolus appeared dispersed, occupying a great nuclear area,

presenting one filamentous and other granular portions (**Fig. 8A**). The perinuclear cytoplasm was occupied by few multivesicular and electron-dense bodies. The rest of the basal cytoplasm exhibited a high concentration of subcellular structures including the endoplasmic reticulum, Golgi complex, mitochondria and ribosomes. By other side, the apical region presented large compacted masses of smooth endoplasmic reticulum, and together with mitochondria, surrounded the differentiating spermatids (not documented).

The most obvious changes suffered by the Sertoli cells during the different periods were linked to the nucleus. In the deactivating period, the nucleus showed a softening of their infoldings and the nucleolus had their filamentous portion increased in relation to the granular (**Fig. 8B**). This softening process had its peak at the regressed period, where the nucleus of the Sertoli cells showed an elongated shape without infoldings. This was a smaller nucleus, which presented a great portion of condensed chromatin and a small and compact nucleolus (**Fig. 8C**).

In the reactivating period, the nucleus began to enlarge, the chromatin began to decondensed and the nucleolus was unpack, returning to present a fibrillar shape (**Fig. 8D**).

#### *Leydig Cell*

The Leydig cells were irregular cells, found singly or in clusters within the interstitial tissue. The nuclei were generally large and undefined; the cytoplasm was vast and presented a highly secretory aspect (**Fig. 8E**), with a great portion of such occupied by the endoplasmic reticulum and vesicles. The endoplasmic reticulum is found predominantly in the smooth form, organized as a compact network of anastomosing cisterns that surrounds the nucleus and other organelles, but in the proximity of the nucleus, the rough form predominated (**Fig. 8G**). Two spherical bodies were frequently observed in their cytoplasm: the lipid droplets the multivesicular bodies. The lipid droplets were relatively large with round vesicles that were

distributed irregularly or in groups (**Fig. 8E-F**). They present a pale and homogeneous component and were not surrounded by membrane. The multivesicular bodies were irregular, membrane-bound vesicles (**Fig. 8E**).

The most obvious difference observed in the Leydig cells during the different periods was linked to the amount of lipid droplets and multivesicular bodies. During the active period, the Leydig cells presented a large amount of multivesicular bodies and few lipid droplets (**Fig. 8E-F**), which reversed in the regressed period (**Fig. 8H**).

## DISCUSSION

Our study confirms that the annual reproductive cycle of *M. nigricans* presents four different phases: active; deactivating; regressed and reactivating periods; with all these presenting distinct characteristics (Beguelini *et al.* 2012a).

The active period was characterized by the complete occurrence of the spermatogenesis, with the spermatogonial stem cells suffering a process of cell renewal, where some spermatogonia divide to replenish the stem cell pool and others undergo mitotic divisions, become committed to further differentiation, and produce spermatocytes, which undergo meiotic divisions that give rise to haploid spermatids that differentiate into mature spermatozoa, which is capable of motility and fertilization (Beguelini *et al.* 2012b).

In most mammals, the spermatogenesis is organized in the seminiferous tubules in well-defined fixed cell associations (Leblond and Clermont 1952), which are species-specific, and can be generally divided in the eight stages of the seminiferous epithelium cycle (Berndtson 1977). However, as *M. nigricans* shows a pattern of testicular regression and reactivation during their annual reproductive cycle, it does not present the fixed cell associations, thus do not following the seminiferous epithelium cycle and explaining the asynchrony observed by Beguelini *et al.* (2009).



Despite the asynchrony in the seminiferous epithelium cycle, in the active period, *M. nigricans* presented testicular cells with similar characteristics to other bats already studied, presenting three main types of spermatogonia: A<sub>d</sub>, A<sub>p</sub> and B (Singwi and Lall 1983; McGuckin and Blackshaw 1987; Saidapur and Patil 1992; Lee 2003; Beguelini *et al.* 2009; Beguelini *et al.* 2011a; Beguelini *et al.* 2012b); and 12 steps in the process of spermatid differentiation (Beguelini *et al.* 2011a; Beguelini *et al.* 2012b). However, variations in the process were observed.

Beguelini *et al.* (2012b) described that the process of acrosome formation in *M. molossus* (Molossidae) is similar to that found in other mammals, with the acrosome being formed by proacrosomal vesicles that already contain an electron-dense granule inside it; however it differs from that found in *P. lineatus* (Phyllostomidae), which produces two different types of proacrosomal vesicles, one electron-dense and other electron-lucid (Beguelini *et al.*, 2011a). Differing from both, *M. nigricans* do not presented proacrosomal vesicles doted of electron-dense materials; on the contrary, their vesicles were only electron-lucid. This difference can be related to the presence of a perforatorium, where these electron-dense materials possibly is the basic substance from its mounting; as *M. nigricans* do not present a perforatorium, it does not have this type of secretion.

*Myotis nigricans* also differed from *M. molossus* and *P. lineatus* in the morphology of the outer dense fibers, presenting the fibers 1, 5, 6 and 9 larger than the others, while the others present only the 1, 5 and 6 larger (Beguelini *et al.* 2011a; Beguelini *et al.* 2012b).

The major changes in the other periods are possibly linked to the functionality of the auxiliary cells, which directly influenced in the process of spermatogenesis, regulating it.

During the deactivating period, the spermatogenesis ceases and, as observed by Beguelini *et al.* (2012a), this process seems not to be connected to a process of apoptosis-phagocytosis (small number of apoptotic figures), being possibly linked to a process of

deactivation. Despite the mechanisms and cascades of reactions linked to this deactivation are not known, the relaxation in the cellular connections between Sertoli cells and spermatids, observed in the adluminal compartment, bring us an interesting insight. According to Holdcraft and Braun (2004) and Wang *et al.* (2009), the maintenance of the adhesion of spermatids to the Sertoli cells was required for their normal differentiation to elongated spermatozoa and this adhesion was mediated by the normal function of the androgen receptors (AR) in Sertoli cells. Moreover, Beguelini *et al.* (2012a) described a low expression of AR in Sertoli cells during the deactivating period (September-October), in *M. nigricans*.

Based on all these data, we can infer that possibly the low expression of AR (low testosterone stimulus) in Sertoli cells disable its support and nurture functions (Wang *et al.* 2009), causing an instability in the adluminal compartment and making it impossible the completion of spermatogenesis, being one mechanism of the deactivation of the spermatogenesis in this period.

Similarly, the decrease in testosterone stimulus seems to be linked to a decrease in the androgen syntheses in Leydig cells. Loh and Gemmell (1980) described that *M. adversus* presented a high plasma androgens concentration and a low amount of lipid droplets in the Leydig cells, during the breeding season, and an inverse proportion in the quiescent phase (regressed period). Thus, the authors suggested that the lipid droplets of Leydig cells contains substrates which are utilized in the production of steroid hormone; and that the amount of lipid droplets observed in the cytoplasm was inversely linked to the steroid production.

In the present work, we observed similar patterns, with the active period presenting a low amount of lipid droplets in Leydig cells and the regressed period a large amount. These facts indicate that possibly the androgen syntheses in Leydig cells decrease in the deactivating and regressed periods, causing a decrease in the paracrine testosterone stimuli of the Sertoli cells, thus possibly generating the process of deactivation.

As the amount of lipids in Leydig cells (present study) and the AR expression in Sertoli cells (Beguelini *et al.* 2012a) remained low during the deactivating and part of the regressed periods, its epithelium presented a deactivated spermatogenic aspect, with almost only spermatogonia and Sertoli cells. However, these cells presented great changes in morphology.

Despite possible errors inherent to the method used in the present analyze (this is not a method of *real time* analysis), we believe that the three main types of spermatogonia generally observed in the seminiferous epithelium of most mammals, including bats (Singwi and Lall 1983; McGuckin and Blackshaw 1987; Saidapur and Patil 1992; Lee 2003; Beguelini *et al.* 2009; Beguelini *et al.* 2011a; Beguelini *et al.* 2012b), are presented in this period; however they seem to suffer considerably changes in morphology and physiology.

The A<sub>d</sub> spermatogonia seem to be similar to that observed in active period, only presenting a more compact and condensed shape. This feature seems to be consistent with the hypothesis that this is the “true spermatogonial stem cell”, which is essential for the renewal and maintenance of the seminiferous epithelium (Beguelini *et al.* 2009; Beguelini *et al.* 2011a; Beguelini *et al.* 2012b). Because of its importance, it would have to be protected from suffering injuries, so a process of compaction, reduction of physiological reactions and chromatin condensation, protect it from external damage, leaving it able to be reactivated in the future.

By other side, the types A<sub>p</sub> and B seem to suffer considerably morphologic changes. The type A<sub>p</sub> possibly correspond to the type 1 spermatogonia and the type B to the type 2. The processes that occur in these cell types are not clear, as it is not clear the function of the increasing in cell size: if it is connected to a process of developmental delay and protection or to a process of no progression in the cell differentiation due to the lack of stimuli. By other side, the presence of B/2 spermatogonia, above the line formed by the nuclei of Sertoli cells,

was possibly linked to the process of elimination of the cells that progress in the differentiation, since the few apoptotic cells, observed in this period, were found in this compartment.

Still within the regressed period, the amount of lipids in Leydig cells (present study) and the AR expression in Sertoli cells (Beguelini *et al.* 2012a) greatly increase, thus possibly causing the reactivation of the spermatogenesis, with the testes entering in reactivating period.

The three main types of spermatogonia return to present their basic morphology; however, it is not clear if the types 1 and 2, when stimulated, develop, turning them into the basic morphology or if the three types are derived from a new wave of differentiation of type A<sub>d</sub> spermatogonia. Adding to this, the observation of a great amount of apoptotic cells in this period leads us to raise some hypotheses: 1. the cells (types 1 and 2) that undamaged survived to the deactivation and reactivation process continue the cellular differentiation, while the damaged cells are eliminated; 2. all the types 1 and 2 cells are eliminated and only the new cells formed entering in cellular differentiation; 3. all types 1 and 2 survive and differentiate, with the apoptotic cells corresponding only to the cells that suffer damage during the accelerated differentiation process. For us, the first proposition seems to be more plausible; however, this is a fact that deserves future detailed studies.

In conclusion, our study described the process of spermatogenesis and the ultrastructure of the spermatozoa of *M. nigricans* and confirmed that the process of testicular regression suffered by it during the spring season can be divided into four different phases, with all those presenting interesting distinct morphologic and physiologic characteristics, which seem to be specific from this species, and deserve to be further studied. It is interesting to remember that this species present another process of testicular regression (June), which has different patterns in relation to this.

## **ACKNOWLEDGEMENTS**

Technical help from Luiz Roberto Falleiros Junior and Rosana Silistino de Souza Santos is highly appreciated. The scholarship awarded to Mateus Rodrigues Beguelini by the Brazilian Research Foundation (CAPES) is also gratefully acknowledged. Financial support from the São Paulo State Research Foundation (FAPESP) and the Brazilian Research Foundation (CAPES) is gratefully acknowledged.



## REFERENCES

- Beguelini, M. R., Moreira, P. R. L., Faria, K. C., Marchesin, S. R. C., and Morielle-Versute, E. (2009). Morphological characterization of the testicular cells and seminiferous epithelium cycle in six species of Neotropical bats. *J. Morphol.* **270**, 943-953.
- Beguelini, M. R., Puga, C. C. I., Taboga, S. R., and Morielle-Versute, E. (2011a). Ultrastructure of spermatogenesis in the white-lined broad-nosed bat, *Platyrrhinus lineatus* (Chiroptera: Phyllostomidae). *Micron* **42**, 586-599.
- Beguelini, M. R., Marchesin, S. R. C., Azeredo-Oliveira, M. T. V., and Morielle-Versute, E. (2011b). Nucleolar behavior during meiosis in four species of phyllostomid bats (Chiroptera, Mammalia). *Genet Mol Res* **10(2)**, 552-565.
- Beguelini, M. R., Góes, R. M., Taboga, S. R., and Morielle-Versute, E. (2012a). Two periods of testicular regression, not directly linked to apoptosis, are peculiar events of the annual reproductive cycle of the black Myotis bat, *Myotis nigricans* (Chiroptera: Vespertilionidae). *Biol. Reprod.* **Artigo a ser submetido**.
- Beguelini, M. R., Taboga, S. R., and Morielle-Versute, E. (2012b). Ultrastructural characteristics of spermatogenesis in Pallas's Mastiff bat, *Molossus molossus* (Chiroptera: Molossidae). *Micros. Res. Techq.* **In press**.
- Berndtson, W. E. (1977). Methods for quantifying mammalian spermatogenesis: a review. *J. Anim. Sci.* **44**, 818-883.
- Breed, W. G., and Leigh, C. (1985). Sperm head morphology of Australian molossid bats with special reference to the acrosomal structure. *Mammalia* **49(3)**, 403-406.
- De Knegt, L. V., Silva, J. A., Moreira, E. C., and Sales, G. L. (2005). Morcegos capturados no município de Belo Horizonte, 1999-2003. *Arq. Bras. Med. Vet. Zootec.* **57**, 576-583.
- Fawcett, D. W., and Ito, S. (1965). The fine structure of bat spermatozoa. *Amer. J. Anat.* **116**, 567-610.

- Holdcraft, R. W., and Braun, R. E. (2004). Androgen receptor function is required in Sertoli cells for the terminal differentiation of haploid spermatids. *Development* **31**, 459-467.
- Krutzsch, P. H. (1919). Male reproductive patterns in nonhibernating bats. *J. Reprod. Fertil.* **56**, 333-344.
- Kurohmaru, M., Saruwatari, T., Kimura, J., Mukohyama, M., Watanabe, G., Taya, K., and Hayashi, Y. (2002). Seasonal changes in spermatogenesis of Japanese Lesser Horseshoe bat, *Rhinolophus cornutus* from a morphological viewpoint. *Okajimas Folia Anat. Japan* **79(4)**, 93-100.
- Leblond, C. P., and Clermont, Y. (1952). Spermiogenesis of rat, mouse, hamster and guinea pig as revealed by the periodic acid-fuchsin sulfuro acid technique. *Am. J. Anat.* **90(2)**, 167-215.
- Lee, J. H. (2003). Cell differentiation and ultrastructure of the seminiferous epithelium in *Myotis macrodactylus*. *Korean J. Electron Micros.* **33(1)**, 25-39.
- Lee, J. H., and Mori, T. (2004). Annual cycle of the seminiferous epithelium of *Myotis macrodactylus*. *J. Fac. Agric. Kyushu Univ.* **49(2)**, 355-365.
- Lee, J. H., Choi, B. J., and Son, S. W. (1992). Spermiogenesis in the Korean Greater Horseshoe Bat, *Rhinolophus ferrumequinum korai*. *Korean J. Electron Micros.* **22(2)**, 97-117.
- Loh, H. S. F., and Gemmell, R. T. (1980). Changes in the fine structure of the testicular Leydig cells of the seasonally-breeding bat, *Myotis adversus*. *Cell Tissue Res.* **210**, 339-347.
- McGuckin, M. A., and Blackshaw, A. W. (1987). Cycle of the seminiferous epithelium in the grey-headed fruit bat, *Pteropus poliocephalus*. *Austral. J. Biol. Sci.* **40**, 203-210.
- Morigaki, T., Kurohmaru, M., Kanai, Y., Mukohyama, M., Hondo, E., Yamada, J., Agungpriyono, S., and Hayashi, Y. (2001). Cycle of the seminiferous epithelium in the

- Java fruit bat (*Pteropus vampyrus*) and the Japanese Lesser Horseshoe bat (*Rhinolophus cornutus*). *J. Vet. Med. Sci.* **63**, 773–779.
- Oh, Y. K., Mori, T., and Uchida, T. A. (1985). Spermiogenesis in the Japanese Greater Horseshoe Bat, *Rhinolophus ferrumequinum* Nippon. *J. Fac. Agric. Kyushu Univ.* **29(4)**, 203-209.
- Phillips, D. M., Rasweiler, J. J., and Murwali, F. (1997). Giant, accorded sperm acrosomes of the greater bulldog bat, *Noctilio leporinus*. *Mol. Reprod. Develop.* **48**, 90-94.
- Saidapur, S. K., and Patil, S. B. (1992). Kinetics of spermatogenesis in megachiropteran bat, *Rousettus leschenaulti* (Desmarest): seminiferous epithelial cycle, frequency of stages, spermatogonial renewal and germ cell degeneration. *Indian J. Exper. Biol.* **30**, 1037-1044.
- Sang-Sick, K., Jung-Hun, L., Sung-Won, S., and Byung-Jin, C. (1999). Morphological comparison of spermatozoa in the Korean greater horseshoe bat (*Rhinolophus ferrumequinum korai*) and long-fingered bat (*Miniopterus schreibersi fuliginosus*). *Korean J. Electron Micros.* **29(1)**, 1-10.
- Sharifi, M., Ghorbani, R., and Akmal, V. (2004). Reproductive cycle in *Pipistrellus kuhlii* (Chiroptera, Vespertilionidae) in western Iran. *Mammalia* **68(4)**, 323-327.
- Singwi, M. S., and Lall, S. B. (1983). Spermatogenesis in the non-scrotal bat – *Rhinopoma kinneari* Wroughton (Microchiroptera: Mammalia). *Acta Anat.* **116**, 136-145.
- Son, S. W., Lee, J. H., and Cheon, H. M. (1997). Spermiogenesis in the Korean Daubenton's Bat (*Myotis daubentonii ussuriensis*). *Develop. Reprod.* **1(1)**, 9-24.
- Wang, R. S., Yeh, S., Tzeng, C. R., and Chang, C. (2009). Androgen receptor roles in spermatogenesis and fertility: lessons from testicular cell-specific androgen receptor knockout mice. *Endocr. Rev.* **30(2)**, 119-132.
- Wilson, D. E. (1971). Ecology of *Myotis nigricans* (Mammalia: Chiroptera) on Barro Colorado Island, Panama Canal Zone. *J. Zool.* **163**, 1-13.

**Figure 1.** Ultrastructural characteristic of the three types of spermatogonia of *Myotis nigricans*, during the active period. **A-B.** Type A<sub>d</sub> spermatogonia. Note the high degree of adhesion to the basal lamina (arrow-head) and the presence of two (**A**) or three nucleoli (**B**). **C-E.** Type A<sub>p</sub> spermatogonia. Note an intermediate degree of adhesion to the basal lamina (**C**, arrow-head), the presence of the chromatoid body (**D**) and extensions of endoplasmic reticulum (**E**). **F-G.** Type B spermatogonia. Note the process of ascension into the adluminal compartment (**F**) and the loss of the contact with the basal lamina (**G**). (BL, basal lamina; Cb, chromatoid body; ER, endoplasmic reticulum; G, Golgi complex; M, mitochondria; My, Myoid cell; N, nucleus; No, nucleolus; Sd, spermatid; Se, Sertoli cell). Scale Bars = 2µm.

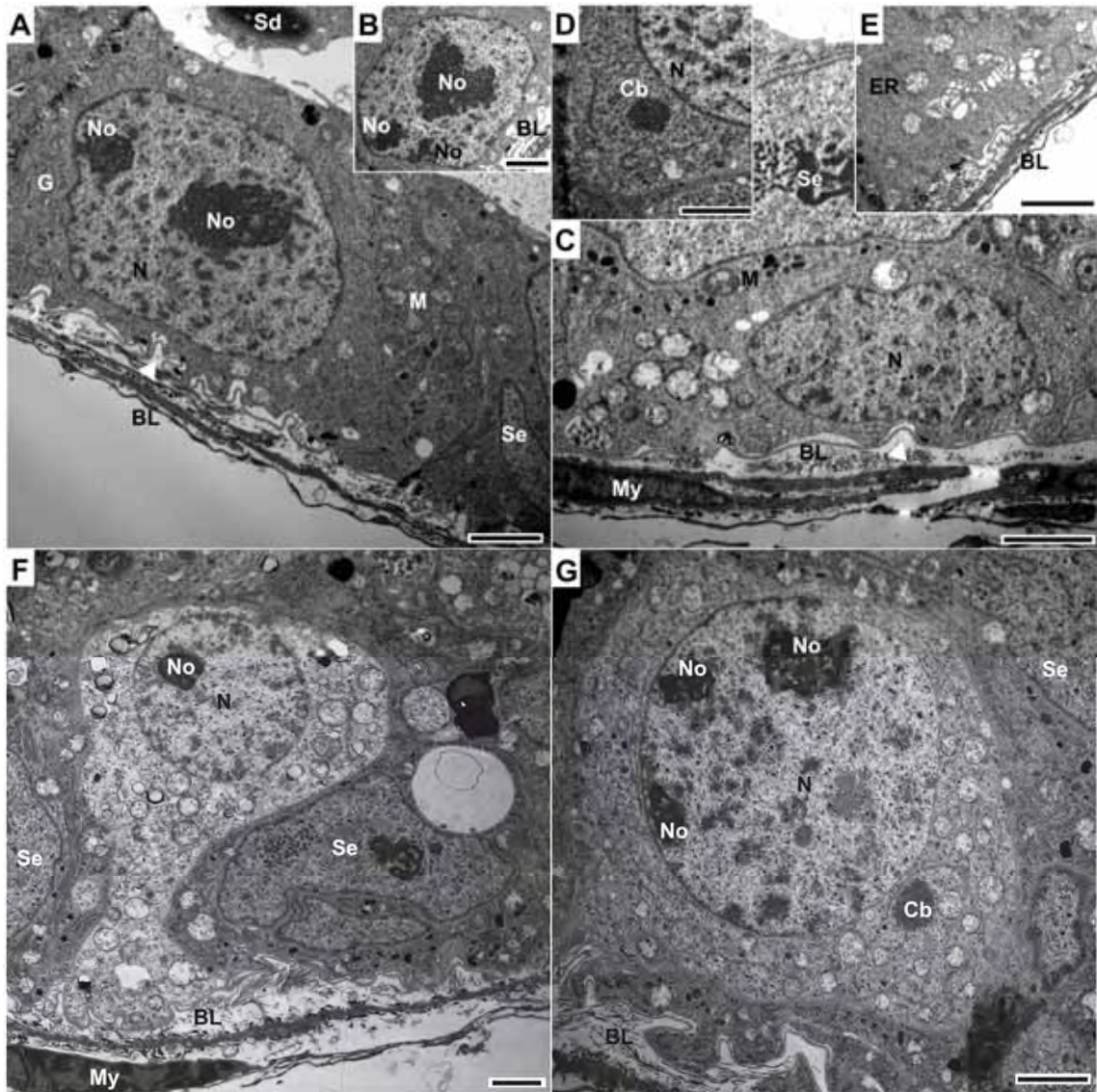




**Figure 2.** Electron micrographs of the meiotic cells (meiosis I) of *Myotis nigricans*, during the active period. **A.** Primary spermatocytes in leptotene. **B.** Primary spermatocytes in zygotene. **C.** Primary spermatocytes in pachytene. **D-E.** Primary spermatocytes in diplotene. **F.** Metaphases. **G.** Secondary spermatocytes. Note the increase in the degree of chromatin condensation around the synaptonemal complexes (**A-D**, arrows); the disruption of the nucleolus (arrow-heads) from leptotene (**A**) to diplotene (**D**); and the large amount of *lamellae anellata* (**E**). (Ch, chromosomes; N, nucleus). Scale Bars = 2 $\mu$ m.

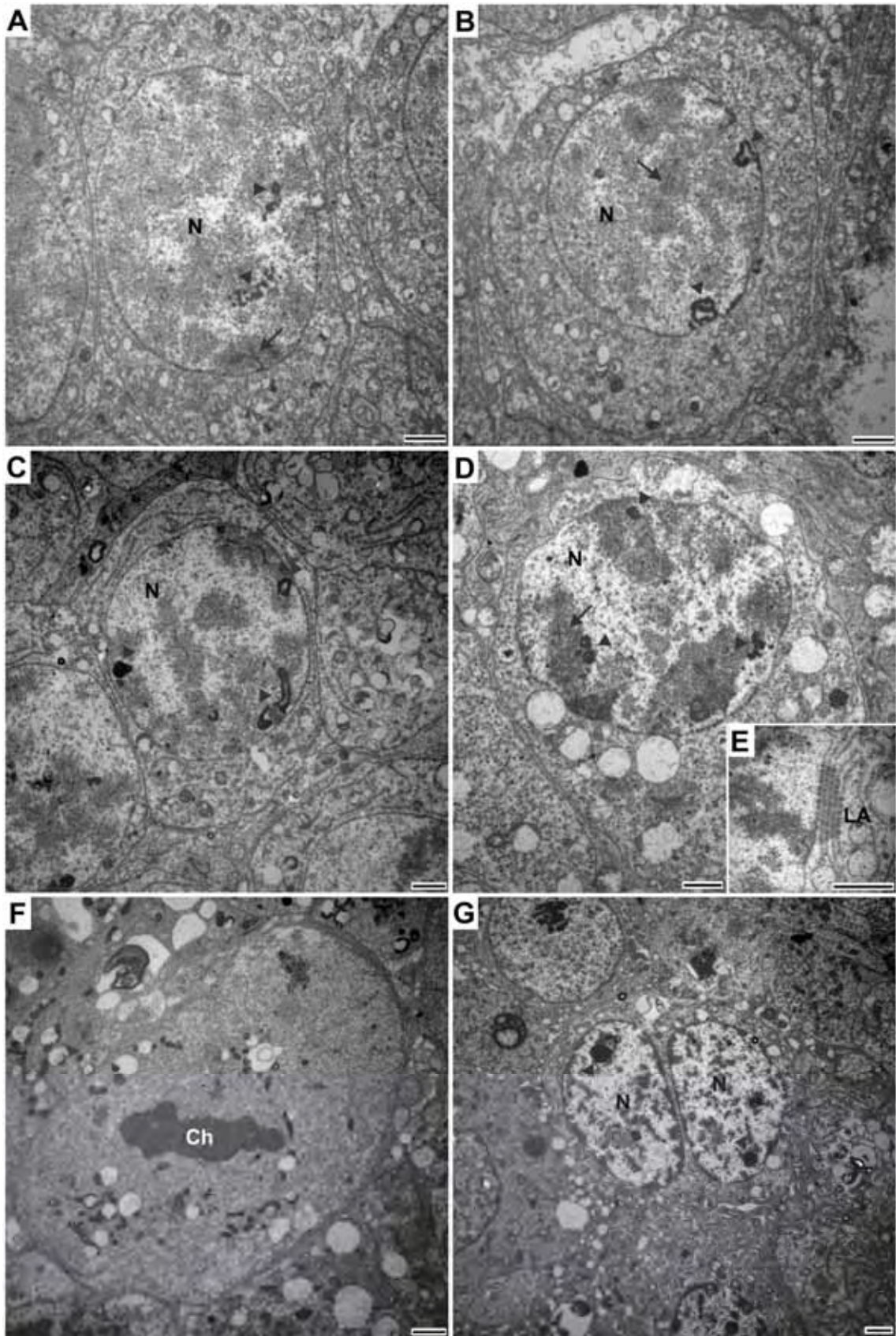


**Figure 3.** Electron micrographs of the spermatids showing the spermiogenesis process in *Myotis nigricans*, during the active period. **A-B.** Step 1 spermatids. Note the little differentiation of this type of spermatid, presenting a spherical nucleus dotted of a single nucleolus; and the presence of few small proacrosomal vesicles associated to the Golgi complex (**B**, arrow). **C.** Step 2 spermatid. Note the formation of proacrosomal vesicles, which tend to increase in number starting to fuse with each other (arrow); and the association of the chromatoid body to this complex. **D-E.** Step 3 spermatids. Note the fusion of the proacrosomal vesicles to form a large proacrosomal vacuole (**D**), which stayed adjacent to the nucleus (**E**). **F-H.** Step 4 spermatids. Note that the proacrosomal vacuole greatly increase during this step and attach to the nuclear envelope; and the dislocation of centrioles to the opposite pole of the acrosome, with the development of the axoneme (**G**). **I-J.** Step 5 spermatids. Note the intimate association of the acrosome with the nuclear envelope and the continuous production and subsequent fusion of proacrosomal vesicles to the acrosome by the Golgi complex (**J**, arrow). **K.** Step 6 spermatid. Note that the acrosome condenses, compacts and expands forming a cap, which covers a large surface of the nucleus. (A, acrosome; An, annulus; Cb, chromatoid body; DC, distal centriole; G, Golgi complex; M, mitochondria; N, nucleus; No, nucleolus; PC, proximal centriole; PV, proacrosomal vacuole; \*, intercellular bridge).



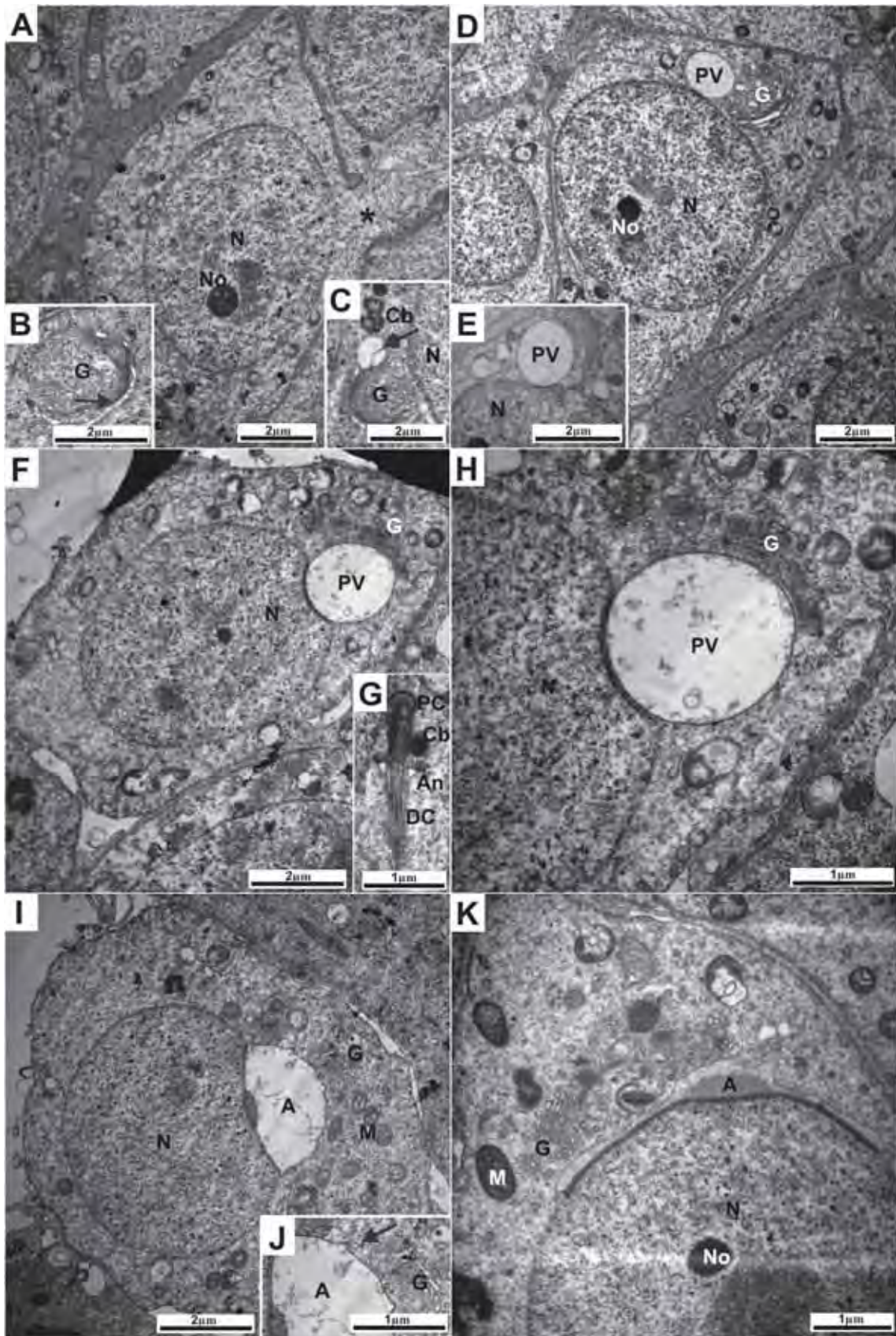


**Figure 4.** Electron micrographs of the spermatids showing the spermiogenesis process in *Myotis nigricans*, during the active period. **A-B.** Step 7 spermatids. Note the migration of the nucleus toward the plasma membrane; the fusion of large proacrosomal vesicles to the acrosome (**A**, arrows); and the development of an elevation in the distal region of the acrosome (**B**, arrows). **C.** Step 8 spermatid. Note the approximation of the nucleus to the plasma membrane and the formation of the microtubular manchette (Mc). **D-H.** Early (**D-E**), middle (**F**) and late (**G-H**) step 9 spermatids. Note that the nuclear elongation occurs in this step, when the longitudinal manchette, connected to the nuclear ring (arrows) has its fibers gradually shortened, pulling the acrosomes and making it cover the entire rostral end of the nucleus, which now assumes an arrow-shape (**H**). **I-L.** Step 10 spermatids. Note that at this step the nuclear ring completes its dislocation to the posterior region of the nucleus (**I-J**); the annulus commences its caudal migration (**I-J**) and the organization of the midpiece begins, with the clusters of mitochondria associating with the axial filament (**L**); and the absence of a perforatorium in the rostral region of the nucleus (**K**). **M-N.** Step 11 spermatids. Note that the mitochondrial sheath, from the midpiece, was almost completely organized (**M**) and the organization of the fibrous sheath, from the principal piece, takes place (**N**). (A, acrosome; Af, axial filament; An, annulus; Ax, axoneme; G, Golgi complex; M, mitochondria; Mc, manchette; MP, midpiece; N, nucleus; Nr, nuclear ring; PP, principal piece; Rnm, redundant nuclear membrane). Scale Bars = 2 $\mu$ m.



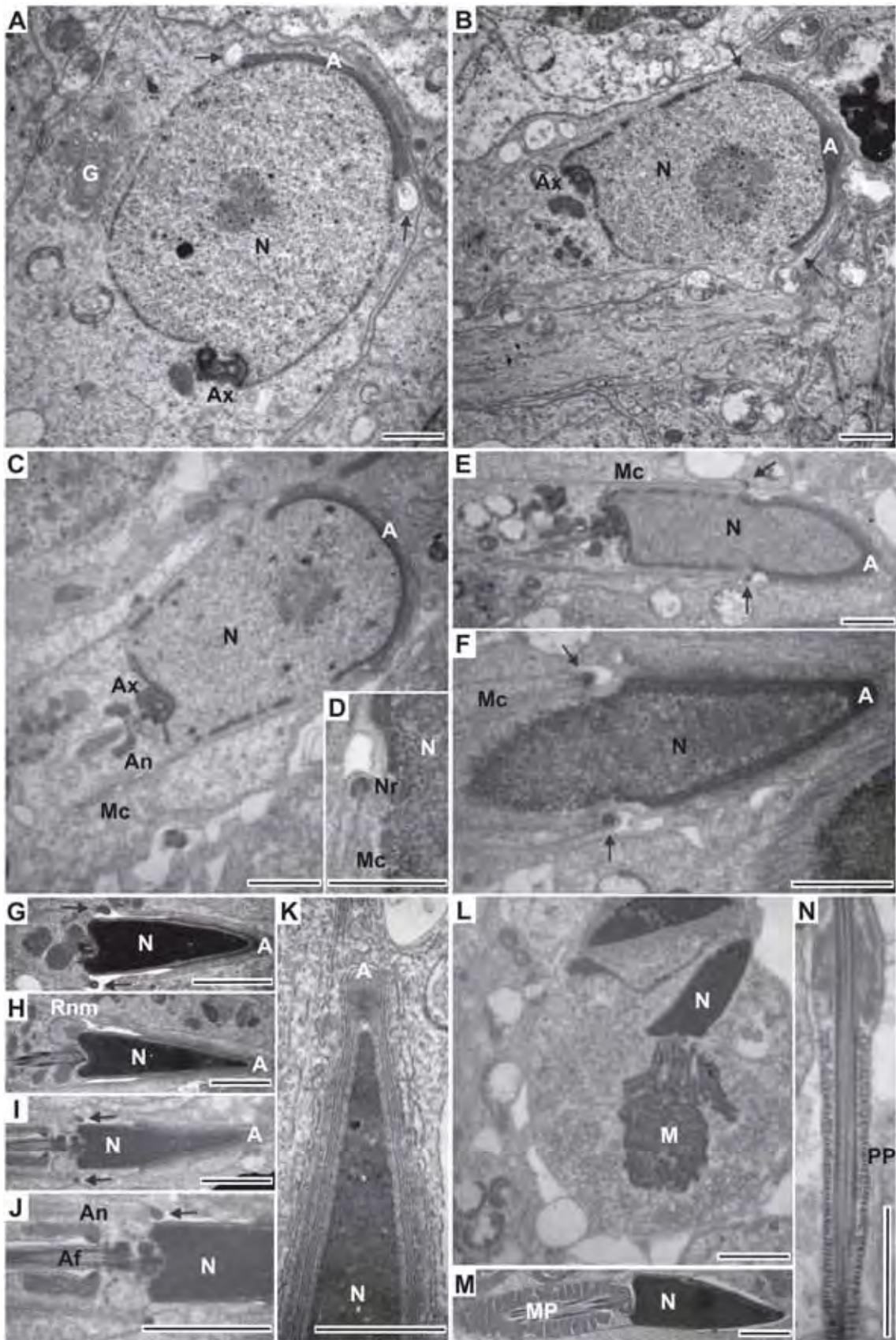


**Figure 5.** Electron micrographs of the spermatozoon of *Myotis nigricans*. **A.** The head region. Note that the nucleus occupied almost completely the space of the arrow-like head, presenting an extremely dense and homogeneous matrix. **B.** The apical portion of the head region. Note the presence of a small acrosome that covers only one third of the nuclear length and the absence of a perforatorium. **C.** The neck region. **D.** Transversal section of the midpiece. Note that the outer dense fibers 1, 5, 6 and 9 were larger than the others. **E.** The transitional region from the midpiece to the principal piece. **F-G.** Transversal sections of the principal piece. **H.** Transversal section of the end piece. **I.** Transversal section of the midpiece, showing the position of the droplet. (A, acrosome; Af, axial filament; An, annulus; Bp, basal plate; C, capitulum; Fs, fibrous sheath; Iam, inner acrosomal membrane; Lc, longitudinal column; M, mitochondria; Mt, microtubules; N, nucleus; Oam, outer acrosomal membrane; Od, outer dense fibers; Pm, plasma membrane; Rnm, redundant nuclear membrane; S, space between the plasma membrane and the outer acrosomal membrane; Ss, subacrosomal space).



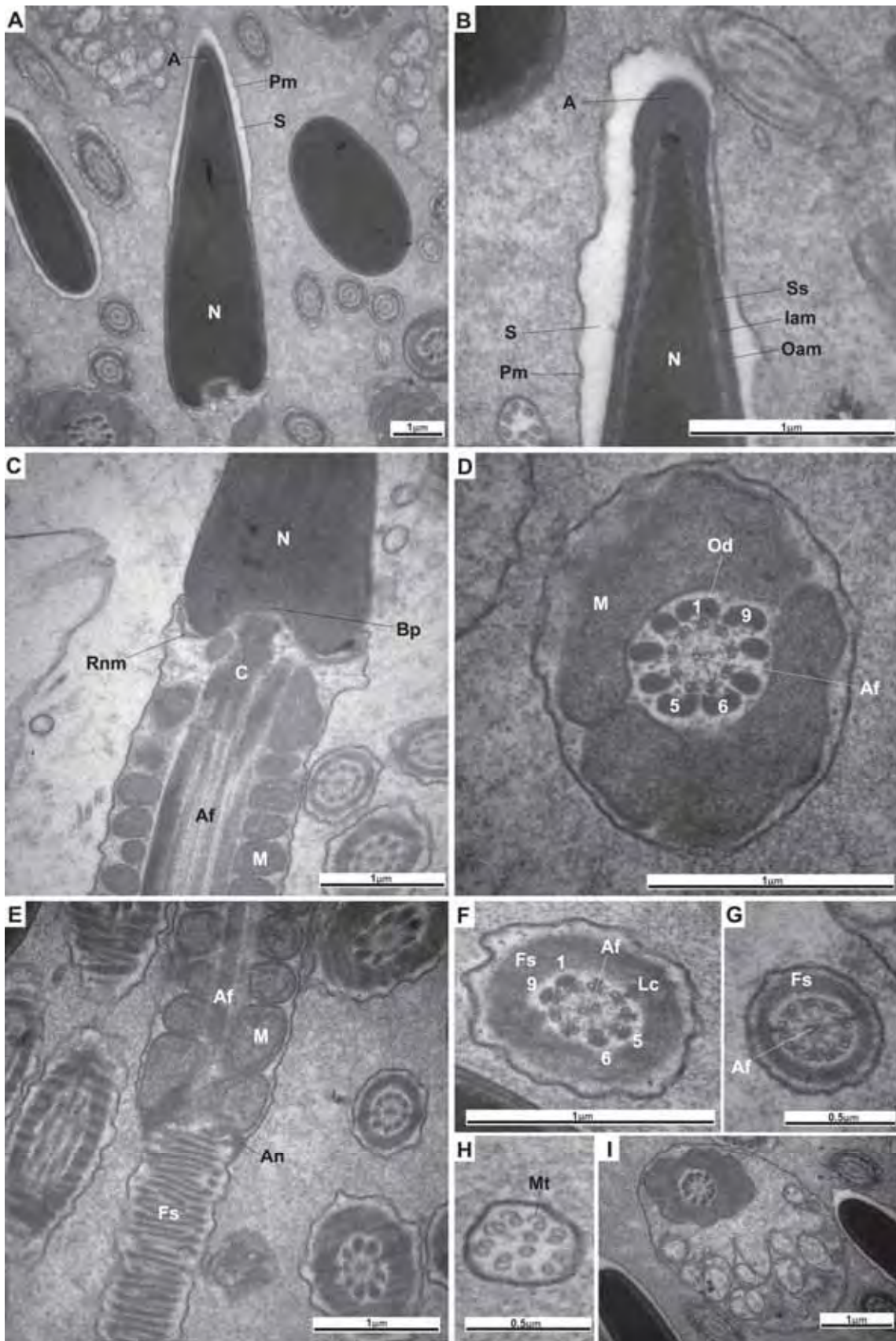


**Figure 6.** Photo (C) and electron micrographs of the testes of *Myotis nigricans* showing the ultrastructural characteristics during the deactivating (A-B) and regressed periods (C-G). **A-B.** Deactivating period. Note the more firmly cell association and the higher electron-density of the basal compartment (A); and the relaxation in the cellular connections, presenting several intra and intercellular vacuoles of the adluminal compartment (A-B). **C.** Photomicrograph of the semi-fine section stained with Toluidine Blue plus Borax, showing the arrangement of the testicular epithelium during the regressed period. Note that the epithelium was composed only by spermatogonia and Sertoli cells; and the presence of three different types of spermatogonia: types A<sub>d</sub> (arrow), 1 e 2. **D-G.** Regressed period. Note that the type 1 spermatogonia were great cells, which could be adhered or released from the basal lamina, were completely surrounded by Sertoli cells (D) and presented large and less electron-dense cytoplasm, dotted of large lipid droplets (F); Observe that the type 2 spermatogonia presented a smaller size than the type 1, presenting a smaller cytoplasm almost entirely occupied by their large nucleus and the absence of lipid droplets in their cytoplasm (G); and the presence of few sporadic apoptotic (E). (I, primary spermatocytes; L, lipid droplet; My, myoid cell; N, nucleus; No, nucleolus; Sd, spermatid; Se, Sertoli cell; Sg, spermatogonia; Sg1, type 1 spermatogonia; Sg2, type 2 spermatogonia; \*, apoptotic cell).

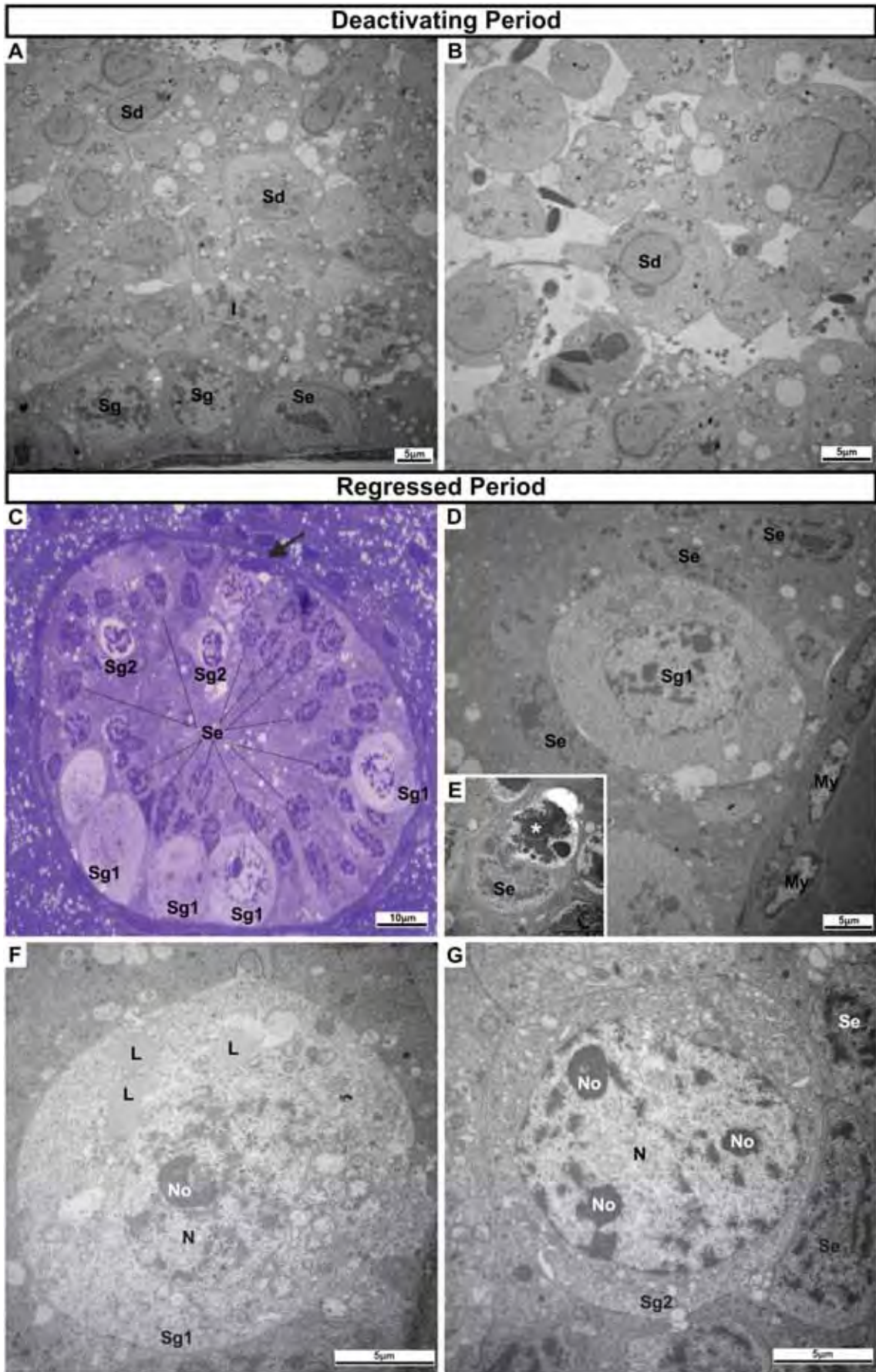




**Figure 7.** Photo (**D**) and electron micrographs of the testes of *Myotis nigricans* showing the ultrastructural characteristics during the reactivating period. Note that the epithelium of the seminiferous tubules was occupied basic by Sertoli cells, spermatogonia and primary spermatocytes (**A**); the three main types of spermatogonia can be seen again: types A<sub>d</sub>, A<sub>p</sub> (**A-B**) and B (**A** and **C**); and the presence of a great amount of apoptotic cells (**D-F**) in both compartments (basal and adluminal) and apoptotic bodies (**E**, arrow). **D.** Photomicrograph of the semi-fine section stained with Toluidine Blue plus Borax, showing the arrangement of the testicular epithelium during the regressed period. Note the great amount of apoptotic cells (arrows). (A<sub>p</sub>, type A<sub>p</sub> spermatogonia; B, type B spermatogonia; BL, basal lamina; Cb, chromatoid body; I, primary spermatocytes; M, mitochondria; My, myoid cell; N, nucleus; No, nucleolus; Se, Sertoli cell, \*, apoptotic cell).

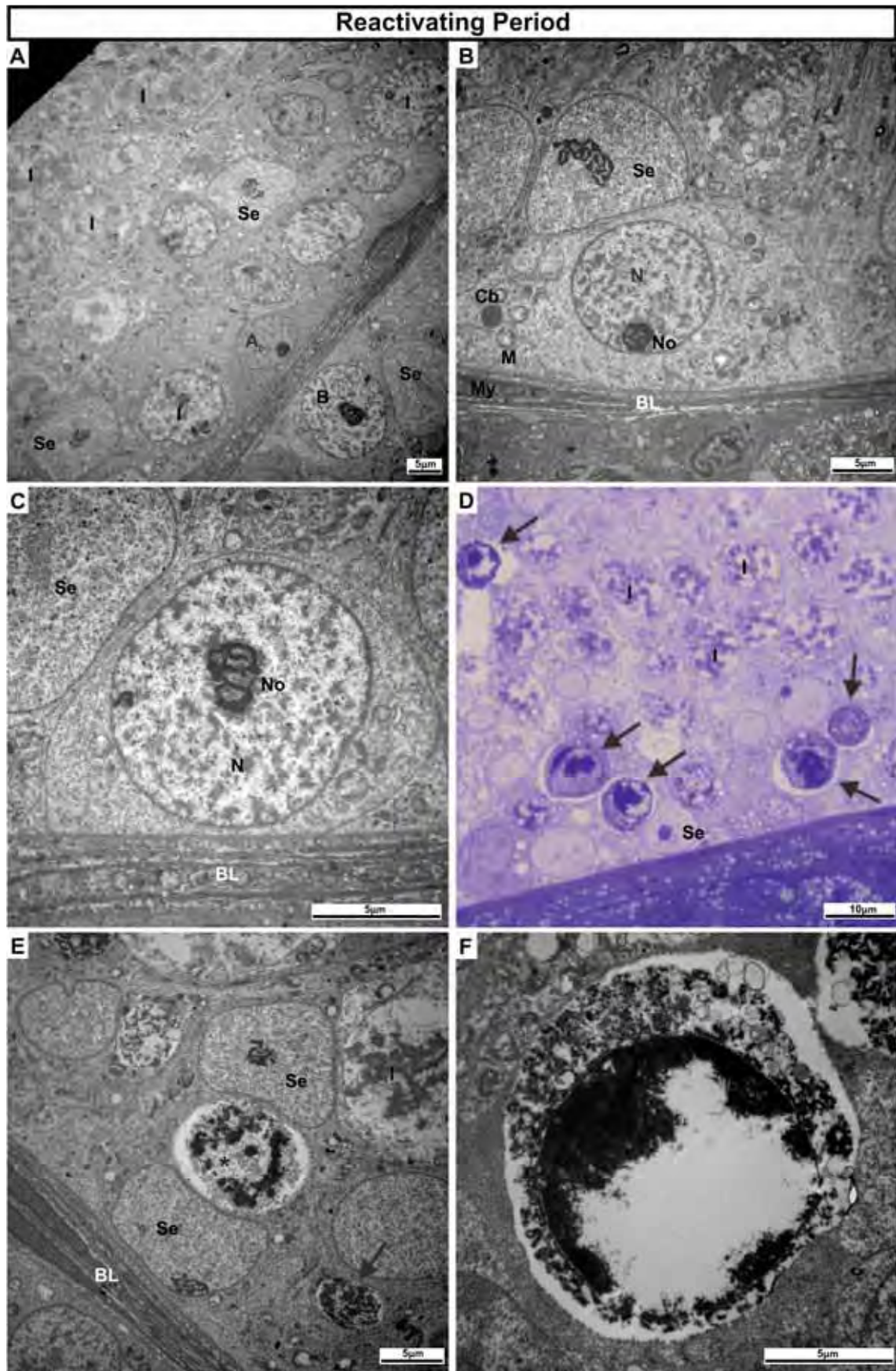
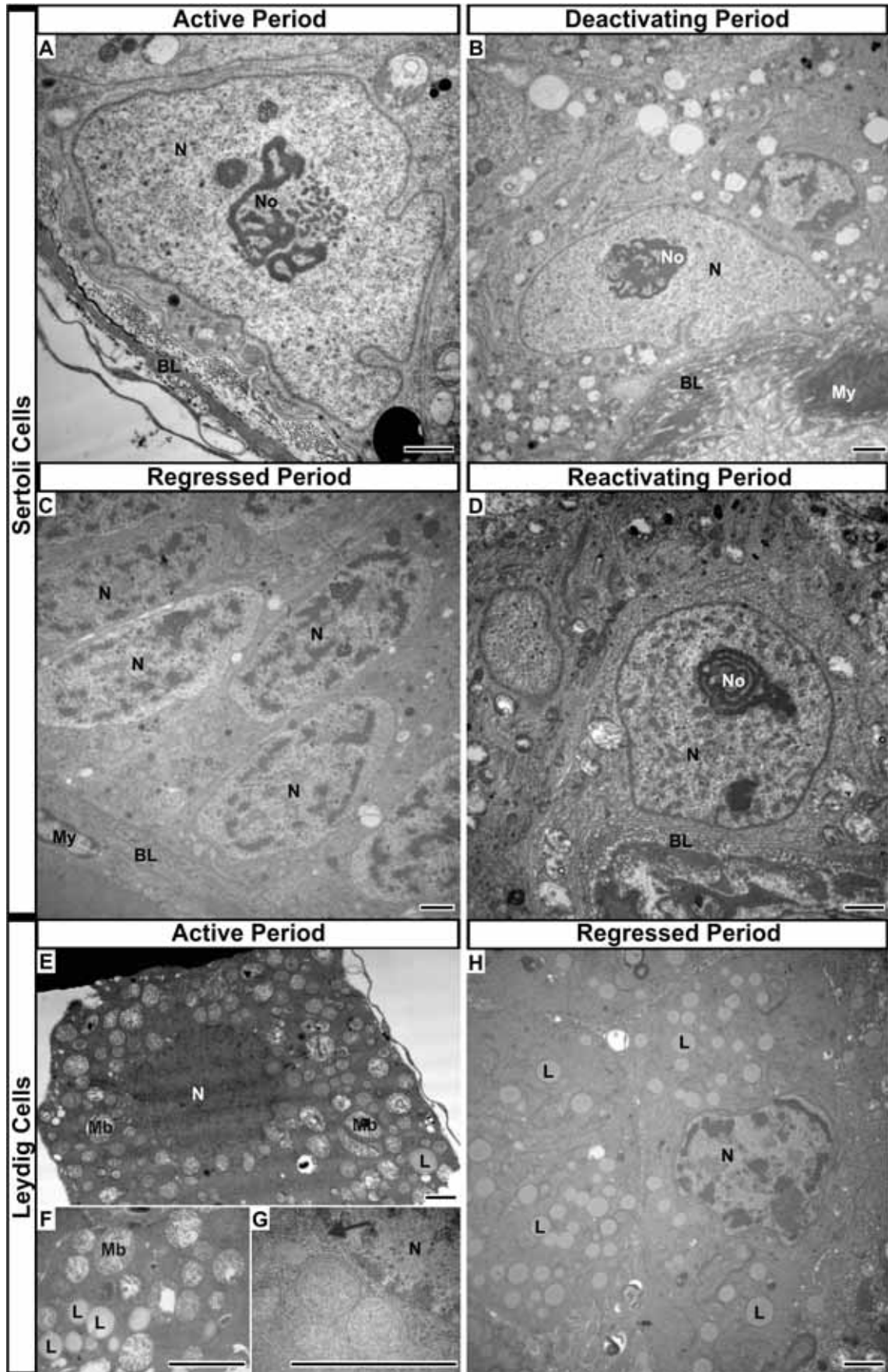


**Figure 8.** Electron micrographs of the auxiliary cells of the bat *Myotis nigricans*, during the four different periods analyzed. **A.** Sertoli cell in the active period. Note the large and irregularly shaped nucleus presenting great infoldings and a dispersed nucleolus, dotted of one filamentous and other granular portions. **B.** Sertoli cell in the deactivating period. Note the softening of their infoldings. **C.** Sertoli cell in the regressed period. Note the peak of the softening process, where the nucleus showed an elongated shape without infoldings. **D.** Sertoli cell in the reactivating period. **E-G.** Leydig cells in the active period. Note the large and undefined nucleus and the vast and highly secretory cytoplasm with great portion of them occupied by the endoplasmic reticulum (**G**) and vesicles (**F**); and the great amount of multivesicular bodies and few lipid droplets. **H.** Leydig cell in the regressed period. Note the large amount of lipid droplets. (BL, basal lamina; L, lipid droplets; Mb, multivesicular bodies; My, myoid cell; N, nucleus; No, nucleolus). Scale Bars = 2 $\mu$ m.





## VI. CAPÍTULO 4

### **Análise comparativa da ultraestrutura das células espermatogênicas e do espermatozóide de morcegos**



Por ser uma célula altamente especializada, é esperado que a morfologia do espermatozóide seja específica a cada espécie, ou ao menos que seja semelhante entre espécies proximamente relacionadas, sendo assim, diferenças estruturais podem indicar, possivelmente, diferenças taxonômicas.

Atualmente a observação e análise da ultraestrutura dos espermatozoides têm sido utilizadas como ferramenta importante na identificação e classificação de táxons de vários grupos de organismos, desde anfíbios (GARDA et al., 2002; COSTA et al., 2004a; COSTA et al., 2004b; GARDA et al., 2004), répteis (GIUGLIANO et al., 2002; TEIXEIRA et al., 2002; VIEIRA et al., 2005; COLLI et al., 2007; CUNHA et al., 2008) e aves (JAMIESON et al., 2006; TRIPEPI et al., 2006) até alguns grupos de mamíferos (JEONG et al., 2006; LUQUE e BÁO, 2006; AMARAL et al., 2010) e mesmo dentro de Chiroptera (ROUSE e ROBSON, 1986; PHILLIPS et al., 1997).

Apesar da escassez de estudos relacionados com a ultraestrutura do espermatozóide em morcegos; esses poucos estudos, quando correlacionados com nossos dados, mostram variações morfológicas interessantes, onde três caracteres da morfologia parecem variar nas diferentes famílias e, possivelmente, interespecificamente: morfologia das fibras densas externas, presença e morfologia do perforatorium e morfologia da cabeça do espermatozóide.

A morfologia das fibras densas externas divide os poucos morcegos já estudados ultraestruturalmente em ao menos dois grupos: um com as fibras 1, 5 e 6 maiores que as outras e o outro com as 1, 5, 6 e 9 sendo maiores. O primeiro grupo inclui as espécies exclusivamente Neotropicais *P. lineatus* - Phyllostomidae (BEGUELINI et al., 2011a) (Fig. 1D) e *M. molossus* - Molossidae (BEGUELINI et al., 2012) (Fig. 1E) e o segundo inclui as espécies de Rhinolophidae (OH et al., 1985; LEE et al., 1992; SANG-SICK et al., 1999) Miniopteridae (SANG-SICK et al., 1999) e Vespertilionidae (FAWCETT e ITO, 1965; SON et al., 1997; LEE, 2003) (Fig. 1F).

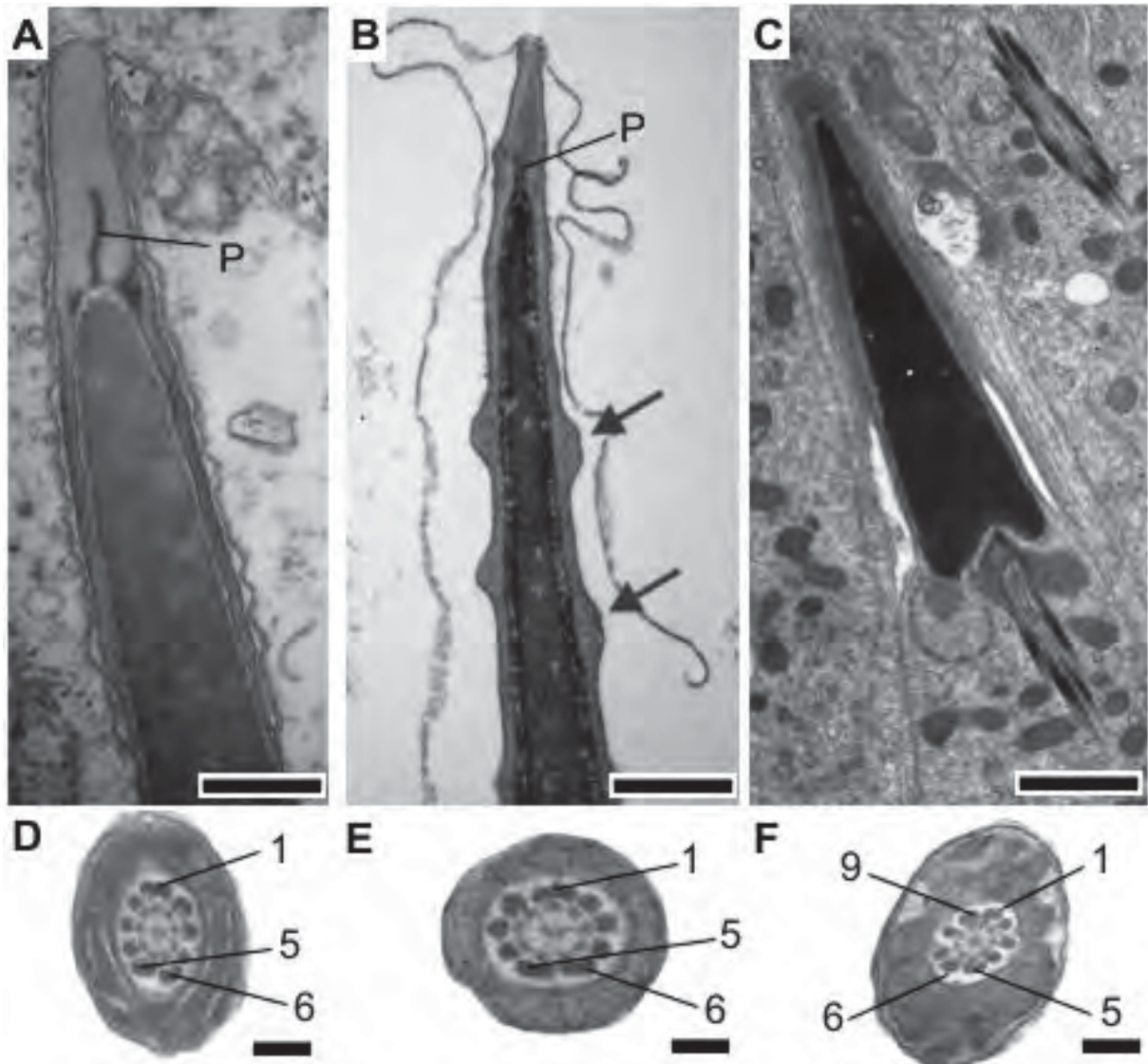


**Figura 1.** Ultraestrutura do espermatozóide de *Platyrrhinus lineatus* (A e D) (Phyllostomidae), *Molossus molossus* (B e E) (Molossidae) e *Myotis nigricans* (C e F) (Vespertilionidae). A-C. Cabeça do espermatozóide em corte longitudinal. Note a presença do perforatorium (P) em *P. lineatus* (A) e *M. molossus* (B) e a ausência em *M. nigricans* (C); as projeções do acrossomo de *M. molossus* (B, setas); e o maior tamanho das fibras densas externas 1, 5 e 6 em *P. lineatus* (D) e *M. molossus* (E) e das 1, 5, 6 e 9 em *M. nigricans* (F). Escalas: A-C - 0,5 $\mu$ m; D-F - 0,2 $\mu$ m.

O perforatorium está ausente ou pouco desenvolvido em Vespertilionidae (Fig. 1C) (FAWCETT e ITO, 1965) e Noctilionidae (PHILLIPS et al., 1997), pouco desenvolvido em Rhinolophidae (OH et al., 1985; LEE et al., 1992) e bem desenvolvido em Molossidae (Fig. 1B) (BREED e LEIGH, 1985; BEGUELINI et al., 2012) e *P. lineatus* - Phyllostomidae (Fig. 1A) (BEGUELINI et al., 2011a).

Morfologias incomuns na cabeça do espermatozóide também são típicas em algumas famílias de morcegos, tais como a cabeça extraordinariamente grande, plana e excentricamente inserida, com dobras em formato de acordeão, típico da família Noctilionidae (PHILLIPS et al., 1997), e as projeções em ondas do acrossomo de Molossidae (Fig. 1B, setas) (BREED e LEIGH, 1985; BEGUELINI et al., 2012).

Analisando esses dados observamos que *M. molossus* está mais intimamente relacionado com Phyllostomidae do que com Rhinolophidae e Vespertilionidae; e essas semelhanças entre Molossidae e Phyllostomidae, indicam que a hipótese de que Phyllostomidae tenha derivado de Molossidae não pode ser descartada. No entanto, futuras investigações da ultraestrutura do espermatozóide de outras espécies dessas famílias, assim como de outras famílias, são necessárias para uma melhor elucidação.

No entanto, esses dados já nos indicam que a morfologia do espermatozóide de morcegos talvez seja um interessante parâmetro a ser caracterizado em diferentes espécies, analisado comparativamente e utilizado em análises filogenéticas e evolutivas.

Além das diferenças na morfologia do espermatozóide, nossa análise ultraestrutural mostrou ainda diferenças no processo da espermiogênese. O processo de formação do acrossomo variou nas três espécies analisadas, apresentando três diferentes parâmetros: 1. Acrossomo formado pela junção de vesículas pró-acrossomais que contém grânulos elétrondensos dentro delas (*M. molossus* – Fig.2A); 2. Acrossomo formado apenas pela junção de vesículas pró-acrossomais elétron-lúcidas (*M. nigricans* – Fig. 2B); 3. Acrossomo formado pela junção de dois diferentes tipos de vesículas pró-acrossomais, uma elétron-densa e outra elétron-lúcida (*P. lineatus* – Fig. 2C-D). Esta diferença parece estar correlacionada com a formação do perforatorium, onde este material elétron-denso, possivelmente, corresponderia à substância básica da sua montagem. Assim teríamos o primeiro caso correspondendo ao padrão encontrado em muitos mamíferos que apresentam o perforatorium, possivelmente a

característica ancestral; o segundo, a animais que não o apresentam, ou por sua perda ou por nunca terem tido; e o terceiro a animais que apresentam uma forma diferente de sua formação, talvez uma apomorfia.

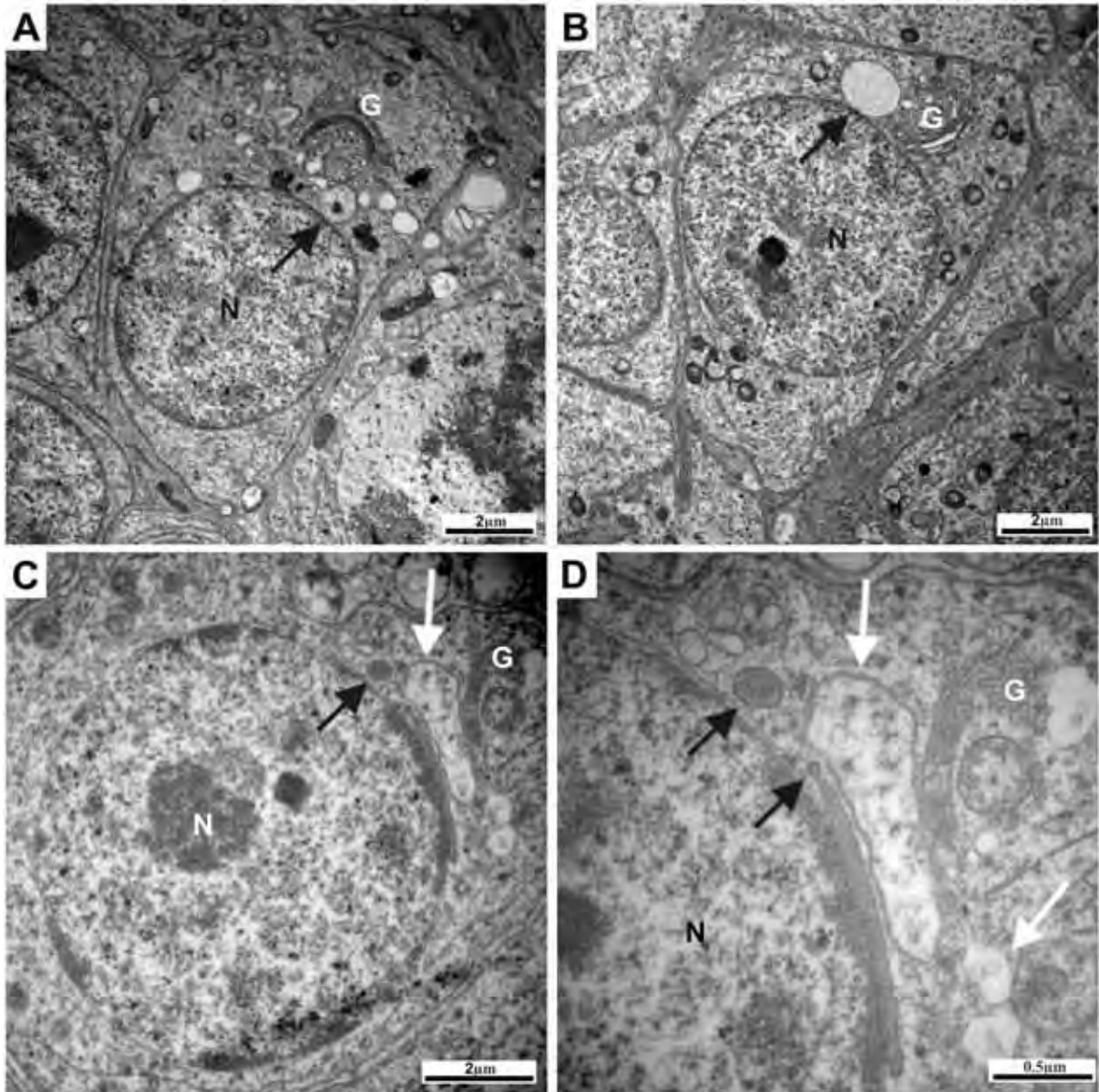


**Figura 2.** Ultraestrutura das espermátides de *Molossus molossus* (A) (Molossidae), *Myotis nigricans* (B) (Vespertilionidae) e *Platyrrhinus lineatus* (C-D) (Phyllostomidae) mostrando a composição das vesículas e vacúolos pré-acrossômicos. Setas em A-B indicam os vacúolos pré-acrossômicos; em C-D, setas negras indicam vesículas e vacúolos elétron densos e setas brancas indicam elétron lúcidos. (G, complexo de Golgi; N, núcleo).

## VII. CAPÍTULO 5

### **Annual Reproductive Cycle of Males of the Flat-faced Fruit-eating Bat, *Artibeus planirostris* (Chiroptera: Phyllostomidae)**

Artigo a ser submetido à publicação na revista “Reproduction”.



**Annual Reproductive Cycle of Males of the Flat-faced Fruit-eating Bat, *Artibeus planirostris* (Chiroptera: Phyllostomidae).**

Mateus R. Beguelini<sup>1</sup>, Cintia C. I. Puga<sup>2</sup>, Sebastião R. Taboga<sup>1</sup>, Eliana Morielle-Versute<sup>2</sup>

<sup>1</sup>*Department of Biology, São Paulo State University – UNESP/IBILCE, São José do Rio Preto, São Paulo, Brazil 15054-000*

<sup>2</sup>*Department of Zoology and Botany, São Paulo State University – UNESP/IBILCE, São José do Rio Preto, São Paulo, Brazil 15054-000*

Running head: Reproduction of *Artibeus planirostris*.

Correspondence should be addressed to Eliana Morielle-Versute; Email: morielle@ibilce.unesp.br

**ABSTRACT**

*Artibeus planirostris* is a relatively large and endemic species of phyllostomid bat from the Neotropical region, which occurs in virtually every tropical and subtropical forest, in Cerrado and Cerradão, and also in Caatingas. Some studies indicated that it exhibits seasonal bimodal polyestry; however, others postulate that it may be able to produce young at any time throughout the year. Due to these characteristics, the aim of this study was to evaluate the effect of seasonality in the testicular morphology and physiology in this species in southeast Brazil. Sixty mature male specimens, collected between June 2009 and May 2010, were submitted to morphometric and immunohistochemical analysis. Our study showed that *A. planirostris* presented a continuous active pattern of spermatogenesis throughout the year, presenting spermatozoa inside its cauda epididymis in all months. However, with two pronounced peaks of spermatogenic production, one in September and another in February. We also observed that the two breeding periods seems to be influenced mainly by the food supplement provided by environments with high temperatures and rainfall. The only median correlations between the temperature and rainfall and the testicular parameters (serum testosterone, AR e PCNA expressions) may be due to this indirect effect, where both do not directly influence the reproduction, but indirectly through the increase in food supplement. In conclusion, we observed that *A. planirostris* is an species of bat that present a bimodal polyestric pattern, with two breeding periods, that seems to be influenced by the food viability and temperature and rainfall.

**Keywords:** Chiroptera, Phyllostomidae, Reproduction, Seasonality.

## INTRODUCTION

The flat-faced fruit-eating bat, *Artibeus planirostris*, is a relatively large and endemic species of phyllostomid bat from the Neotropical region, which present the body mass ranging from 40-69g (Bárquez *et al.* 1993) and the length of forearm from 62-73mm (Guerrero *et al.* 2003, Hollis 2005). They can be found from south Colombia and southern Venezuela, south to northern Argentina and east to eastern Brazil (Koopman 1982, 1994). Known elevational range is from sea level to 1,660 m (Eisenberg 1989); however, higher locations have been described in Bolivia and Peru, reaching to 2000 m (Anderson *et al.* 1982).

This species occurs in virtually every tropical and subtropical forest (Eisenberg 1989, Hollis 2005), in Cerrado and Cerradão, and also in Caatingas (Mares *et al.* 1981, Willig & Mares 1989), but was most abundant in transitional forests (Bárquez *et al.* 1991). It roosts in trees, being captured close to several fruit-bearing trees or just above/in proximity of rivers (Bárquez *et al.* 1991, 1993); and presents a predominantly frugivorous habit, but with a great plasticity, consuming less often floral resources (pollen/nectar) and insects (Reis *et al.* 2007).

The specimens are solitary or form small colonies of 5 to 16 individuals. The gestation period is approximately 3.5 months, with usually a single young produced in each gestation. The ovaries can remained functional during pregnancy and a new ovulation can occur after birth (Taddei 1976).

According to Willig (1985), it exhibits seasonal bimodal polyestry, with peaks in reproduction from February to March and October-November. However, Graham (1987) and Taddei (1976) postulate that it may be able to produce young at any time throughout the year, by the observation of females simultaneously lactating and pregnant, and scrotal males, doted of epididymal sperm, throughout the year.

Due to all these interesting characteristics, the aim of this study was to evaluate the annual reproductive cycle of the males of this species in Southeast Brazil and to analyze the effect of seasonality in the testicular and epididymal morphology and physiology.

## RESULTS

### *Climatic Conditions*

The mean monthly temperature varied little throughout the year, staying close to 25°C (**Fig. 1A**). The period October-March had the highest average temperatures, however a great reduction was observed in June-July (Minimum temperature = 3 °C).

The mean monthly rainfall recorded to the area analyzed is shown in **Fig. 1B**. The data indicated an intense rainfall in September, followed by a period of peak in rainfall from November to March (above 100mm) and a low rainfall from May-July.

The mean monthly daylength recorded to the area analyzed is shown in **Fig. 1C**. We observed a maximum daylength in the period November-January and a minimum in June-July.

Analyzing the data we confirm the abiotic pattern of the region studied, observing the presence of two marked and different seasons: a rainy summer, with high temperatures and great daylengths; and a dry winter, with low temperatures and small daylengths.

### *Body and Gonad Weights and Gonad-Somatic Index*

The body weights of the bats studied showed little seasonal variation (**Fig. 1D**), with mean body weight close to 45g.

Differently from the body weight, the gonad weight showed two significant great peaks (**Fig. 1E**), one in September ( $0.292 \pm 0.115$ g) and another in February ( $0.489 \pm 0.114$ g). We observed that both peaks were followed by a gradual reduction in the weight, with some

posterior months presenting very low values (December:  $0.134 \pm 0.016g$  and April:  $0.155 \pm 0.062g$ , respectively).

The gonad-somatic index presented a similar pattern to that observed for the gonad weight, with two peaks followed by low values (**Fig. 1F**).

### ***Testicular Reproductive Cycle***

*Artibeus planirostris* showed an active pattern in the testes throughout the entire year, with no periods of testicular regression (**Fig. 2**). The stereological analysis showed a great abundance of epithelium in relation to other tissues; however, no accentuated variations in the proportion of tissues were observed during the year (**Fig. 3A**), with only few periods presenting small statistically significant differences. On the other hand, the morphometry confirm the presence of two major peaks of spermatogenic activity, in September and in February (**Fig. 3B**), and the gradual reduction in posterior months. These data show that, possibly, the seasonal increase and decrease of testicular mass should occur proportionally in each tissue (epithelium, lumen and interstitial tissue).

The immunohistochemistry for proliferating cells (PCNA) showed three different patterns (**Fig. 4A**): months with a significantly higher expression (May-July) (**Fig. 4B-C**); months with a median expression (December-March); and months with a low expression (August-November and April) (**Fig. 4D**); with the three groups presenting significant differences between them. The first group corresponded to autumn and early winter months; the second, to summer months; and the third, to late winter and early spring months. We observed that the expressions in the first and second groups do not vary markedly; however, in the third we noted a gradual decrease in the late winter and a gradual increase in the early spring. Surprisingly, the months with greater spermatogenic activity (greater gonads weights,



epithelium height, etc.), September and February, presented the lowest and a median expressions of PCNA, respectively. The **Fig. 4E** is the negative control of the reaction.

The expression of AR in Sertoli cells showed considerable seasonal variation (**Fig. 4F**). There were two peaks of great expression, one in May-July (**Fig. 4G**) and other in December (**Fig. 4H**). Each of them was followed by a gradual decrease until months with low expressions. Similar to the PCNA expression, the months with greater spermatogenic activity, September and February, presented again the lowest expressions. The **Fig. 4I** is the negative control of the reaction.

The TUNEL method showed no significant differences throughout the year (**Fig. 4L**), presenting only a basal expression (**Fig. 4J**). The **Fig. 4K** is the positive control of the reaction. By other side, the circulating serum testosterone showed a significantly much higher concentration in the summer months, December-February, than in other months of the year (**Fig. 4M**).

### *Epididymal Reproductive Cycle*

*Artibeus planirostris* presented sperm inside their epididymis throughout the year. The stereological analysis showed small variations in the proportion of tissues during the year for the caput and the corpus epididymis (**Fig. 3C and 3E**), on the other hand, the cauda showed large fluctuations (**Fig. 3G**). In morphometry, we confirmed the presence of two peaks in the three regions, one in September and another in February (**Fig. 3D, 3F and 3H**).

The immunohistochemistry for PCNA showed a low expression in the caput (**Fig. 6A and D**) and corpus epididymis (less than 10%) (**Fig. 6B**). This low expression was also presented in the cauda epididymis in most months (**Fig. 6F**); however, two peaks of high expression were observed (**Fig. 6C**), one in July (**Fig. 6E**) and another in January.

Interestingly, both are months that precede the months of greatest testicular activity. The **Fig. 6G** is the negative control of the reaction.

The expression of AR in epididymis was high in the three regions: close to 70% in the caput (**Fig. 6K**), to 80% in the corpus (**Fig. 6L**) and to 75% in the cauda (**Fig. 6M**); with no accentuated differences observed in the three regions during the year (**Fig. 6H-J**). The **Fig. 6N** is the negative control of the reaction.

### *Correlation Tests*

The correlation tests are exposed in **Table 1**.

The body weight had the higher (negative) correlation with the rainfall, while the gonad weight seemed to be equality correlated with the rainfall and temperature. The epithelium height, tubular and luminal diameters were weakly correlated with all parameters analyzed.

The PCNA expression presented a median correlation with the temperature and the AR expression and serum testosterone, median correlations with all abiotic factors.

The testicular epithelium height presented only weak correlations with the AR and PCNA and serum testosterone level.

## DISCUSSION

The Phyllostomidae is an exclusively Neotropical family of bats that is distributed from the southern United States to northern Argentina (Reis *et al.* 2007). Within this wide distribution, they inhabit from tropical to subtropical regions, in a great diversity of habitats, thus being submitted to a large variety of abiotic factors, including variations in latitude, temperature, rainfall, photoperiod, etc. (Fleming *et al.* 1972). In response to all these factors, phyllostomid bats have evolved different reproductive patterns, such as seasonal monoestry, aseasonal polyestry, seasonal polyestry or species that breed all year round (Baumgarten & Vieira 1994, Mello & Fernandez 2000, Racey & Entwistle 2000, Duarte & Talamoni 2010).

Differing from *A. lituratus* (Ortêncio-Filho *et al.* 2007; Oliveira *et al.* 2009), our study showed that *A. planirostris* presented a continuous active pattern of spermatogenesis throughout the year, presenting spermatozoa inside its cauda epididymis in all months and no periods of testicular regression. However, two pronounced peaks of spermatogenic production, one in September and another in February, were observed, indicating that, as postulated by Willig (1985), this species possibly presented a bimodal polyestric pattern. The polyestry with two or more breeding periods seems to be the most common pattern of phyllostomid bats, already been described for various species, like *A. lituratus* (Ortêncio-Filho *et al.* 2007, Duarte & Talamoni 2010), *A. jamaicensis*, *Carollia perspicillata* and *Uroderma bilobatum* (Fleming *et al.* 1972), *A. watsoni* (Chaverri & Kunz 2006), *Platyrrhinus lineatus* (Costa *et al.* 2007), among others (Crichton & Krutzsch 2000).

The continuous annual spermatogenic activity, the presence of spermatozoa in the cauda epididymis throughout the year, together with the harems structure, possibly enables this species the ability of, under favorable conditions, to generate young at different times of the year, as described by Taddei (1976) and Graham (1987).

Despite this ability, we know that the reproductive cycle is greatly influenced and regulated by the female cycle. Many papers discuss about the female regulation of the reproductive process, where the control of the reproduction is linked to the female, due to its regulation of the periods of copulation, ovulation and fertilization. Thus, many species have adapted their reproductive cycles according to the female physiology, usually synchronizing the reproduction in a manner that the lactation, which is an energetically expensive activity (Speakman & Thomas 2003), occurs in the period of greater availability of resources (Fleming *et al.* 1972, Heideman 1995, Zortúa 2003).

Thus, we corroborated with Willig (1985), affirming that *A. planirostris* presented a bimodal polyestric pattern, with two breeding periods synchronized/influenced mainly by the food supplement provided by the environment with high temperatures and rainfall. This explains the presence of the two peaks of spermatogenic production; as it is a preferentially frugivorous species, it is expected that the lactation synchronize with the fruiting period, which is normally connected to high temperature and rainfall (Kunz *et al.* 1998, De Knegt *et al.* 2005).

The only median correlations between the temperature and rainfall and the testicular parameters (serum testosterone, AR e PCNA expressions) may be due to this indirect effect, where both do not directly influence the reproduction, but indirectly through the increase in food supplement.

In conclusion, we observed that *A. planirostris* is an exclusively Neotropical species of bat that present a bimodal polyestric pattern, with two breeding periods, that seems to be directly influenced by the food viability and indirectly by temperature and rainfall.

## **MATERIALS AND METHODS**

### ***Study Area, Capture, Climatic Conditions and Licenses***

The animals were collected in the city of São José do Rio Preto, in northwest of São Paulo State, Brazil, (49W22'45" 20S49'11"), which is located at 500 meters above sea level. This is a semi-flat region, inserted in a degraded Cerrado biome, with mesothermal climate (with rainy summers and dry winters).

The capture was performed at night, using five mist-nets (3 m x 6 m) set to intercept bats flying 1–3 m above the ground. The nets were precisely set on possible flight paths or exit shelters. At least five captures were performed in each month, except for the nights of full moon.

The climatic conditions (temperature, rainfall and photoperiod) during the period of collection were measured by the Integrated Center for Agrometeorological Information (CIIAGRO-Brazil: <http://www.ciiagro.sp.gov.br>).

The capture and captivity of bats were authorized by the Brazilian institution responsible for wild animal care (Instituto Brasileiro do Meio Ambiente, IBAMA – Processes: 02027.001957/2006-02 and 21707-1) whereas the ethics committee IBILCE-UNESP authorized all experimental procedures (Process: 013/09 – CEEA). The animals were treated according to the recommendations of the Committee on Care and Use of Laboratory Animals from the Institute of Laboratory Animal Resources, National Research Council, “Guide for the Care and Use of Laboratory Animals” (Committee on Care and Use of Laboratory Animals, 1980).

### ***Species, Aging and Experiment***

The species analyzed was the exclusively Neotropical Phyllostomidae bat, *Artibeus planirostris* (Spix 1823). It is a species not listed as endangered in the International Union for Conservation of Nature (IUCN) Red List of Threatened Species.



The bats were aged as adult based on the body weight, complete ossification of the metacarpal-phalangeal epiphyses, wear of the teeth (De Knecht *et al.* 2005; Dinerstein 1986), positioning of the testes and the presence of sperm inside the testes and/or cauda epididymis.

Sixty sexually male mature specimens were used in this study, with five specimens collected each month between June 2009 and May 2010. One testis and one epididymis of each animal were subject to the morphometric analysis and the others were analyzed by immunohistochemistry. Blood samples were collected to test the serum hormone concentration of all animals.

#### ***Processing of Animals and Serological and Histological Analyses***

The animals were deeply anesthetized and, after the measured of the body weight, blood samples were collected by endocardial puncturing, after this, the testes and epididymides were also removed to the analysis.

The blood samples were sent for analysis of plasma testosterone concentration in a commercial clinical laboratory, using automated equipment VITROS ECI-Johnson and Johnson for Ultra-sensitive Chemiluminescent Analysis.

The testes and epididymides were: immersed in Bouin fixative solution for at least 24 hours, dehydrated in graded series of ethanol, embedded in glycol methacrylate (Historesin, Leica Instruments), sectioned (1  $\mu\text{m}$  thickness), stained with hematoxylin-eosin (Ribeiro & Lima, 2000) and morphometrically analyzed; or, immersed in a methanol: chloroform: acetic acid (6:3:1) fixative solution for three hours at 4°C, dehydrated in graded series of ethanol, clarified in xylene, embedded in paraffin, sectioned (4  $\mu\text{m}$  thickness) and submitted to the immunohistochemical procedures for localization of specific androgen receptor (AR), cell proliferation marker (PCNA) and detection of apoptotic cells (TUNEL).

All the specimens are housed in the Chiroptera collection at the São Paulo State University (DZSJRP- UNESP).

### ***Morphometric-Stereological Analysis***

The following measurements were performed in testicular and epididymis (caput, corpus and cauda) cross sections using the Axiovision 3.1 for Windows® computer software for image analysis: Stereology - the relative percentage of tissue (epithelium, lumen and interstitial tissue); and Morphometry - tubular and luminal diameters, and epithelium height (excluding the stereocilia).

The relative percentage of epithelium, lumen and interstitial tissue were estimated according to the procedure of Weibel and collaborators (1966) using a 168-point grid test system. The data were obtained from 30 random microscopic fields per animal at 200x magnification. The relative percentage (%) was calculated after counting the number of points that coincided with each of the tissue compartments (epithelium, lumen of ducts and interstitial tissue).

The analysis of the tubular and luminal diameters and the epithelium height were performed in 200 tubule cross sections per animal at 400x magnification. Only transverse sections were included in this study. The epithelium height was taken as the linearly length from the base of the epithelium (basal lamina) to the apical edge (excluding the stereocilia); the luminal diameter, as the more elongated measurement from one apical edge to the other; and the tubular diameter as the more elongated distance between basal-basal laminas.

### ***Immunohistochemistry***

After microwaving for antigen retrieval, non-specific antibody binding was blocked using 3% BSA prior to incubation with the primary antibodies: specific androgen receptor (AR - rabbit polyclonal IgG, N-20, Santa Cruz Biotechnology, EUA, 1:75); cell proliferation

marker (PCNA - monoclonal anti-mouse, PC10 sc-56, Santa Cruz Biotechnology, EUA, 1:100); and detection of apoptotic cells (TUNEL - TdT-Fragel-Calbiochem, according to manufacturer's instructions). The immunoreaction was visualized by the reaction with the diaminobenzidine (DAB) and the sections were counterstained with Harrys hematoxylin. For negative controls, the sections received phosphate buffer saline (PBS) in place of the primary antibody or the enzyme (TUNEL).

The incidence of AR positive cells, apoptosis and cell proliferation in the testes was estimated by calculating the mean number of AR positive, apoptotic or proliferating cells per  $\mu\text{m}^2$  of seminiferous tubule, according to the formula:  $X = C_{ST} / A_{ST}$ , where  $C_{ST}$  is the number of cells counted per seminiferous tubule section and  $A_{ST}$  is the area of the seminiferous tubule section (expressed in  $\mu\text{m}^2$ ).

The incidence of AR positive cells and cell proliferation in the epididymis was estimated by calculating the proportion of AR or proliferating positive cells per tubule section.

### ***Statistical Analysis***

Means and standard deviations were calculated for all data sets. Differences between groups were evaluated using one-way analysis of variance (ANOVA) followed by pairwise comparisons using a Tukey test, of the program Statistica 7.0 (Statsoft Inc., Tulsa, OK).. A  $p$  value of  $\leq 0.05$  was accepted as statistically significant.

### ***Correlation Tests***

The correlation tests were performed using the Correlation Matrices of the program Statistica 7.0 (Statsoft Inc., Tulsa, OK). The tests were performed to investigate the correlation between: 1. Abiotic factors and testicular measurements and expressions; 2. Serum

testosterone and the expressions of testicular PCNA and AR; 3. Variation on testicular epithelium and PCNA, Serum Testosterone and AR expressions; and 4. Variation in body and gonad weights and serum testosterone. A correlation coefficient  $r \geq \pm 0.7$  was interpreted as a high correlation factor and a  $r \leq \pm 0.4$  as a weak correlation factor.

#### **DECLARATION OF INTEREST**

The authors declare that there is no conflict of interest that could be perceived as prejudicing the impartiality of the research reported.

#### **FUNDING**

This work was supported by the São Paulo State Research Foundation (FAPESP: processes - 09/16181-9 and 09/03470-2).

#### **ACKNOWLEDGEMENTS**

Technical help from Luiz Roberto Falleiros Junior is highly appreciated. The scholarship awarded to Mateus Rodrigues Beguelini by the Brazilian Research Foundation (CAPES) is also gratefully acknowledged.

#### **REFERENCES**

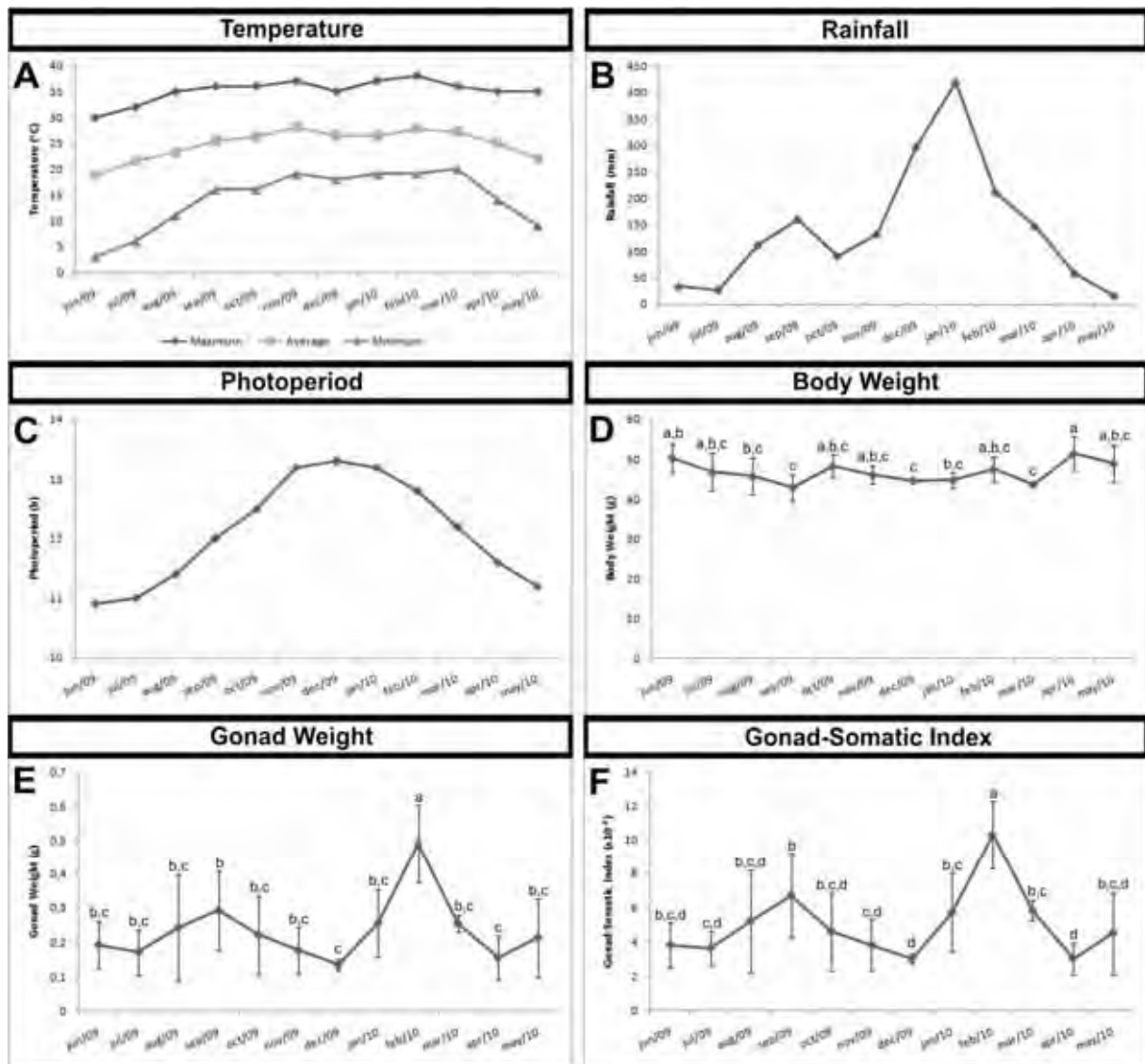
- Anderson S, Koopman KF & Creighton GK** 1982 Bats of Bolivia: an annotated checklist. *American Museum Novitates* **2750** 1–24.
- Bárquez RM, Giannini NP & Mares MA** 1993 Guide to the bats of Argentina. Oklahoma Museum of Natural History, Norman.
- Bárquez RM, Mares MA, Ojeda RA & Giannini NP** 1991. Mammals of Tucuman (Mamíferos de Tucuman). Oklahoma Museum of Natural History, Norman.

- Baumgarten JE & Vieira EM** 1994 Reproductive seasonality and development of *Anoura geoffroyi* (Chiroptera: Phyllostomidae) in central Brazil. *Mammalia* **58** 415–422.
- Chaverri G & Kunz TH** 2006 Reproductive biology and postnatal development in the tent-making bat *Artibeus watsoni* (Chiroptera: Phyllostomidae). *Journal of Zoology* **270** 650–656.
- Costa LM, Almeida JC & Esbérard CEL** 2007 Dados de reprodução de *Platyrrhinus lineatus* em estudo de longo prazo no Estado do Rio de Janeiro (Mammalia, Chiroptera, Phyllostomidae). *Lheringia, Série Zoológica* **97(2)** 152-156.
- Crichton EG & Krutzsch PH** 2000 **Reproductive biology of bats**. Academic Press, London, United Kingdom. 528 p.
- De Knegt LV, Silva JA, Moreira EC & Sales GL** 2005 Bats found in the city of Belo Horizonte, MG, 1999-2003. *Arquivo Brasileiro de Medicina Veterinária e Zootecnia* **57(5)** 576-583.
- Dinerstein E** 1986 Reproductive Ecology of Fruit Bats and the Seasonality of Fruit Production in a Costa Rican Cloud Forest. *Biotropica* **18(4)** 307-318.
- Duarte APG & Talamoni AS** 2010 Reproduction of the large fruit-eating bat *Artibeus lituratus* (Chiroptera: Phyllostomidae) in a Brazilian Atlantic forest area. *Mammalian Biology* **75** 320-325.
- Eisenberg JF** 1989 **Mammals of the Neotropics: Panama, Columbia, Venezuela, Guyana, Suriname, French Guiana**. University of Chicago Press, Illinois.
- Fleming TH, Hooper ET & Wilson DE** 1972 Three Central American bat communities: structure, reproductive cycles and movement patterns. *Ecology* **53** 555-569.
- Graham GL** 1987 Seasonality of reproduction in Peruvian bats. In *Studies in Neotropical mammalogy, essays in honor of Philip Hershkovitz*, pp **173–181**. Eds BD Patterson and RM Timm. *Fieldiana: Zoology (New Series)* **39** 1–506.

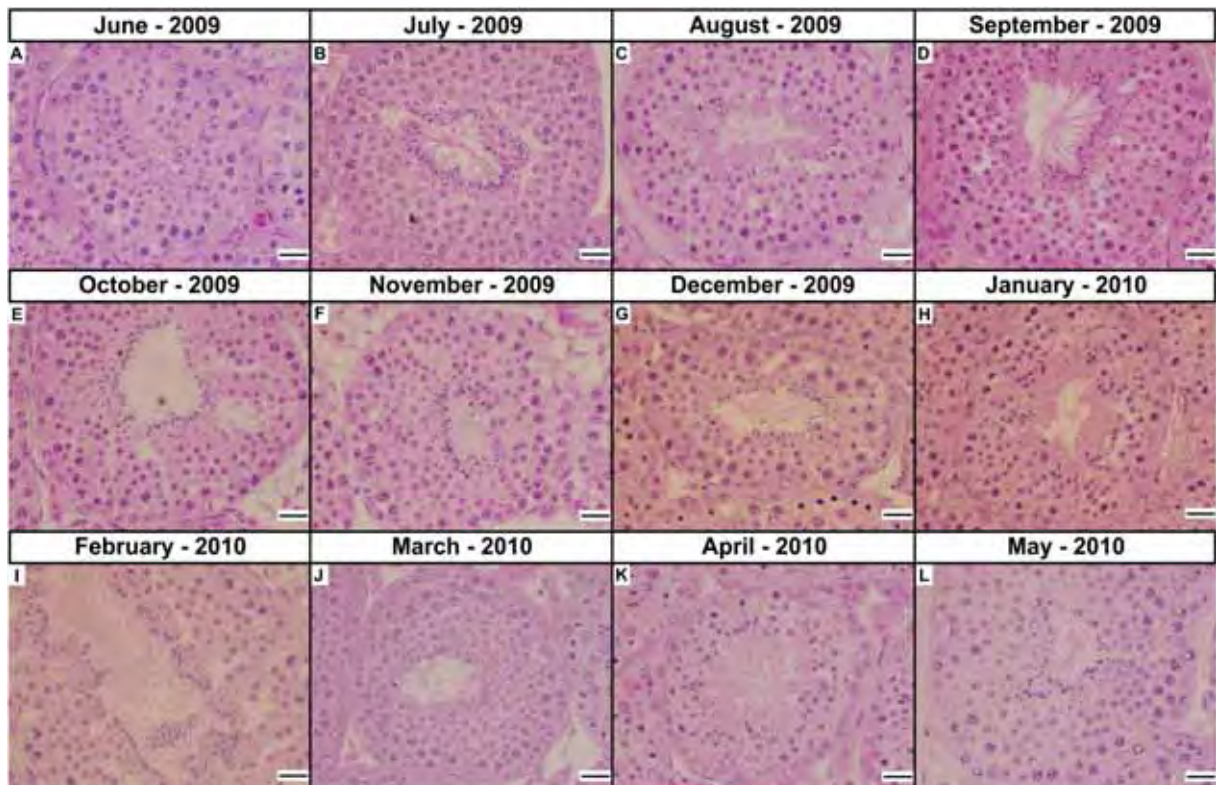


- Guerrero JA, de Luna E & Sánchez-Hernández C** 2003 Morphometrics in the quantification of character state identity for the assessment of primary homology: an analysis of character variation of the genus *Artibeus* (Chiroptera: Phyllostomidae). *Biological Journal of the Linnean Society* **80** 45–55.
- Heideman PD** 1995 Synchrony and seasonality of reproduction in tropical bats. *Symposia of the Zoological Society of London* **67** 151–165.
- Hollis L** 2005 *Artibeus planirostris* *Mammalian Species* **775** 1–6.
- Koopman KF** 1982 Biogeography of the bats of South America. In *Mammalian biology in South America*, pp 273–302. Eds MA Mares and HH Genoways. Pennsylvania: University of Pittsburg.
- Koopman KF** 1994 Chiroptera: Systematics. In *Handbook of zoology: a natural history of the phyla of the animal kingdom*, pp 1–217. Eds J Niethammer, H Schliemann and D Starck. Berlin, Germany: Walter de Gruyter and Co.
- Kunz TH, Robson SK & Nagy KA** 1998 Economy of harem maintenance in the greater spear-nosed bat *Phyllostomus hastatus*. *Journal of Mammalogy* **79** 631–642.
- Mares MM, Willig MR, Streilein KE & Lacher TEJR** 1981 The mammals of northeastern Brazil: a preliminary assessment. *Annals of Carnegie Museum* **50** 81–137.
- Mello MAR & Fernandez FA** 2000 Reproduction ecology of the bat *Carollia perspicillata* (Chiroptera, Phyllostomidae) in a fragment of the Brazilian Atlantic coastal forest. *Mammalian Biology* **65** 340–349.
- Oliveira RL, Oliveira AG, Mahecha GAB, Nogueira JC & Oliveira CA** 2009 Distribution of estrogen receptors (ER $\alpha$  and ER $\beta$ ) and androgen receptor in the testis of big fruit-eating bat *Artibeus lituratus* is cell- and stage-specific and increases during gonadal regression. *General and Comparative Endocrinology* **161** 283–292.

- Ortêncio-Filho H, Reis NR, Pinto D & Vieira DC** 2007 Aspectos reprodutivos de *Artibeus lituratus* (Phyllostomidae) em fragmentos florestais na região de Porto Rico, Paraná, Brasil. *Chiroptera Neotropical* **13(2)** 313-318.
- Racey PA & Entwistle AC** 2000 **Life-history and reproductive strategies of bats**. In: Crichton EG, Krutzsch PH (Eds.). *Reproductive Biology of Bats*. Academic Press, London, pp.363–414.
- Reis NR, Peracchi AL, Pedro WA & Lima IP** 2007 *Morcegos do Brasil*. Londrina: Universidade Estadual de Londrina.
- Ribeiro MG & Lima SR** 2000 *Iniciação às técnicas de preparação de material para o estudo e pesquisa em morfologia*. Belo Horizonte: SEGRAC – Editora e Gráfica Limitada.
- Speakman JR & Thomas DW** 2003 **Physiological Ecology and Energetics of Bats**. In: Kunz TH, Fenton, MB (Eds.). *Bat Ecology*. University of Chicago Press, Chicago, pp. 430–490.
- Taddei VA** 1976 The reproduction of some Phyllostomidae (Chiroptera) from the northwestern region of the State of São Paulo. *Biol. Zool. Univ. São Paulo*. **1** 313-330.
- Weibel ER, Kistler GS & Scherle WF** 1966 Practical stereological methods for morphometric cytology. *Journal of Cell Biology* **30(1)** 23-38.
- Willig MR** 1985 Reproductive patterns of bats from Caatingas and Cerrado biomes in northeast Brazil. *Journal of Mammalogy* **66** 668–681.
- Willig MR & Mares MA** 1989 Mammals from the Caatinga: an updated list and summary of recent research. *Revista Brasileira de Biologia* **49** 361–367.
- Zortéa M** 2003 Reproductive patterns and feeding habitats of three nectarivorous bats (Phyllostomidae: Glossophaginae) from Brazilian Cerrado. *Revista Brasileira de Biologia* **63(1)** 159-168.

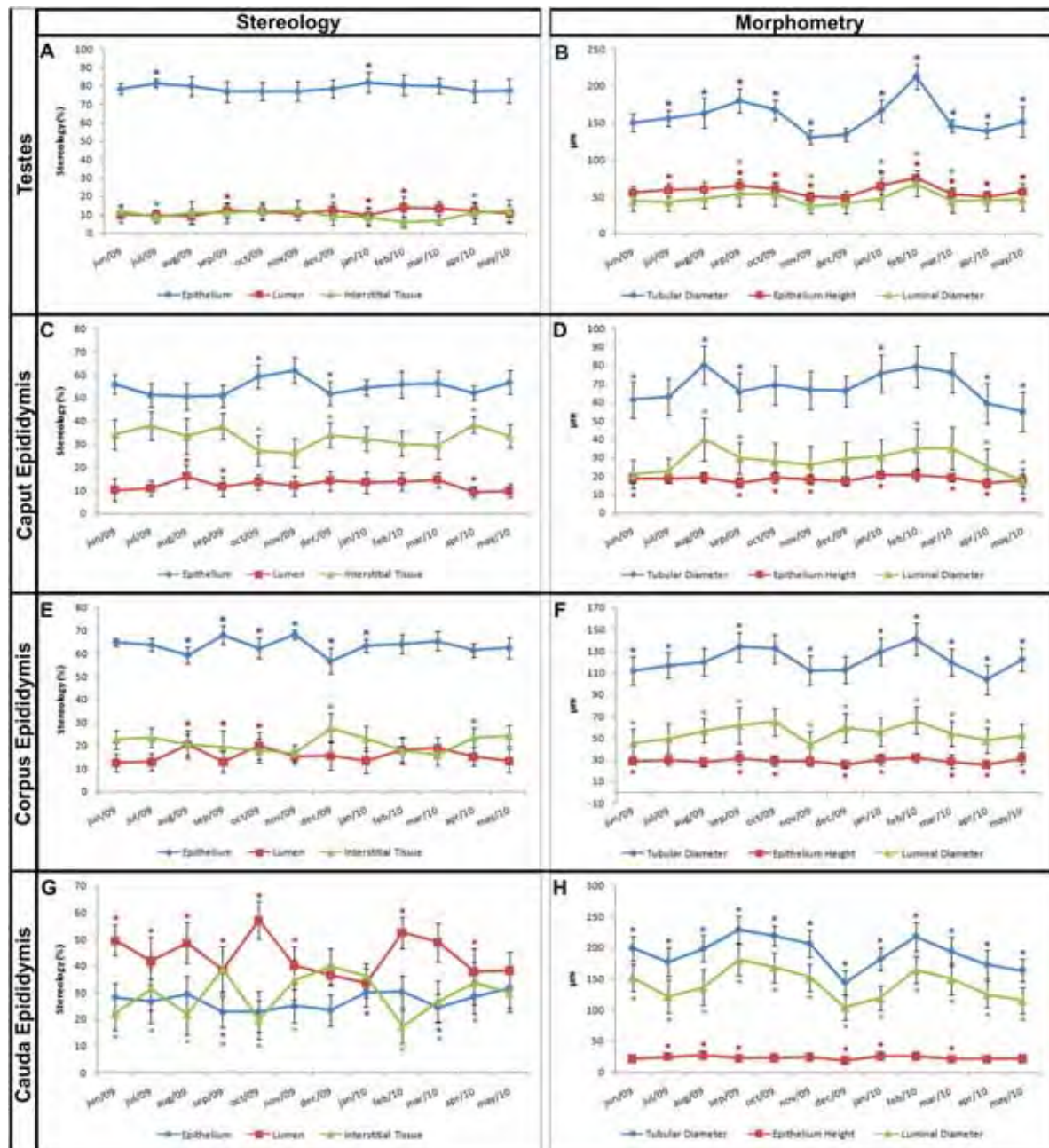


**Figure 1.** Seasonal changes in climatic conditions of the area studied and in the body and gonad weights and gonad-somatic index of *Artibeus planirostris* from Southeast Brazil from June 2009 to May 2010. **A.** Interannual monthly variations in temperature. **B.** Interannual monthly variations in rainfall. **C.** Interannual monthly variations in daylength. **D.** Seasonal variations in the mean body weight. **E.** Seasonal variations in the mean gonad weight (both testes). **F.** Seasonal variations in the gonad-somatic index. Different letters indicate statistically significant differences (ANOVA at  $p < 0.05$ ;  $n = 5$ ).



**Figure 2.** Testicular morphology of *Artibeus planirostris* from Southeast Brazil from June 2009 to May 2010. Hematoxylin-eosin stain. **A.** June 2009. **B.** July 2009. **C.** August 2009. **D.** September 2009. **E.** October 2009. **F.** November 2009. **G.** December 2009. **H.** January 2010. **I.** February 2010. **J.** March 2010. **K.** April 2010. **L.** May 2010. Note the active pattern of the testicular epithelium throughout the year. Scale bars = 20 $\mu$ m.

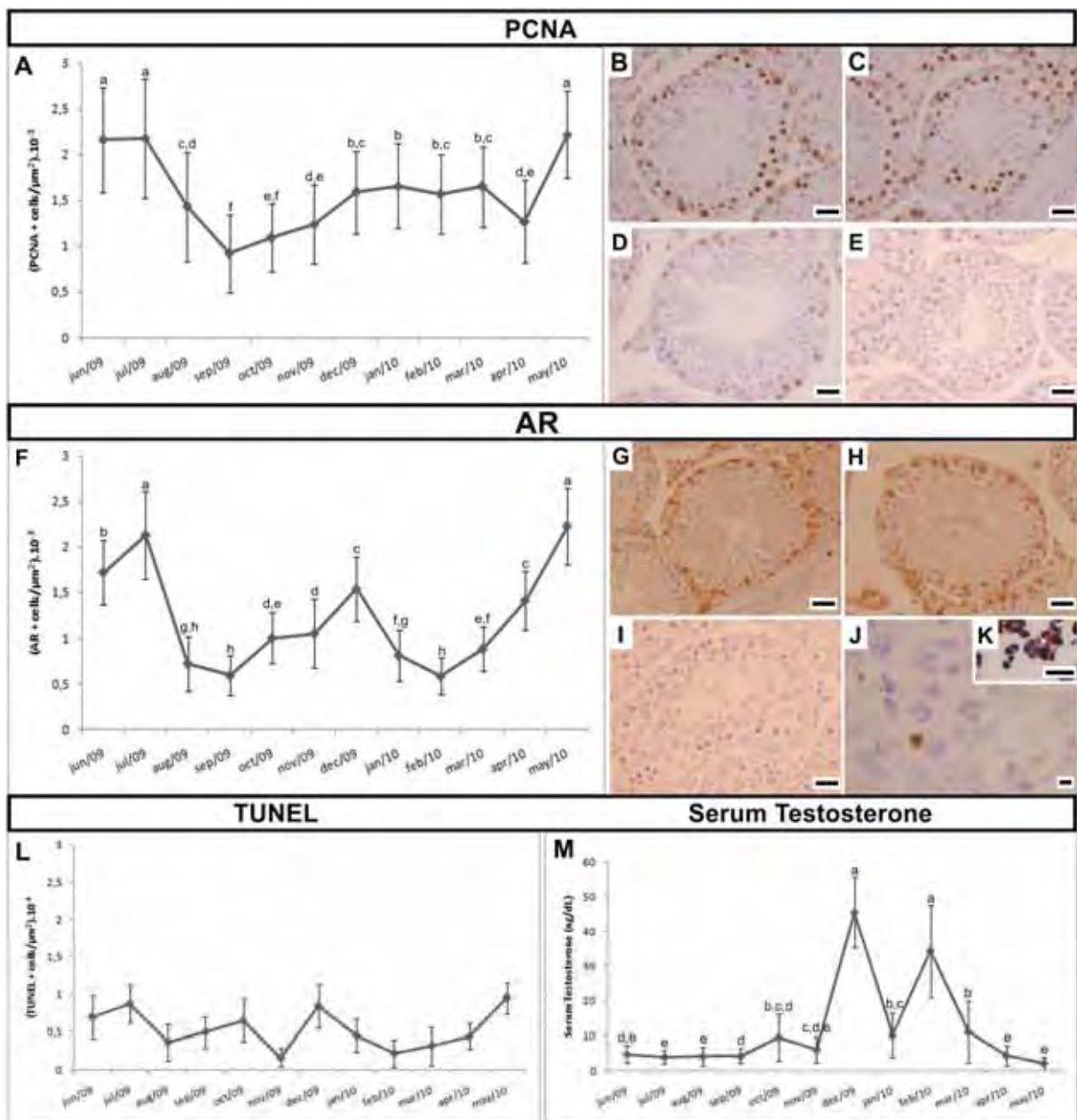




**Figure 3.** Stereology (amount of epithelium, lumen and interstitial tissue) and morphometry (tubular and luminal diameters and epithelial height) of the testes and epididymis of *Artibeus planirostris* from Southeast Brazil from June 2009 to May 2010. **A-B.** Testes. **C-D.** Caput epididymis. **E-F.** Corpus epididymis. **G-H.** Cauda epididymis. (\* = significantly different with respect to the value of the previous month - ANOVA at  $p < 0.05$ ;  $n = 5$ ).



**Figure 4.** Seasonal changes in amount of proliferating cells (PCNA: **A-E**), expression of androgen receptor (AR: **F-I**) and amount of apoptotic cells (TUNEL: **J-L**) in testes; and circulating serum testosterone (**M**) of *Artibeus planirostris* from Southeast Brazil from June 2009 to May 2010. **A.** Graphic showing the number of PCNA+ cells by testicular area. **B-D.** Expression of PCNA in animals from June (**B**), July (**C**) and September (**D**). **E.** Negative control of the PCNA immunoreaction. **F.** Graphic showing the number of AR+ cells by testicular area. **G-H.** Expression of AR in Sertoli cells of animals from July (**G**) and December (**H**). **I.** Negative control of the AR immunoreaction. **J.** TUNEL reaction in testes of animals from December. **K.** Positive control of the TUNEL immunoreaction. **L.** Graphic showing the number of TUNEL+ cells by testicular area. **M.** Graphic showing the annual variation in the concentration of circulating serum testosterone. Different letters indicate statistically significant differences (ANOVA at  $p < 0.05$ ;  $n = 5$ ). Scale bars = 20 $\mu$ m.



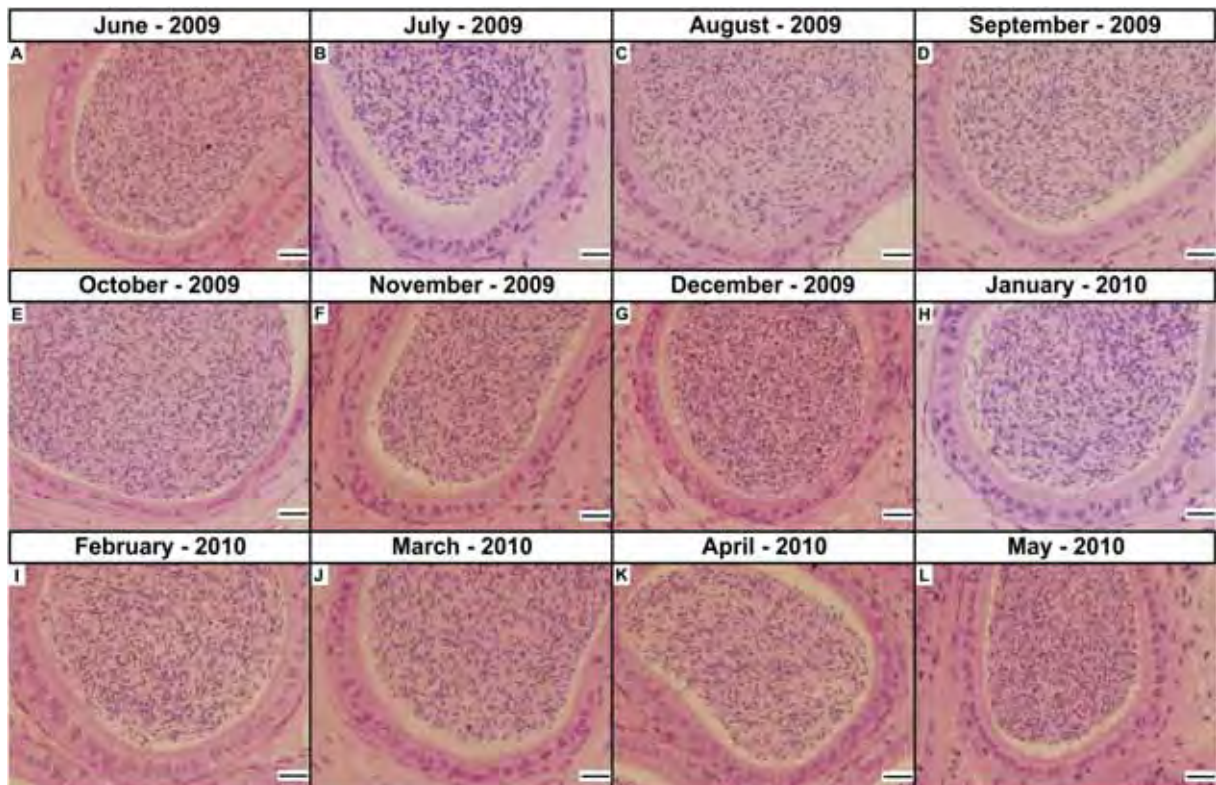


**Figure 5.** Morphology of the cauda epididymis of *Artibeus planirostris* from Southeast Brazil from June 2009 to May 2010. Hematoxylin-eosin stain. **A.** June 2009. **B.** July 2009. **C.** August 2009. **D.** September 2009. **E.** October 2009. **F.** November 2009. **G.** December 2009. **H.** January 2010. **I.** February 2010. **J.** March 2010. **K.** April 2010. **L.** May 2010. Note the abundant presence of spermatozoa in the lumen in all months. Scale bars = 20 $\mu$ m.

**Figure 6.** Seasonal changes in amount of proliferating cells (PCNA: **A-G**) and in expression of androgen receptor (AR: **H-N**) in epididymis of *Artibeus planirostris* from Southeast Brazil from June 2009 to May 2010. **A.** Graphic showing the number of PCNA+ cells in caput epididymis. **B.** Graphic showing the number of PCNA+ cells in corpus epididymis. **C.** Graphic showing the number of PCNA+ cells in cauda epididymis. **D.** Expression of PCNA in caput epididymis of animal from June. **E-F.** Expression of PCNA in cauda epididymis of animals from July (**E**) and August (**F**). **G.** Negative control of the PCNA immunoreaction. **H.** Graphic showing the number of AR+ cells in caput epididymis. **I.** Graphic showing the number of AR+ cells in corpus epididymis. **J.** Graphic showing the number of AR+ cells in cauda epididymis. **K.** Expression of AR in caput epididymis of animal from June. **L.** Expression of AR in corpus epididymis of animal from July. **M.** Expression of AR in cauda epididymis of animal from July. **N.** Negative control of the AR immunoreaction. Different letters indicate statistically significant differences (ANOVA at  $p < 0.05$ ;  $n = 5$ ). Scale bars =  $10\mu\text{m}$ .

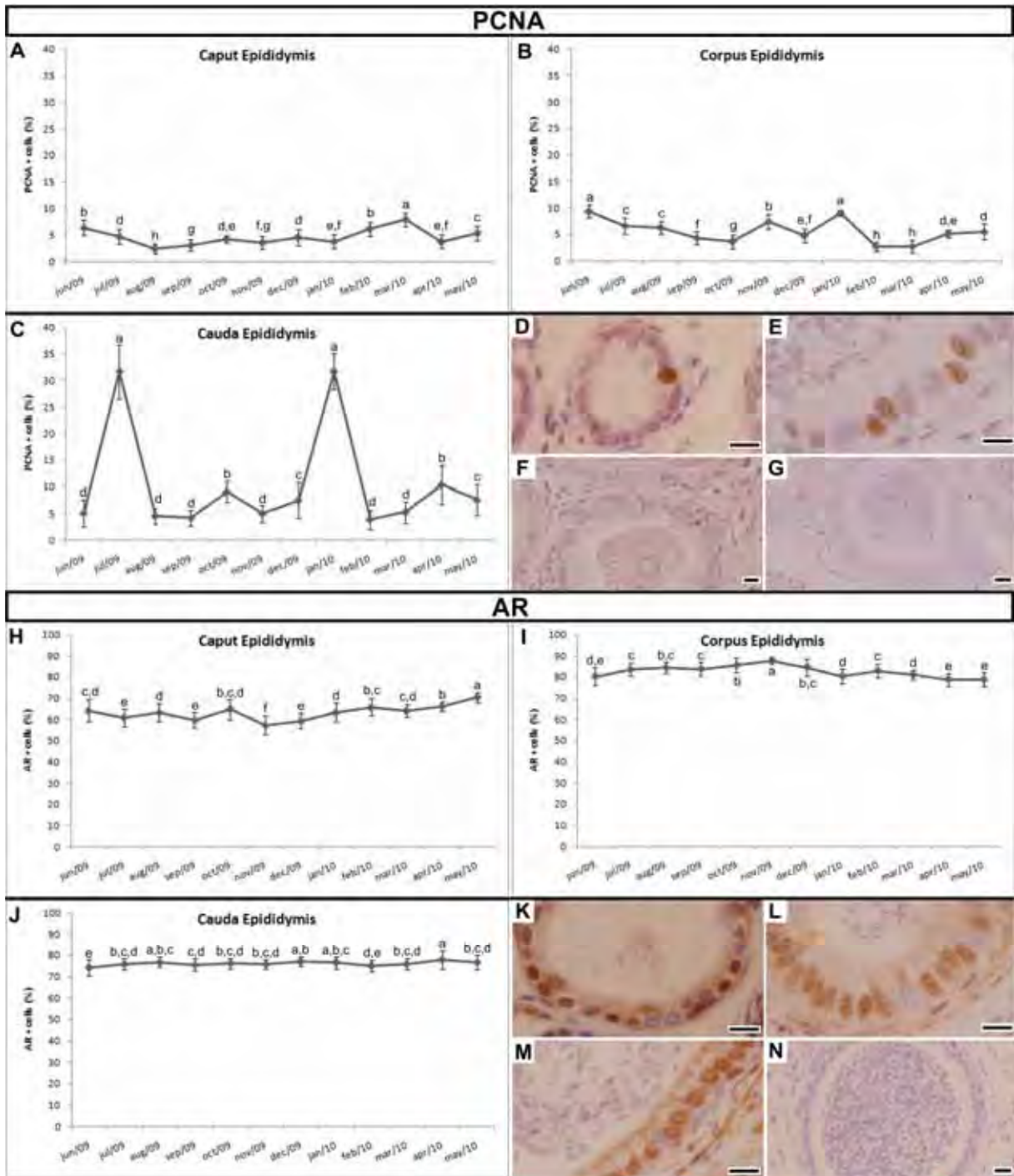




**Table 1.** Correlation coefficients (r) for relationships.

<b>1) Abiotic factors and testicular measurements and expressions</b>				
	<b>Body Weight</b>	<b>Gonad Weight</b>	<b>Tubular Diameter</b>	<b>Luminal Diameter</b>
<b>Temperature</b>	-0.2946	0.22863	0.12256	0.11117
<b>Rainfall</b>	-0.3461	0.19343	0.16051	0.07010
<b>Photoperiod</b>	-0.2837	0.13377	0.04270	0.04493
	<b>Epithelium Height</b>	<b>PCNA</b>	<b>AR</b>	<b>Serum Testosterone</b>
<b>Temperature</b>	0.05811	<b>-0.4307</b>	<b>-0.5711</b>	<b>0.49385</b>
<b>Rainfall</b>	0.14597	-0.1619	<b>-0.4486</b>	<b>0.57614</b>
<b>Photoperiod</b>	0.01983	-0.3183	<b>-0.4596</b>	<b>0.62858</b>
<b>2) Serum testosterone and the expressions of PCNA and AR</b>				
	<b>PCNA</b>	<b>AR</b>		
<b>Testosterone</b>	-0.0478	-0.2161		
<b>3) Variation on testicular epithelium and PCNA, Testosterone and AR expressions</b>				
	<b>PCNA</b>	<b>Testosterone</b>	<b>AR</b>	
<b>Epithelium Height</b>	-0.0246	0.13868	-0.2455	
<b>4) Variation in body and gonad weights and serum testosterone</b>				
	<b>Body Weight</b>	<b>Gonad Weight</b>		
<b>Testosterone</b>	-0.1650	0.26048		

Bold numbers indicate median correlations.

## VIII. CAPÍTULO 6

**Two Process of Testicular Regression, not Directly Linked to Apoptosis, Are Peculiar Events of the Annual Reproductive Cycle of the Black Myotis Bat, *Myotis nigricans* (Chiroptera: Vespertilionidae)**

Artigo a ser submetido à publicação na revista “Biology of Reproduction”.

**Two Process of Testicular Regression, not Directly Linked to Apoptosis, Are Peculiar Events of the Annual Reproductive Cycle of the Black *Myotis* Bat, *Myotis nigricans* (Chiroptera: Vespertilionidae)**

**Short title:** Testicular Regression in *Myotis nigricans*.

**Summary sentence:** *Myotis nigricans* is a Neotropical species of bat that present two process of testicular regression, in the same annual reproductive cycle, which are not directly linked to apoptosis and seems to be weakly influenced by abiotic factors.

**Keywords:** Apoptosis, Chiroptera, Testicular regression, Seasonality.

**Authors:** Mateus R. Beguelini,<sup>1</sup> Rejane M. Góes<sup>1</sup>, Sebastião R. Taboga,<sup>1</sup> Eliana Morielle-Versute<sup>2</sup>

<sup>1</sup> *Department of Biology, UNESP – Univ Estadual Paulista, São José do Rio Preto, São Paulo, Brazil, 15054-000;*

<sup>2</sup> *Department of Zoology and Botany, UNESP – Univ Estadual Paulista, São José do Rio Preto, São Paulo, Brazil, 15054-000*

**Grant support:** Supported by grant 2009/16181-9 from the São Paulo State Research Foundation (FAPESP).

**Corresponding author:** Eliana Morielle-Versute – Rua Cristóvão Colombo nº 2265, Jardim Nazareth, 15054-000, São José do Rio Preto, São Paulo, Brazil. Tel.: +55 17 32212369. FAX: + 55 17 32212374. E-mail address: morielle@ibilce.unesp.br

**ABSTRACT**

*Myotis nigricans*, an endemic Neotropical species of vespertilionid bat, present few and controversial reproductive data, which indicate a geographical variation in reproduction. Thus, this study aimed to evaluate the seasonal modifications in its testicular morphology in a tropical environment. Twenty-eight mature specimens, collected between September 2008 and August 2009, were submitted to morphometric and immunohistochemical analysis. The observations revealed that it presented two peaks of spermatogenic activity that were followed by two process of testicular regression (November and June) that also seems to be synchronized with decreasing in caput and corpus epididymis, but not present in the cauda epididymis in June (sperm storage). The two process of regression presented different patterns: 1. in November, the regression occurs with a great decrease of the epithelium and a great increase of interstitial tissue proportions; however, in June, the interstitial tissue do not showed an increase; 2. the reactivation process that followed the regression in November occurs more slowly (December-March) than that from June, which occurs rapidly (July); Despite the impossibility of evaluating the circulating plasma testosterone, the expression of androgen receptor indicated a great link between testosterone and the reproductive cycle of *M. nigricans*, with a great connection between the periods of testicular increase and high AR expression. In conclusion, *Myotis nigricans* is an exclusively Neotropical species of bat that present two process of testicular regression, in the same annual reproductive cycle, which are not directly linked to apoptosis and seems to be weakly influenced by abiotic factors.

## INTRODUCTION

Studies show that most bat species reproduce seasonally [1-3]. The reproductive patterns in bats are intimately dependent on both physiological and environmental factors [4]. Temperate bats are seasonal breeders and this character is directly associated with hibernation and low temperatures [2]; however, the summer food availability and precipitation intensity also influence in this pattern [5, 6].

Bats from tropics do not hibernate and their reproduction are strongly linked to the habitat in which they are inserted, been directly influenced by the seasonal temperature changes, latitude, rainfall, and feeding resources [7, 8]. Thus, tropical bats may exhibit a great variation in reproductive patterns, showing from monoestric or polyestric patterns, to species that reproduce continuously throughout the year [9-11].

*Myotis nigricans* is an endemic species of vespertilionid bat from the Neotropical region, with records from the southern edge of the Mexican plateau to just below the Tropic of Capricorn. Known elevational range is from sea level to 3,150m, with specimens occurring in virtually every tropical and subtropical forest, as well as in areas of savanna and scrub [12].

Data from females indicated that it has a unique reproductive cycle, presenting three parturition peaks in the Panama [13]. The gestation period is approximately 60 days and the first parturition peak occurs in February. This is followed by post-partum estrus and repetitions of the cycle resulting in birth peaks in April-May and August. The third peak is followed by a period of declining reproductive activity until late December when a new annual cycle begins [12].

The young remain attached to their mother only for the first two or three days, then are left behind in large groups when the mothers leave to feed at night; it gained adult proportions, weights and measurements, with fusion of epiphyses of the long bones to the



diaphyses, until the thirteenth week [14]; and males become reproductively active at weeks 15 to 17 [15].

Wilson and Findley [15] described that the males undergo a spermatogenic cycle that is similar to the female cycle, with spermatogenesis slows or stops during September, October and November, and no sperm storage occurring. However, they observed that specimens from Mexico more closely resemble temperate zone bats in their reproductive condition at certain times of the year. Thus, these authors proposed that *M. nigricans* is geographically variable with regard to reproductive cycle and that the controlling factor in the seasonality in this species lies with the males.

Due to all these interesting characteristics and the lack of information about the reproduction of this species in South America, the aim of this study was to evaluate the effect of seasonality in the testicular morphology and physiology in this species in a tropical environment.

## **MATERIALS AND METHODS**

### ***Study Area, Capture, Climatic Conditions and Licenses***

The animals were collected in the city of São José do Rio Preto, in northwest of São Paulo State, Brazil, (49W22'45" 20S49'11"), which is located at 500 meters above sea level. This is a semi-flat region, inserted in a degraded Cerrado biome, with mesothermal climate (with rainy summers and dry winters).

The capture was performed at night, using five mist-nets (3 m x 6 m) set to intercept bats flying 1–3 m above the ground. The nets were precisely set on possible flight paths or exit shelters. At least five collections were performed in each month, except for the nights of full moon.

The climatic conditions (temperature, rainfall and photoperiod) during the period of collection were measured by the Integrated Center for Agrometeorological Information (CIIAGRO-Brazil: <http://www.ciiagro.sp.gov.br>).

The capture and captivity of bats were authorized by the Brazilian institution responsible for wild animal care (Instituto Brasileiro do Meio Ambiente, IBAMA – Processes: 02027.001957/2006-02 and 21707-1) whereas the ethics committee at IBILCE-UNESP authorized all experimental procedures (Process: 013/09 – CEEA). The animals were treated according to the recommendations of the Committee on Care and Use of Laboratory Animals from the Institute of Laboratory Animal Resources, National Research Council, “Guide for the Care and Use of Laboratory Animals” (Committee on Care and Use of Laboratory Animals, 1980).

### ***Species, Aging and Experiment***

The species analyzed was the exclusively Neotropical Vespertilionidae bat, *Myotis nigricans*. It is not listed as endangered in the International Union for Conservation of Nature (IUCN) Red List of Threatened Species, however, it is a scarce and difficult to collect species, thus we took care to not disturb the females and only few adult males were used in this study.

The bats were aged as adult based on the body weight, complete ossification of the metacarpal-phalangeal epiphyses, wear of the teeth [16, 17], positioning of the testes and the presence of sperm inside the testes and/or cauda epididymis.

Twenty-eight sexually male mature specimens were used in this study, with at least two specimens collected each month between September 2008 and August 2009. One testis and one epididymis of each animal were subject to the morphometric analysis and the others were analyzed by immunohistochemistry. Four specimens were collected later, two in November 2009 and two in June 2010, to confirm the periods of testicular regression.

### ***Processing of Animals and Histological Analyses***

The animals were sacrificed by cervical compression and, after the measured of the body weight, had the testes and epididymides removed to the analysis. The testes were also weighted.

The testes and epididymides were: immersed in Bouin fixative solution for at least 24 hours, dehydrated in graded series of ethanol, embedded in glycol methacrylate (Historesin, Leica Instruments), sectioned (1  $\mu\text{m}$  thickness), stained with hematoxylin-eosin [18] and morphometrically analyzed; or, immersed in a methanol: chloroform: acetic acid (6:3:1) fixative solution for three hours at 4°C, dehydrated in graded series of ethanol, clarified in xylene, embedded in paraffin, sectioned (4  $\mu\text{m}$  thickness) and submitted to the immunohistochemical procedures for localization of specific androgen receptor (AR), cell proliferation marker (PCNA) and detection of apoptotic cells (TUNEL).

All the specimens are housed in the Chiroptera collection at the São Paulo State University (DZSJRP- UNESP).

### ***Morphometric-Stereological Analyses***

The following measurements were performed in testicular and epididymal (caput, corpus and cauda) cross sections using the Axiovision 3.1 for Windows® computer software for image analysis: Stereology - the relative percentage of tissue (epithelium, lumen and interstitial tissue); and Morphometry - tubular and luminal diameters, and epithelium height (excluding the stereocilia).

The relative percentage of epithelium, lumen and interstitial tissue were estimated according to the procedure of Weibel and collaborators [19] using a 168-point grid test system. The data were obtained from 30 random microscopic fields per animal at 200x magnification. The relative percentage (%) was calculated after counting the number of points

that coincided with each of the tissue compartments (epithelium, lumen of ducts and interstitial tissue).

The analysis of the tubular and luminal diameters and the epithelium height were performed in 200 tubule cross sections per animal at 400x magnification. Only transverse sections were included in this study. The epithelium height was taken as the linearly length from the base of the epithelium (basal lamina) to the apical edge (excluding the stereocilia); the luminal diameter, as the more elongated measurement from one apical edge to the other; and the tubular diameter as the more elongated distance between basal-basal laminas.

### ***Immunohistochemistry***

After microwaving for antigen retrieval, non-specific antibody binding was blocked using 3% BSA prior to incubation with the primary antibodies: specific androgen receptor (AR - rabbit polyclonal IgG, N-20, Santa Cruz Biotechnology, EUA, 1:75); cell proliferation marker (PCNA - monoclonal anti-mouse, PC10 sc-56, Santa Cruz Biotechnology, EUA, 1:100); and detection of apoptotic cells (TUNEL - TdT-Fragel-Calbiochem, according to manufacturer's instructions). The immunoreaction was visualized by the reaction with the diaminobenzidine (DAB) and the sections were counterstained with Harrys hematoxylin. For negative controls, the sections received phosphate buffer saline (PBS) in place of the primary antibody or the enzyme (TUNEL). The immunofluorescence was performed using a FITC-conjugated secondary antibody followed by a counterstained with 4-6-Diamidino-2-phenylindole (DAPI).

The incidence of AR positive cells, apoptosis and cell proliferation in the testes was estimated by calculating the mean number of AR positive, apoptotic or proliferating cells per  $\mu\text{m}^2$  of seminiferous tubule, according to the formula:  $X = C_{ST} / A_{ST}$ , where  $C_{ST}$  is the number

of cells counted per seminiferous tubule section and  $A_{ST}$  is the area of the seminiferous tubule section (expressed in  $\mu\text{m}^2$ ).

The incidence of AR positive cells and cell proliferation in the epididymis was estimated by calculating the proportion of AR or proliferating positive cells per tubule section.

### ***Statistical Analysis***

Means and standard deviations were calculated for all data sets. Differences between groups were evaluated using one-way analysis of variance (ANOVA), followed by pairwise comparisons using a Tukey test, of the program Statistica 7.0 (Statsoft Inc., Tulsa, OK). A  $p$  value of  $\leq 0.05$  was accepted as statistically significant.

### ***Correlation Tests***

The correlation tests were performed using the Correlation Matrices of the program Statistica 7.0 (Statsoft Inc., Tulsa, OK). The tests were performed to investigate the correlation between: 1. Abiotic factors and testicular measurements and expressions; 2. Period of testicular regression (TUNEL) and the expressions of PCNA and AR; 3. Variation on testicular epithelium and PCNA, TUNEL and AR expression; and 4. Variation in testicular and epididymal epithelium height. A correlation coefficient  $r \geq \pm 0.7$  was interpreted as a high correlation factor and a  $r \leq \pm 0.4$  as a weak correlation factor.



## RESULTS

### *Climatic Conditions*

The mean monthly temperature varied little throughout the year, staying close to 25°C (**Fig. 1A**). The period December-March had the highest average temperatures, however a great reduction was observed in June-July (Minimum temperature = 3 °C).

The mean monthly rainfall recorded to the area analyzed is shown in **Fig. 1B**. The data indicated an increase in rainfall from December to March (above 150mm) and a low rainfall from May-July.

The mean monthly daylength recorded to the area analyzed is shown in **Fig. 1C**. We observed a maximum daylength in the period November-January and a minimum in June-July.

Analyzing the data we confirm the abiotic pattern of the region studied, observing the presence of two marked and different seasons: a rainy summer, with high temperatures and great daylengths; and a dry winter, with low temperatures and small daylengths.

### *Body and Gonad Weights and Gonad-Somatic Index*

The body weights of the bats studied showed a marked variation (**Fig. 1D**), presenting a significant great body weight in May ( $4.6 \pm 0.25\text{g}$ ), preceded (March:  $3.63 \pm 0.08\text{g}$ ) and also followed (June:  $3.74 \pm 0.09$  and July:  $3.69 \pm 0.02$ ) by a lower value. The mean body weight during the other months was close to 4g.

Differently from the body weight, the gonad weights presented two significant great peaks (**Fig. 1E**), one in September ( $46 \pm 24.8\text{mg}$ ) and another in April ( $56 \pm 39.7\text{mg}$ ). We observed that both peaks were followed by a great reduction in the gonad weight, with some posterior months presenting very low weights (November:  $7.2 \pm 1.6\text{mg}$  and June:  $15.6 \pm 3.5\text{mg}$ , respectively).

The gonad-somatic index presented a similar pattern to that observed for the gonad weight, with two peaks followed by very low values (**Fig. 1F**).

### ***Testicular Reproductive Cycle***

The testes of *M. nigricans* undergo considerable changes in morphology (**Fig. 2**) and morphometric patterns during the year. They underwent a profound involution in October (**Fig. 2B**) and were totally regressed in November (**Fig. 2C**), where only Sertoli cells and spermatogonia could be observed. Afterwards, in December they began a recrudescence process (**Fig. 2D-F**) that extended to the production of the first spermatozoa in March (**Fig. 2G**). In April, the testes reached their highest level of development and activity during the year (**Fig. 2H**). In May occurred another process of testicular regression (**Fig. 2I**), which culminated in the regressed testes of June (**Fig. 2J**). The process of testicular regression in June seems to be less accentuated than in November since, despite the presence of only Sertoli cells and spermatogonia, the tubular size does not seem to slow sharply and the amount of interstitial tissue does not appear to increase. Adding this, in July the testes were again active (**Fig. 2K**), showing that the process of recrudescence in July occurred rapidly. In August and September the testes showed an active pattern (**Figs. 2L and 2A**, respectively). Both periods of regression were confirmed in the subsequent year, November 2009 and June 2010.

Analyzing these data, we observed that the annual reproductive cycle of *M. nigricans* presented four different phases, which was repeated twice in the year, in the same order (active, deactivating, regressed and reactivating periods). Thus we had: 1. Active periods: August-September and March-April; 2. Deactivating periods: October and May; 3. Regressed periods: November and June; 4. Reactivating periods: December-February and July.

The stereological and morphometrical analyses of the testes confirmed the presence of two periods of testicular regression, one in November and another in June; and peaks of spermatogenic activity in September-October and April (**Fig. 3A-B**). The data of morphometry clearly indicated the two periods of testicular regression (**Fig. 3B**); however, the stereology clearly indicated only the November period, where there was an inversion in the proportion of tissues, with the percentage of epithelium sharply decreased ( $30.1\pm 5\%$ ) and of interstitial tissue greatly increased ( $65.8\pm 5.6\%$ ), a fact not observed in June (**Fig. 3A**). These data show that the testicular regression observed in June differed from that of November and was less accentuated than it, not presenting a significant “substitution” of the epithelium by the interstitial tissue, as in November.

The immunohistochemistry for proliferating cells (PCNA) confirmed the presence of two great peaks of spermatogonial proliferation (**Fig. 4A**), one in November-December (**Fig. 4B**) and other in June (**Fig. 4C**). These periods corresponded to regression periods, where the testes already reach their regressive point and begin to reactivate. The data also indicated two periods of little proliferation, showing that October (**Fig. 4D**) and May are periods of testicular deactivation, which proceed the two periods of regression. The **Fig. 4E** is the negative control of the reaction.

The PCNA also showed considerable seasonal changes in the Leydig cells proliferation (**Fig. 4F**), with three great peaks of proliferation: November (**Fig. 4G**), January and June (**Fig. 4H**); and two periods of little proliferation, August-October (**Fig. 4I**) and May (**Fig. 4J**).

The TUNEL method also showed two great peaks of apoptosis in the seminiferous tubules (**Fig. 4K**), one in December (**Fig. 4L-M**) and other in June (**Fig. 4N**). The proportion of apoptotic cells in other months stayed basal (**Fig. 4O**). The **Fig. 4P** is the positive control of the reaction.

The expression of AR in Sertoli cells showed considerable seasonal variation (**Fig. 4Q**), not only quantitatively but also qualitatively. There were two peaks of great expression, one in December (**Fig. 4R**) and other in June (**Fig. 4S**), and two periods of low expression, in September (**Fig. 4T**) and March. The **Fig. 4U** is the negative control of the reaction. By other side, the expression of AR in Leydig cells was more qualitatively, with all cells of the same month expressing or not expressing the receptor. The expression in Leydig cells was completely opposed to that in Sertoli cells, i.e. when the expression in Sertoli cells was high, the Leydig cells do not express the receptor and, when the expression in Sertoli cells was low, the Leydig cells express the receptor. Thus, the expression was absent in December-January (**Fig. 4V**), high from February to May (**Fig. 4X**), absent in June and high from July to November (**Fig. 4Y**). Another interesting feature was that the expression of AR in Leydig cells was only cytoplasmatic (**Fig. 4X-Y**), a fact confirmed in the immunofluorescence (**Fig. 4Z**).

### *Epididymal Reproductive Cycle*

The caput and corpus epididymis showed changes in morphology and morphometric patterns during the year similar to testes, presenting two clear periods of regression in morphometry, November and June (**Fig. 3D** and **F**, respectively), and only one in stereology, November (**Fig. 3C** and **E**, respectively). The two peaks of great development, September-October and April, were also observed in both regions (**Fig. 3C-D** and **E-F**, respectively). The data indicate that the caput and corpus epididymis vary in a way similar to the testes; however, the cauda epididymis varies differently.

The cycle of the cauda epididymis of *M. nigricans* started in November, where it presented its minimum size (**Fig. 5C**); from December to February, the cauda epididymis tubules developed gradually (**Fig. 5D-F**); however, the first spermatozoa was observed within

it only in March (**Fig. 5G**). From April, the cauda epididymis started to store spermatozoa, reaching the maximum size in June (**Fig. 5J**). The storage of spermatozoa extended until October (**Fig. 5B**), and in November no spermatozoa were observed inside it again.

The stereological and morphometric data confirmed the peak of regression in cauda epididymis in November and the maximum development in June (**Fig. 3G-H**, respectively). During the period of regression, the percentage of interstitial tissue predominance upon the other tissues (**Fig. 3G**), and the morphometric measurements presented their lowest values for luminal and tubular diameters, with the absence of spermatozoa inside it (**Fig. 3H**). By other side, with the storage of spermatozoa, the lumen increased greatly, predominating upon the other tissues (**Fig. 3G**), and the morphometric measurements presented their greatest values (**Fig. 3H**).

The immunohistochemistry for PCNA showed a similar variation for the three epididymal regions during the year, with two peaks of proliferation (**Fig. 6A-C**), one in September (**Fig. 6D**) and other in January (**Fig. 6E**), and two periods of little proliferation, one in October and other in June-July (**Fig. 6F**). The **Fig. 6G** is the negative control of the reaction.

The expression of AR in epididymis showed considerable differences among the three regions. The caput presented one period of low expression in September-October; however, the other months showed a high expression, around 80% (**Fig. 6H**). Interestingly, the expression of AR in this region is higher than that of others. The expression in the corpus varied little during the year, with three periods of slight reduction in the expression, in September, December and May. Its expression was intermediate between the caput and cauda, remaining at approximately 60% in most months (**Fig. 6I**). The cauda had the lowest expression, around 50% (**Fig. 6J**), presenting one period of low expression in March-May



(**Fig. 6K**), which was preceded and also followed by peaks of high expression, January (**Fig. 6L**) and July (**Fig. 6M**), respectively. The **Fig. 6N** is the negative control of the reaction.

### *Correlation Tests*

The correlation tests are exposed in **Table 1**. We observed that the temperature presented the higher correlation with the AR expression, however this negative correlation was only median; and the photoperiod presented only a median positive correlation with the PCNA expression. The correlations between rainfall and all parameters analyzed and between temperature and photoperiod and others parameters showed only weak correlations.

The body weight had the higher (negative) correlation with the rainfall, while the gonad weight seemed to be equality correlated with the rainfall and photoperiod. The epithelium height seemed to be equality correlated with the temperature and rainfall, while the luminal diameter, with the rainfall and photoperiod.

The PCNA expression presented a median correlation with the photoperiod, but seemed to be also correlated with the rainfall. The AR expression seemed to be correlated only with the temperature and the TUNEL with any abiotic factor. Similarly, the testicular TUNEL expression showed only weak positive correlations with the PCNA and AR expressions.

The testicular epithelium height presented only a median (negative) correlation with the AR, with weak correlations with PCNA and TUNEL expressions. Moreover, it presented a median correlation with the epithelium height of the caput and corpus epididymis, but a weak correlation to the cauda.

## **DISCUSSION**

The Vespertilionidae family presents the widest distribution of any living chiropteran family: north to the Arctic Circle in Palearctic and Nearctic regions, south to the southern parts of Africa, Australia and South America, including many oceanic islands, as Hawaii, Indonesia, Madagascar and New Zealand [2, 20]. Within this wide distribution, they inhabit a great variety of habitats, colonizing from natural to urban environments, and thus are submitted to a large variety of abiotic factors, including latitude, temperature, rainfall, photoperiod, etc. [7, 21].

In response to all these factors, vespertilionid bats have evolved some unique reproductive cycles. The majority of vespertilionid bats are seasonally monoestrous, mainly in temperate zones [1, 3], where the prolonged hibernation period during the winter restricts the reproductive process to summer, with the spermatogenesis and copulation having to occur during this period [22]. However, there are a number of nonhibernating species that also exhibit this pattern: *Scotophilus heathi* [22] and *S. wroughtoni* [23] in India; *Nycticeius schlieffenii* [24] and *Pipistrellus rusticus* [25] in South Africa; *Lasiurus ega* in Paraguay [26]; *Corynorhinus mexicanus* in Mexico [27], among others. These species are usually found in regions where winter temperatures are mild or in regions that present a great reduced seasonally variation in abiotic patterns, and frequently present the annual reproductive cycle synchronized with the female reproductive events [2]. By other side, vespertilionid species that inhabit in low latitudes, in tropical or subtropical regions, tend to be polyestrous, presenting two or three parturition peaks annually [2].

Species of the *Myotis* genera also present a great variation in their reproductive cycles; having since a seasonally monoestrous cycle in hibernating species of temperate regions, as *M. daubentonii* [28], *M. lucifugus* [29, 30], *M. macrodactylus* [31], *M. thysanodes* [32] and *M. velifer* [33]; to polyestrous cycles, in species that inhabit low latitudes, in tropical or subtropical regions: *M. adversus* demonstrated two male reproductive peaks with a

reduced/regressed period between both in Australia [34]; *M. albescens* breeds two or three times annually, with spermatogenesis occurring only from autumn to spring in Paraguay [26], among others.

The data concerning the reproductive cycle of *M. nigricans* is scarce, presenting only few old studies [12-15]. Wilson and Findley [15] and subsequently, Krutzsch [2] proposed that its reproductive cycle was geographically variable, with animals from Paraguay presenting an active pattern trough the entire year; from Panama presenting an active pattern during most of the year, but becomes reproductively quiescent for approximately three months (September-November); and animals from Mexico more closely resembling temperate zone bats in their reproductive condition.

Despite the geographic proximity to the Paraguay, our study demonstrated that specimens from São Paulo State - Brazil, are not reproductively active during the entire year, since during the November-February period they do not present spermatozoa capable of fertilization in their reproductive tract. Comparing to Panama specimens, we also observed a period of regression in November; however, differing to they, our specimens presented not one but two periods of testicular regression in the same annual reproductive cycle, a pattern never observed in any other species or study.

The observation of periods of testicular regression from 1 to 6 months in hibernating species is common, but the observation of two periods, one of whom presenting a large amount of sperm storage in the cauda epididymis, in a tropical species, seems to be specific to *M. nigricans*. Thus, similar to Wilson and Findley [15], we propose that this species has a unique pattern of reproduction, geographically variable, that present since a hibernating pattern in some regions; an active pattern throughout the year in others, to two peaks of great spermatogenic activity followed by two periods of regression in Southeast Brazil.

Fleming et al. [7] proposed that the reproductive cycles of tropical bat species are directly influenced by climatic factors (temperature, rainfall, photoperiod, etc.) and also by the availability of the food supplement. In insectivorous bats, the temperature may have a direct physiological influence in reproduction or present an indirect role, acting in the prey availability, which influences the energy resources [35]. Similarly, the continuous rainfall negatively affects the reproduction by reducing the prey abundance and increasing the energetic costs of homeothermy [36]; however, it can indirectly influence, with the post-rain acting in the prey availability. It is predicted that the photoperiod enforces the seasonality in temperate zone bats [37], acting by at least two ways: turn on or turn off a breeding season or influencing the endogenous circannual rhythm [38]; however, little is known about its effects in low latitudes.

In the present study, we observed that only the AR expression seems to be influenced by the temperature and that this influence was, possibly, directly determined. By other side, the temperature and rainfall do not appear to have a strong direct influence in any parameter analyzed; however, the post-action of both can not be neglected, deserving future accurate studies. Similarly, the photoperiod presented only a median correlation with the gonad weight, also do not appear to strongly influence any other parameter analyzed. These data indicate that abiotic parameters had only a minimal effect on reproduction of *M. nigricans*, showing that its seasonal reproductive cycle is regulated by other factors (physiologic, behavior, female cycle, etc.) or that it has not been properly regulated to the ambient where the species live (recent dispersion + short time of adaptation of species to the environment = species already shows patterns of their ancestral region - temperate region – merged with new patterns).

The gonad weight and the morphometric data show that *M. nigricans* present two peaks of spermatogenic activity, one in September and other in April, which seems to be

synchronized in the testes and caput and corpus epididymis, indicating that, possibly, they are regulated in a similar form. However, the cauda epididymis presents a different pattern, presenting a late peak (June). This difference may be explained by sperm storage that occurs from March to October. The presence of spermatozoa in the cauda epididymis of *M. nigricans* from March to October shows that this species is able to reproduce during 7-8 months per year, with the number of breeds and fertilizations depending on the reproductive cycle of the females.

The two peaks of spermatogenic activity were followed by two periods of testicular regression (November and June) that also seems to be synchronized with decreasing in caput and corpus epididymis, but not present in the cauda epididymis in June (sperm storage). The two periods of regression presented different patterns: 1. in November, the regression occurs with a great decrease of the epithelium and a great increase of interstitial tissue proportions; however, in June, the interstitial tissue do not showed an increase; 2. the reactivation process that followed the regression in November occurs more slowly (December-March) than that from June, which occurs rapidly (July);

Despite the impossibility of evaluating the circulating plasma testosterone, due to the minimum size of the species (very little blood); the expression of AR receptor indicated a great link between testosterone and the reproductive cycle of *M. nigricans*. The AR expression showed great connection with the periods of testicular increase, where, during the year, it is high in periods of testicular recrudescence and low in periods of deactivation.

The regression in November seems to be more strong/drastic, with an accentuated decreasing of the epithelium, which should be caused by the large decrease in the stimulus (low AR expression) in previous months. With the gradual increase in AR expression, the testes begin the recrudescence process that occurs slowly and extends until March, with the production of the first spermatozoa. This slow recrudescence process, possibly occur in



response to this slow and gradual increase in AR expression; however, the detailed mechanisms that regulate this response still seem uncertain.

Wang et al [39] described that the AR expression in Sertoli cells plays the most important role in the spermatogenesis during the meiosis I, with knockout mice to Sertoli cell AR arresting the process at diplotene primary spermatocytes stage; and that the AR expression in Leydig cells influences on steroidogenic functions, with the lack of functional AR leading to arrest at round spermatid stage. Similarly, Holdcraft and Braun [40] proposed that the AR normal function in Sertoli cells is also required for the terminal differentiation of spermatids. Comparing to our data, we observed that the stages of the spermatogenesis proceed according to the one proposed by these authors: with the increase in Sertoli cell AR expression (November-January) the spermatogonia differentiate into spermatocytes (December) and later to round spermatids (January), and the differentiation to elongated spermatids was linked to a peak of AR expression in Leydig cell (February). However, the meaning of the inverse expression in Sertoli and Leydig cell remains unclear.

By other side, the recrudescence process in June seems to occur rapidly, possibly due to the great and quick peak of stimulus (AR expression) and the less accentuated regression.

Apoptosis, the active, physiologic and genetically controlled, signal-induced process of selective cell death [41], is normally conspicuous during normal spermatogenesis in most mammalian species [42, 43]; however, it appears to present different roles in seasonally breeding species. It seems to directly contributed to testicular regression in Chinese soft-shelled turtle, hamsters, white-footed mice, European brown hare [44] and the bat *Miniopterus inflatus* [45]; however, similarly to that observed by Dadhich et al [46] in the Iberian mole, in *M. nigricans*, the apoptosis was not linked to the periods of testicular regression, on the contrary, it is linked to the periods of spermatogenic peak, indicating that it is not linked to the testicular regression but with the elimination of errors caused by the rapidly reactivation of

the spermatogenesis. The detailed mechanisms that regulate the testicular regression remain unclear but, possibly it was linked to a deactivation or absence of activation of the stimuli to the division.

In conclusion, *Myotis nigricans* is an exclusively Neotropical species of bat that present two periods of testicular regression, in the same annual reproductive cycle, which are not directly linked to apoptosis and seems to be weakly influenced by abiotic factors.

## ACKNOWLEDGEMENTS

Technical help from Luiz Roberto Falleiros Junior is highly appreciated.

## REFERENCES

1. Gustafson AW. Male reproductive patterns in hibernating bats. *J Reprod Fertil* 1979; 56(1):317-331.
2. Krutzsch PH. Male reproductive patterns in nonhibernating bats. *J Reprod Fertil* 1979; 56:333-344.
3. Crichton EG, Krutzsch PH. Reproductive biology of bats. London-United Kingdom: Academic Press; 2000: 528 p.
4. Racey PA, Entwistle AC. Life-history and reproductive strategies of bats. In: Crichton EG, Krutzsch PH (eds.), Reproductive biology of bats. London-United Kingdom: Academic Press; 2000: 363-414.
5. Grindal SD, Collard TS, Brigham RM, Barclay RMR. The influence of precipitation on reproduction by *Myotis* bats in British Columbia. *Amer Mid Nat* 1992; 128:339-344.
6. Lewis SE. Effect of climatic variation on reproduction by pallid bats (*Antrozous pallidus*). *Can J Zool* 1993; 71:1429-1433.

7. Fleming TH, Hooper ET, Wilson DE. Three Central American Bat Communities: Structure, Reproductive Cycles, and Movement Patterns. *Ecology* 1972; 53:555-569.
8. Taddei VA. The reproduction of some Phyllostomidae (Chiroptera) from the northwestern region of the state of São Paulo. *Bol Zool Univ São Paulo* 1976; 1:313-330.
9. Taddei VA. Biologia reprodutiva de Chiroptera: perspectivas e problemas. *Inter-facies Escrit Doc* 1980; 6:1-18.
10. Zortéa M. Reproductive patterns and feeding habits of three nectarivorous bats (Phyllostomidae: Glossophaginae) from the Brazilian Cerrado. *Braz J Biol* 2003; 63(1):159-168.
11. Beguelini MR, Moreira PR, Faria KC, Marchesin SR, Morielle-Versute E. Morphological characterization of the testicular cells and seminiferous epithelium cycle in six species of Neotropical bats. *J Morphol* 2009; 270(8):943-953.
12. Wilson DE, Laval RK. *Myotis nigricans*. *Mammal Spec* 1974; 39:1-3.
13. Wilson DE, Findley JS. Reproductive cycle of a neotropical insectivorous bat, *Myotis nigricans*. *Nature* 1970; 225(5238):1155.
14. Wilson DE. Ecology of *Myotis nigricans* (Mammalia: Chiroptera) on Barro Colorado Island, Panama Canal Zone. *J Zool* 1971; 163:1-13.
15. Wilson DE, Findley JS. Spermatogenesis in Some Neotropical Species of *Myotis*. *J Mammal* 1971; 52(2):420-426.
16. Dinerstein E. Reproductive Ecology of Fruit Bats and the Seasonality of Fruit Production in a Costa Rican Cloud Forest. *Biotropica* 1986; 18(4):307-318.
17. De Knecht LV, Silva JA, Moreira EC, Sales GL. Bats found in the city of Belo Horizonte, MG, 1999-2003. *Arq Bras Med Vet Zootec* 2005; 57(5):576-583.

18. Ribeiro MG, Lima SR. Iniciação às técnicas de preparação de material para o estudo e pesquisa em morfologia. Belo Horizonte: SEGRAC – Editora e Gráfica Limitada. 2000: 106p.
19. Weibel ER, Kistler GS, Scherle WF. Practical stereological methods for morphometric cytology. *J Cell Biol* 1966; 30(1):23-38.
20. Simmons NB. Order Chiroptera. In: Wilson DE, Reeder DM (eds.), *Mammal Species of the World: a taxonomic and geographic reference*. Baltimore: Johns Hopkins University Press; 2005: 312-529.
21. Beguelini MR, Taboga SR, Morielle-Versute E. Ultrastructural characteristics of spermatogenesis in Pallas's Mastiff bat, *Molossus molossus* (Chiroptera: Molossidae). *Microsc Res Tech* 2011; *in press*.
22. Krishna A, Singh K. The relationship between testicular activity, accessory sex glands, and circulating steroid concentration during the reproductive cycle in a male Indian vespertilionid bat, *Scotophilus heathi*. *Can J Zool* 1997; 75:1042-1050.
23. Gopalakrishna A. Studies on the embryology of microchiroptera. Part II. Reproduction in the male vespertilionida bat *Scotophilus wroughtoni* (Thomas). *Proc Indian Acad Sci B* 1948; 27:137-151.
24. Van der Merwe M, Rautenbach IL. Reproduction in Schlieffen's bat, *Nycticeius schlieffenii*, in the eastern Transvaal lowveld, South Africa. *J Reprod Fertil* 1987; 81:41-50.
25. Van der Merwe M, Rautenbach IL. Reproduction in rusty bat, *Pipistrellus rusticus*, in the northern Transvaal bushveld, South Africa. *J Reprod Fertil* 1990; 89:537-542.
26. Myers P. Patterns of reproduction of four species of vespertilionid bats in Paraguay. *Univ Calif Publs Zool* 1977; 107:1-41.

27. León-Galván MA, López-Wilchis R, Hernández-Pérez O, Arenas-Ríos E, Rosado A. Male reproductive cycle of Mexican big-eared bats, *Corynorhinus mexicanus* (Chiroptera: Vespertilionidae). *Southwest Nat* 2005; 50(4):453-460.
28. Encarnação JA, Dietz M, Kierdorf U. Reproductive condition and activity pattern of male Daubenton's bats (*Myotis daubentonii*) in the summer habitat. *Mammal Biol* 2004; 69(3):163-172.
29. Gustafson AW, Shemesh M. Changes in plasma testosterone levels during the annual reproductive cycle of the hibernating bat, *Myotis lucifugus lucifugus* with a survey of plasma testosterone levels in adult male vertebrates. *Biol Reprod* 1976; 15:9-24.
30. Gustafson AW, Damassa DA. Annual variations in plasma sex steroid-binding protein and testosterone concentrations in the adult little brown bat: relation to the asynchronous recrudescence of the testis and accessory reproductive organs. *Biol Reprod* 1985; 33:1126-1137.
31. Lee JH, Mori T. Annual cycle of the seminiferous epithelium of *Myotis macrodactylus*. *J Fac Agr, Kyushu Univ* 2004; 49(2):355-365.
32. O'Farrell MJ, Studier EH. Reproduction, growth, and development in *Myotis thysanodes* and *M. lucifugus* (Chiroptera: Vespertilionidae). *Ecology* 1973; 54(1):18-30.
33. Krutzsch PH. The reproductive biology of the cave *Myotis* (*Myotis velifer*). *Acta Chiropter* 2009; 11(1):89-104.
34. Dwyer PD. Latitude and breeding season in a polyestrous species of *Myotis*. *J Mammal* 1970; 51(2):405-410.
35. Racey PA, Speakman JR, Swift SM. Reproductive adaptations of heterothermic bats at the northern borders of their distribution. *S Afr J Sci* 1987; 83:635-638.
36. Tuttle MD, Stevenson D. Growth and survival of bats. In: Kunz TH (ed.), *Ecology of bats*. New York: Plenum Press; 1982:105-150.



37. Heideman PD, Deoraj P, Bronson FH. Seasonal reproduction of a tropical bat, *Anoura geoffroyi*, in relation to photoperiod. *J Reprod Fertil* 1992; 96:765-773.
38. Heideman PD, Bronson FH. An endogenous circannual rhythm of reproduction in a tropical bat, *Anoura geoffroyi*, is not entrained by photoperiod. *Biol Reprod* 1994; 50:607-614.
39. Wang RS, Yeh S, Tzeng CR, Chang C. Androgen receptor roles in spermatogenesis and fertility: lessons from testicular cell-specific androgen receptor knockout mice. *Endocr Rev* 2009; 30(2):119-132.
40. Holdcraft RW, Braun RE. Androgen receptor function is required in Sertoli cells for the terminal differentiation of haploid spermatids. *Development* 2004; 131:459-467.
41. Schwartzman RA, Cidlowski JA. Apoptosis: the biochemistry and molecular biology of programmed cell death. *Endocr Rev* 1993; 14:133-151.
42. Sinha-Hikim AP, Swerdloff RS. Hormonal and genetic control of germ cell apoptosis in the testis. *Rev Reprod* 1999; 4:38-47.
43. Print CG, Lakoski-Loveland K. Germ cell suicide: new insights into apoptosis during spermatogenesis. *BioEssays* 2000; 22:423-430.
44. Zhang L, Han XK, Qi YY, Liu Y, Chen QS. Seasonal effects on apoptosis and proliferation of germ cells in the testes of the Chinese soft-shelled turtle, *Pelodiscus sinensis*. *Theriogenology* 2008; 69:1148-1158.
45. Onyango DW, Gachoka GE, Otianga'a-Owiti GE, Hendrickx AG. Seasonally dependent testicular apoptosis in the tropical Long-fingered bat (*Miniopterus inflatus*). *Z Säugetierkunde J Mammal Biol* 1995; 60:206-214.
46. Dadhich RK, Real FM, Zurita F, Barrionuevo FJ, Burgos M, Jiménez R. Role of apoptosis and cell proliferation in the testicular dynamics of seasonal breeding mammals: a study in the Iberian mole, *Talpa occidentalis*. *Biol Reprod* 2010; 83:83-91.

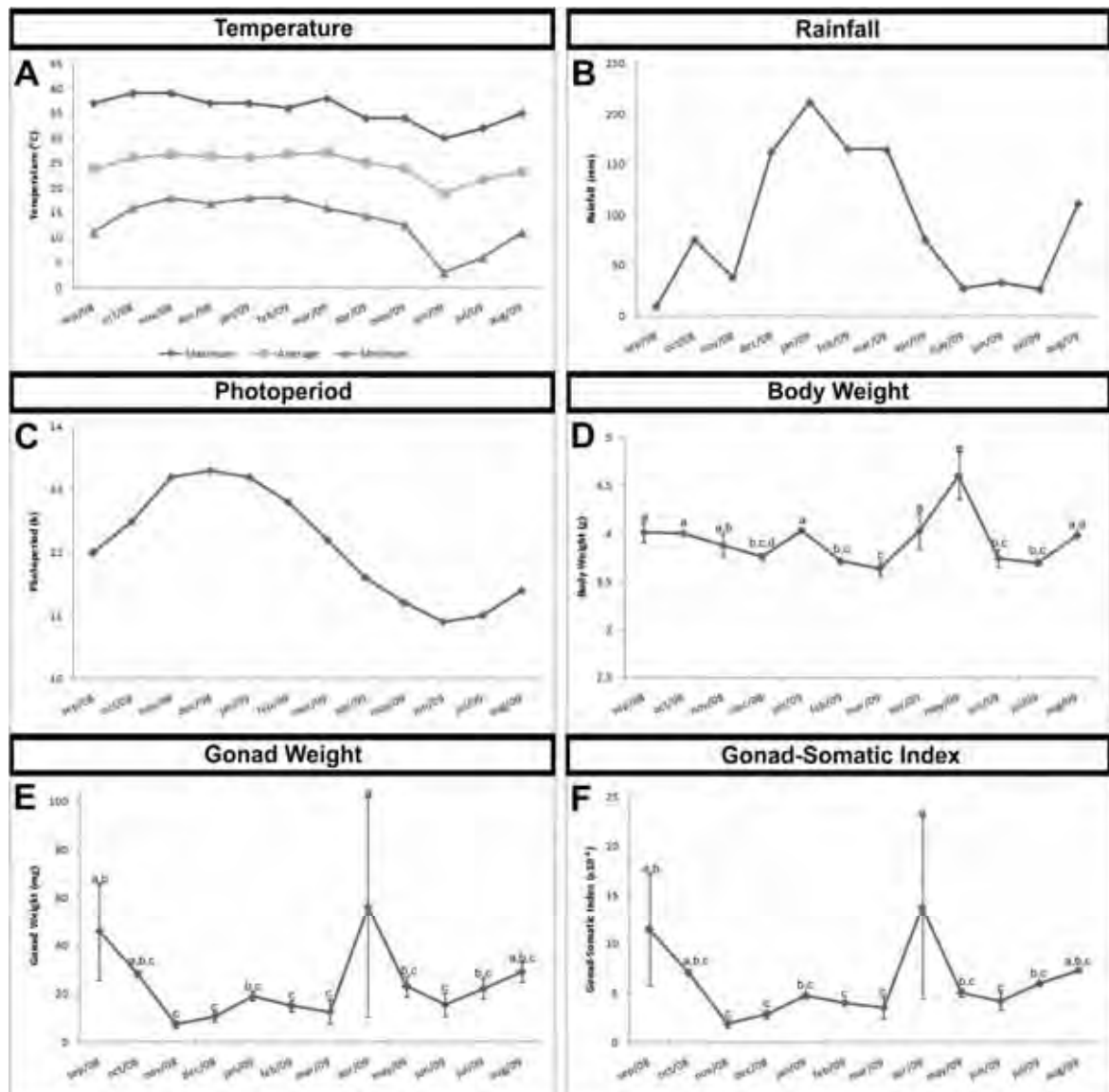


**Figure 1.** Seasonal changes in climatic conditions of the area studied and in the body and gonad weights and gonad-somatic index of *Myotis nigricans* from Southeast Brazil from September 2008 to August 2009. **A.** Interannual monthly variations in temperature. **B.** Interannual monthly variations in rainfall. **C.** Interannual monthly variations in daylength. **D.** Seasonal variations in the mean body weight. **E.** Seasonal variations in the mean gonad weight (both testes). **F.** Seasonal variations in the gonad-somatic index. Different letters indicate statistically significant differences (ANOVA at  $p < 0.05$ ).

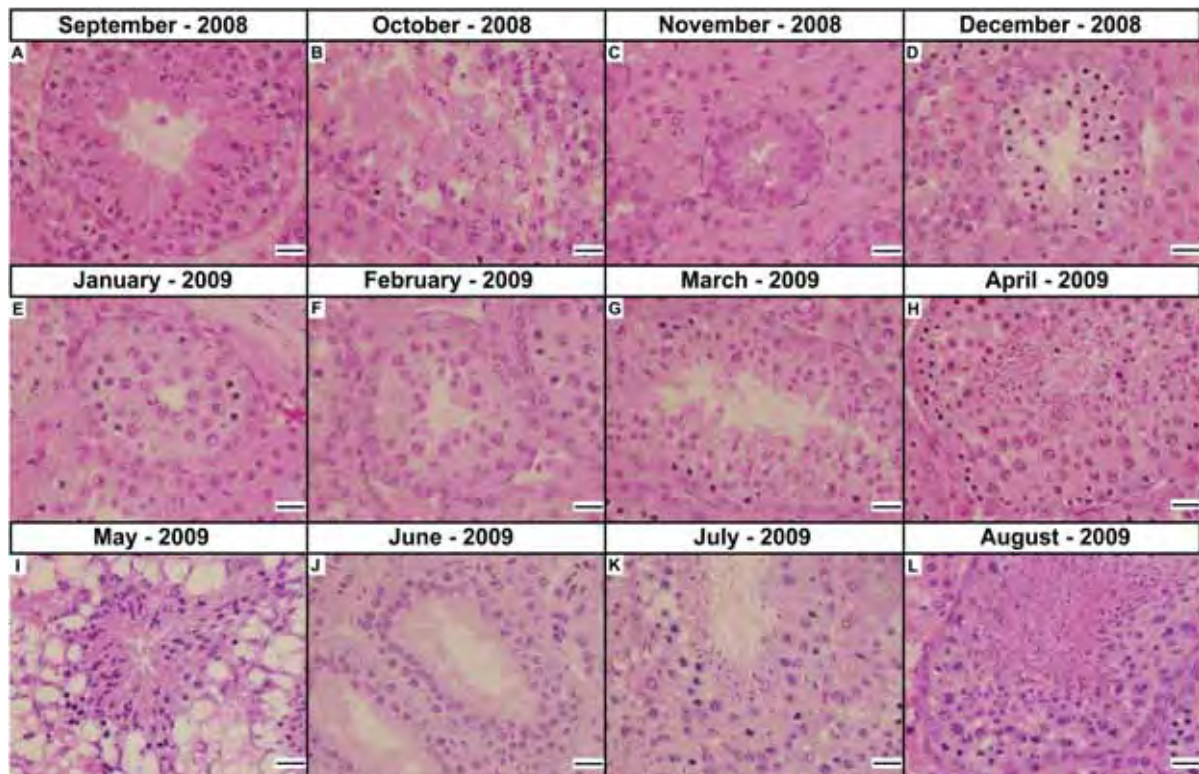


**Figure 2.** Seasonal changes in testicular morphology of *Myotis nigricans* from Southeast Brazil from September 2008 to August 2009. Hematoxylin-eosin stain. **A.** September 2008. **B.** October 2008. **C.** November 2008. **D.** December 2008. **E.** January 2009. **F.** February 2009. **G.** March 2009. **H.** April 2009. **I.** May 2009. **J.** June 2009. **K.** July 2009. **L.** August 2009. Note that the testes underwent a profound involution in October (**B**) and were totally regressed in November (**C**). Afterwards, in December they began a recrudescence process (**D-F**) that extended to the production of the first spermatozoa in March (**G**). In April, the testes reached their highest level of development and activity during the year (**H**). In May occurred a rapid process of testicular regression (**I**), which culminated in the regressed testes of June (**J**). In July the testes reactive (**K**) and in August and September the testes showed an active pattern (**L** and **A**, respectively). Scale bars = 20 $\mu$ m.

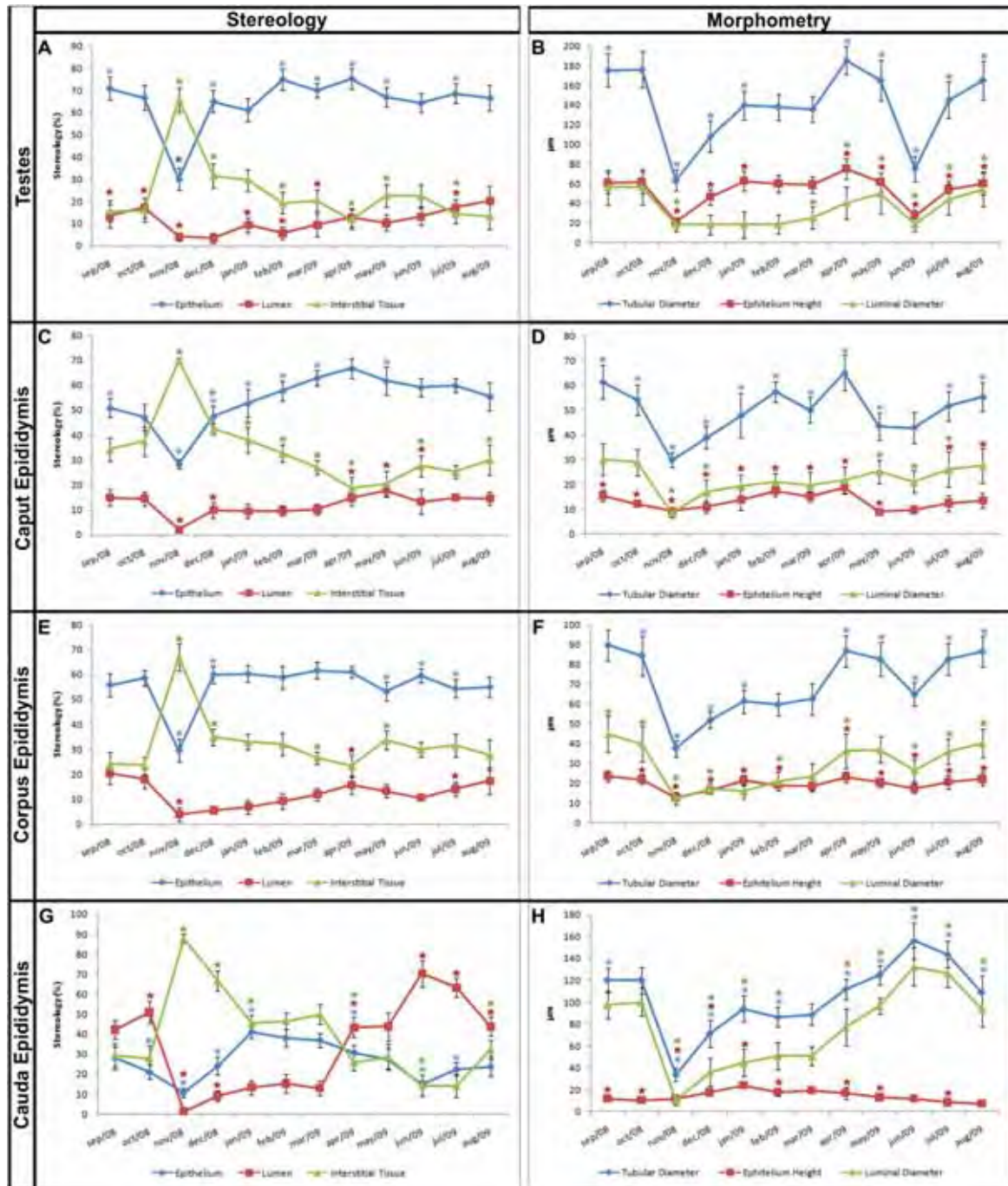
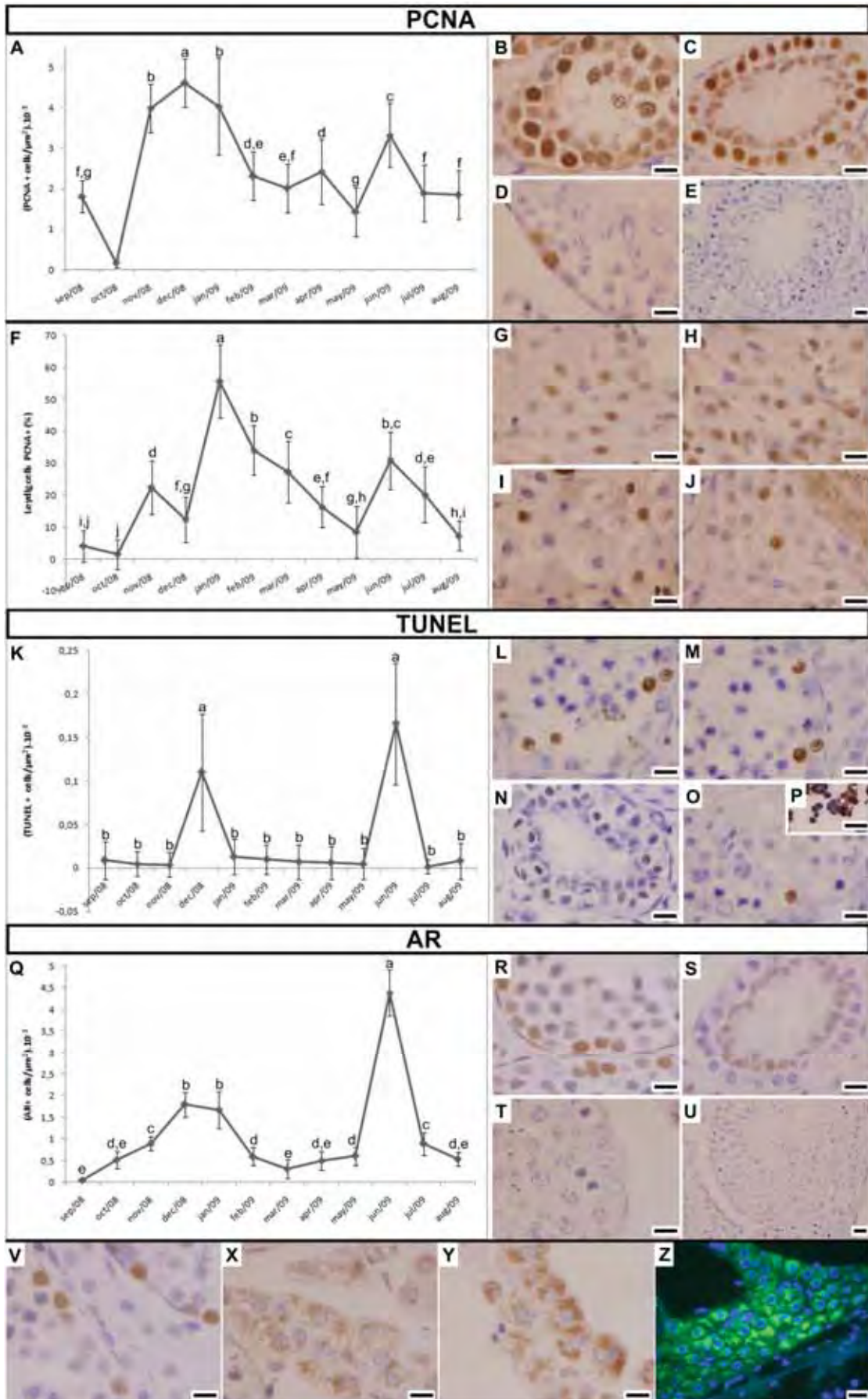


**Figure 3.** Seasonal changes in stereology (amount of epithelium, lumen and interstitial tissue) and morphometry (tubular and luminal diameters and epithelial height) of the testes and epididymis of *Myotis nigricans* from Southeast Brazil from September 2008 to August 2009. **A-B.** Testes. **C-D.** Caput epididymis. **E-F.** Corpus epididymis. **G-H.** Cauda epididymis. (\* = significantly different with respect to the value of the previous month - ANOVA at  $p < 0.05$ ).



**Figure 4.** Seasonal changes in amount of proliferating cells (PCNA: **A-J**), apoptosis (TUNEL: **K-P**) and in expression of androgen receptor (AR: **Q-Z**) in testes of *Myotis nigricans* from Southeast Brazil from September 2008 to August 2009. **A.** Graphic showing the number of PCNA+ cells by testicular area. **B-D.** Expression of PCNA in animals from December (**B**), June (**C**) and October (**D**). **E.** Negative control of the PCNA immunoreaction. **F.** Graphic showing the number of PCNA+ Leydig cells. **G-J.** Expression of PCNA in Leydig cells of animals from November (**G**), June (**H**), October (**I**) and May (**J**). **K.** Graphic showing the number of TUNEL+ cells by testicular area. **L-O.** TUNEL reaction in testes of animals from December (**L-M**), June (**N**) and October (**O**). **P.** Negative control of the TUNEL immunoreaction. **Q.** Graphic showing the number of AR+ cells by testicular area. **R-T.** Expression of AR in Sertoli cells of animals from December (**R**), June (**S**) and September (**T**). **U.** Negative control of the AR immunoreaction. **V-Y.** Expression of AR in Leydig cells of animals from December (**V**), May (**X**) and September (**Y**). **Z.** Immunofluorescence showing the cytoplasmatic expression of AR in Leydig cells. Different letters indicate statistically significant differences (ANOVA at  $p < 0.05$ ). Scale bars = 10 $\mu$ m.





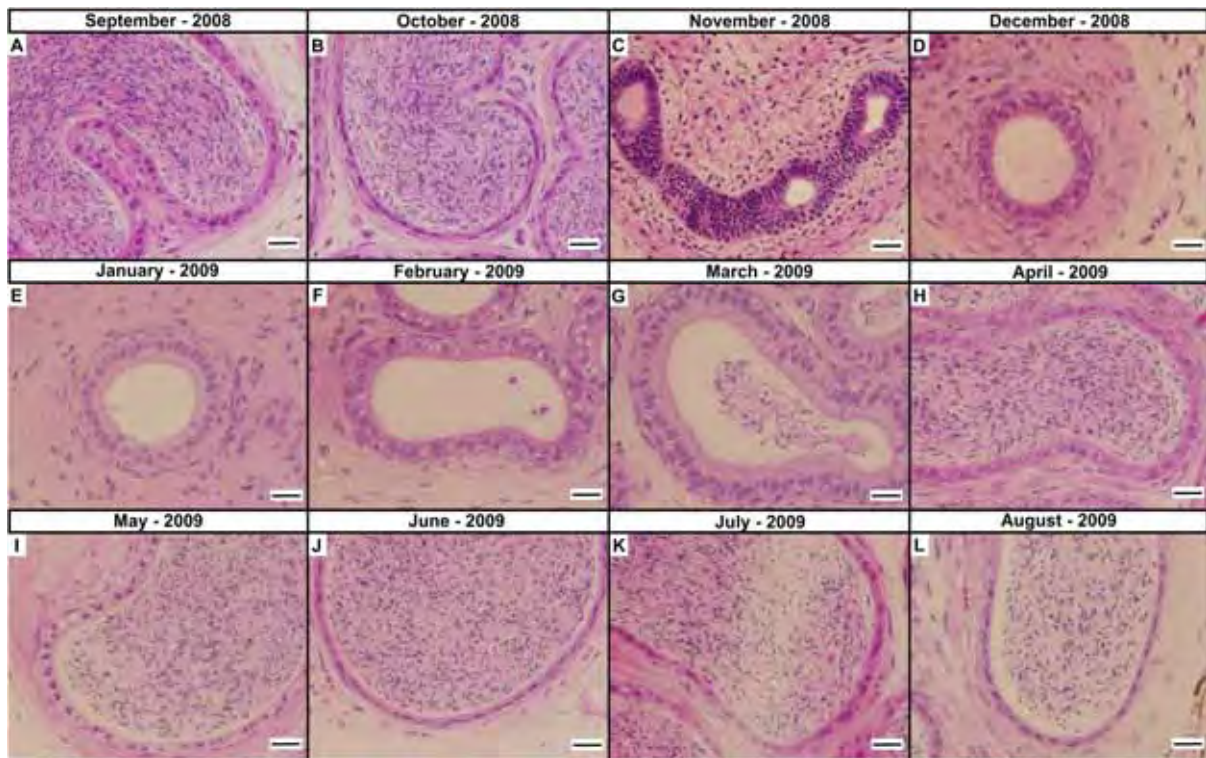


**Figure 5.** Seasonal changes in morphology of the cauda epididymis of *Myotis nigricans* from Southeast Brazil from September 2008 to August 2009. Hematoxylin-eosin stain. **A.** September 2008. **B.** October 2008. **C.** November 2008. **D.** December 2008. **E.** January 2009. **F.** February 2009. **G.** March 2009. **H.** April 2009. **I.** May 2009. **J.** June 2009. **K.** July 2009. **L.** August 2009. Note that the cycle of the cauda epididymis started in November, where it presented its minimum size (**C**); from December to February, the cauda epididymis tubules developed gradually (**D-F**); however, the first spermatozoa was observed within it only in March (**G**). From April (**H**), the cauda epididymis started to store spermatozoa, reaching the maximum size in June (**J**). The storage of spermatozoa extended until October (**B**), and in November no spermatozoa were observed inside it again. Scale bars = 20 $\mu$ m.

**Figure 6.** Seasonal changes in amount of proliferating cells (PCNA: **A-G**) and in expression of androgen receptor (AR: **H-N**) in epididymis of *Myotis nigricans* from Southeast Brazil from September 2008 to August 2009. **A.** Graphic showing the number of PCNA+ cells in caput epididymis. **B.** Graphic showing the number of PCNA+ cells in corpus epididymis. **C.** Graphic showing the number of PCNA+ cells in cauda epididymis. **D-F.** Expression of PCNA in cauda epididymis of animals from September (**D**), January (**E**) and July (**F**). **G.** Negative control of the PCNA immunoreaction. **H.** Graphic showing the number of AR+ cells in caput epididymis. **I.** Graphic showing the number of AR+ cells in corpus epididymis. **J.** Graphic showing the number of AR+ cells in cauda epididymis. **K-M.** Expression of AR in cauda epididymis of animals from May (**K**), January (**L**) and July (**M**). **N.** Negative control of the AR immunoreaction. Different letters indicate statistically significant differences (ANOVA at  $p < 0.05$ ). Scale bars = 10 $\mu$ m.

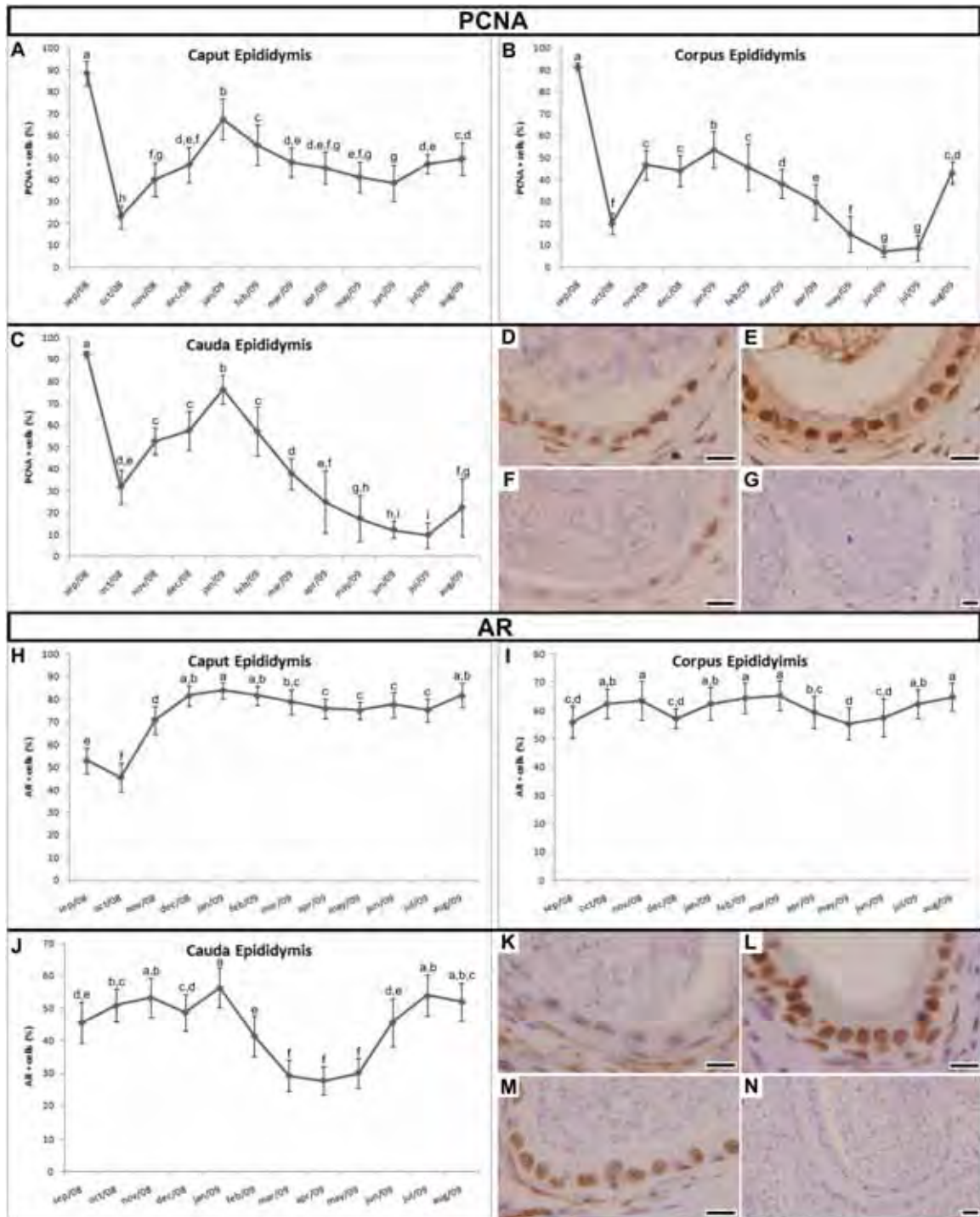




**Table 1.** Correlation coefficients (r) for relationships.

<b>1) Abiotic factors and testicular measurements and expressions</b>				
	<b>Body Weight</b>	<b>Gonad Weight</b>	<b>Tubular Diameter</b>	<b>Luminal Diameter</b>
<b>Temperature</b>	-0.0252	-0.1237	0.0959	-0.1661
<b>Rainfall</b>	-0.2866	-0.2549	-0.0162	-0.3826
<b>Photoperiod</b>	-0.1863	-0.2870	-0.2477	-0.3730
	<b>Epithelium Height</b>	<b>PCNA</b>	<b>TUNEL</b>	<b>AR</b>
<b>Temperature</b>	0.2194	0.0835	-0.1785	<b>-0.5700</b>
<b>Rainfall</b>	0.2325	0.3059	-0.0055	-0.0196
<b>Photoperiod</b>	-0.0997	<b>0.4070</b>	-0.0402	-0.1600
<b>2) Period of testicular regression (TUNEL) and the expressions of PCNA and AR</b>				
	<b>PCNA</b>	<b>AR</b>		
<b>TUNEL</b>	0.1330	0.2947		
<b>3) Variation on testicular epithelium and PCNA, TUNEL and AR expressions</b>				
	<b>PCNA</b>	<b>TUNEL</b>	<b>AR</b>	
<b>Epithelium Height</b>	-0.3536	-0.1562	<b>-0.4924</b>	
<b>4) Variation in testicular and epididymal epithelium heights</b>				
	<b>Caput</b>	<b>Corpus</b>	<b>Cauda</b>	
<b>Testes</b>	<b>0.4549</b>	<b>0.5540</b>	0.1616	

Bold numbers indicate median correlations.



## **IX. CAPÍTULO 7**

### **Análise da nucleogênese em morcegos**

## INTRODUÇÃO

A compartimentalização das funções nucleolares é, em parte, uma consequência do recrutamento de grandes complexos e maquinarias em seus diferentes domínios, cada qual estando associada a uma função biológica diferente. Essa separação de funções em sítios específicos parece estar sincronizada com um alto desempenho, onde, com essa conformação, o nucléolo pode desenvolver múltiplas funções ao mesmo tempo (BOISVERT et al., 2007; BEGUELINI et al., 2011b; HERNANDEZ-VERDUM, 2011).

Assim, a localização e arranjo dos subcompartimentos nucleolares estão relacionados à sua função na produção das subunidades ribossômicas e em suas diferentes funções. Cadeias de RNAr em transcrição são localizadas na junção dos CFs com o CFD e se acumulam no CFD (CMARKO et al., 2000; GUILLOT et al., 2005). Por outro lado, o processamento dos pré-RNAr é iniciado junto ao sítio de transcrição no CFD (CMARKO et al., 2000) e continua durante a migração intra-nucleolar do RNA até o CG. Do mesmo modo, as proteínas nucleolares que participam das primeiras etapas do processamento do RNAr, como a fibrilarina e a nucleolina, localizam-se no CFD (GINISTY et al., 1998), enquanto que proteínas como a NPM/B23 e a PM-Scl 100, que estão envolvidas nas etapas intermediárias e tardias do processamento, localizam-se no CG (GAUTIER et al., 1994).

A nucleolina, também conhecida como proteína C23, é uma fosfo-proteína ácida abundantemente expressa em tecidos em crescimento, e está localizada principalmente no CFD do nucléolo. Ela está envolvida no controle da transcrição dos genes de RNAr pela polimerase I, na maturação e formação do ribossomo, e no transporte núcleo-citoplasma dos componentes ribossomais (SRIVASTAVA et al., 1990).

Essa compartimentalização parece influenciar no comportamento dos subcompartimentos nucleolares durante as divisões celulares, onde estudos revelam que cada um desses subcompartimentos existentes dentro do nucléolo apresenta uma distribuição

diferencial ao longo da divisão, dispersando-se para diferentes partes da célula durante a divisão mitótica e voltando a se reorganizar nas células filhas ao fim da telófase (DUNDR et al., 1997; LEUNG et al., 2004). Como apresentado, os mecanismos dessa desorganização e reorganização já foram extensivamente estudados, no entanto, algumas lacunas ainda são observadas, além de que a maior parte das informações é relatada com base em observações de células mitóticas, sendo o fenômeno muito pouco descrito em células meióticas.

Assim, este estudo tem como objetivo avaliar o comportamento do nucléolo durante a divisão meiótica em espécies de morcegos que apresentam diferentes números e posicionamentos das regiões organizadoras nucleolares (RONs), através da junção de análises em microscopia eletrônica de transmissão e análises citogenéticas (impregnação por íons prata e marcações imunocitoquímicas de proteínas nucleolares); investigando se o padrão de desorganização nucleolar meiótico difere do mitótico e se diferenças no número e posicionamentos das RONs interferem nesse processo.

## **MATERIAL E MÉTODOS**

### ***Coletas e Licenças***

A captura dos morcegos foi autorizada pelo Instituto Brasileiro do Meio Ambiente (IBAMA - Processos: 02027.001957/2006-02 e 21.707-1), enquanto o comitê de ética do IBILCE-UNESP autorizou todos os procedimentos experimentais (Processo: 013/09 - CEEA).

### ***Espécies e Delineamento Experimental***

As espécies analisadas no presente estudo foram: *Carollia perspicillata* (RON no cromossomo X: 1 par na fêmea e uma RON no macho); *Molossus molossus* e *Platyrrhinus lineatus* (1 par de RONs autossômicas); *Artibeus planirostris* (3 pares de RONs autossômicas) e *Myotis nigricans* (5 pares de RONs autossômicas). Com os testículos de 5 animais de cada

espécie analisados em microscopia eletrônica de transmissão; 3 incluídos em parafina, para as análises de imunohistoquímica e ao menos 3 foram processados e transformados em suspensões celulares e submetidas a impregnação por íons prata e a imunocitoquímica.

### ***Microscopia Eletrônica de Transmissão***

Os testículos retirados para a análise em microscopia eletrônica foram cortados em pedaços pequenos e, amostras dos túbulos seminíferos, picotadas e fixadas por imersão em solução de glutaraldeído 3% acrescido de 0,25% ácido tânico em solução tampão Millonig (pH 7,3) contendo 0,54% de glicose por 24 horas. Após lavagem com o mesmo tampão, as amostras foram pós-fixadas com tetróxido de ósmio 1% durante 2 horas, lavadas em solução tampão Millonig, desidratadas em séries graduadas de acetona, e incluídas em resina Araldite. Cortes semi-finos foram realizados a fim de se analisar a qualidade do material e localizar o material de pesquisa, após o que cortes ultra-finos foram realizados, com o uso de lâminas de diamante. Esses foram corados com acetato de uranila 2% por 30 minutos, seguido pelo citrato de chumbo 2% em hidróxido de sódio por 10 minutos e analisados em Microscópio Eletrônico de Transmissão.

### ***Imunohistoquímica***

Os testículos foram imersos em uma solução fixadora metanol: clorofórmio: ácido acético (06:03:01) por três horas a 4°C, desidratados em série gradual de etanol, clarificadas em xilol, incluídos em parafina, seccionados (4 µm de espessura) e submetidos aos procedimentos de imunohistoquímica para a localização da nucleolina (C23), que consistiram: na desparafinização, recuperação antigênica, bloqueio, incubação no anticorpo primário ‘monoclonal anti-mouse C23 (SC-8031 – Santa Cruz Biotechnology)’, incubação no anticorpo secundário anti-nucleolina - ‘monoclonal anti-mouse-FITC’ e por fim a montagem

em meio contendo antifade e 4',6-diamidino-2-phenylindole (DAPI) e analisado em microscópio de epifluorescência da Zeiss com lâmpada de 100 watts, em filtro apropriado, com o software de captura e análise de imagens (Axiovision 4.8.2).

### ***Suspensão Celular***

Os testículos foram colocados em solução hipotônica de KCl (0,075M), na qual foi adicionada colquicina [0,1%], e macerados durante 40 minutos. A suspensão obtida foi centrifugada a 1000 RPM por 6 minutos; o sobrenadante foi desprezado e o precipitado fixado em Metanol: Ácido Acético (3:1) por 15 minutos. A suspensão foi centrifugada e a fixação repetida por mais duas vezes. A suspensão final foi pingada em lâminas de vidro úmidas, e submetida à impregnação por íons prata e a imunocitoquímica para nucleolina.

### ***Impregnação por íons prata (Ag-NOR)***

As lâminas contendo o material a ser analisado, foram tratadas com uma gota de solução reveladora (solução de gelatina a 1%, acrescida de 0,25% ácido fórmico), sobre a qual foram adicionadas duas gotas de solução de nitrato de prata a 25%, misturadas e cobertas com lamínula de vidro. Esse preparado foi incubado em forno microondas por 5 segundos em alta potência. Após a incubação, as lâminas foram lavadas em água deionizada, até que a lamínula se soltasse, deixadas secar ao ar, contra-coradas com Giemsa a 5% por 30 segundos e analisadas.

### ***Imunocitoquímica para nucleolina***

As lâminas contendo o material a ser analisado, foram submetidas à recuperação antigênica, permeabilização, bloqueio, incubação no anticorpo primário 'monoclonal anti-mouse C23 (SC-8031 – Santa Cruz Biotechnology)', incubação no anticorpo secundário anti-



nucleolina - 'monoclonal anti-mouse-FITC' e por fim a montagem em meio contendo antifade e 4',6-diamidino-2-phenylindole (DAPI) e analisado em microscópio de epifluorescência da Zeiss com lâmpada de 100 watts, em filtro apropriado, com o software de captura e análise de imagens (Axiovision 4.8.2).

## RESULTADOS PARCIAIS

### 1. Análises em *Carollia perspicillata*: espécie com uma única RON localizada no cromossomo X.

A análise das células de *C. perspicillata* submetidas à impregnação por nitrato de prata revelou que o número de nucléolos marcados pela prata nas espermatogônias em intérfase não variou, sendo observada a presença de um único nucléolo (Fig. 1A). No entanto, em microscopia eletrônica, apesar de todas as espermatogônias apresentarem um único e grande nucléolo, em algumas encontramos uma segunda marcação, geralmente de menor tamanho (Fig. 2A).

Nas espermatogônias em mitose, apenas um cromossomo apareceu marcado pela prata em região intersticial, local onde se encontra a RON (Fig. 1B).

Nos espermatócitos I em leptóteno observamos a presença de um único nucléolo (Fig. 1C e 2B) que, com o avanço da compactação cromossômica, começa a se desorganizar dispersando-se para diferentes partes da célula (Fig. 2B-D e 3A), com seus componentes podendo ser visualizados como: marcações irregulares no nucleoplasma (Fig. 1D-E); marcações pontuais que se dissociam do nucléolo e tendem a sair do núcleo em direção ao citoplasma (Fig. 1E-F); marcações pontuais associadas a certas regiões pericromossomais (Fig. 1F-G); ou associadas à RON, onde são observados durante toda a divisão celular (Fig. 1C-H).

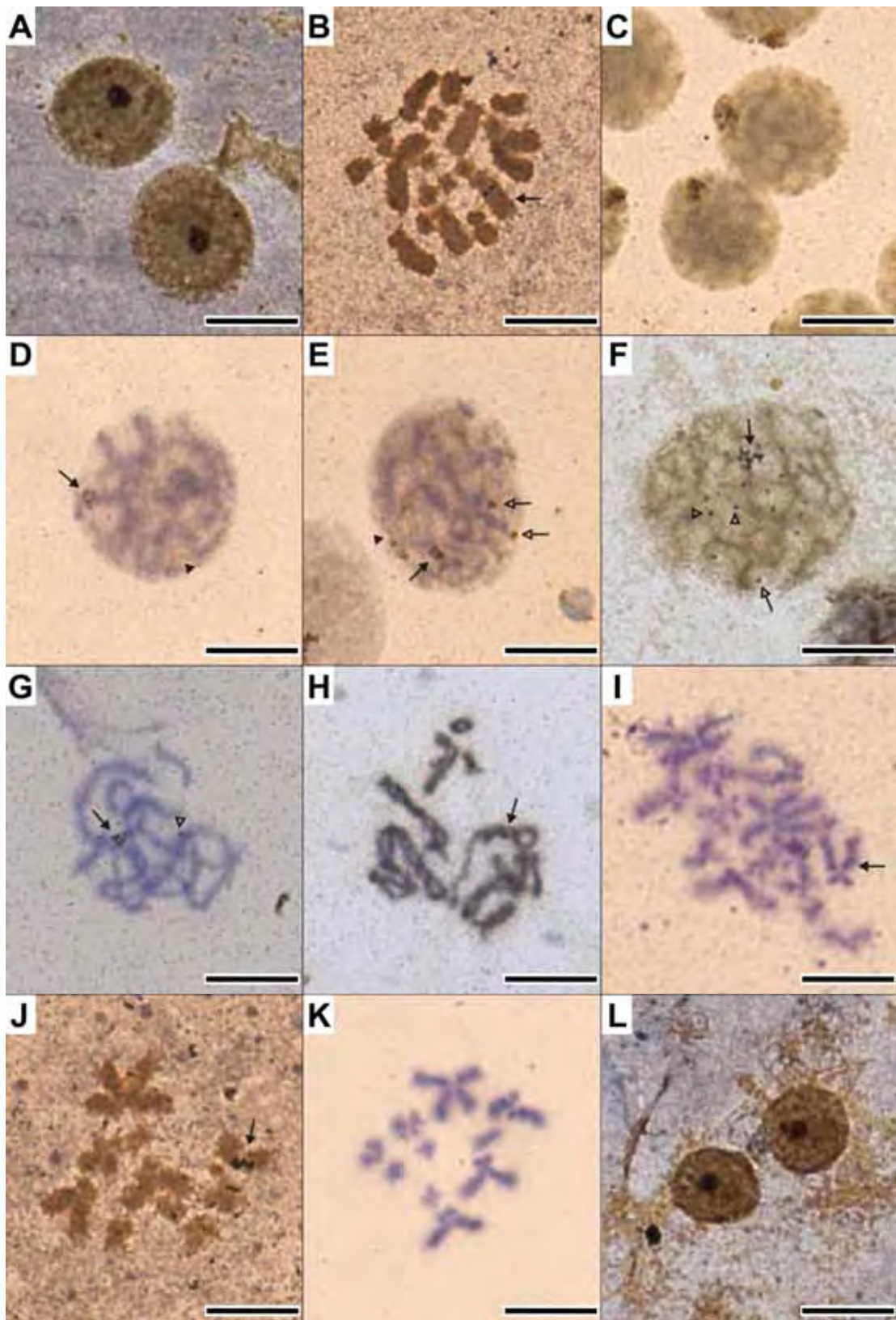
Em diplóteno-diacinese o material nucleolar ainda foi visível associado a RON, identificando o cromossomo organizador nucleolar, o cromossomo X, que apareceu associado formando o trivalente (cromossomos X-Y<sub>1</sub>-Y<sub>2</sub>) (Fig. 1H). No entanto, outros pontos apareceram marcados, tanto associados a cromossomos, quanto isolados (Fig. 3A).

Em metáfase meiótica I o único material nucleolar ainda visível foi aquele associado a RON, localizada na região intersticial do cromossomo X (Fig. 1I); com nenhuma outra marcação (Fig. 3B). Nas células em metáfase meiótica II, duas situações foram registradas, uma apresentando 10 cromossomos, com a marcação do cromossomo X (Fig. 1J) e a outra apresentando 11 cromossomos, sem a presença de cromossomos marcados (Fig. 1K).

Nas espermatídes iniciais, um único nucléolo foi observado (Fig. 1L e 3C). Com a entrada das espermatídes no processo de espermiogênese esse nucléolo se desorganizou e nenhum material nucleolar foi observado nas próximas fases (Fig. 3D).

A análise das células marcadas com o anticorpo específico para a nucleolina mostrou que essa proteína está presente em grande quantidade no nucléolo das espermatogônias em intérfase (Figs. 4A e 5B). Similarmente, durante a divisão meiótica, ela está presente em ao menos três das quatro sub-frações nucleolares: marcações irregulares no nucleoplasma (Fig. 4C); marcações pontuais associadas a certas regiões pericromossomais (Fig. 4D-E) e marcações pontuais que se dissociam do nucléolo e tendem a sair do núcleo em direção ao citoplasma (Figs. 4D-E e 5A e C). E ao fim da divisão, novas marcações são observadas junto ao nucléolo das espermatídes (Fig. 4F).

**Figura 1.** Células espermatogênicas de *Carollia perspicillata* submetidas à marcação pelo nitrato de prata. **A.** Espermatogônias em intérfase com um único nucléolo. **B.** Espermatogônia em mitose evidenciando a posição da RON em região intersticial do braço longo do cromossomo X (seta). **C-F.** Espermatócitos I de leptóteno (**C**) a paquíteno (**E-F**). Note o início da desorganização do nucléolo no zigóteno (**D**), com os fragmentos espalhados pelo nucleoplasma (ponta de seta), e deslocados para a periferia em direção ao citoplasma (setas ocas) e associado a regiões pericromossomais (pontas de setas ocas) nas células em paquíteno (**E e F**). **G.** Espermatócito I em final de paquíteno evidenciando apenas uma concentração de material nucleolar em área pericromossomal. **H.** Espermatócito I em diplóteno apontando a marcação no trivalente  $XY_1Y_2$  (seta). **I.** Metáfase meiótica I com a marcação no cromossomo X (seta). **J.** Metáfase meiótica II com 10 cromossomos e com um cromossomo marcado (seta). **K.** Metáfase meiótica II com 11 cromossomos e sem marcações. **L.** Espermátides com um nucléolo. Barras = 10 $\mu$ m.



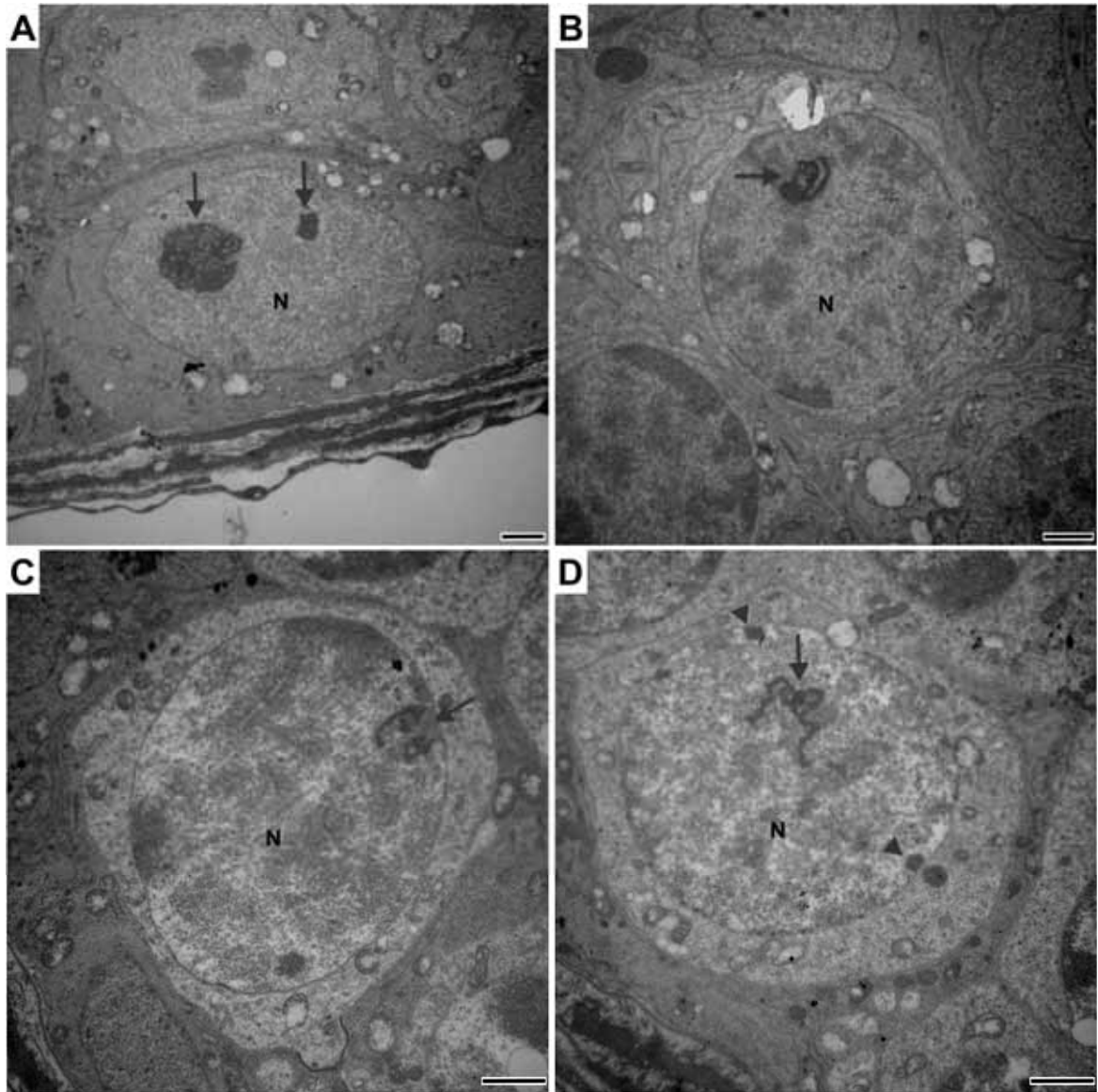


**Figura 2.** Células espermatogênicas de *Carollia perspicillata* submetidas à Microscopia Eletrônica de Transmissão. **A.** Espermatogônia. **B.** Espermatócito I em zigóteno. **C.** Espermatócito I em paquíteno inicial. **D.** Espermatócito I em paquíteno tardio. Note o grande nucléolo e a marcação de mais uma região elétron densa, nas espermatogônias; e a gradual desorganização do nucléolo, nos espermatócitos. (seta, nucléolo; ponta de seta, material nucleolar; N, núcleo). Barras = 2 $\mu$ m.



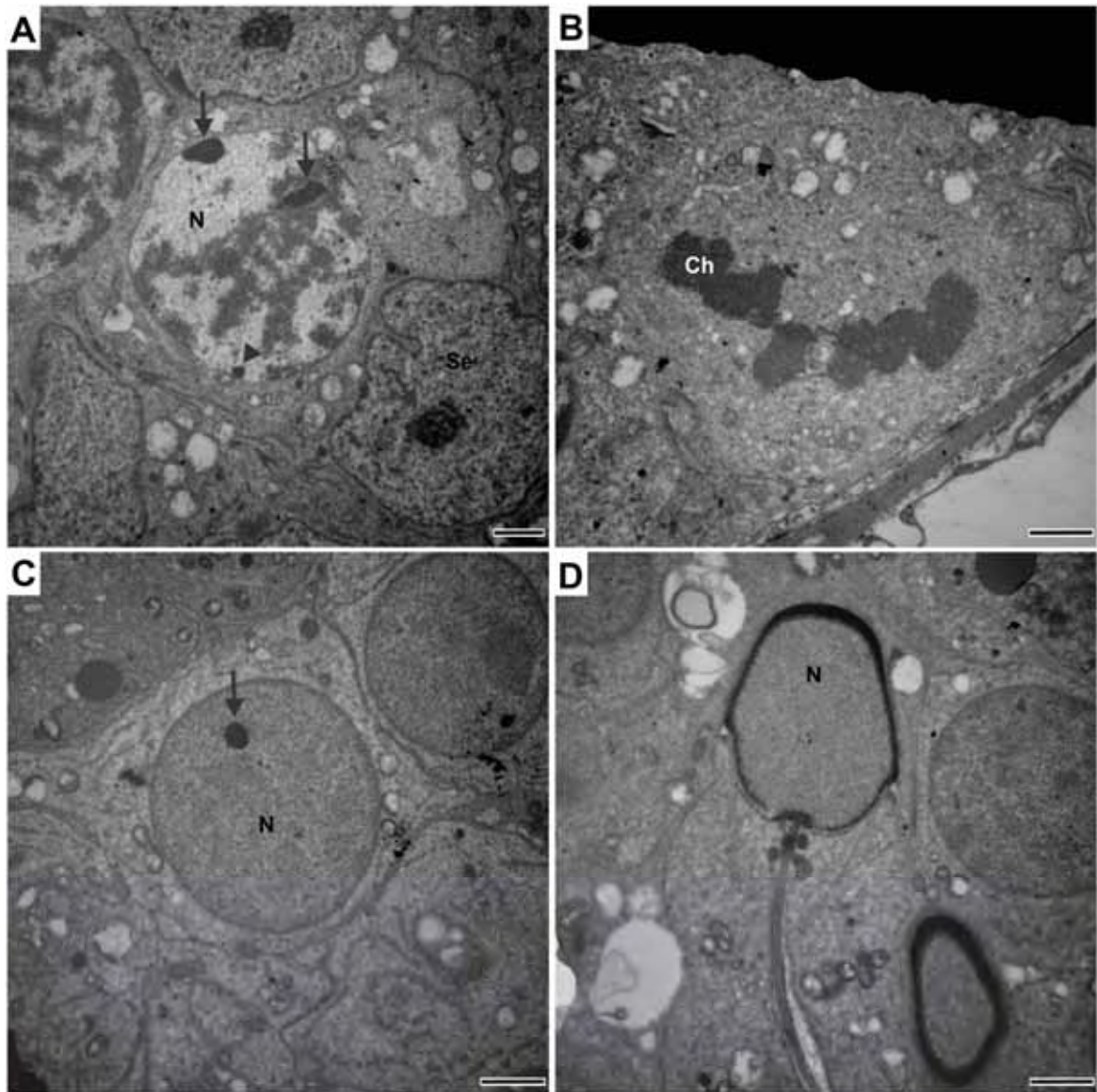


**Figura 3.** Células espermatogênicas de *Carollia perspicillata* submetidas à Microscopia Eletrônica de Transmissão. **A.** Espermatócito I em diplóteno. **B.** Metáfase. **C.** Espermátide inicial. **D.** Espermátide alongada. Note a marcação de um único nucléolo nas espermátides iniciais (**C**) e a ausência de marcações nas alongadas (**D**). (seta, nucléolo; ponta de seta, material nucleolar; N, núcleo). Barras = 2 $\mu$ m.

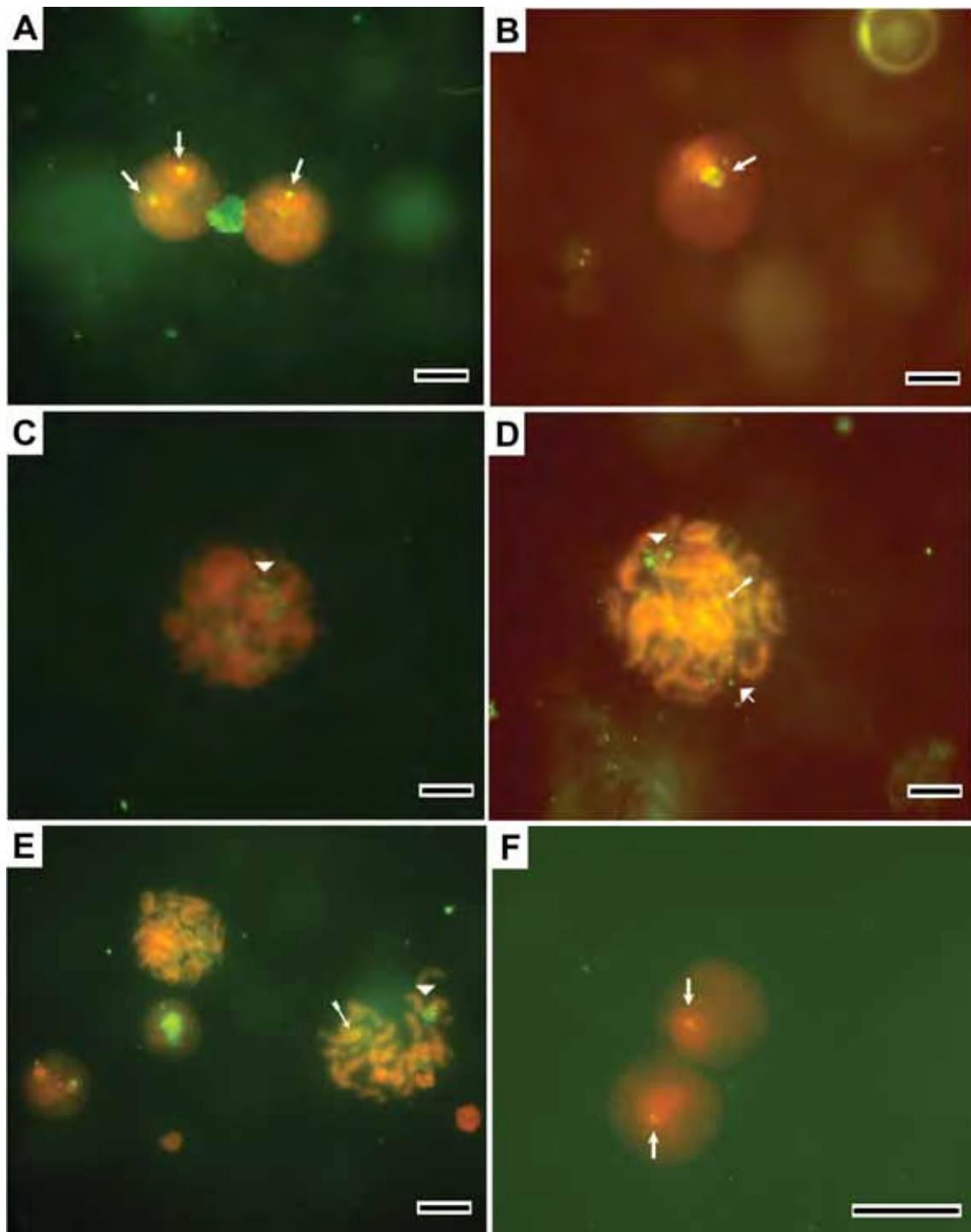


**Figura 4.** Células espermatogênicas de *Carollia perspicillata* submetidas à imunoreações com o anticorpo específico contra a proteína nucleolina. **A.** Espermatogônias. Note as marcações indicativas de nucleolina (setas). **B.** Espermatócito I em início de divisão. Note a nucleolina localizada em uma única grande região (seta), possivelmente o nucléolo. **C-E.** Espermatócito I em leptóteno, zigóteno e diacinese. Note as marcações indicativas de nucleolina espalhadas pelo nucleoplasma (cabeça de seta); sobre os cromossomos (flecha) e na periferia do núcleo (ponta de seta). **F.** Espermatídes com uma única marcação (setas). Barras = 10 $\mu$ m.

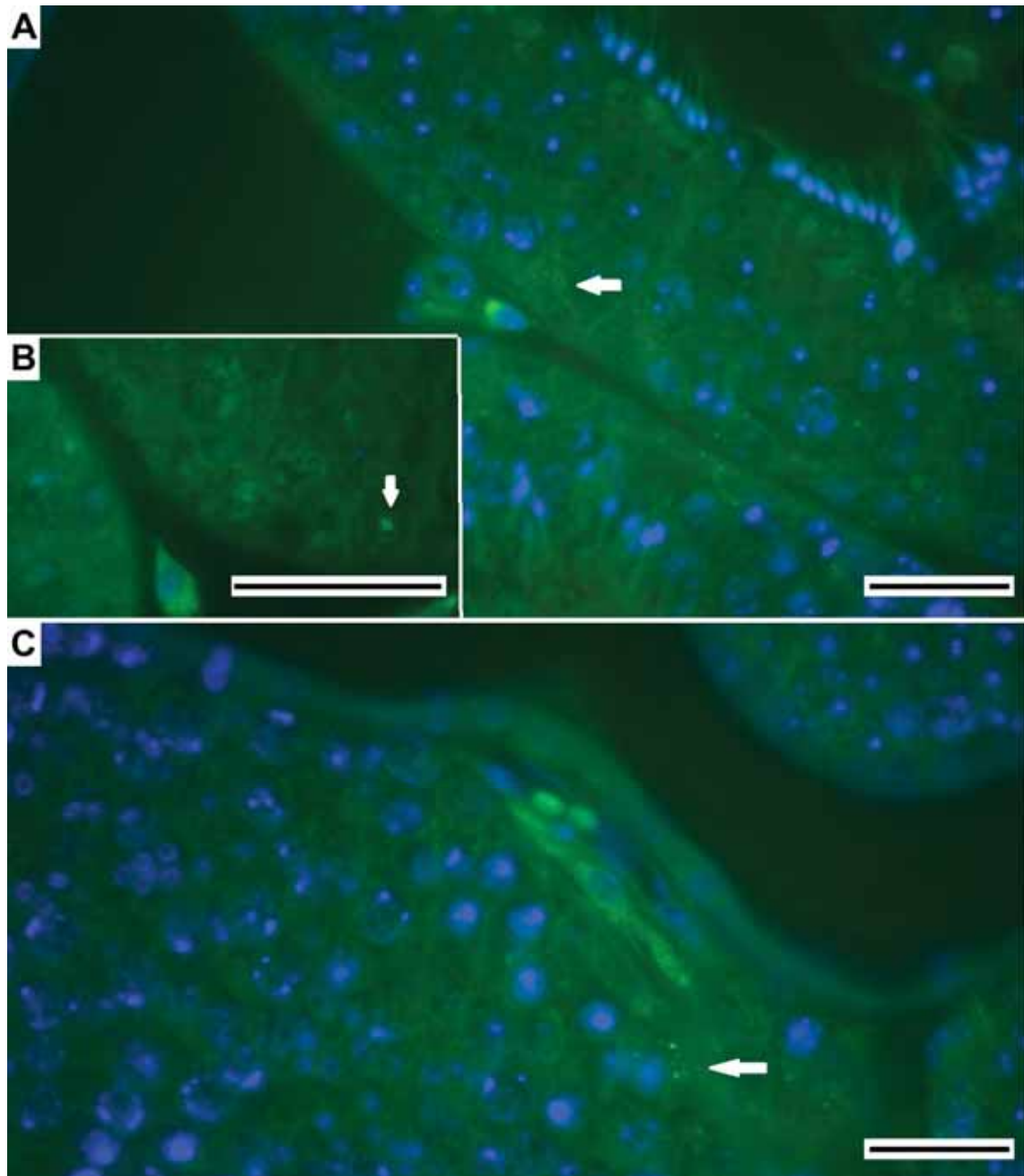


**Figura 5.** Seções espermatogênicas de *Carollia perspicillata* submetidas à imunoreações com o anticorpo específico contra a proteína nucleolina. Observe a espermatogônia, na base do epitélio, apresentando marcação indicativa da presença de nucleolina espalhada pelo nucléolo (B, seta) e as marcações no citoplasma dos espermátócitos I (A e C, setas). Barras = 10µm.

## 2. Análises em *Molossus molossus* (Molossidae) e *Platyrrhinus lineatus* (Phyllostomidae): espécies com um par de RONS autossômicas.

A análise das espermatogônias revelou em ambas as espécies, a presença de apenas um nucléolo na maioria das células e, raramente, dois (Figs. 6A-B e 7A-B). Em *P. lineatus*, o nucléolo parece estar ainda morfológicamente organizado durante o leptóteno e início de zigóteno, apresentando uma forma elétron-densa e compacta (Fig. 6C-F). Em zigóteno tardio e/ou paquíteno inicial, com o aumento da condensação cromossômica, o nucléolo perde sua morfologia e inicia sua desorganização (Fig. 6G-H). Em *M. molossus* a organização nucleolar permanece até zigóteno tardio (Fig. 7E-F) e a desorganização nucleolar começa somente em paquíteno inicial (Fig. 7G-H).

Em ambas as espécies os componentes nucleolares são vistos em diferentes locais da célula: como marcações irregulares espalhadas no nucleoplasma, como marcas inespecíficas associadas a regiões pericromossomais; como materiais que dissociam do nucléolo e tendem a deixar o núcleo para o citoplasma, e materiais que permanecem associados com as RONS durante toda a meiose. Em diplóteno/diacinése a quantidade de fragmentos nucleolares diminui muito (Fig. 8C-D e 9E-F), mas algumas partes ainda podem ser observadas associadas com uma única região cromossômica, possivelmente a RON. Em metáfase, a marcação pela prata foi restrita as RONS (Fig. 8E-F e 9G-H), e apenas um único nucléolo foi observado nas espermátides iniciais das duas espécies (Fig. 8G-H e 9I-J).



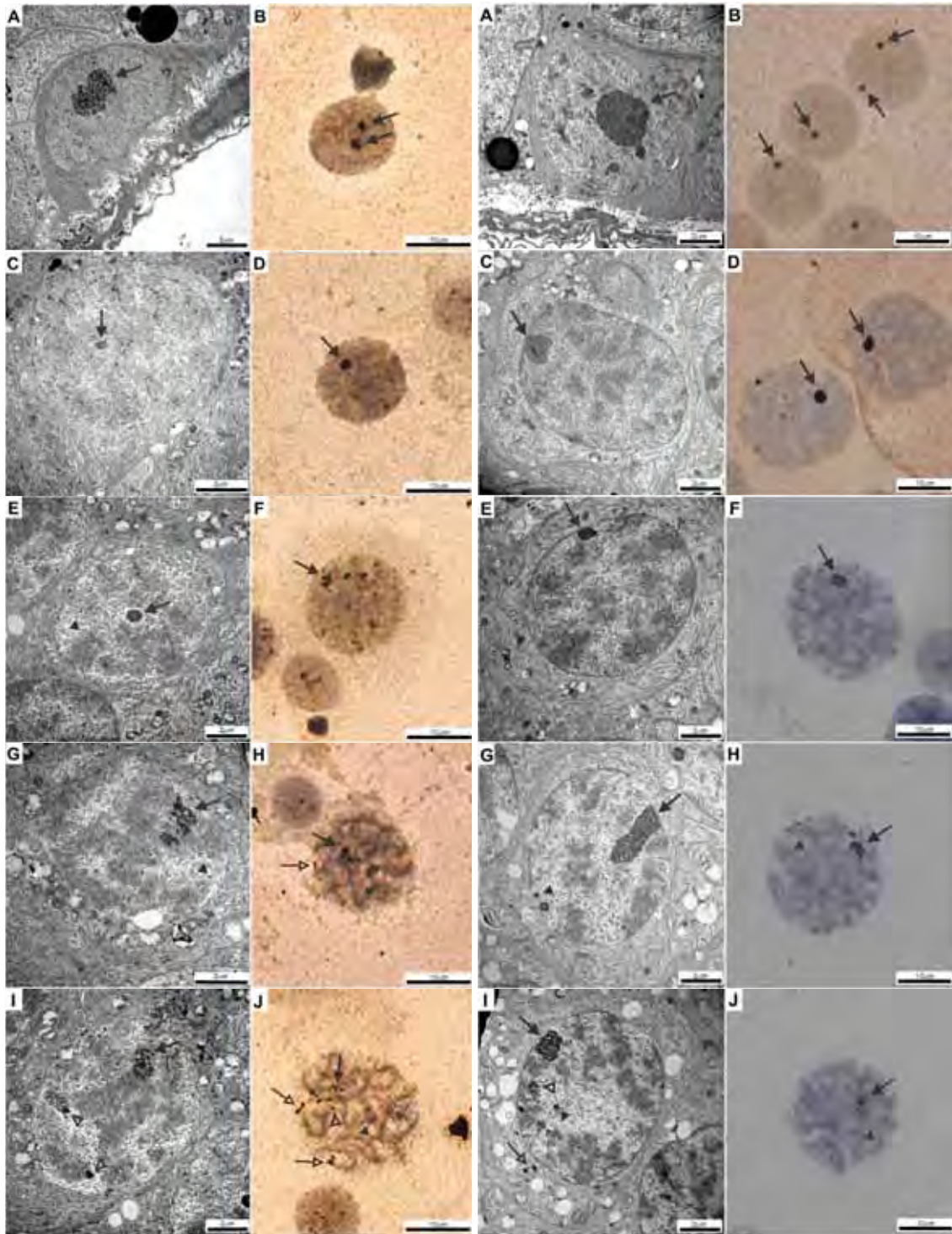


**Figura 6.** Células espermatogênicas de *Platyrrhinus lineatus* submetidas à microscopia eletrônica de transmissão (A, C, E, G e I) e impregnação por nitrato de prata (B, D, F, H e J). A-B. Espermatogônias. C-D. Espermatócitos primários em leptóteno. E-F. Espermatócitos primários em zigóteno. G-H. Espermatócitos primários em paquíteno inicial. I-J. Espermatócitos primários em paquíteno tardio.

**Figura 7.** Células espermatogênicas de *Molossus molossus* submetidas à microscopia eletrônica de transmissão (A, C, E, G e I) e impregnação por nitrato de prata (B, D, F, H e J). A-B. Espermatogônias. C-D. Espermatócitos em leptóteno. E-F. Espermatócitos em zigóteno. G-H. Espermatócitos primários em paquíteno inicial. I-J. Espermatócitos primários em paquíteno tardio. (setas, nucléolo ou local de desorganização nucleolar; cabeças de seta, material que se dissolve no nucleoplasma; setas ocas, material que se move para o citoplasma; cabeças de setas ocas, material que está associado com as regiões pericromossomais). Barras = 2 $\mu$ m (MET) e 10 $\mu$ m (microscopia de luz).



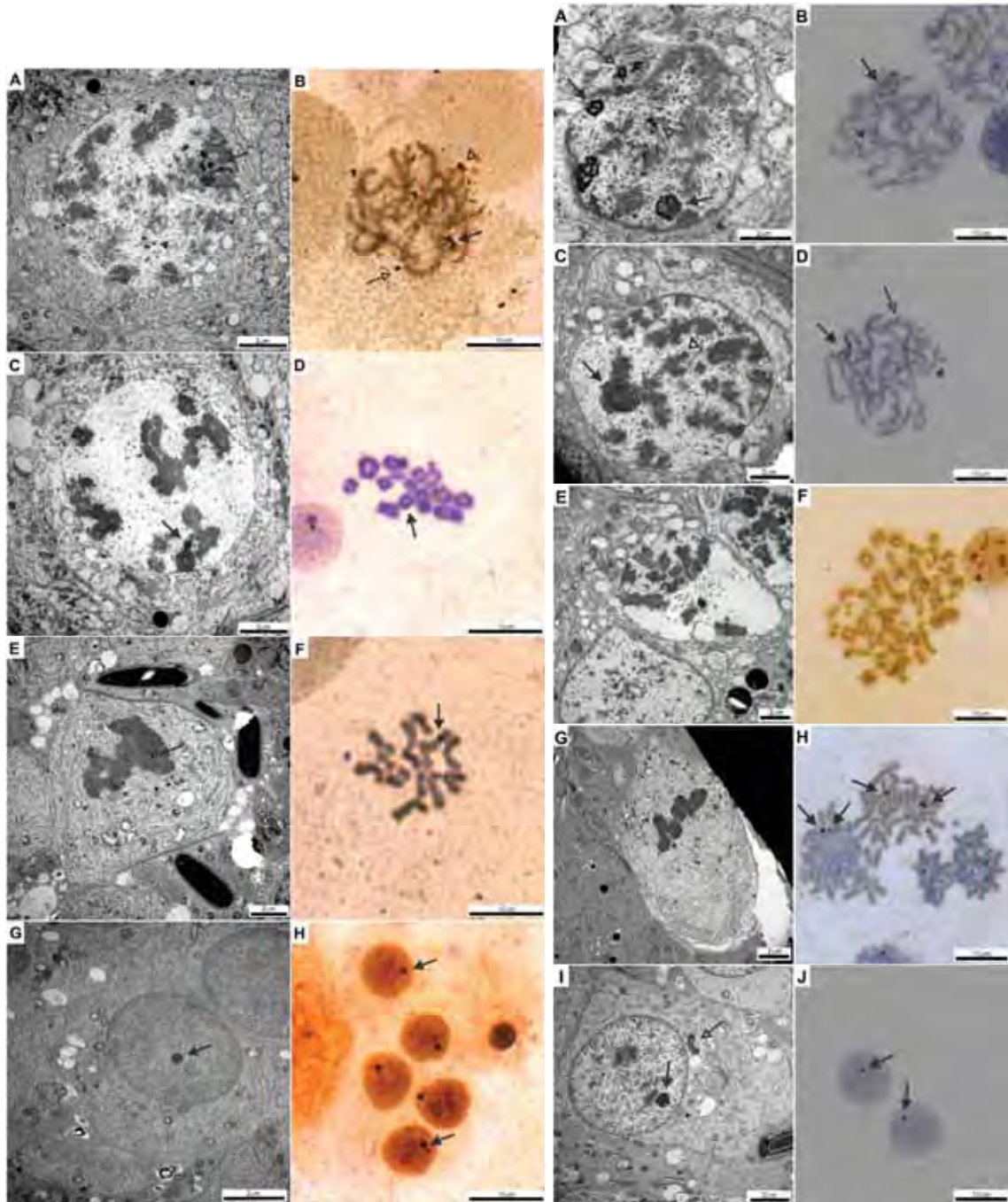


**Figura 8.** Células espermatogênicas de *Platyrrhinus lineatus* submetidas à microscopia eletrônica de transmissão (A, C, E e G) e impregnação por nitrato de prata (B, D, F e H). A-B. Espermatócitos em diplóteno. C-D. Espermatócitos em diacinese. E-F. Metáfase. G-H. Espermátides.

**Figura 9.** Células espermatogênicas de *Molossus molossus* submetidas à microscopia eletrônica de transmissão (A, C, E, G e I) e impregnação por nitrato de prata (B, D, F, H e J). A-B. Espermatócitos primários em diplóteno inicial. C-D. Espermatócitos primários em diplóteno tardio. E-F. Espermatócitos em diacinese. G-H. Metáfase. I-J. Espermátides. (setas, nucléolo, RONS ou local de desorganização nucleolar; cabeças de seta, material que se dissolve no nucleoplasma; setas ocas, material que se move para o citoplasma; cabeças de setas ocas, material que está associado com as regiões pericromossomais). Barras = 2 $\mu$ m (MET) e 10 $\mu$ m (microscopia de luz).

Em ambas as espécies, a imunohistoquímica indicou a presença de nucleolina espalhada pelo nucléolo das espermatogônias (Fig. 10A e 11A-C), assim como junto às frações nucleolares durante a divisão celular. Observamos uma gradual dispersão das marcações no nucleoplasma de leptóteno para diplóteno (Fig. 10A-B e 11B-C); a presença de marcações no citoplasma de leptóteno para diplóteno (Fig. 10A-D e 11A-D) e a marcação de uma única região pericromossomal em diplóteno (Fig. 10D e 11D).

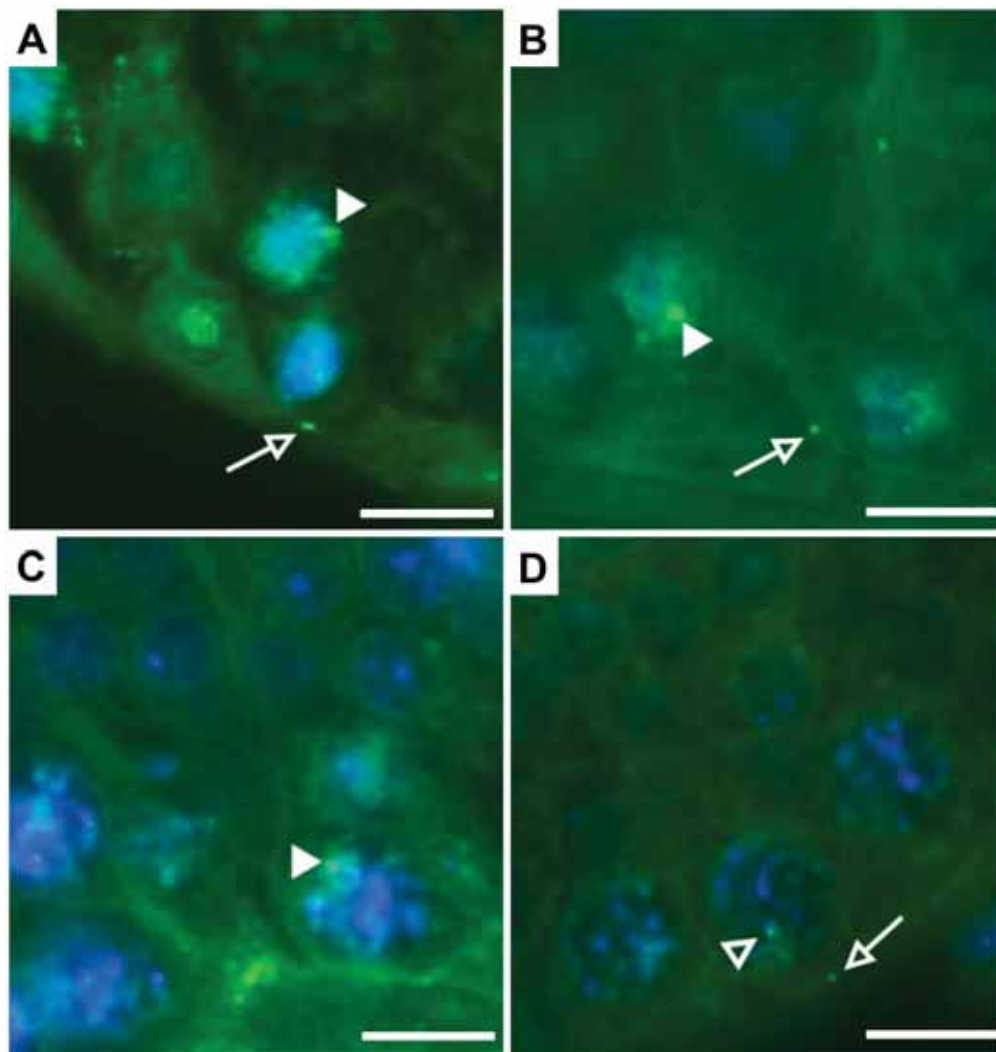


**Figura 10.** Seções testiculares de *Platyrrhinus lineatus* submetidas à imunoreações com o anticorpo específico contra a proteína nucleolina. **A.** Espermatogônias e espermatócitos I em leptóteno. **B.** Espermatócitos I em zigóteno. **C.** Espermatócitos I em paquíteno. **D.** Espermatócitos I em diplóteno. Observe as espermatogônias, na base do epitélio, apresentando marcações indicativas da presença de nucleolina espalhadas pelo nucléolo (**A**); a gradual dispersão das marcações no nucleoplasma de leptóteno para diplóteno (cabeças de seta); presença de marcações no citoplasma de leptóteno para diplóteno (setas ocas) e à marcação de uma única região pericromossomal em diplóteno (ponta de seta oca). Barras = 10  $\mu\text{m}$ .

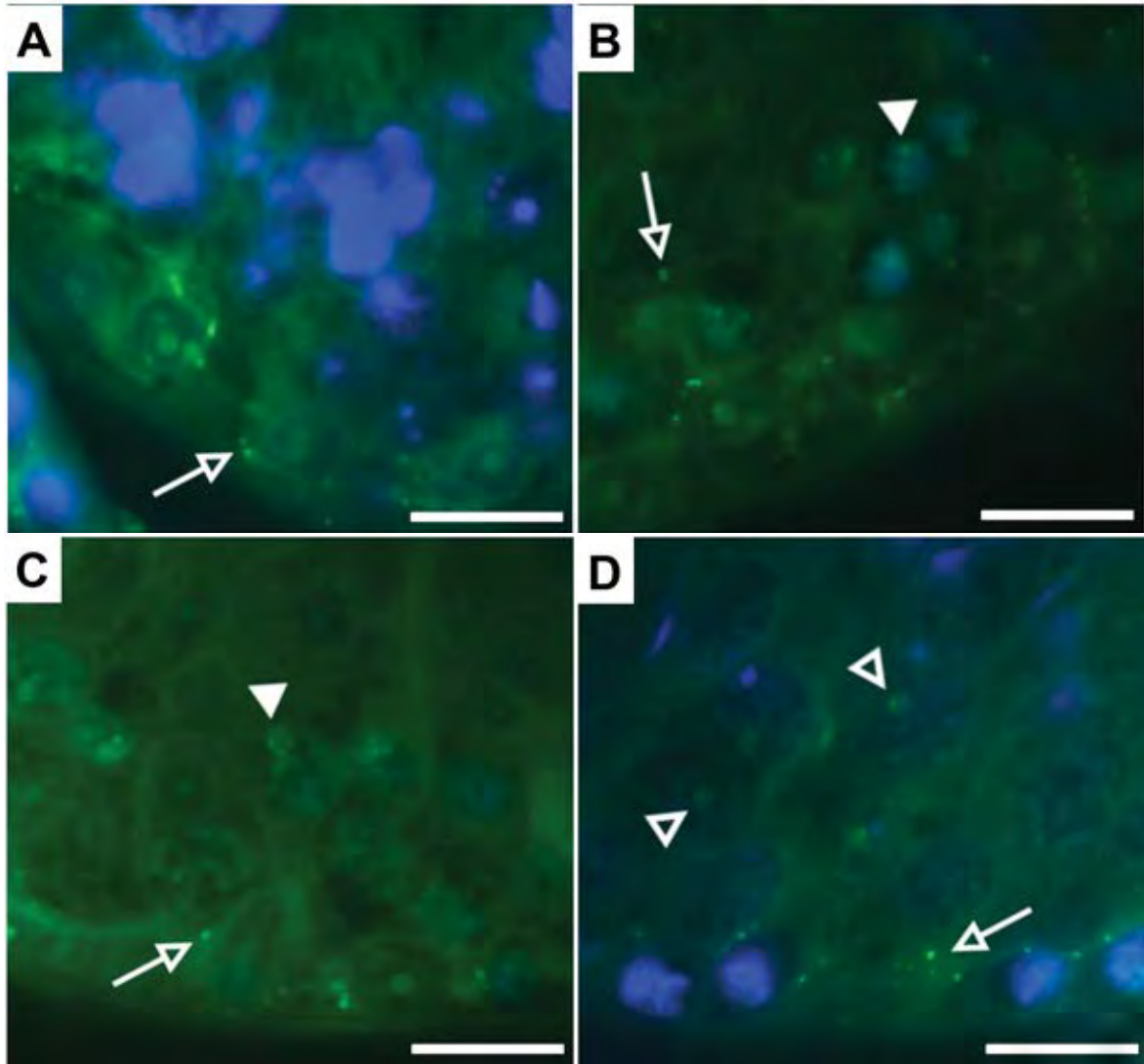


**Figura 11.** Seções testiculares de *Molossus molossus* submetidas à imunoreações com o anticorpo específico contra a proteína nucleolina. **A.** Espermatogônias. **B.** Espermatócitos I em leptóteno. **C.** Espermatócitos I em paquíteno. **D.** Espermatócitos I em diplóteno. Observe as espermatogônias, na base do epitélio, apresentando marcações indicativas da presença de nucleolina espalhadas pelo nucléolo (**A**) e também no citoplasma (seta oca); a gradual dispersão das marcações no nucleoplasma de leptóteno para diplóteno (cabeças de seta); a presença de marcações no citoplasma de leptóteno para diplóteno (setas ocas) e à marcação de uma única região pericromossomal em diplóteno (ponta de seta oca). Barras = 10  $\mu$ m.

### 3. Análises em *Artibeus planirostris* (Phyllostomidae): espécie com três pares de RONS autossômicas.

Em *A. planirostris*, observamos de um a seis nucléolos nas espermatogônias em intérfase, sendo três, quatro ou cinco nucléolos os mais freqüentemente encontrados (Fig. 12A), e nas em mitose, três pares de autossomos dotados de RONS (não documentado), com as células apresentando de um a seis cromossomos marcados por metáfase. A marcação de três ou quatro nucléolos nos espermátocitos iniciais (leptóteno) foi o mais freqüente. Esses formam no máximo três sítios individuais de desorganização (Fig. 12E) que, a semelhança do observado para as outras espécies, com a compactação cromossômica desorganiza-se, e seus componentes são visualizados no nucleoplasma, deslocando para o citoplasma, associados às regiões pericromossomais e às RONS (Figs. 12B–G). Em diplóteno o único material nucleolar ainda visível é aquele associado às RONS (Fig. 12H). As células em metáfase meiótica I apresentaram até seis cromossomos marcados e em metáfase II de um a três cromossomos marcados. Nas espermátides observamos de um a três nucléolos (Fig. 12I).

A análise da imuno-reação a nucleolina mostrou que essa proteína está presente em grande quantidade em todos os nucléolos das espermatogônias em intérfase (Fig. 13A) e, similar as outras espécies, durante a divisão meiótica, ela está presente em nas três sub-frações nucleolares (Fig. 13A-D). No entanto, observamos uma maior reação a nucleolina pelas células de *A. planirostris* do que das outras espécies, notada pela maior quantidade e tamanho dos sinais fluorescente. Esse fato indica que, possivelmente, a existência de um maior número de nucléolos pressupõe uma maior quantidade de nucleolina para estabelecer seus CFD.



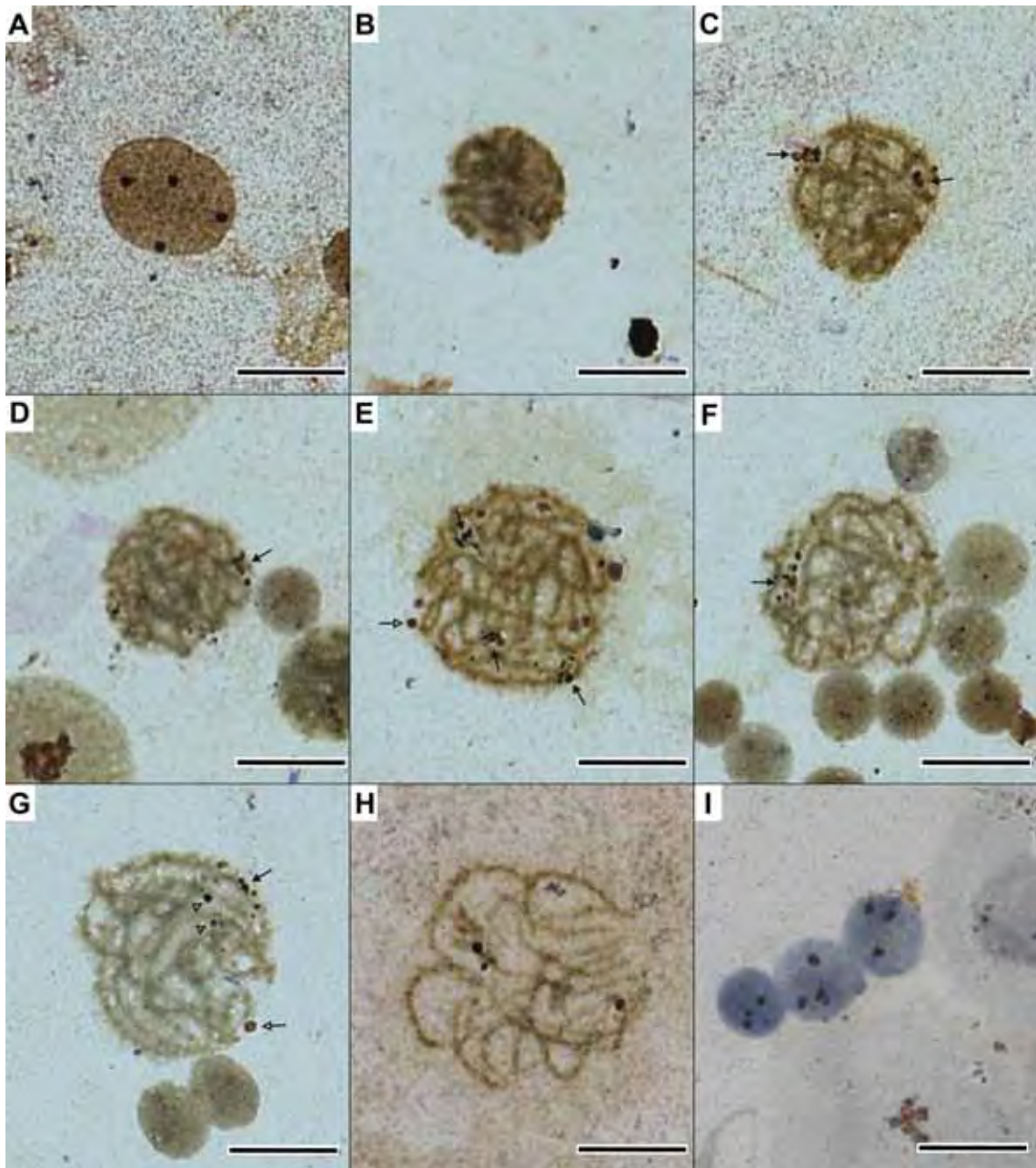


**Figura 12.** Células espermatogênicas de *Artibeus planirostris* submetidas à impregnação por nitrato de prata. **A.** Espermatogônia em interfase apresentando quatro nucléolos. **B.** Espermatócito I em leptóteno. **C-D.** Espermatócitos I em zigóteno. Notar a presença de um ou dois sítios de desorganização (setas). **E-G.** Espermatócitos I em paquíteno. Notar a presença de até três sítios de desorganização (setas), o material que desloca para o citoplasma (seta oca) e o material que se associa as regiões pericromossomais (ponta de seta oca). **H.** Espermatócito I em diplóteno. Notar a diminuição das marcações. **I.** Espermátides com até três nucléolos. Barras = 10 µm.



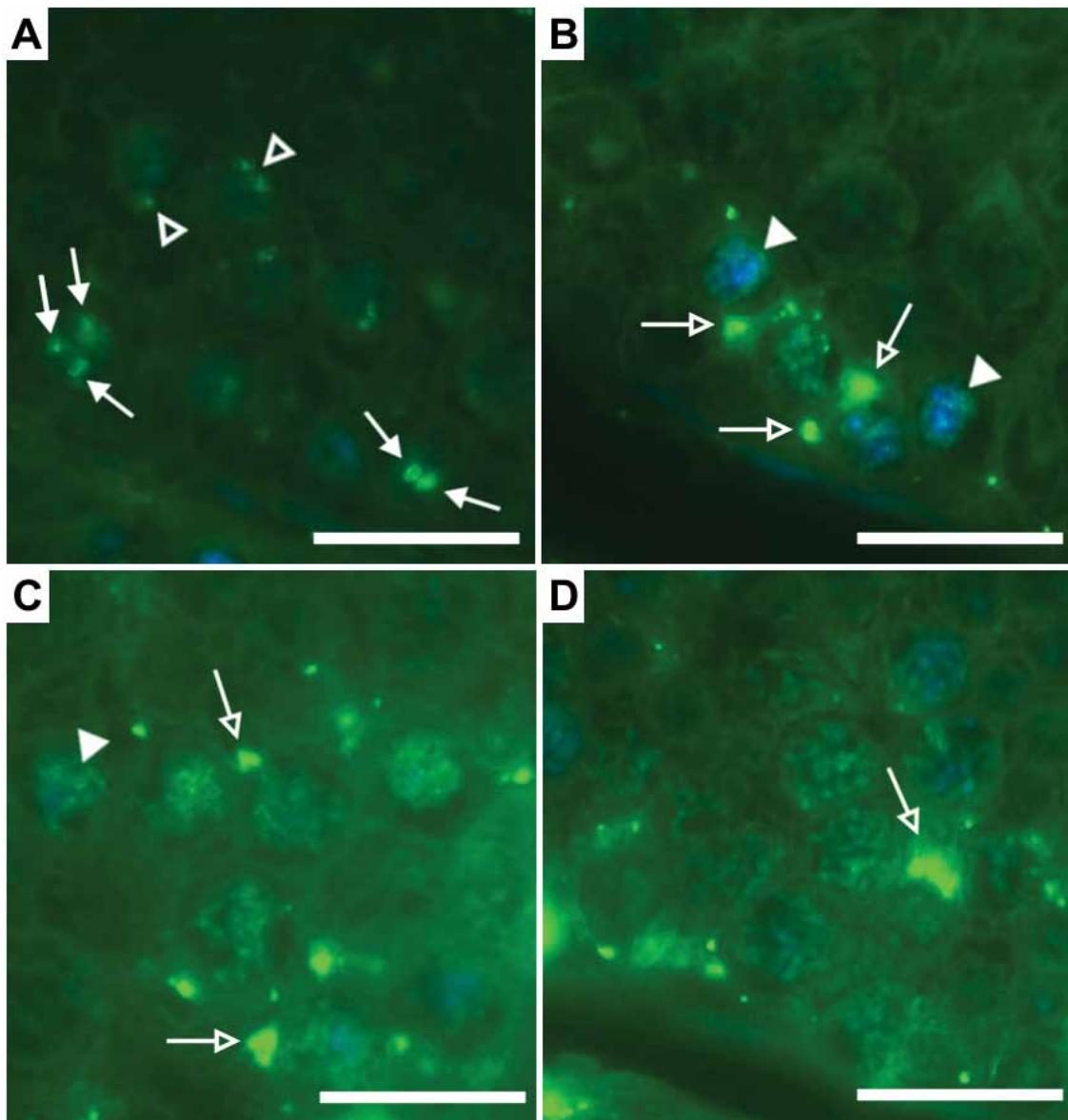


**Figura 13.** Seções testiculares de *Artibeus planirostris* submetidas imunoreações com o anticorpo específico contra a proteína nucleolina. **A.** Espermatogônias e espermatócitos I em diplóteno. **B.** Espermatócitos I em leptóteno. **C.** Espermatócitos I em paquíteno. **D.** Espermatócitos I em diplóteno. Observe as espermatogônias, na base do epitélio, apresentando marcações indicativas da presença de nucleolina espalhadas em todos os seus nucléolos (setas); a gradual dispersão das marcações no nucleoplasma de leptóteno para diplóteno (cabeças de seta); a presença de marcações no citoplasma de leptóteno para diplóteno (setas ocas) e à marcação de regiões pericromossomais em diplóteno (ponta de seta oca). Barras = 10  $\mu$ m.

**4. Análises em *Myotis nigricans* (Vespertilionidae): espécie com cinco pares de RONS autossômicas.**

Em *M. nigricans* foram observadas espermatogônias com cinco a dez marcações (Fig. 14A) que se desorganizam e passam a ser observadas como pontos escuros sobre os cromossomos durante a divisão (Figura 14B-D). Nas metáfases I até dez cromossomos marcados (5 bivalentes) foram visualizados (Figura 14E) e nas espermátides uma a cinco marcações foram características (Fig. 14F).

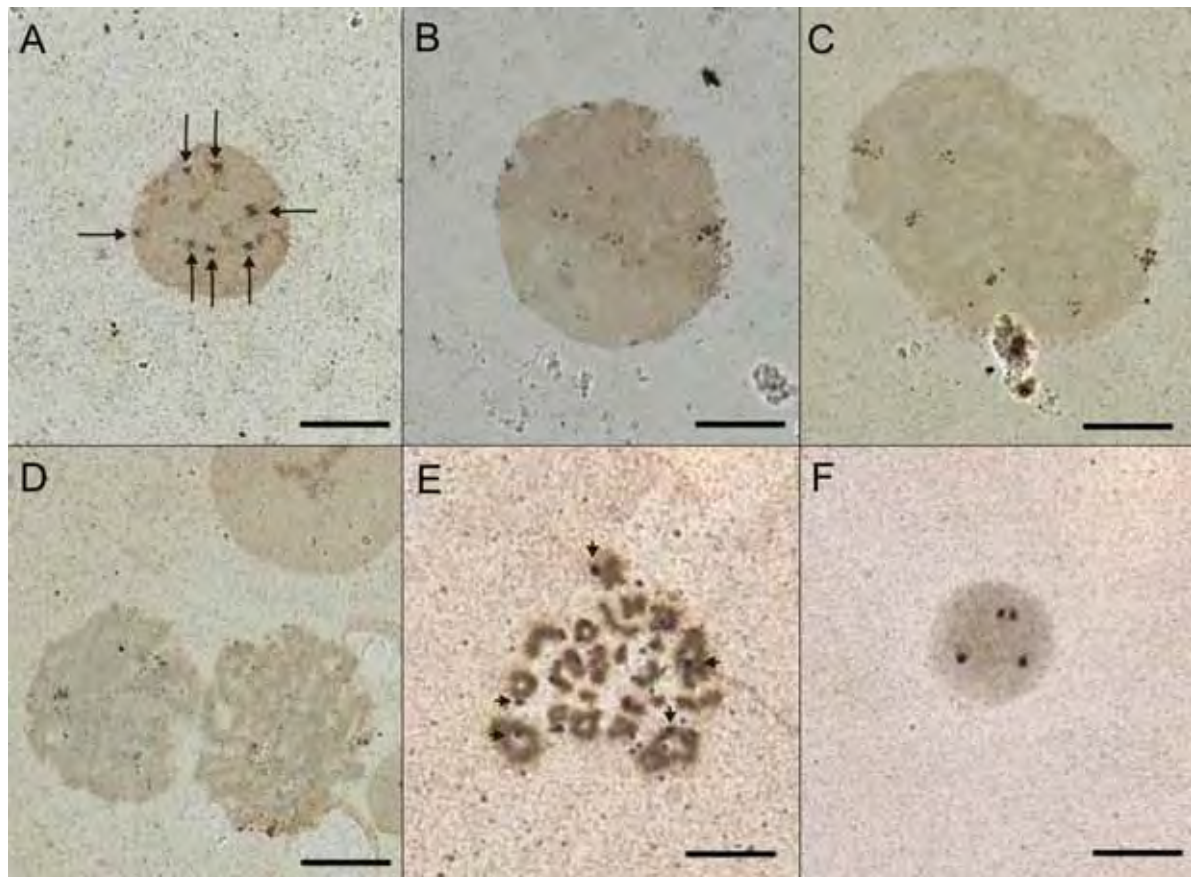


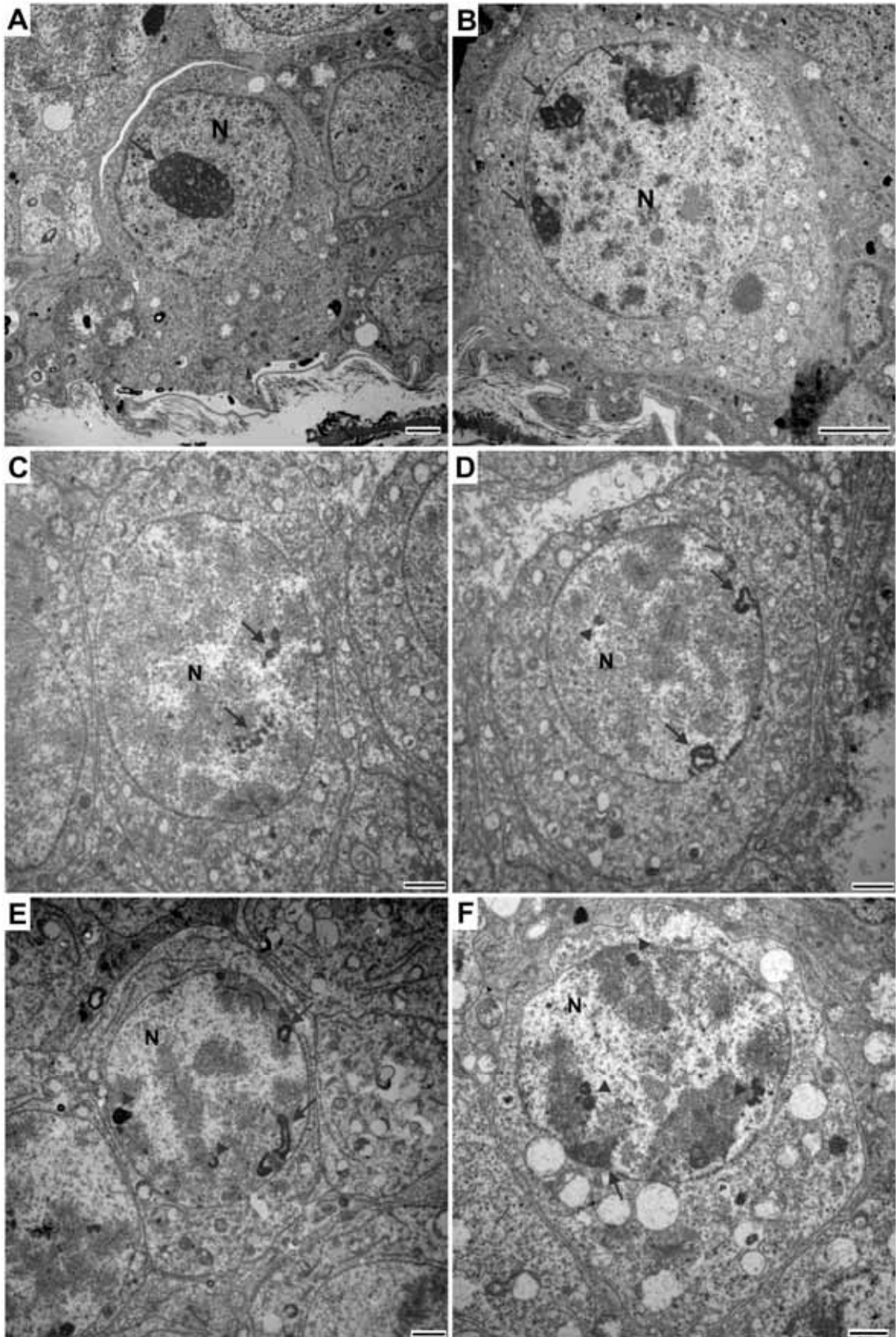
**Figura 14.** Células espermatogênicas de *Myotis nigricans* submetidas à impregnação por nitrato de prata. **A.** Espermatogônia com sete marcações (setas). **B.** Espermatócito I em início de paquíteno. **C.** Espermatócitos I em paquíteno. **D.** Espermatócito I em paquíteno-diplóteno. **E.** Metáfase I, com cinco marcações (pontas de seta). **F.** Espermátide com quatro marcações. Barras = 10 µm.

Em MET observamos que a variação no número de nucléolos está ligada também a uma variação em seu tamanho, onde células com menor número de nucléolos tendem a apresentá-los com maior tamanho (Fig. 15A-B). O número de sítios de desorganização variou de um a cinco, variação possivelmente ligada ao número de nucléolos que a célula apresentava na interfase anterior.

Durante a divisão celular, observamos que o material nucleolar se dispersa no núcleo (Fig. 15C-F), ficando associado a algumas regiões pericromossomais (Fig. 15D-F e 16A) e as vezes deslocando-se para o citoplasma. Em metáfase nenhuma marcação foi observada (Fig. 16B). Nos espermatócitos II marcações nucleolares são novamente notadas, geralmente sendo uma única marcação (Fig. 16C), mesmo número de marcação observada nas espermátides recém formadas (Fig. 16D).

**Figura 15.** Células espermatogênicas de *Myotis nigricans* submetidas à microscopia eletrônica de transmissão. **A-B.** Espermatogônias. Note a presença ou de um único e enorme nucléolo (**A**, seta) ou de dois, ou mais, menores (**B**, setas). **C.** Espermatócito I em leptóteno. **D.** Espermatócito I em zigóteno. **E.** Espermatócito I em paquíteno. **F.** Espermatócito I em diplóteno. Note a presença de um a três sítios de desorganização nucleolar (**C-F**, setas) e os fragmentos nucleolares dissipados pelo núcleo (**C-F**, ponta de setas). (N, núcleo). Barras = 2 $\mu$ m.







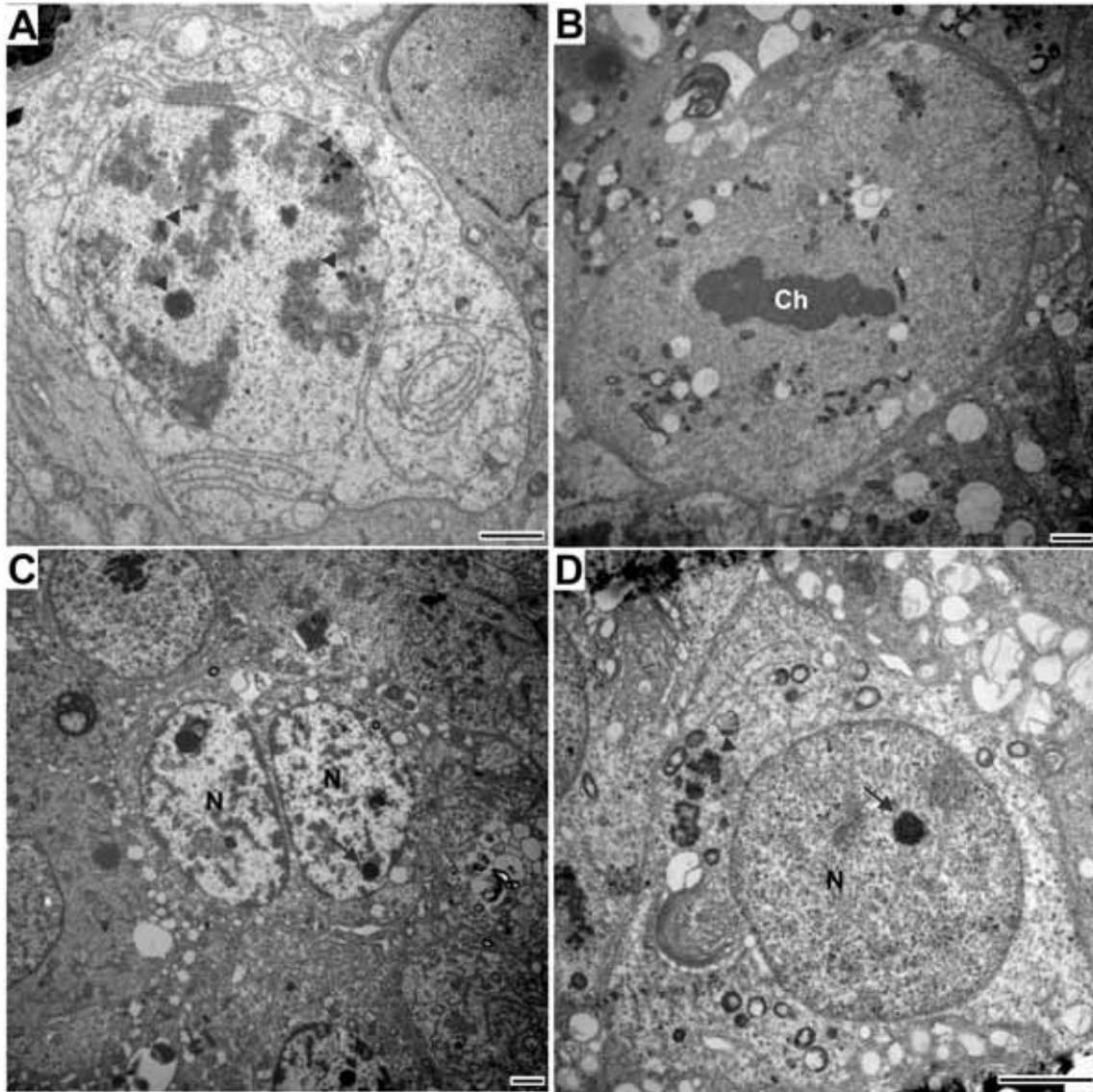


**Figura 16.** Células espermatogênicas de *Myotis nigricans* submetidas à microscopia eletrônica de transmissão. **A.** Espermatócito I em diplóteno. Note a grande quantidade de fragmentos nucleolares dissipados pelo núcleo (A, pontas de seta). **B.** Metáfase I. Note a ausência de marcações. **C.** Espermatócitos II. Note a marcação de um nucléolo (setas). **D.** Espermátide. Note a marcação de um nucléolo (seta). (Ch, cromossomo; N, núcleo). Barras = 2 $\mu$ m.

## DISCUSSÃO

Como podemos perceber a nucleologênese meiótica apresenta grande similaridade com a mitótica, possuindo um comportamento semelhante de seus subcomponentes durante a divisão, no entanto, notamos que o processo meiótico apresenta características únicas, como um maior período de transcrição, uma maior dispersão de subcomponentes nucleolares e alguns comportamentos próprios, não vistos na mitose. Essas características únicas podem, possivelmente, ser influenciadas pelos mecanismos próprios do processo meiótico, como o pareamento das RONS homólogas durante toda divisão, a ocorrência de duas divisões consecutivas e a formação de células haplóides, entretanto, a influência de outros fatores não pode ser descartada.

No presente estudo, a análise da espécie *C. perspicillata* demonstrou que, apesar dessa espécie apresentar a RON no cromossomo X, o comportamento do nucléolo durante a divisão meiótica não foi diferente das outras espécies que apresentam RONS autossômicas. Da mesma forma, avaliando o posicionamento cromossômico das RONS nas diferentes espécies, poderemos perceber que as RONS e os nucléolos apresentam características semelhantes mesmo que estejam localizadas em diferentes cromossomos ou em diferentes regiões cromossômicas, seja em cromossomos metacêntricos, subtelocêntricos ou acrocêntricos, ou estando em regiões intersticiais ou terminais. Isso indica que, possivelmente, o locus cromossômico não influencia significativamente na nucleologênese meiótica.

Por outro lado, percebemos que o número de RONS exerce alguma influência na nucleologênese onde, espécies que possuem maior número de RONS, apresentam maior número de nucléolos por célula interfásica, maior número de sítios de desorganização e uma maior quantidade de material nucleolar e expressão de nucleolina nas células em divisão.

## **X. DISCUSSÃO GERAL E CONCLUSÕES**

Apesar de a reprodução ser um processo intensamente estudado em várias espécies de roedores, no ser humano e em outros mamíferos, relativamente poucos estudos foram feitos em Chiroptera, uma grande e diversa ordem que apresenta mais de mil espécies distribuídas mundialmente em vários habitats. Devido a essa grande diversidade de espécies, sua ampla distribuição geográfica e a grande variação de seus aspectos biológicos, é possível que processos fisiológicos, como os reprodutivos, apresentem acentuadas diferenças entre essas espécies.

Devido, possivelmente, a adaptação ao período de hibernação, muitas espécies de morcegos de ambiente temperado desenvolveram características únicas e, embora morcegos Neotropicais não apresentem um período de hibernação, muitas de suas características reprodutivas variam acentuadamente.

A variação reprodutiva em Chiroptera é ampla e complexa, onde observamos diferenças desde em características simples, como o posicionamento dos testículos, forma e tamanho do epidídimo, etc., até o desenvolvimento de características complexas, como a regressão testicular com armazenamento de espermatozóides ou os atrasos na fertilização, implantação e desenvolvimento do embrião.

Dentro desses aspectos, no presente estudo procuramos analisar diferentes aspectos relacionados à reprodução e também a nucleogênese de algumas espécies de morcegos, procurando entender melhor esses múltiplos mecanismos que governam a fisiologia reprodutiva de Chiroptera.

No epitélio seminífero de mamíferos, as células espermatogênicas movem-se da camada basal em direção ao lúmen tubular, sofrendo processos de divisão e diferenciação celular, até sua liberação no lúmen como espermatozóides. A fonte dessas células espermatogênicas são as células-tronco espermatogoniais ou espermatogônias. O

reconhecimento e classificação dessas células têm sido feita em conformidade com sua disposição topográfica em relação à membrana basal, morfologia e fisiologia; e a classificação mais complexa reconhece, nas espécies de roedores, uma série de nove tipos de espermatogônias, que, após 9-11 divisões mitóticas, produzem os espermatócitos (VAN HAASTER e de ROOIJ, 1993; de ROOIJ, 2001; CHIARINI-GARCIA *et al.*, 2001, 2003, CHIARINI-GARCIA e RUSSELL, 2002).

No presente estudo, três tipos principais de espermatogônias foram reconhecidos, com o uso de microscopia de luz, para as espécies de molossídeos *E. glaucinus*, *M. molossus*, *M. rufus* e *M. temminckii*: tipos A<sub>d</sub>, A<sub>p</sub> e B. Esses mesmos tipos já foram descritos para outras seis espécies de morcegos Neotropicais das famílias Phyllostomidae e Vespertilionidae (BEGUELINI *et al.*, 2009), assim como para outros morcegos (SINGWI e LALL, 1983; McGUICKIN e BLACKSHAW, 1987; SAIDAPUR e PATIL, 1992; LEE, 2003). Os mesmos três tipos também foram observados em *P. lineatus*, *M. molossus* e *M. nigricans* em microscopia eletrônica.

Baseado nessas considerações e nos nossos resultados, podemos propor que o processo de diferenciação em morcegos começa com a célula tronco espermatogonial, denominada A<sub>d</sub>, que quando estimulada divide-se mitoticamente, assim mantendo o estoque de células-tronco do epitélio (A<sub>d</sub>) e formando novas células que tornam-se destinadas a futura diferenciação (A<sub>p</sub>). Essas novas células passam por outras divisões mitóticas que, ao fim, produzem um tipo de espermatogônia diferente, o tipo B, que é a célula predestinada a sofrer diferenciação até espermatócitos e entrar em divisão meiótica.

Outro processo interessante do epitélio seminífero que tem atraído vários estudos, em várias espécies, refere-se à espermiogênese, processo pelo qual espermátides arredondadas diferenciam-se em espermatozóides maduros. O número de etapas na transformação das espermátides em espermatozóides varia em diferentes espécies e

diferentes estudos descrevem entre 6 a 16 passos, dependendo dos métodos utilizados (CAVAZOS e MELAMPY, 1954; GUNAWARDANA, 1977; SINGWI e LALL, 1983; LIN e JONES, 1993; GÓES e DOLDER, 2002).

Com base na morfologia nuclear, condensação da cromatina e posição das células dentro do epitélio seminífero, sete etapas da espermiogênese foram observadas para as espécies de Molossidae em microscopia de luz. Isto está em acordo com o observado por BEGUELINI e colaboradores (2009), mas em contraste com SINGWI e LALL (1983), que, com base no sistema de formação do acrossomo, identificaram 16 etapas em *Rhinopoma kinneari* e SAIDAPUR e PATIL (1992), utilizando os mesmos critérios, identificou 14 etapas em *Rousettus leschenaulti*. Nestes estudos, o número de etapas da espermiogênese estava estritamente relacionadas ao número de fases do ciclo do epitélio seminífero, para o qual diferentes critérios de classificação foram utilizados.

Observamos também que, para *P. lineatus*, *M. molossus* e *M. nigricans*, foram identificadas 12 etapas na espermiogênese em microscopia eletrônica, as quais estão muito acima das 7 observadas na mesma espécie em estudos prévios (BEGUELINI et al., 2009). Essa diferença está relacionada com os métodos utilizados em cada estudo, onde a análise ultraestrutural é mais distintiva do que as colorações em microscopia de luz. Esse número também é maior que o observado por LEE (2003) em *Myotis macrodactylus*, apesar de ambos os estudos utilizaram análise ultraestrutural. Além disso, este número é menor que o observado em alguns roedores (CLERMONT, 1972; SEGATELLI et al., 2002) e em espécies de Monotremata (LIN et al., 1997; LIN e JONES, 2000), possivelmente devido a uma morfologia final mais simples.

Observamos que o processo de espermiogênese ocorre de forma semelhante em *P. lineatus*, *M. molossus* e *M. nigricans* e que os espermatozóides de *P. lineatus* e *M. molossus* apresentam semelhanças como o formato mais alongado da cabeça, a presença do



perforatorium e espessamentos nas fibras densas externas 1, 5 e 6. Observamos ainda, que o acrossomo e o perforatorium, de *M. molossus* são formados pela junção de vesículas proacrossomais que apresentam ambos os tipos de secreção (uma secreção elétron-densa e uma elétron-lúcida) dentro da mesma vesícula, muito semelhante ao observado em roedores e outros mamíferos. Por outro lado, em *P. lineatus* observamos a produção de dois tipos distintos vesículas proacrossomais, com as vesículas elétron-densas associando-se primeiro ao envelope nuclear que as elétron-lúcidas; e a ausência de perforatorium e espessamentos nas fibras axilares 1, 5, 6 e 9 em *M. nigricans*.

Comparando os padrões reprodutivos de *A. planirostris* e *M. nigricans*, observamos que, apesar de ambos serem espécies Neotropicais, eles diferem acentuadamente em sua reprodução. *Artibeus planirostris* apresenta um perfil de espermatogênese ativo durante todo o ano, possivelmente apresentando, como exposto por WILLIG (1985), um padrão poliétrico bimodal, com dois picos de acentuada produção espermatogênica, um em setembro e outro em fevereiro. Muitos trabalhos discorrem sobre a regulação feminina do processo de reprodução, onde o controle estaria ligado ao sexo feminino, devido à sua regulação dos períodos de ovulação e fertilização. No entanto, a contínua atividade espermatogênica anual e a existência de espermatozóides na cauda do epidídimo durante todo o ano, aliada a estrutura de haréns que essa espécie exibe possivelmente possibilita a esta espécie a habilidade de, em condições favoráveis de alimentação, abrigo, etc. poder gerar jovens em diferentes períodos do ano, como o descrito por TADDEI (1976) e GRAHAM (1987).

Por outro lado, *M. nigricans* apresentou um padrão totalmente diferente, apresentando um ciclo reprodutivo anual dotado de dois períodos de regressão testicular, um perfil nunca antes observado em nenhum outro morcego ou mamífero. A observação de períodos de regressão testicular de um a seis meses em espécies de morcegos hibernantes

de clima temperado é comum, no entanto a observação desse padrão em espécies de clima tropical é rara. Já a observação de dois períodos, um dos quais apresentando grande armazenamento de espermatozóides foi exclusiva de *M. nigricans*, mostrando que a semelhança do observado por WILSON e FINDLEY (1971), essa espécie apresenta um padrão exclusivo de reprodução, variando geograficamente, de ambientes onde ele se comporta como uma espécie hibernante, a ambientes onde ele é ativo durante todo o ano.

A nucleogênese nas diferentes espécies analisadas ocorre de maneira semelhante ao observado na divisão mitótica de muitos mamíferos, onde os componentes nucleolares podem se comportar de até quatro formas durante a divisão meiótica, dissolver-se no nucleoplasma, deslocar-se para o citoplasma, associar-se às regiões pericromossomais ou ficar ligado às RONS durante toda a divisão; Com a variação no posicionamento cromossômico não influenciando significativamente na nucleogênese meiótica.

Por outro lado, percebemos que o número de RONS exerce alguma influência na nucleogênese onde, espécies que possuem maior número de RONS, apresentam maior número de nucléolos por célula interfásica, maior número de sítios de desorganização e uma maior quantidade de material nucleolar e expressão de nucleolina nas células em divisão.

A análise conjunta dos resultados evidencia que as características reprodutivas dos morcegos estudados estão intimamente relacionadas às espécies as quais pertencem e que, apesar de possuírem um perfil de nucleogênese semelhante, as espécies ainda apresentam diferenças importantes em relação ao nucléolo. Com esses estudos esclarecemos alguns aspectos da espermatogênese e da nucleogênese de morcegos, assim como levantamos dados que podem ser utilizados em análises filogenéticas multifatoriais, para uma melhor elucidação das relações filogenéticas entre as espécies de morcegos.

Assim, são conclusões deste trabalho:

- a espermatogênese dos morcegos analisados assemelha-se a de outros mamíferos, apresentando células de Leydig e de Sertoli com características similares e três tipos principais de espermatogônias ( $A_d$ ,  $A_p$  e B).
  
- o processo de diferenciação em morcegos começa com a célula-tronco espermatogonial, denominada  $A_d$ , que quando estimulada divide-se mitoticamente, assim mantendo o estoque de células-tronco do epitélio ( $A_d$ ) e formando novas células que tornam-se destinadas a futura diferenciação ( $A_p$ ). Essas novas células passam por outras divisões mitóticas que, ao fim, produzem um tipo de espermatogônia diferente, o tipo B, que é a célula predestinada a sofrer diferenciação até espermatócitos e entrar em divisão meiótica.
  
- apesar das diferenças encontradas na espermiogênese, todas as espécies apresentaram um processo semelhante, podendo ser subdividido em doze passos, em MET.
  
- a ultraestrutura mais simples do espermatozóide de morcegos mostra um padrão mais intimamente relacionado com o de humanos e outros primatas.
  
- a ultraestrutura do espermatozóide dos morcegos analisados mostra variações morfológicas interessantes, onde três caracteres da morfologia parecem variar nas diferentes famílias: morfologia das fibras densas externas, presença e morfologia do perforatorium e morfologia da cabeça do espermatozóide.

- os dados de MET indicam que *M. molossus* está mais intimamente relacionado com o Phyllostomidae do que com Rhinolophidae e Vespertilionidae; e essas semelhanças indicam que a hipótese de que Phyllostomidae tenha derivado de Molossidae não pode ser descartada.
- a morfologia do espermatozóide de morcegos talvez seja um interessante parâmetro a ser caracterizado em diferentes espécies, analisado comparativamente e utilizado em análises filogenéticas e evolutivas.
- *Artibeus planirostris* apresenta um padrão poliétrico bimodal de reprodução, com dois períodos de copula, que parecem ser diretamente influenciados pela viabilidade de suplemento alimentar e indiretamente pela temperatura e pluviosidade.
- *Myotis nigricans* apresenta dois períodos de regressão testicular, no mesmo ciclo reprodutivo anual, que não está diretamente ligado a apoptose e parece ser fracamente influenciado por fatores abióticos.
- *Myotis nigricans* apresenta uma assincronia no ciclo do epitélio seminífero, apresentado sobreposição de fases, o que é devido a seus períodos de regressão testicular e reativação.
- um dos mecanismos da desativação da espermatogênese em *Myotis nigricans* parece estar ligado a baixa expressão do AR nas células de Sertoli, que desativam sua função de suporte, nutrição e estímulo tornando a complementação da espermatogênese impossível.

– outro mecanismo parece estar relacionado a diminuição da síntese de andrógenos pelas células de Leydig (diminuição na quantidade de lipídeos), que causam uma diminuição do estímulo parácrino das células de Sertoli.

– a nucleogênese nas diferentes espécies analisadas ocorre de maneira semelhante ao observado na divisão mitótica de muitos mamíferos, onde os componentes nucleolares podem se comportar de até quatro formas durante a divisão meiótica: dissolver-se no nucleoplasma; deslocar-se para o citoplasma; associar-se às regiões pericromossomais; ou ficar ligado às RONS durante toda a divisão.

– a variação no posicionamento cromossômico das RONS não influencia significativamente na nucleogênese meiótica. Por outro lado, o número de RONS exerce alguma influência na nucleogênese onde, espécies que possuem maior número de RONS, apresentam maior número de nucléolos por célula interfásica, maior número de sítios de desorganização e uma maior quantidade de material nucleolar e expressão de nucleolina nas células em divisão.

Com esses resultados inéditos esclarecemos alguns aspectos da espermatogênese e da nucleogênese de morcegos, assim como levantamos dados que podem ser utilizados em análises filogenéticas multifatoriais, para uma melhor elucidação das relações filogenéticas entre as espécies de morcegos.



## XI. REFERÊNCIAS BIBLIOGRÁFICAS

AMARAL, R. S. et al. Morphology, morphometry and ultrastructure of the Amazonian manatee (Sirenia: Trichechidae) spermatozoa. **Zoologia**, v. 27(6), p. 1014-1017, 2010.

AMORY, J. K.; BREMNER, W. Endocrine regulation of testicular function in men: implications for contraceptive development. **Molecular and Cellular Endocrinology**, v. 182, p. 175–179, 2001.

ANAND-KUMAR, T. C. Reproduction in the rat-tailed bat *Rhinopoma kinneari*. **Journal of Zoology**, v. 147, p. 147-155, 1965.

BAKER, R. J.; HOOD, C. S.; HONEYCUTT, R. L. Phylogenetic relationships and classification of the higher categories of the New World bat family Phyllostomidae. **Systematic Zoology**, v. 38, p. 228-238, 1989.

BAKER, R. J. et al. Diversification among New World leaf-nosed bats: an evolutionary hypothesis and classification inferred from digenomic of DNA sequence. **Occasional Papers of the Museum of Texas Technology University**, v. 230, p. 1-32, 2003.

BARCLAY, R. M. R. Does energy or calcium availability constrain reproduction by bats. **Symposia of the Zoological Society of London**, v. 67, p. 245–258, 1995.

BARCLAY, R. M. R.; BRIGHAM, R. M. Prey detection, dietary niche breadth, and body size in bats: why are aerial insectivorous bats so small? **The American Naturalist**, v. 137, p. 693-703, 1991.

BEGUELINI, M. R. et al. Morphological characterization of the testicular cells and seminiferous epithelium cycle in six species of Neotropical bats. **Journal of Morphology**, v. 270, p. 943-953, 2009.

BEGUELINI, M. R. et al. Ultrastructure of spermatogenesis in the white-lined broad-nosed bat, *Platyrrhinus lineatus* (Chiroptera: Phyllostomidae). **Micron**, v. 42(6), p. 586-599, 2011a.

BEGUELINI, M. R. et al. Nucleolar behavior during meiosis in males of phyllostomid bats (Chiroptera, Mammalia). **Genetics and Molecular Research**, v. 10(2), p. 552-565, 2011b.

BEGUELINI, M. R.; TABOGA, S. R.; MORIELLE-VERSUTE, E. Ultrastructural characteristics of spermatogenesis in Pallas's Mastiff bat, *Molossus molossus* (Chiroptera: Molossidae). **Microscopy Research and Technique**, 2012. *in press*. DOI: 10.1002/jemt.22005

BOISVERT, F.M.; et al. The multifunctional nucleolus. **Nature Reviews: Molecular Cell Biology**, v. 8, p. 574-585, 2007.

BOYLES, J. G. et al. Economic importance of bats in agriculture. **Science**, v. 332, p. 41-42, 2011.

BRADBURY, J.; VEHRENCAMP, S. Social organization and foraging in emballonurid bats. III. Mating systems. **Behavior Ecology and Sociobiology**, v. 2, p. 1-17, 1977.

BREED, W. G.; LEIGH, C. Sperm head morphology of Australian molossid bats with special reference to the acrosomal structure. **Mammalia**, v. 49, p. 403-406, 1985.

CARMO-FONSECA, M.; MENDES-SOARES, L.; CAMPOS, I. To be or not to be in the nucleolus. **Nature Cell Biology**, v. 2, p. E107-E112, 2000.

CAVAZOS, L. F.; MELAMPY, R. M. A comparative study of periodic acid-reactive carbohydrates in vertebrates testes. **American Journal of Anatomy**, v. 95, p. 467-497, 1954.

CHIARINI-GARCIA, H.; RUSSELL, L. D. Characterization of mouse spermatogonia by transmission electron microscopy. **Reproduction**, v. 123, p. 567-577, 2002.

CHIARINI-GARCIA, H.; RAYMER, A. M.; RUSSELL, L. D. Non-random distribution of spermatogonia in rats: evidence of niches in the seminiferous tubules. **Reproduction**, v. 126, p. 669-680, 2003.

CHIARINI-GARCIA, H. et al. Distribution of type A spermatogonia in the mouse is not random. **Biology of Reproduction**, v. 65, p. 1179-1185, 2001.

CLERMONT, Y. Kinetics of spermatogenesis in Mammals: Seminiferous epithelium cycle and spermatogonial renewal. **Physiological Reviews**, v. 52, p. 198-236, 1972.

CMARKO, D. et al. Ultrastructural analysis of nucleolar transcription in cells microinjected with 5-bromo-UTP. **Histochemistry and Cell Biology**, v. 113, p. 181-187, 2000.

COLLI, G. R. et al. Comparative study of sperm ultrastructure of five species of teiid lizards (Teiidae, Squamata), and *Cercosaura ocellata* (Gymnophthalmidae, Squamata). **Tissue Cell**, v. 39, p. 59-78, 2007.

COSTA, D. S.; PAULA, T. A. R. Espermatogênese em Mamíferos. **Scientia Vila Velha** (ES), v. 4 (1/2), p. 53-72, 2003.

COSTA, G. C. et al. Comparative analysis of the sperm ultrastructure of three species of *Phyllomedusa* (Anura, Hylidae) **Acta Zoologica**, v. 85, p. 257-262, 2004a.

COSTA, G. C. et al. An ultrastructural comparative study of the sperm of *Hyla pseudopseudis*, *Scinax rostratus*, and *S. squalirostris* (Amphibia: Anura: Hylidae). **Zoomorphology**, v. 123, p. 191-197, 2004b.

CRICHTON, E. G.; KRUTZSCH, P. H. **Reproductive biology of bats**. Academic Press, London, United Kingdom. 528 p., 2000.

CUNHA, L. D.; TAVARES-BASTOS, L.; BÁO, S. N. Ultrastructural description and cytochemical study of the spermatozoon of *Crotallus durissus* (Squamata, Serpentes). **Micron**, v. 39, p. 915-925, 2008.

de ROOIJ, D. G. Proliferation and differentiation of spermatogonial stem cells. **Reproduction**, v. 121, p. 347-354, 2001.

DOUSSET, T. et al. Initiation of nucleolar assembly is independent of RNA polymerase I transcription. **Molecular Biology of Cell**, v. 11, p. 2705-2717, 2000.

DUNDR, M.; OLSON, M. O. J. Partially processed pre-rRNA is preserved in association with processing components in nucleolus-derived foci during mitosis. **Molecular Biology of Cell**, v. 9, p. 2407-2422, 1998.

DUNDR, M.; MISTELLI, T.; OLSON, O. J. The dynamics of postmitotic reassembly of the nucleolus. **Journal of Cell Biology**, v. 150, p. 433-446, 2000.

DUNDR, M. et al. A class of nonribosomal nucleolar components is located in chromosome periphery and in nucleolus-derived foci during anaphase and telophase. **Chromosoma**, v. 105, p. 407-417, 1997.

ENCARNAÇÃO, J. A.; DIETZ, M.; KIERDORF, U. Reproductive condition and activity pattern of male Daubenton's bats (*Myotis daubentonii*) in the summer habitat. **Mammalian Biology**, v. 69, p. 163-172, 2004.

FARIA, K. C.; MORIELLE-VERSUTE, E. Genetic relationships between Brazilian species of Molossidae and Phyllostomidae (Chiroptera, Mammalia). **Genetica**, v. 126, p. 215-225, 2006.

FAWCETT, D. W.; ITO, S. The fine structure of bat spermatozoa. **American Journal of Anatomy**, v. 116, p. 567-610, 1965.

FENTON, M. B. **Bats**. New York: Facts On File, Inc., 207p., 1992.

FLEMING, T. H.; HOOPER, E. T.; WILSON, D. E. Three Central American bat communities: structure, reproductive cycles and movement patterns. **Ecology**, v. 53, p. 555-569, 1972.

FOMPROIX, N.; GÉRBRANE-YOUNÉS, J.; HERNANDEZ-VERDUN, D. Effects of anti-fibrillar antibodies on building of functional nucleoli at the end of mitosis. **Journal of Cell Science**, v. 111, p. 359-372, 1998.

GARDA, A. A. et al. The ultrastructure of the spermatozoa of *Epipedobates flavopictus* (Amphibia, Anura, Dendrobatidae), with comments on its evolutionary significance. **Tissue Cell**, v. 34(5), p. 356-64, 2002.

GARDA, A. A. et al. Spermatozoa of Pseudinae (Amphibia, Anura, Hylidae), with a test of the hypothesis that sperm ultrastructure correlates with reproductive modes in anurans. **Journal of Morphology**, v. 261(2), p. 196-205, 2004.

GAUTIER, T. et al. Fate of specific nucleolar perichromosomal proteins during mitosis: cellular distribution and association with U3 snoRNA. **Biology of Cell**, v. 82, p. 81-93, 1994.

GINISTY, H.; AMALRIC, F.; BOUVET, P. Nucleolin functions in the first step of ribosomal RNA processing. **EMBO Journal**, v. 17, p. 1476-1486, 1998.

GIUGLIANO, L. G. et al. Ultrastructure of spermatozoa of the lizard *Ameiva ameiva*, with considerations on polymorphism within the family Teiidae (Squamata). **Journal of Morphology**, v. 253(3), p. 264-271, 2002.

GOPALAKRISHNA, A.; BADWAIK, N. Breeding habits and associated phenomenon in some Indian bats – Part XIV. **Journal of the Bombay Natural History Society**, v. 90, p. 1–10, 1993.

GRAHAM, G. L. Seasonality of reproduction in Peruvian bats. In Studies in Neotropical mammalogy, essays in honor of Philip Hershkovitz, pp 173–181. Eds BD Patterson and RM Timm. **Fieldiana: Zoology (New Series)**, v. 39, p. 1–506, 1987.

GREGORIN, R.; TADDEI, V. A. Chave artificial para a identificação de molossídeos brasileiros (Mammalia, Chiroptera). **Journal of Neotropical Mammalogy**, v. 9, p. 13-32, 2002.

GUILLOT, P.V.; MARTIN, S.; POMBO, A. The organization of transcription in the nucleus of mammalian cells. In: HEMMERICH, P.; DIEKMANN, S. **Visions of the cell nucleus**. ASP, CA, p. 95–105, 2005.

GUNAWARDANA, V. K. Stages of spermatids in the domestic fowl: A light microscope study using Araldite sections. **Journal of Anatomy**, v. 123, p. 351-360, 1977.

GÉBRANE-YOUNÈS, J.; FOMPROIX, N.; HERNANDEZ-VERDUN, D. When rDNA transcription is arrested during mitosis, UBF is still associated with non-condensed rDNA. **Journal of Cell Science**, v. 110, p. 2429-2440, 1997.

GÓES, R. M.; DOLDER, H. Cytological steps during spermiogenesis in the house sparrow (*Passer domesticus*, Linnaeus). **Tissue Cell**, v. 34, p. 273-282, 2002.

HAYSEN, V.; VAN TIENHOVEN, A.; VAN TIENHOVEN, A. **Asdell's Patterns of Mammalian Reproduction**. Cornell University Press, Ithaca, New York, 1993.

HECKERT, L. L.; GRISWOLD, M. D. The expression of the follicle-stimulating hormone receptor in spermatogenesis. **Recent Progress in Hormone Research**, v. 57, p. 129–148, 2002.

HEIX, J. et al. Mitotic silencing of human rRNA synthesis: inactivation of the promoter selectivity factor SL1 by cdc2/cyclin B-mediated phosphorylation. **EMBO Journal**, v. 17, p. 7373-7381, 1998.

HERNANDEZ-VERDUN, D. Assembly and disassembly of the nucleolus during the cell cycle. **Nucleus**, v. 2(3), p. 189-194, 2011.

HERNANDEZ-VERDUN, D.; ROUSSEL, P.; GÉBRANE-YOUNÈS, J. Emerging concepts of nucleolar assembly. **Journal of Cell Science**, v. 115, p. 2265-2270, 2002.

HISCOX, J. A. RNA viruses: hijacking the dynamic nucleolus. **Nature Reviews: Microbiology**, v. 5, p. 119-127, 2007.

- HOCKMAN, D. et al. The role of early development in Mammalian limb diversification: a descriptive comparison of early limb development between the Natal Long-Fingered Bat (*Miniopterus natalensis*) and the mouse (*Mus musculus*). **Developmental Dynamics**, v. 238, p. 965-979, 2009.
- HOLDCRAFT, R. W.; BRAUN, R. E. Hormonal regulation of spermatogenesis. **International Journal of Andrology**, v. 27, p. 335–342, 2004a.
- HOLDCRAFT, R. W.; BRAUN, R. E. Androgen receptor function is required in Sertoli cells for the terminal differentiation of haploid spermatids. **Development**, v. 31, p. 459-467, 2004b.
- HOOD, C. S.; BAKER, R. J. G. G- and C-banding chromosoma studies of bats of the family Emballonuridae. **Journal of Mammalogy**, v. 67, p. 705-711, 1986.
- JAMIESON, B. G. M.; HODGSON, A.; SPOTTISWOODE, C. N. Ultrastructure of the spermatozoon of *Myrmecocichla formicivora* (Vieillot, 1881) and *Philetairus socius* (Latham, 1790) (Aves; Passeriformes), with a new interpretation of the passeridan acrosome. **Acta Zoologica**, v. 87, p. 297-304, 2006.
- JEONG, S. J. et al. Comparative fine structure of the epididymal spermatozoa from three Korean shrews with considerations on their phylogenetic relationships. **Biocell**, v. 30(2), p. 279-86, 2006.
- JONES, K. E. et al. A phylogenetic supertree of the bats (Mammalia: Chiroptera). **Biology Reviews**, v. 77, p. 223-259, 2002.
- JONES, K. E.; CARTER, D. C. Annotated checklist, with keys to subfamilies and genera. **Special Publications of Museum Texas Technology University**, v. 10, p. 7-38, 1976.
- KOOPMAN, K. F. Zoogeography of bats. In: SLAUGHTER, B. H.; WALTON, D. W. (Ed.). **About bats: a chiropteran biology symposium**. Dallas: Southern Methodist University Press, 1970. p. 29-46.
- KOOPMAN, K. F. A synopsis of the families of bats. **Bat Research News**, v. 25, p. 25- 29, 1984.
- KOOPMAN, K. F. Order Chiroptera. In: WILSON, D. E.; REEDER, D. M. (Ed.) **Mammals species of the world: a taxonomic and geographic reference**. Washington: Smithsonian Institution Press, p. 137-241, 1993.
- KOOPMAN, K. F. Chiroptera: systematics. handbook of zoology. **Mammalia**, v. 8, p. 1-217, 1994.
- KUROHMARU, M. et al. Seasonal changes in spermatogenesis of Japanese Lesser Horseshoe bat, *Rhinolophus cornutus* from a morphological viewpoint. **Okajimas Folia Anatomica Japonica**, v. 79(4), p. 93-100, 2002.
- KURTA, A.; KUNZ, T. H. Size of bats at birth and maternal investment during pregnancy. **Symposia of the Zoological Society of London**, v. 57, p. 79–106, 1987.



- LEE, J. H. Cell differentiation and ultrastructure of the seminiferous epithelium in *Myotis macrodactylus*. **Korean Journal of Electron Microscopy**, v. 33(1), p. 25-39, 2003.
- LEE, J. H.; MORI, T. Annual cycle of the seminiferous epithelium of *Myotis macrodactylus*. **Journal of Faculty of Agriculture, Kyushu University**, v. 49(2), p. 355-365, 2004.
- LEE, J. H.; CHOI, B. J.; SON, S. W. Spermiogenesis in the Korean horseshoe bat, *Rhinolophus ferrumequinum korai*. **Korean Journal of Electron Microscopy**, v. 22, p. 97-117, 1992.
- LEE, K. H. et al. Estrogen receptor alpha has a functional role in the mouse rete testis and efferent ductules. **Biology of Reproduction**, v. 63, p. 1873-1880, 2000.
- LEI, Z. M. et al. Targeted disruption of luteinizing hormone/human chorionic gonadotropin receptor gene. **Molecular Endocrinology**, v. 15, p. 184-200, 2001.
- LEUNG, A.K. et al. Quantitative kinetic analysis of nucleolar breakdown and reassembly during mitosis in live human cells. **Journal of Cell Biology**, v. 166, p. 787-800, 2004.
- LIM, B. K. Review of the origins and biogeography of bats in South America. **Chiroptera Neotropical**, v. 15(1), p. 391-410, 2009.
- LIN, M.; JONES, R. C. Spermiogenesis and spermiation in the Japanese quail (*Coturnix coturnix japonica*). **Journal of Anatomy**, v. 183, p. 525-535, 1993.
- LIN, M.; JONES, R. C. Spermiogenesis and spermiation in a monotreme mammal, the platypus, *Ornithorhynchus anatinus*. **Journal of Anatomy**, v. 196, p. 217-232, 2000.
- LIN, M.; HARMAN, A.; RODGER, J. C. Spermiogenesis and spermiation in a marsupial, the tammar wallaby (*Macropus eugenii*). **Journal of Anatomy**, v. 190, p. 377-395, 1997.
- LINDZEY, J. et al. Molecular mechanisms of androgen action. **Vitamins and Hormones**, v. 49, p. 383-432, 1994.
- LODISH, H. et al. **Molecular Cell Biology**, 5ed. Nova Iorque: WH Freeman & Co, 2005.
- LUQUE, M. C. A.; BÁO, S. N. Structural and ultrastructural characterization of zebu (*Bos indicus*) spermatozoa. **Biocell**, v. 30(1), p. 33-38, 2006.
- MAEKAWA, M.; KAMIMURA, K.; NAGANO, T. Peritubular myoid cells in the testis: their structure and function. **Archives of Histology and Cytology**, v. 59, p. 1-13, 1996.
- MARCHESIN, S. R. C.; MORIELLE-VERSUTE, E. **Análise citogenética em espécies de Vespertilionidae dos gêneros *Eptesicus*, *Histiotus*, *Lasiurus* e *Myotis* (Chiroptera, Mammalia)**. 2002. 98f. Dissertação (Mestrado em Genética) Instituto de Biociências, Letras e Ciências Exatas, São José do Rio Preto, 2002.
- MARCHESIN, S. R. C.; MORIELLE-VERSUTE, E. **Divergência Genética e Relacionamento Filogenético em Espécies de Morcegos das Famílias Molossidae e Phyllostomidae Baseado em Análises de PCR-RFLP**. 2006. 118f. Tese (Doutorado em Genética) Instituto de Biociências, Letras e Ciências Exatas, São José do Rio Preto, 2006.

- MATSUMOTO, A. M. Spermatogenesis. **Reproductive Endocrinology, Surgery and Technology**. Lippincott-Raven Publishers, Philadelphia, 1996.
- MELLO, M. L. S. Nucléolo. **A Célula** 2001. Editora Manole Ltda, Barueri – SP. p. 101-110, 2001.
- McGUCKIN, M. A.; BLACKSHAW, A. W. Cycle of the seminiferous epithelium in the grey-headed fruit bat, *Pteropus poliocephalus*. **Australian Journal of Biological Sciences**, v. 40, p. 203-210, 1987.
- McLACHLAN, R. I. et al. Identification of specific sites of hormonal regulation in spermatogenesis in rats, monkeys, and man. **Recent Progress in Hormone Research**, v. 57, p. 149–179, 2002.
- MENDIS-HANDAGAMA, S. M. Luteinizing hormone on Leydig cell structure and function. **Histology and Histopathology**, v. 12, p. 869-882, 1997.
- MORIELLE, E.; VARELLA-GARCIA, M. Variability of nucleolus organizer regions in Phyllostomid bats. **Brazilian Journal of Genetics**, v. 11, p. 853-871, 1988.
- MORIELLE-VERSUTE, E.; VARELLA-GARCIA, M.; TADDEI, V. A. Karyotypic patterns of seven species of Molossid bats (Molossidae, Chiroptera). **Cytogenetic and Cell Genetics**, v. 72, p. 26-33, 1996.
- MURO, E. et al. The traffic of proteins between nucleolar organizer regions and prenucleolar bodies governs the assembly of the nucleolus at exit of mitosis. **Nucleus**, v. 1, p. 202-211, 2010.
- NEGI, S. S.; OLSON, M. O. Effects of interphase and mitotic phosphorylation on the mobility and location of nucleolar protein B23. **Journal of Cell Science**, v. 119, p. 3676-3685, 2006.
- NIKAIDO, M. et al. Monophyletic origin of the order Chiroptera and its phylogenetic position among Mammalia, as inferred from the complete sequence of the mitochondrial DNA of a Japanese megabat, Ryukyu flying fox (*Pteropus dasymallus*). **Journal of Molecular Evolution**, v. 51, p. 318-328, 2000.
- NOLTE, M.J. et al. Embryonic staging system for the Black Mastiff Bat, *Molossus rufus* (Molossidae), correlated with structure-function relationships in the adult. **Anatomical Record**, v. 292, p. 155–168, 2009.
- NOVACEK, M. J. Aspects of morphology of the cochlea in microchiropteran bats: an investigation of character transformation. **Bulletins of American Museum of Natural History**, v. 206, p. 84-100, 1991.
- NOWAK, R. M. **Chiroptera**. In: Walker's mammals of the world. 6.ed. Baltimore: Johns Hopkins University Press. v. 1, p. 253-489, 1999.

OH, Y. K.; MORI, T.; UCHIDA, T. A. Spermogenesis in the Japanese Greater Horseshoe Bat, *Rhinolophus ferrumequinum nippon*. **Journal of Faculty of Agriculture: Kyushu University**, v. 29(4), p. 203-209, 1985.

PARVINEN, M. et al. *In vitro* stimulation of stage-specific deoxyribonucleic acid synthesis in rat seminiferous tubule by interleukin- 1alfa. **Endocrinology**, v. 129, p. 1614-1620, 1991.

PETTIGREW J. D. Flying primates? Megabats have the advanced pathway from eye to midbrain. **Science**, v. 231(4743), p. 1304-1306, 1986.

PETTIGREW J. D. Flying primates: crashed, or crashed through? In: Ecology, evolution and behavior of bats. **Symposium of the Zoological Society of London**, v. 67, p. 3-26, 1995.

PETTIGREW, J. D.; JAMIESON, B. G. M. Are flying foxes (Chiroptera: Pteropodidae) really primates? **Australian Mammalogy**, v. 10, p. 119-124, 1987.

PETTIGREW, J. D. et al. Phylogenetic relations between microbats, megabats and primates (Mammalia: Chiroptera and Primates). **Philosophical Transactions of Royal Society of London B**, v. 325, p. 489-559, 1989.

PHILLIPS, D. M.; RASWEILER IV, J. J.; FAROUK, M. Giant, Accordioned Sperm Acrosomes of the Greater Bulldog Bat, *Noctilio leporinus*. **Molecular Reproduction and Development**, v. 48, p. 90-94, 1997.

PIERSON, E. D. **Molecular systematics of the Microchiroptera: higher taxon relationships and biogeography**. Ph.D. dissertation, University of California, Berkeley, 1986.

RACEY, P. A. The reproductive cycle in male noctule bats, *Nyctalus noctula*. **Journal of Reproduction and Fertility**, v. 41, p. 169-182, 1974.

RACEY, P. A. The prolonged storage and survival of spermatozoa in Chiroptera. **Journal of Reproduction and Fertility**, v. 56, p. 391-402, 1979.

RANNIKKI, A. S.; ZHANG, F. P.; HUHTANIEMI, I. T. Ontogeny of follicle-stimulating hormone receptor gene expression in the rat testis and ovary. **Molecular and Cellular Endocrinology**, v. 107, p. 199-208, 1995.

RASWEILER, J. J. Pregnancy in Chiroptera. **Journal of Experimental Zoology**, v. 266, p. 495-513, 1993.

REIS, N. L. et al. Ordem Chiroptera. 1.ed. In: **Mamíferos do Brasil**. Universidade Estadual de Londrina. v. 1, p. 153-230, 2006.

REIS, N. R. et al.. **Morcegos do Brasil**. Londrina: Universidade Estadual de Londrina. 2007.

ROSA, E. S. T. et al. Bat-transmitted Human Rabies Outbreaks, Brazilian Amazon. **Emerging Infectious Diseases**, v. 12(8), p. 1197-1202, 2006.

ROUSE, G. W.; ROBSON, S. K. An ultrastructural study of megachiropteran (Mammalia: Chiroptera) spermatozoa: implications for chiropteran phylogeny. **Journal of Submicroscopic Cytology**, v. 18, p. 137-152, 1986.

RUSSELL, L. D.; GRISWOLD, M. D. **The Sertoli cell**. Clearwater, Florida: Cache River Press., 1993.

RUSSELL, L. D. et al. **Mammalian spermatogenesis**. In: Russell LD, Ettlín RA, Sinha Hikin AP, Clegg ED, eds. Histological and histopathological evaluation of the testis. Clearwater: Cache River Press, p. 1-40, 1990.

SAIDAPUR, S. K.; PATIL, S. B. Kinetics of spermatogenesis in megachiropteran bat, *Rousettus leschenaulti* (Desmarset): seminiferous epithelial cycle, frequency of stages, spermatogonial renewal and germ cell degeneration. **Indian Journal of Experimental Biology**, v. 30, p. 1037-1044, 1992.

SANG-SICK, K. et al. Morphological comparison of spermatozoa in the Korean greater horseshoe bat (*Rhinolophus ferrumequinum korai*) and long-fingered bat (*Miniopterus schreibersi fuliginosus*). **Korean Journal of Electron Microscopy**, v. 29(1), p. 1-10, 1999.

SAVINO, T. M. et al. Nucleolar assembly of the rRNA processing machinery in living cells. **Journal of Cell Biology**, v. 115, p. 1097-1110, 2001

SCHEER, U.; HOCK, R. Structure and function of the nucleolus. **Current Opinion on Cell Biology**, v. 11, p. 385-390, 1999.

SCHEER, U.; THIRY, M.; GOESSENS, G. Structure, function and assembly of the nucleolus. **Trends Cell Biology**, v. 3, p. 236-241, 1993.

SEARS, K.E. Molecular Determinants of Bat Wing Development. **Cells Tissues Organs**, v. 187, p. 6-12, 2008.

SEARS, K.E. et al. Development of bat flight: Morphologic and molecular evolution of bat wing digits. **PNAS**, v. 103(17), p. 6581-6586, 2006.

SEGATELLI, T. M. et al. Kinetics of spermatogenesis in the Mongolian gerbil (*Meriones unguiculatus*). **Tissue Cell**, v. 34(1), p. 7-13, 2002.

SHARIFI, M.; GHORBANI, R.; AKMALI, V. Reproductive cycle in *Pipistrellus kuhlii* (Chiroptera, Vespertilionidae) in western Iran. **Mammalia**, v. 68(4), p. 323-327, 2004.

SHARPE, R. M. **Regulation of Spermatogenesis**. In: The Physiology of Reproduction (eds E. Knobil & J. D. Neill), Raven Press, Ltd, New York, NY. 1994.

SHEN, Y-Y. et al. Adaptive evolution of energy metabolism genes and the origin of flight in bats. **PNAS**, v. 107(19), p. 8666-8671, 2010.

SIMMONS, N. B. The case for chiropteran monophyly. **American Museum Novitates**, v. 3103, 54 p., 1994.

SIMMONS, N. B. Bat relationships and the origin of flight. In: Ecology, evolution and behavior of bats. **Symposium of the Zoological Society of London**, v. 67, p. 27-43, 1995.

SIMMONS, N. B. A reappraisal of interfamilial relationships of bats. p.3-26. In: KUNZ, T. H.; RACEY, P. A. (Eds), **Bats: Phylogeny, Morphology, Echolocation and Conservation Biology**. Smithsonian Institution Press, London, 365p., 1998.

SIMMONS, N. B. **Order Chiroptera**. In: Mammal species of the world: a taxonomic and geographic reference (Wilson D.E. and Reeder D.M., eds.). 3rd edn. Johns Hopkins University Press: Baltimore, p. 312-529, 2005.

SIMMONS, N. B.; GEISLER, J. H. Phylogenetic relationships of *Icaronycteris*, *Archeonycteris*, *Hassianycteris*, and *Palaeochiropteryx* to extant bat lineages, with comments on the evolution of echolocation and foraging strategies in Microchiroptera. **Bulletin of American Museum of Natural History**, v. 235, p. 1-182, 1998.

SINGWI, M. S.; LALL, S. B. Spermatogenesis in the non-scrotal bat – *Rhinopoma kinneari* Wroughton (Microchiroptera: Mammalia). **Acta Anatomica**, v. 116, p. 136-145, 1983.

SIRRI, V.; ROUSSEL, P.; HERNANDEZ-VERDUN, D. The mitotically phosphorylated form of the transcription termination factor TTF-1 is associated with the repressed rDNA transcription machinery. **Journal of Cell Science**, v. 112, p. 3259-3268, 1999.

SIRRI, V.; ROUSSEL, P.; HERNANDEZ-VERDUN, D. The AgNOR proteins: qualitative and quantitative changes during the cell cycle. **Micron**, v. 31, p. 121-126, 2000.

SIRRI, V.; HERNANDEZ-VERDUN, D.; ROUSSEL, P. Cyclindependent kinases govern formation and maintenance of the nucleolus. **Journal of Cell Biology**, v. 156, p. 969-981, 2002.

SMITH, J. D. Chiropteran evolution. **Special Publication of Museum of Texas Technology University**, v. 10, p. 49-69, 1976.

SMITH, J. D.; MADKOUR, G. Penial morphology and the question of chiropteran phylogeny. In: Proceedings Fifth International Bat Research Conference. Lubbock: **Texas Technology Press**, p. 347-365, 1980.

SON, S. W.; LEE, J. H.; CHEON, H. M. Spermiogenesis in the Korean Daubenton's Bat (*Myotis daubentonii ussuriensis*). **Development and Reproduction**, v. 1(1), p. 9-24, 1997.

SPEAKMAN, J. R. The evolution of flight and echolocation in bats: another leap in the dark. **Mammalian Review**, v. 31(2), p. 111-130, 2001.

SRIVASTAVA, M. et al. Genomic organization and chromosomal localization of the human nucleolin gene. **Journal of Biology and Chemistry**, v. 265, p. 14922-14931, 1990.

SUDMAN, P. D.; BARKELEY L. J.; HAFNER, M. S. Familial affinity of *Tomopeas ravus* (Chiroptera) based on protein electrophoretic and cytochrome b sequence data. **Journal of Mammalogy**, v. 75, p. 365-377, 1994.



TADDEI, V. A. The reproduction of some Phyllostomidae (Chiroptera) from the northwestern region of the State of São Paulo. **Biologia e Zoologia Universidade de São Paulo**, v. 1, p. 313-330, 1976.

TADDEI, V. A. Biologia reprodutiva de Chiroptera: perspectivas e problemas. **Inter-Facies, Escr. e Doc.** v. 6, p. 1-18, 1980.

TEELING, E. C. et al. A molecular phylogeny for bats illuminates biogeography and the fossil record. **Science**, v. 307, p. 580-584, 2005.

TEIXEIRA, R. D. et al. A comparative ultrastructural study of spermatozoa of the teiid lizards *Cnemidophorus gularis gularis*, *Cnemidophorus ocellifer*, and *Kentropyx altamazonica* (Reptilia, Squamata, Teiidae). **Tissue Cell**, v. 34(3), p. 135-42, 2002.

TRIPEPI, S.; JAMIESON, B. G. M.; BRUNELLI, E. Ultrastructure of the Spermatid of *Caprimulgus europaeus* Linnaeus 1758, the European Nightjar (Aves; Caprimulgidae), With Phylogenetic Implications. **Journal of Morphology**, v. 267(10), p. 1157-1164, 2006.

VAN DEN BUSSCHE, R. A.; HOOFER, S. R. Phylogenetic relationships among recent chiropteran families and the importance of choosing appropriate out-group taxa. **Journal of Mammalogy**, v. 85(2), p. 321-330, 2004.

VAN HAASTER, L. H.; de ROOIJ, D. G. Cycle of the seminiferous epithelium in the Djungarian Hamster (*Phodopus sungorus sungorus*). **Biology of Reproduction**, v. 48, p. 515-521, 1993.

VAN VALEN, T. A. The evolution of bats. **Evolutionary Theory**, v. 4, p. 104-121, 1979.

VIEIRA, G. H. C.; COLLI, G. R.; BÁO, S. N. Phylogenetic relationships of corytophanid lizards (Iguania, Squamata, Reptilia) based on partitioned and total evidence analyses of sperm morphology, gross morphology, and DNA data. **Zoologica Scripta**, v. 34, p. 605-625, 2005.

VOLLETH, M. Differences in location of nucleolus organizer regions in European Vespertilionid bats. **Cytogenetic and Cell Genetics**, v. 44, p. 186-197, 1987.

WACHTLER, F.; STAHL, A. The nucleolus: a structural and functional interpretation. **Micron**, v. 24, p. 473-505, 1993.

WANG, R. S.; YEH, S.; TZENG, C. R.; CHANG, C. Androgen receptor roles in spermatogenesis and fertility: lessons from testicular cell-specific androgen receptor knockout mice. **Endocrinology Reviews**, v. 30(2), p. 119-132, 2009.

WARD, S. W.; COFFEY, D. S. DNA packaging and organization in mammalian spermatozoa: Comparison with somatic cells. **Biology of Reproduction**, v. 44, p. 569-574, 1991.

WEATHERBEE, S.D. et al. Interdigital webbing retention in bat wings illustrates genetic changes underlying amniote limb diversification. **PNAS**, v. 103(41), p. 15103-15107, 2006.

WETTERER, A. L.; ROCKMAN, M. V.; SIMMONS, N. B. Phylogeny of Phyllostomid bats (Mammalia: Chiroptera). Data from diverse morphological systems, sex chromosome, and restriction sites. **Bulletins of American Museum of Natural History**, v. 248, p. 1-200, 2000.

WILLIG, M. R. Reproductive patterns of bats from Caatingas and Cerrado biomes in northeast Brazil. **Journal of Mammalogy**, v. 66, p. 668–681, 1985.

WILSON, D. E.; FINDLEY, J. S. Spermatogenesis in Some Neotropical Species of *Myotis*. **Journal of Mammalogy**, v. 52(2), p. 420-426, 1971.

ZHOU, Q.; NIE, R.; PRINS, G. S.; SAUNDERS, P. T.; KATZENELLENBOGEN, B. S.; HESS, R. A. Localization of androgen and estrogen receptors in adult male mouse reproductive tract. **Journal of Andrology**, v. 23, p. 870–881, 2002.

Autorizo a reprodução xenográfica para fins de pesquisa.

São José do Rio Preto, 08/03/2012.

---

Assinatura